

INFORMATION TO USERS

This manuscript has been reproduced from the microfilm master. UMI films the text directly from the original or copy submitted. Thus, some thesis and dissertation copies are in typewriter face, while others may be from any type of computer printer.

The quality of this reproduction is dependent upon the quality of the copy submitted. Broken or indistinct print, colored or poor quality illustrations and photographs, print bleedthrough, substandard margins, and improper alignment can adversely affect reproduction.

In the unlikely event that the author did not send UMI a complete manuscript and there are missing pages, these will be noted. Also, if unauthorized copyright material had to be removed, a note will indicate the deletion.

Oversize materials (e.g., maps, drawings, charts) are reproduced by sectioning the original, beginning at the upper left-hand corner and continuing from left to right in equal sections with small overlaps. Each original is also photographed in one exposure and is included in reduced form at the back of the book.

Photographs included in the original manuscript have been reproduced xerographically in this copy. Higher quality 6" x 9" black and white photographic prints are available for any photographs or illustrations appearing in this copy for an additional charge. Contact UMI directly to order.

UMI

A Bell & Howell Information Company
300 North Zeeb Road, Ann Arbor MI 48106-1346 USA
313/761-4700 800/521-0600

University of Alberta

**TRANSIENT-PRESSURE ANALYSIS IN COMPARTMENTALIZED
RESERVOIRS**

by

N. M. ANISUR RAHMAN



A thesis submitted to the Faculty of Graduate Studies and Research in partial fulfillment
of the requirements for the degree of DOCTOR OF PHILOSOPHY
in
PETROLEUM ENGINEERING

DEPARTMENT OF CIVIL AND ENVIRONMENTAL ENGINEERING

EDMONTON, ALBERTA
SPRING, 1998



National Library
of Canada

Acquisitions and
Bibliographic Services

395 Wellington Street
Ottawa ON K1A 0N4
Canada

Bibliothèque nationale
du Canada

Acquisitions et
services bibliographiques

395, rue Wellington
Ottawa ON K1A 0N4
Canada

Your file Votre référence

Our file Notre référence

The author has granted a non-exclusive licence allowing the National Library of Canada to reproduce, loan, distribute or sell copies of this thesis in microform, paper or electronic formats.

The author retains ownership of the copyright in this thesis. Neither the thesis nor substantial extracts from it may be printed or otherwise reproduced without the author's permission.

L'auteur a accordé une licence non exclusive permettant à la Bibliothèque nationale du Canada de reproduire, prêter, distribuer ou vendre des copies de cette thèse sous la forme de microfiche/film, de reproduction sur papier ou sur format électronique.

L'auteur conserve la propriété du droit d'auteur qui protège cette thèse. Ni la thèse ni des extraits substantiels de celle-ci ne doivent être imprimés ou autrement reproduits sans son autorisation.

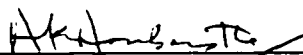
0-612-29096-4

University of Alberta
Faculty of Graduate Studies and Research

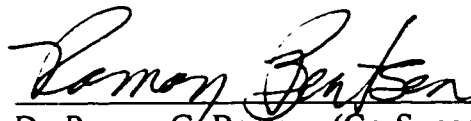
The undersigned certify that they have read, and recommend to the Faculty of Graduate Studies and Research for acceptance, a thesis entitled "TRANSIENT-PRESSURE ANALYSIS IN COMPARTMENTALIZED RESERVOIRS" submitted by N. M. ANISUR RAHMAN in partial fulfillment of the requirements for the degree of DOCTOR OF PHILOSOPHY in PETROLEUM ENGINEERING.



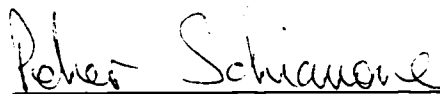
Dr. Nallamuthu Rajaratnam (Chairman)



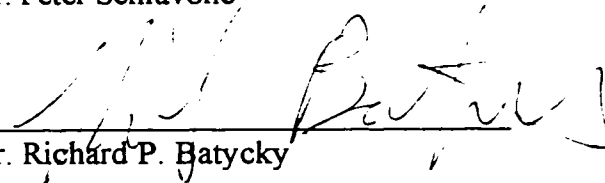
Dr. Anil K. Ambastha (Co-Supervisor)



Dr. Ramon G. Bentsen (Co-Supervisor)



Dr. Peter Schiavone



Dr. Richard P. Batycky

Dr. Roland N. Horne



Dated: November 27, 1997

To all the vivid memories of

my father,

M. Azizur Rahman

B.A., M.A. (Economics), C.M.I.B.P.
(1939-1990)

and

my brother,

FLIGHT LIEUTENANT

N. M. Aminur Rahman

B.Sc. (Aeronautics), G.D.(P.), B.A.F.
(1967-1995)

who never stopped searching until their last breaths for
their faith in the power of knowledge.

ABSTRACT

A compartmentalized reservoir is made up of a number of hydraulically-communicating compartments. Usually the communication between a pair of neighboring compartments is poor due to the presence of faults or low-permeability barriers. Here a new approach is taken to understand the transient-pressure behavior of compartmentalized reservoirs. Analytical solutions are developed for transient flow in compartmentalized systems described by one-, two- and three-dimensional Cartesian coordinate systems. Solutions are derived for dimensionless pressure in one- and two-dimensional systems and for dimensionless potential in three-dimensional flow systems. The solutions for one- and two-dimensional systems are useful for the purpose of studying areally-compartmentalized reservoirs. Consideration of potential is important in a three-dimensional system due to the importance of the effects of gravity. Such a situation can be encountered in reservoir compartmentalization especially with vertical extent. The new solutions have been validated by comparing a number of their simplified cases with those available in the literature.

Interference due to production through multiple wells from a compartmentalized system has been characterized. In addition, a compartmentalized system has been characterized in terms of a homogeneous system. Conditions under which the principle of reciprocity is applicable in the new analytical solutions have been determined.

Transient behavior in compartmentalized systems has been examined using the solutions developed in this study. These include a linear system, a two-compartment system, a system of small compartment in communication with a big one and a stacked channel realization. Pressure-derivatives have been used to identify different flow regimes while observing transient responses at the wellbore. Type-curves and simple solutions for late times have been presented for the purpose of identifying the geological structure and of quantifying the flow resistance at the interface boundary in terms of a skin factor.

A partially-communicating barrier between adjoining compartments has been observed to behave as a sealing interface temporarily for a period of time. Using this observation, a simple diagnostic technique has been developed for detection of poor hydraulic communication between compartments from extended drawdown data. Methods have been proposed to compute the pore volume in each compartment, the total reserve, and the average reservoir pressure from stabilized drawdown data.

ACKNOWLEDGMENTS

I express my deep appreciation for the support, encouragement and understanding that I received from my co-supervisor Dr. Anil Kumar Ambastha. He was always there for me in good times and in bad, and without him my graduate studies would have been far more challenging. There is no doubt in my mind that I received a great favor from him when he assigned me the topic for my research on compartmentalized reservoirs. It was quite a learning experience for me to work with such a serious researcher. I take this opportunity to wish him the best in his future endeavors.

I am also grateful to my other co-supervisor, Dr. Ramon G. Bentsen, for his crucial support for over a year. I thank him for joining my supervisory panel in a difficult situation last year. I particularly admire his free-thinking approach to science and engineering. His understanding of the Hubbert potential has caused me to share his concern with the abuse of this classic concept. I value his appreciation and enthusiasm for the work which encouraged me a lot along the way. I did not waste the opportunity to learn a lot from such a very effective editor.

I am very proud of my family members who provided me with extra-academic support without which my graduate studies would never have been possible in the first place. My mother, Noorjahan Aziz, was the first one in the family who removed all the primary obstacles on my way to graduate studies and who worked very hard to maintain this way obstacle-free, believing in its worth. Iris, my beloved wife, has successfully fulfilled her firm commitment to provide me with whatever I have been in need of all these years. I express my deep gratitude to this outstanding lady in my life without whose sacrifice my dreams would never have come true. It is our children, Mohua, Shapan and Barna, who took the most troubles out of my roller-coaster ride during graduate studies. Their patience knew no bound, putting up with my odd working hours. I would like to thank my sister, Parveen, very much for doing a lot of things behind the scenes, which saved me from much trouble on various occasions.

I thank the Bangladesh University of Engineering and Technology, Dhaka, for conceiving of the 'brilliant' idea of sending me over here for graduate studies and also for granting me the necessary leave of absence.

I gratefully acknowledge the financial support towards my graduate studies from the Canadian International Development Agency, provided through the UofA-BUET Linkage Project. I am very proud of being sponsored by such a successful project and having the privilege to come across two highly regarded individuals from the engineering profession, Drs. George Ford and Fred D. Otto. I consider myself very lucky to have gotten to know these mentors. I will definitely rely on my perception of their teachings, wisdom and vision while making judgments in the future. Besides, Fred has been more than a friend who has kept his door open to me to listen to my problems for last couple years. Also,

Ms. Lori Constantine, Project Manager, has worked very hard to keep our stay in Canada as pleasant as possible. As far as I know, she never complained about having to listen to my complains. I am grateful for her patience and quick responses to my rescue calls. I should also express my sincere appreciation to Mr. Bob Schmidt, former Project Manager, for his friendly approach.

I am also thankful to Mrs. Key Whiting at the School of Mining and Petroleum Engineering whom I bothered at least zillion times, mostly with unusual questions and unconventional requests.

I also acknowledge the productive discussions with Drs. K. Nandakumar, P. Steffler, P. Schiavone, R.P. Batycky and Mr. D. Clyburn at the UofA, Professor R.N. Horne at the Stanford University, California, and Professor M.K. Mikhailov at the University Federal of Rio de Janeiro, Brazil.

There are a lot more extended family, friends, colleagues and well-wishers whom I am indebted to for their support and understanding. I gratefully acknowledge their crucial help and take this opportunity to thank them all.

TABLE OF CONTENTS

CHAPTER 1: INTRODUCTION

1.1 Background.....	1
1.2 Geology of Compartmentalized Reservoirs.....	3
1.3 Literature Review.....	6
1.4 Statement of the Problem.....	8
1.5 Objectives of the Study.....	10
1.6 Formulation of the Problem.....	11
1.7 Solution Methodology.....	20
1.8 Summary of the Following Chapters.....	21

CHAPTER 2: LINEAR, ONE-DIMENSIONAL FLOW SYSTEM

2.1 Introduction.....	25
2.2 Development of the Analytical Solution.....	28
2.2.1 Setting up Governing Differential Equations.....	28
2.2.2 Solving the Differential Equations.....	31
2.2.3 Summary of the Solution Procedure.....	44
2.2.4 Computer Program for Numerical Values.....	44
2.2.5 Determination of Cumulative Flux at an Interface.....	45
2.2.6 Special Cases.....	46
2.3 Validation of New Solution.....	50
2.4 Scope of the Model.....	56
2.5 Example Problems.....	57

CHAPTER 3: TWO-DIMENSIONAL FLOW SYSTEM

3.1 Introduction.....	64
3.2 Development of the Analytical Solution.....	65
3.2.1 Setting up Governing Differential Equations.....	66
3.2.2 Solution of Differential Equations.....	71
3.2.3 Computer Program for Numerical Values.....	78
3.2.4 Average Compartment Pressure.....	78
3.2.5 Cumulative Influx through an Interface.....	79
3.2.6 Relationship between Skin Factor and Barrier Transmissibility.....	80
3.2.7 Modification of Solution for Special Cases.....	82
3.3 Validation of New Solution.....	84
3.4 Application of New Model.....	91

CHAPTER 4: THREE-DIMENSIONAL FLOW SYSTEM

4.1 Introduction.....	93
4.2 Development of the Analytical Solution.....	94

4.2.1 Setting up Governing Differential Equations.....	95
4.2.2 Solution of Differential Equations.....	101
4.2.3 Computer Program for Numerical Values.....	110
4.2.4 Average Compartment Potential.....	110
4.2.5 Cumulative Influx through an Interface.....	112
4.2.6 Relationship between Skin Factor and Barrier Transmissibility.....	113
4.2.7 Modification of Solution for Special Cases.....	114
4.3 Validation of New Solution.....	117
4.4 Application of New Model.....	121

CHAPTER 5: INTERFERENCE OF WELLS DUE TO PRODUCTION

5.1 Introduction.....	124
5.2 Mathematical Consideration.....	126
5.2.1 Two-Dimensional System.....	127
5.2.2 Three-Dimensional System.....	130
5.3 Results and Discussion.....	133
5.4 Applicability of the Principle of Reciprocity.....	137

CHAPTER 6: TRANSIENT-PRESSURE BEHAVIOR OF COMPARTMENTALIZED SYSTEMS

6.1 Introduction.....	139
6.2 Linear System.....	141
6.3 A Small Compartment in Communication with a Big one.....	147
6.3.1 Drawdown.....	152
6.3.2 Buildup.....	166
6.3.3 General Discussion.....	166
6.4 Two-Compartment System.....	171
6.5 Stacked Channel Realization.....	180

CHAPTER 7: EXTENDED DRAWDOWN ANALYSIS IN COMPARTMENTALIZED RESERVOIRS

7.1 Introduction.....	188
7.2 Relationship between Average Reservoir Pressure and Production Rate.....	189
7.3 Analysis of Extended Drawdown Data.....	190
7.3.1 Detection of Poor Hydraulic Communication	190
7.3.2 Compartment Volumes and Hydrocarbon Reserve.....	192
7.3.3 Average Reservoir Pressure.....	196

CHAPTER 8: DISCUSSION, CONCLUSIONS AND RECOMMENDATIONS

8.1 General Discussion.....	205
8.2 Conclusions.....	207
8.3 Recommendations.....	210

REFERENCES.....	212
APPENDICES.....	225
APPENDIX A: Computer Program for One-Dimensional Compartmentalized System.....	225
APPENDIX B: Computer Program for Two-Dimensional Compartmentalized System.....	233
APPENDIX C: Computer Program for Three-Dimensional Compartmentalized System.....	246
APPENDIX D: Three-Dimensional Flow in a Homogeneous and Isotropic Rectangular Parallelepiped	267
APPENDIX E: Proof of Applicability of Principle of Reciprocity.....	277

LIST OF TABLES

Table 6.1:	Dimensionless time to the end of infinite-acting linear flow, t_{DL} , and the start of pseudosteady-state flow, t_{DPSS}	145
Table 6.2:	Location, extent and specification of skin factor of communicating boundaries.....	150
Table 6.3:	Combinations of skin factors at the boundaries of a small compartment.....	150
Table 6.4:	Dimensionless time to the start of steady-state flow, t_{DS} , in “Combination 1”.....	164
Table 6.5:	Dimensionless time to the start of steady-state flow, t_{DS} , in “Combination 2”.....	164
Table 6.6:	Dimensionless time to the start of steady-state flow, t_{DS} , in “Combination 3”.....	164
Table 6.7:	Dimensionless time to the start of steady-state flow, t_{DS} , in “Combination 4”.....	165
Table 6.8:	Dimensionless time to the start of steady-state flow, t_{DS} , in “Combination 5”.....	165
Table 7.1:	Buildup time required for different skin factors.....	197
Table 7.2:	Values of C_w for well locations in a compartmentalized system with $XY = 0.5, s = 100$	199
Table 7.3:	Values of C_w for well locations in a compartmentalized system with $XY = 0.5, s = 1000$	200
Table 7.4:	Values of C_w for well locations in a compartmentalized system with $XY = 0.5, s = 10000$	200
Table 7.5:	Values of C_w for well locations in a compartmentalized system with $XY = 1.0, s = 100$	200
Table 7.6:	Values of C_w for well locations in a compartmentalized system with $XY = 1.0, s = 1000$	201

Table 7.7:	Values of C_w for well locations in a compartmentalized system with $XY = 1.0, s = 10000$.	201
Table 7.8:	Values of C_w for well locations in a compartmentalized system with $XY = 2.0, s = 100$.	201
Table 7.9:	Values of C_w for well locations in a compartmentalized system with $XY = 2.0, s = 1000$.	202
Table 7.10:	Values of C_w for well locations in a compartmentalized system with $XY = 2.0, s = 10000$.	202
Table 7.11:	Average values of C_w for different values of skin factor in a compartmentalized system.	202
Table D.1:	Kernel functions for auxiliary solutions for closed boundaries.	272

LIST OF FIGURES

Figure 1.1:	Linear, one-dimensional flow system with skin boundary	14
Figure 1.2:	Two-dimensional flow system with skin boundary.....	14
Figure 1.3:	Three-dimensional flow system with skin boundary.....	14
Figure 1.4:	Schematic illustrating Linear-Segment Approximation Method.....	17
Figure 1.5:	Schematic illustrating use of the Heaviside unit-step function.....	19
Figure 1.6:	Schematic illustrating steps of the integral-transform technique for finite, composite domains.....	22
Figure 2.1:	Schematic of a linear, compartmentalized system ($n = 4$).....	27
Figure 2.2:	Two-rate flow condition at the inner boundary and closed outer boundary in a homogeneous system.....	52
Figure 2.3:	Comparison of dimensionless cumulative influx at the constant pressure inner boundary while the outer boundary is closed.....	52
Figure 2.4:	Shut-in followed by production in the inner boundary and constant pressure at the outer boundary.....	54
Figure 2.5:	Comparison of the dimensionless pressure at the producing boundary of a homogeneous system with the modified solution of Ambastha and Sageev (1987).....	54
Figure 2.6:	Comparison of the dimensionless pressure at the producing boundary of a composite system with the modified solution of Ambastha and Sageev (1987).....	55
Figure 2.7:	Schematic of a reservoir-aquifer system.....	58
Figure 2.8:	The variation of flow rate at the inner boundary.....	60
Figure 2.9:	Comparison of dimensionless cumulative influxes at the inner boundary and the reservoir-aquifer interface.....	60
Figure 2.10:	Comparison of dimensionless pressures at the inner boundary and reservoir-aquifer interface.....	61

Figure 2.11:	Comparison of dimensionless cumulative influxes at the inner boundary and the reservoir-aquifer interface.....	61
Figure 2.12:	Dimensionless pressure response at the reservoir-aquifer interface for a homogeneous system.....	63
Figure 2.13:	Comparison of dimensionless cumulative influxes at the inner boundary and the reservoir-aquifer interface for a homogeneous system.....	63
Figure 3.1:	Schematic illustrating the geometry of a two-dimensional, areally-compartmentalized system.....	67
Figure 3.2:	Comparison of dimensionless pressure responses in a closed homogeneous reservoir.....	85
Figure 3.3:	Comparison of dimensionless pressure responses for a 3-rate situation in a closed homogeneous system.....	85
Figure 3.4:	Comparison of buildup responses in a closed homogeneous system.....	87
Figure 3.5:	Comparison of dimensionless pressure responses in a homogeneous reservoir with constant-pressure boundaries.....	87
Figure 3.6:	Comparison of dimensionless pressure responses for a 3-rate situation in a homogeneous system with constant-pressure boundaries.....	88
Figure 3.7:	Comparison of buildup responses in a homogeneous system with constant-pressure boundaries.....	90
Figure 3.8:	Comparison of semilog derivative responses with those from Hovanessian (1961).....	90
Figure 4.1:	Schematic of a general arrangement in a three-dimensional compartmentalized system.....	96
Figure 4.2:	Schematic showing location of wells in <i>ith</i> compartment.....	97
Figure 4.3:	Comparison of the dimensionless potential response and its derivatives from the solution of a compartmentalized system with those from a closed, homogeneous system.....	118

Figure 4.4:	Comparison of the dimensionless potential response and its Cartesian derivative from the solution of a compartmentalized system with those from a closed, homogeneous system and Hovanessian (1961).....	120
Figure 4.5:	Comparison of the dimensionless potential response and its Cartesian derivative from the solution of a compartmentalized system with those from a homogeneous system.....	120
Figure 4.6:	Comparison of the dimensionless potential response and its Cartesian derivative generated from the solution of a compartmentalized system with those from a homogeneous system.....	122
Figure 5.1:	A homogeneous rectangular reservoir with a two-dimensional flow system	129
Figure 5.2:	A homogeneous rectangular parallelepiped with a three-dimensional flow system.....	132
Figure 5.3	Profiles of equivalent dimensionless production rate for a two-compartment system producing through two wells.....	134
Figure 5.4:	Effect of skin factor on profiles of equivalent dimensionless production rate due to interference of wells in a two-well, two-compartment system.....	134
Figure 5.5:	Profiles of equivalent dimensionless production rate compared with a homogeneous system due to interference of wells in a two-well, two-compartment system.....	136
Figure 5.6:	Effect of skin factor on profiles of equivalent dimensionless production rate due to interference of wells in a two-well, two-compartment system with respect to a homogeneous system.....	136
Figure 6.1:	Dimensionless wellbore pressure responses in a linear system.....	143
Figure 6.2:	Specific derivative profile of dimensionless wellbore pressure responses for a linear system.....	143
Figure 6.3:	Cartesian derivative profile of dimensionless wellbore pressure responses in a linear system.....	144
Figure 6.4:	Effect of storativity ratio on the Cartesian derivative of dimensionless pressure responses in a linear system for $M_2 = 10$	146

Figure 6.5:	Effect of storativity ratio on the Cartesian derivative of dimensionless pressure responses in a linear system for $M_2 = 100$	146
Figure 6.6:	A schematic showing a small compartment in communication with a big one.....	149
Figure 6.7:	Dimensionless pressure responses in drawdown for different values of skin factors considered in "Combination 1".....	153
Figure 6.8:	Dimensionless pressure responses in drawdown for different values of skin factors considered in "Combination 2".....	153
Figure 6.9:	Dimensionless pressure responses in drawdown for different values of skin factors considered in "Combination 3".....	154
Figure 6.10:	Dimensionless pressure responses in drawdown for different values of skin factors considered in "Combination 4".....	154
Figure 6.11:	Dimensionless pressure responses in drawdown for different values of skin factors considered in "Combination 5".....	155
Figure 6.12:	Semilog derivative of dimensionless pressure responses in drawdown for different values of skin factors considered in "Combination 1".....	158
Figure 6.13:	Semilog derivative of dimensionless pressure responses in drawdown for different values of skin factors considered in "Combination 2".....	158
Figure 6.14:	Semilog derivative of dimensionless pressure responses in drawdown for different values of skin factors considered in "Combination 3".....	159
Figure 6.15:	Semilog derivative of dimensionless pressure responses in drawdown for different values of skin factors considered in "Combination 4".....	159
Figure 6.16:	Semilog derivative of dimensionless pressure responses in drawdown for different values of skin factors considered in "Combination 5".....	160
Figure 6.17:	Cartesian derivative of dimensionless pressure responses in drawdown for different values of skin factors considered in "Combination 1".....	160
Figure 6.18:	Cartesian derivative of dimensionless pressure responses in drawdown for different values of skin factors considered in "Combination 2".....	161

Figure 6.19:	Cartesian derivative of dimensionless pressure responses in drawdown for different values of skin factors considered in "Combination 3"	161
Figure 6.20:	Cartesian derivative of dimensionless pressure responses in drawdown for different values of skin factors considered in "Combination 4".....	162
Figure 6.21:	Cartesian derivative of dimensionless pressure responses in drawdown for different values of skin factors considered in "Combination 5"	162
Figure 6.22:	Dimensionless pressure responses at the wellbore for a shut-in period being followed by a production period where the well is shut in at $t_D = 4$ for "Combination 1"	167
Figure 6.23:	Dimensionless pressure responses at the wellbore for a shut-in period being followed by a production period where the well is shut in at $t_D = 4$ for "Combination 2"	167
Figure 6.24:	Dimensionless pressure responses at the wellbore for a shut-in period being followed by a production period where the well is shut in at $t_D = 4$ for "Combination 3"	168
Figure 6.25:	Dimensionless pressure responses at the wellbore for a shut-in period being followed by a production period where the well is shut in at $t_D = 4$ for "Combination 4"	168
Figure 6.26:	Dimensionless pressure responses at the wellbore for a shut-in period being followed by a production period where the well is shut in at $t_D = 4$ for "Combination 5"	169
Figure 6.27:	Effect of skin factor on the dimensionless pressure responses at the wellbore in a two-compartment system.....	173
Figure 6.28:	Effect of skin factor on the semilog derivative of dimensionless pressure responses at the wellbore in a two-compartment system.....	173
Figure 6.29:	Effect of skin factor on Cartesian derivative of dimensionless pressure responses at the wellbore of a two-compartment system.....	174
Figure 6.30:	Effect of mobility and storativity ratios on Cartesian derivative of dimensionless pressure responses at the wellbore of a two-compartment system with $M_2 = 10$, $s = 100$	176

Figure 6.31:	Effect of mobility and storativity ratios on Cartesian derivative of dimensionless pressure responses at the wellbore of a two-compartment system with $M_2 = 100$, $s = 100$	176
Figure 6.32:	Effect of mobility and storativity ratios on Cartesian derivative of dimensionless pressure responses at the wellbore of a two-compartment system with $M_2 = 0.1$, $s = 100$	177
Figure 6.33:	Effect of mobility and storativity ratios on Cartesian derivative of dimensionless pressure responses at the wellbore of a two-compartment system with $M_2 = 10$, $s = 1000$	177
Figure 6.34:	Effect of mobility and storativity ratios on Cartesian derivative of dimensionless pressure responses at the wellbore of a two-compartment system with $M_2 = 100$, $s = 1000$	178
Figure 6.35:	Effect of mobility and storativity ratios on Cartesian derivative of dimensionless pressure responses at the wellbore of a two-compartment system with $M_2 = 0.01$, $s = 1000$	178
Figure 6.36:	Effect of mobility and storativity ratios on Cartesian derivative of dimensionless pressure responses at the wellbore of a two-compartment system with $M_2 = 0.1$, $s = 1000$	179
Figure 6.37:	Schematic of a stacked channel realization.....	181
Figure 6.38a:	Schematic illustrating the geometry of a stacked channel realization in areal view.....	183
Figure 6.38b:	Schematic illustrating the geometry of a stacked channel realization in plan view.....	183
Figure 6.39:	Effect of storativity ratio on the Cartesian derivative of dimensionless potential responses at a wellbore in a stacked channel realization for $s = 0$	184
Figure 6.40:	Effect of storativity ratio on the Cartesian derivative of dimensionless potential responses at a wellbore in a stacked channel realization for $s = 100$	184
Figure 6.41:	Cartesian derivative of dimensionless potential responses at wellbore for different values of skin factor in a stacked channel realization.....	186

Figure 7.1:	Cartesian derivative responses to detect poor hydraulic communication between compartments.....	191
Figure 7.2:	Determination of intercept values from Cartesian derivative profile plotted with well test data from a compartmentalized system.....	194
Figure 7.3:	Buildup behavior at a well in the first compartment for different values of skin factor after a production period of $t_D = 100$	197
Figure 7.4:	Well locations considered for determining C_w for different values of X/Y	199
Figure 7.5:	Comparison of the predicted dimensionless wellbore pressure at late time with that from the analytical solution with $X/Y = 2$	204
Figure 7.6:	Comparison of the predicted dimensionless wellbore pressure at late time with that from the analytical solution with $X/Y = 0.5$	204
Figure D.1:	Schematic of three-dimensional flow in a homogeneous parallelepiped...	269

NOMENCLATURE

Chapter 1

- B_p = Reference formation volume factor of fluid, L^3/L^3
- $H(t-T)$ = Heaviside unit step function, equal to 0 when $t < T$ and 1 when $t \geq T$
- h_p = Reference pay thickness, L
- k_p = Reference permeability, L^2
- $[p_j - p_i]_{\partial R_{ij}}$ = Pressure-drop across the interface, ∂R_{ij} , m/Lt^2
- q_{ij} = Flow rate through the interface between *ith* and *jth* compartments, L^3/t
- q_{ij}^* = Flow rate per unit width through the interface between *ith* and *jth* compartments, L^2/t
- q_{ij}^{**} = Flow rate per unit area through the interface between *ith* and *jth* compartments, L/t
- q_{i-1}, q_i = Production rates at the nodal points, t_{i-1} and t_i , respectively, illustrated in Fig. 1.4
- s_{ij} = Skin factor at the interface between *ith* and *jth* compartments
- t = Time, t
- ∂R_{ij} = Interface boundary between *ith* and *jth* compartments
- X_p = Reference length, L
- μ_p = Reference viscosity of fluid, m/Lt
- $[\Phi_j - \Phi_i]_{\partial R_{ij}}$ = Potential-drop across the interface, ∂R_{ij} , m/Lt^2
- $\psi(t)$ = Time-dependent function
- ψ_1, ψ_2, ψ_3 = Stepped values of ψ in respective time ranges, illustrated in Fig. 1.5

Chapter 2

- a_m = Distance between the plane-sink in m th compartment from the boundary at $x = X_m$, L
- B_m = Formation volume factor of fluid in m th compartment, L^3/L^3
- $A_{0m} B_{0m}$ = Coefficients in Eq. (2.19)
- $A_{nm} B_{nm}$ = Coefficients in Eq. (2.22)
- c_{tm} = Total compressibility of rock-fluid system in m th compartment, Lt^2/m
- $[D]$ = Coefficient matrix, defined in Eqs. (2.48)
- E_m = Constant eigenfunction considered when the extreme boundary conditions are of homogeneous, Neumann-type
- $f_0(t_D)$ = Time-dependent boundary function at $x_D = X_{1D}$, as in Eq. (2.10)
- $f_n(t_D)$ = Time-dependent boundary function at $x_D = X_{n+1D}$, as in Eq. (2.11)
- F_m = Storativity ratio in m th compartment, $\frac{(\phi_m c_{tm})}{(\phi_p c_{tp})}$
- $g_0(t_D)$ = Source-function in case of zero eigenvalue, defined in Eq. (2.58)
- $g(t_D)$ = Source-function, defined in Eq. (2.40)
- $g_0^*(\tau)$ = Source-function, defined in Eq. (2.62)
- G_m = Function, defined in Eq. (2.18b)
- h_m = Height of m th compartment, L
- k_m = Permeability of formation in m th compartment, L^2
- $L_{0m}(x_D)$ = Linear set, defined in Equation (2.16) for m th compartment
- $L_{nm}(x_D)$ = Linear set, defined in Equation (2.17) for m th compartment
- M_m = Mobility ratio in m th compartment, $\frac{(k_m/\mu_m)}{(k_p/\mu_p)}$
- n = Total number of compartments
- N_0 = Norm in case of zero-eigenvalue, defined in Eq. (2.60)
- N_l = Norm, defined in Eq. (2.32)
- $p_m(x, t)$ = Pressure at m th compartment as function of x and t , m/Lt^2
- p_{0m} = Initial pressure in m th compartment, m/Lt^2

p_p = Reference pressure, m/Lt^2

$P_{m i}(\lambda_i, x_D)$ = Function, defined in Eq. (2.47a)

$q_m(t)$ = Production rate from the plane-sink in m th compartment as a function of time, L^3/t

$q_i''(t)$ = Influx rate at the i th interface, L^3/t

$Q_{c, i}(t)$ = Cumulative influx at $x = X_i$ over a period, t , L^3 , defined as,

$$\frac{k h_i w_i}{\mu_i B_i} \int_0^t \left. \frac{\partial p_i(x, \tau)}{\partial x} \right|_{x_i} d\tau$$

$Q_{c, i D}(t_D)$ = Dimensionless cumulative influx at $x_D = X_{i D}$ over a dimensionless period, t_D , defined as, $\frac{Q_{c, i}(t) k_p}{q_p \mu_p \phi_p c_{i p} X_{i D}^2}$

$[R_{L o}]$ = Coefficient matrix, defined in Eq. (2.21a)

$[R_{L n}]$ = Coefficient matrix, defined in Eq. (2.24a)

R_m = The region within the m th compartment

s_i = Skin factor at the interface boundary at $x = X_{i-1}$ or at $x_D = X_{i-1 D}$,

defined as, $\frac{k_{i-1} h_{i-1} [p_i - p_{i-1}]_{x_i}}{\mu_{i-1} B_{i-1} q^*}$, where q^* is the fluid flow rate through

the skin boundary at $x = X_{i-1}$

$\{S_{L o}\}$ = Vector, defined in Eq. (2.21b)

$\{S_{L n}\}$ = Vector, defined in Eq. (2.24b)

t = Time, t

$T_{m i}(\lambda_i, x_D)$ = Function, defined in Eq. (2.47b)

u_i = Transmissibility parameter for i th interface, defined in Eq. (2.14)

$U_{m i}(\lambda_i, x_D)$ = Function, defined in Eq. (2.45a)

$V_{m i}(\lambda_i, x_D)$ = Function, defined in Eq. (2.45b)

w_m = Width of m th compartment, L

$\{W_{L o}\}$ = Vector, defined in Eq. (2.21c)

- $\{W_{L n}\} =$ Vector, defined in Eq. (2.24c)
- $x =$ Space variable, L
- $X_m, X_{m-1} =$ Boundaries of *mth* compartment, L
- $\{Y\} =$ Vector, defined in Eq. (2.49n)
- $z_l =$ Coefficient in Eq. (2.25) and later determined in Eq. (2.34)
- $\alpha_m =$ Transmissibility coefficient for *mth* compartment, defined in Eq. (2.7)
- $\eta_m =$ Diffusivity ratio for *mth* compartment, defined in Eq. (2.6), also F_m/M_m
- $\delta(X - a) =$ Dirac delta function
- $\delta_{ll'} =$ Kronecker delta, equal to 1 when $l = l'$ and 0 when $l \neq l'$
- $\lambda_l =$ *lth* eigenvalue
- $\mu_m =$ Viscosity of fluid in *mth* compartment, m/Lt
- $\phi_m =$ Formation porosity in *mth* compartment
- $\psi_{m l} =$ *lth* eigenfunction in *mth* compartment
- $\psi_{m l}^{\cdot}, \psi_{m l}^{\cdot\cdot} =$ Values of $\psi_{m l}$ at $x_D = X_{m D}, x_D = X_{m-1 D}$, respectively, in Eq. (2.44)
- $\Theta_m(x_D, t_D) =$ Dependent variable of the homogeneous problem, defined in Eqs. (2.18a) through (2.18f)
- $\bar{\Theta}_0^*(t_D = 0) =$ Function, defined in Eq. (2.61)
- $\tau =$ Dummy variable, in Eqs. (2.42), (2.43), (2.51) through (2.54), (2.56), (2.58), (2.59) and (2.62)
- $\gamma_0, \zeta_0 =$ Parameters in Eq. (2.10) to be preset for obtaining an appropriate condition at the extreme boundary at $x_D = X_{1 D}$
- $\gamma_n, \zeta_n =$ Parameters in Eq. (2.11) to be preset for obtaining an appropriate condition at the extreme boundary at $x_D = X_{n+1 D}$

Subscripts

D = Dimensionless

i = i th interface at $x = X_i$ or at $x_D = X_{i,D}$

l = l th eigenvalue, eigenfunction, norm, function or transformed
dimensionless pressure

m = m th compartment

p = Reference compartment or parameter

Chapter 3

A_i = Defined in Eq. (3.48)

$a_i^{(m)}, b_i^{(m)}$ = Co-ordinates of m th well in i th compartment, L

B_i = Formation volume factor in i th compartment

$c_{i,t}$ = Total compressibility in i th compartment, Lt^2/m

e_i = Defined in Eq. (3.18)

$F(\tau)$ = Function defined in Eq. (3.55)

f_{ax}, f_{oy} = Specified conditions at extreme boundaries of i th compartment as a
function of dimensionless time

h_p = Reference pay thickness, L

$h_{p,D}$ = Defined in Eq. (3.15)

k_x, k_y = Permeability in x - and y -direction (principal axes), respectively, L^2

n = Total number of compartments

$N_{w,i}$ = Number of wells in i th compartment

N_l = Norm corresponding to l th eigenvalue, defined in Eq. (3.33)

N_0 = Norm corresponding to zero-eigenvalue, defined in Eq. (3.65)

$p_{D\ add}$ = Defined in Eq. (3.63)

$\bar{p}_{D\ add}(t_D = 0)$ = Defined in Eq. (3.66)

\bar{p}_{Dl} = Transformed value corresponding to l th eigenvalue

- \bar{p}_i, \bar{p}_j = Average pressures at *ith* and *jth* compartment, m/Lt^2
- $p_i(x, y, t)$ = Pressure in *ith* compartment as a function of (x, y, t) , m/Lt^2
- p_{iD} = Dimensionless pressure in *ith* compartment, defined in Eq. (3.9)
- $p_{\alpha i}$ = Initial pressure in *ith* compartment, m/Lt^2
- $p_{\alpha iD}$ = Dimensionless initial pressure in *ith* compartment, defined in Eq. (3.2)
- $Q_{ijD}(t_D)$ = Dimensionless cumulative influx through interface at ∂R_{ij}
- q_{ij} = Rate of influx at interface between *ith* and *jth* compartments, L^3/t
- $q_{ijD} = q_{ij}/q_p$
- $q_i^{(m)}(t)$ = Production rate of the *mth* well in *ith* compartment as a function of time, L^3/t
- R_i = Region within *ith* compartment
- s = Skin factor at an interface
- t = Time, t
- T_{ij} = Barrier transmissibility between *ith* and *jth* compartments, $L^4/t/m$
- U_{i1} = *lth* eigenfunction for *x*-direction in *ith* compartment
- U_{11b}, U_{21l} = Defined in Eqs. (3.43), (3.44), respectively
- U_{i1}^*, U_{i1}^{**} = Value of U_{i1} at $x_D = X_{iD}, X_{i+1D}$, respectively
- \bar{U}_{i1} = Defined in Eq. (3.50)
- V_{i1} = *lth* eigenfunction for *y*-direction in *ith* compartment
- V_{11b}, V_{21l} = Defined in Eqs. (3.45), (3.46), respectively
- V_{i1}^*, V_{i1}^{**} = Value of V_{i1} at $y_D = Y_{iD}, Y_{i+1D}$, respectively
- \bar{V}_{i1} = Defined in Eq. (3.51)
- X_i, X_{i+1} = Location of boundaries of *ith* compartment parallel to *y*-axis, L
- $X_{iD} = X_i/X_p$
- X_p = Reference length, L
- x = Abscissa, L
- x_D = Dimensionless abscissa, defined in Eq. (3.10)

- Y_i, Y_{i+1} = Location of boundaries of *ith* compartment parallel to x-axis, L
 $Y_{i,D} = Y_i / X_p$
 y = Ordinate, L
 y_D = Dimensionless ordinate, defined in Eq. (3.11)
 $\alpha_{x,i}, \alpha_{y,i}$ = Defined in Eqs. (3.16), (3.17), respectively
 $\delta(x - a)$ = Dirac delta function
 δR_{ij} = Interface boundary between compartments, *i* and *j*
 δR_{in} = Interface boundary between compartments, *i* and *n*
 $\eta_{x,i}, \eta_{y,i}$ = Defined in Eqs. (3.21), (3.26), respectively
 λ_l = Defined in Eq. (3.36)
 μ_i = Viscosity in *ith* compartment, m/Lt
 ϕ_i = Porosity in *ith* compartment
 $\sigma_{i,l}$ = *lth* eigenvalue for y-direction in *ith* compartment
 $\theta_{i,l}$ = *lth* eigenvalue for x-direction in *ith* compartment
 τ, τ' = Dummy variables
 $\gamma_{ox,i}, \zeta_{ox,i}$ = Parameters for conditions at extreme boundaries parallel to y-axis
 $\gamma_{oy,i}, \zeta_{oy,i}$ = Parameters for conditions at extreme boundaries parallel to x-axis

Subscripts

- D = Dimensionless
 i = *ith* compartment, $i = 1, 2, 3, \dots, n$
 ij = interface between *ith* and *jth* compartments
 in = interface between *ith* and *nth* compartments
 j = *jth* compartment
 l = *lth* eigenvalue, eigenfunction or parameter
 m = *mth* well in a compartment

p = Reference compartment or parameter
 x, y = Along x or y direction

Chapter 4

- A_i = Defined in Eq. (4.66)
- $a_i^{(m')}, b_i^{(m')}$ = Areal coordinates of m' th well in i th compartment, L
- $a_{i,D}^{(m')}, b_{i,D}^{(m')}$ = Defined in Eqs. (4.18), (4.19), respectively
- B_i = Formation volume factor in i th compartment
- c_{ti} = Total compressibility in i th compartment, Lt^2/m
- C_{hp} = Defined in Eq. (4.73)
- e_i = Defined in Eq. (4.25)
- $F_i(\tau)$ = Function defined in Eq. (4.75)
- $f_{\alpha_x}, f_{\alpha_y}, f_{\alpha_z}$ = Specified conditions at extreme boundaries of i th compartment as a function of dimensionless time
- g = Acceleration due to gravity, L/t^2
- g_l = Defined in Eq. (4.49)
- g_o = Defined in Eq. (4.84)
- $h_{1_i}^{(m')}, h_{2_i}^{(m')}$ = Extent of pay thickness of m' th well in i th compartment, illustrated in Fig. 4.2, L
- $h_{1,D}^{(m')}, h_{2,D}^{(m')}$ = Defined in Eqs. (4.20), (4.21), respectively
- h_p = Pay thickness of the reference compartment, L
- k_x, k_y, k_z = Permeability in x -, y - and z -direction (principal axes), respectively, L^2
- n = Total number of compartments
- N_{wi} = Number of wells in i th compartment
- N_l = Norm corresponding to l th eigenvalue, defined in Eq. (4.45)
- N_0 = Norm corresponding to zero-eigenvalue, defined in Eq. (4.85)

- $p_i(x, y, z, t)$ = Pressure at i th compartment as a function of x, y, z and t , m/Lt^2
- $Q_{ijD}(t_D)$ = Dimensionless cumulative influx through interface at ∂R_{ij}
- q_{ij} = Rate of influx at interface between i th and j th compartments, L^3/t
- $q_{ijD} = q_{ij}/q_p$
- $q_i^{(m)}(t)$ = Production rate of the m th well in i th compartment as a function of time, L^3/t
- R_i = Bounded region within i th compartment
- s = Skin factor at an interface
- t = Time, t
- t_D = Dimensionless time, defined in Eq. (4.17)
- T_{ij} = Barrier transmissibility between i th and j th compartments, L^4t/m
- $U_{i,l}$ = l th eigenfunction for x -direction in i th compartment
- $U_{1,l}, U_{2,l}$ = Defined in Eqs. (4.59), (4.60), respectively
- $U_{i,l}^*, U_{i,l}^{**}$ = Value of $U_{i,l}$ at $x_D = X_{iD}, X_{i-1D}$, respectively
- $\bar{U}_{i,l}$ = Defined in Eq. (4.68)
- $V_{i,l}$ = l th eigenfunction for y -direction in i th compartment
- $V_{1,l}, V_{2,l}$ = Defined in Eqs. (4.61), (4.62), respectively
- $V_{i,l}^*, V_{i,l}^{**}$ = Value of $V_{i,l}$ at $y_D = Y_{iD}, Y_{i-1D}$, respectively
- $\bar{V}_{i,l}$ = Defined in Eq. (4.69)
- $W_{i,l}$ = l th eigenfunction for z -direction in i th compartment
- $W_{1,l}, W_{2,l}$ = Defined in Eqs. (4.63), (4.64), respectively
- $W_{i,l}^*, W_{i,l}^{**}$ = Value of $W_{i,l}$ at $z_D = Z_{iD}, Z_{i-1D}$, respectively
- $\bar{W}_{i,l}$ = Defined in Eq. (4.70)
- X_i, X_{i-1} = Location of boundaries of i th compartment parallel to y -axis, L
- $X_{iD} = X_i/X_p$
- X_p = Reference length, L
- x = Abscissa, L

- x_D = Dimensionless abscissa, defined in Eq. (4.14)
 Y_i, Y_{i-1} = Location of boundaries of i th compartment parallel to x -axis, L
 $Y_{i,D} = Y_i / X_p$
 y = Ordinate, L
 y_D = Dimensionless ordinate, defined in Eq. (4.15)
 Z_i, Z_{i-1} = Location of boundaries of i th compartment parallel to z -axis, L
 $Z_{i,D} = Z_i / Z_p$
 Z_p = Reference length, L
 z = Distance from x - y -plane, L
 z_D = Dimensionless abscissa, defined in Eq. (4.16)
 $\alpha_{x,i}, \alpha_{y,i}, \alpha_{z,i}$ = Defined in Eqs. (4.22), (4.23), (4.24), respectively
 $\delta(x - a)$ = Dirac delta function
 δR_{ij} = Interface boundary between compartments i and j
 δR_{in} = Interface boundary between compartments i and n
 $\epsilon_{i,l}$ = l th eigenvalue for z -direction in i th compartment
 $\eta_{x,i}, \eta_{y,i}, \eta_{z,i}$ = Defined in Eqs. (4.28), (4.33), (4.38), respectively
 $\kappa_{1,i}^{(m')}, \kappa_{2,i}^{(m')}$ = Defined in Eqs. (4.50), (4.51), respectively
 λ_l = Defined in Eq. (4.48)
 μ_i = Viscosity in i th compartment, m/Lt
 ϕ_i = Porosity in i th compartment
 $\Phi_{D\,add}$ = Defined in Eq. (4.83)
 $\bar{\Phi}_{D\,add}(t_D = 0)$ = Defined in Eq. (4.86)
 $\bar{\Phi}_{D\,i}$ = Transformed value corresponding to l th eigenvalue
 $\bar{\Phi}_i, \bar{\Phi}_j$ = Volumetric average potentials at i th and j th compartment, m/Lt²
 $\Phi_i(x, y, z, t)$ = Potential in i th compartment as a function of x, y, z and t , m/Lt²

$\Phi_{i,D}$ = Dimensionless potential in *ith* compartment, defined in Eq. (4.13)

Φ_{α} = Initial potential in *ith* compartment, m/Lt^2

$\Phi_{\alpha i,D}$ = Dimensionless initial potential in *ith* compartment, defined in Eq. (4.3)

ρ = Density of fluid, m/L^3

$\sigma_{i,l}$ = *lth* eigenvalue for *y*-direction in *ith* compartment

$\theta_{i,l}$ = *lth* eigenvalue for *x*-direction in *ith* compartment

τ, τ' = Dummy variables

$\gamma_{\alpha i}, \zeta_{\alpha i}$ = Parameters for conditions at extreme boundaries parallel to *y-z*-plane

$\gamma_{\alpha y i}, \zeta_{\alpha y i}$ = Parameters for conditions at extreme boundaries parallel to *x-z*-plane

$\gamma_{\alpha z i}, \zeta_{\alpha z i}$ = Parameters for conditions at extreme boundaries parallel to *x-y*-plane

Subscripts

D = Dimensionless

i = *ith* compartment, $i = 1, 2, 3, \dots, n$

ij = interface between *ith* and *jth* compartments

in = interface between *ith* and *nth* compartments

j = *jth* compartment

l = *lth* eigenvalue, eigenfunction or parameter

m = *mth* well in a compartment

p = Reference compartment or parameter

x, y, z = Along *x, y* or *z* direction

Superscript

(*m*') = *m*'*th* well in a compartment

Chapter 5

D_{EC}	= Defined in Eqs. (5.3) and (5.8)
D_{EH}	= Defined in Eqs. (5.5) and (5.10)
q_{ECD}	= Defined in Eqs. (5.2) and (5.7)
q_{EHD}	= Defined in Eqs. (5.4) and (5.9)

Chapter 6

$$e = (\phi c_r/B) (B_p/\phi_p c_{rp})$$

$$h_D = h/h_p$$

$$p_w = \text{Wellbore pressure, m/Lt}^2$$

$$p_{wD} = \text{Dimensionless wellbore pressure, } (k_p h_p/q_p \mu_p B_p) (p_p - p_w)$$

Subscripts

l = Lower body

u = Upper body

Chapter 7

A_i = Dimensionless area of i th compartment, defined in Eq. (3.48), Chapter 3

C_w = A constant depending on location of well at producing compartment

e_i = Defined in Eq. (3.18), Chapter 3

h_p = Reference pay thickness, L

$$h_{pD} = h_p/X_p$$

k_i = Permeability in i th compartment

N_S = Hydrocarbon reserve per unit pressure drawdown, defined in Eq. (7.12), L^4t^2/m

N_{S1}, N_{S2} = Hydrocarbon reserve per unit pressure drawdown in compartments 1 and 2, defined in Eqs. (7.8) and (7.9), respectively, L^4t^2/m

N_0 = Defined in Eq. (3.65), Chapter 3

p_o = Initial pressure, m/Lt^2

p_w = Wellbore pressure, m/Lt^2

p_w' = Cartesian derivative of wellbore pressure with respect to time, m/Lt^3

p_{wD} = Dimensionless wellbore pressure, $(k_p h_p/q_p \mu_p B_p) (p_o - p_w)$

p_{wD}' = Cartesian derivative of dimensionless wellbore pressure with respect to dimensionless time

\bar{p} = Average reservoir pressure, m/Lt^2

\bar{p}_D = Defined in Eq. (7.2)

q = Constant rate of production, L^3/t

q_D = Defined in Eq. (7.3)

V_i = Volume of *i*th compartment

X, Y = Dimensions illustrated in Fig. 7.4, L

X_p = Reference length, L

Subscripts

i = *i*th compartment

p = Reference compartment or parameter

r = Infinite-acting radial-flow regime

CHAPTER 1

INTRODUCTION

1.1 Background

A compartmentalized reservoir is made up of a number of hydraulically-communicating compartments. Rock and fluid properties in each compartment may be distinct. The hydraulic communication between any two neighboring compartments is usually poor due to the presence of faults or low-permeability barriers. However, *Smalley and England* (1994) mention that these barriers could be of different strengths, ranging from relatively minor features that might retard fluid flow to major features that will not allow any fluid communication. Evidence of reservoir compartmentalization has been observed in both oil and gas reservoirs (*Junkin et al.*, 1992). *Bradley and Powley* (1994) have pointed out that multiple compartments may be found both areally and vertically. A number of compartmentalized reservoirs have been discovered in different parts of the world including those in the North Sea (*Fox et al.*, 1988), Texas Gulf Coast (*Lord and Collins*, 1991; *Lord et al.*, 1992; *Junkin et al.*, 1992) and Australia (*Malavazos and McDonough*, 1991)

Lord et al. (1992) have given an example of a compartmentalized reservoir in South Texas. In this reservoir, the producing compartment of 8 MMcf is in communication with a secondary compartment of 24.7 MMcf through a barrier with a transmissibility of 4 md-ft (the barrier is 8000 ft long, 1000 ft across, and 1 ft high with a permeability of 0.5 md).

Reservoir compartmentalization is detected primarily from observation of the discontinuities in pressure both areally for areal compartmentalization and vertically for vertical compartmentalization that have been found in produced fields when wireline formation tester surveys have been run in newly-drilled wells (*Stewart and Whaballa*, 1989). Besides mentioning this primary method, *Bradley and Powley* (1994) list a number of other ways the reservoir compartmentalization can be indicated, which are:

- by differing brine and hydrocarbon chemistries;
- by mineralogical differences;
- by electrical resistivity, sonic velocity, and density of shales;
- by mud weight requirements and drilling rate changes.

Also, *Smalley and England* (1994) have proposed a method to assess the behavior of reservoir compartmentalization by analyzing the natural process of fluid mixing. These authors have used the data from reservoir fluid with compositional heterogeneity to get information about how fluids have been able to move through the reservoir over a geologic time scale.

It is important to identify reservoir compartmentalization, if there is any. In the case of detection of an unexpected reservoir compartmentalization later during production, sometimes it becomes essential to drill more wells and build more facilities which could force re-evaluation of the whole development project based on economics. Therefore, it is essential to have as much information about the compartmentalization of a reservoir as possible to avoid any unpleasant surprises in the future. *Smalley and England* (1994) note, for example, that an unexpected detection of the presence of any compartment with a high gas-oil ratio might cause oil production rates to be constrained due to the limited capacity of the gas-handling facilities located at surface.

Massonnet and Bandiziol (1991) emphasize that the geology of a reservoir and the selection of the most suitable solution for well-test interpretation are inter-dependent and that these can complement and improve interpretation of the geology and the well test. According to *Norris et al.* (1993), the results coming from the well-test interpretation contribute to an improvement of the understanding and modeling of the geology. *Mikhailov and Ozisik* (1984) have suggested that analytical solutions, when available, are advantageous in that they provide good insight into the significance of various parameters in the system affecting the transport phenomena, as well as accurate benchmarks for a numerical approach. Along the same line, *Massonnet et al.* (1993) have opined that the

interpretation of transient pressure by the use of analytical models leads to a simplified description of the geological heterogeneities around the well. *Stewart and Whaballa (1989)* prefer the use of analytical solutions for identifying and quantifying major compartments and flow barriers before running a reservoir simulation. *Badgett et al. (1996)* have observed that the production performance of a well is dependent on a number of variables including formation permeability, completion efficiency, reservoir heterogeneities, fluid properties, reservoir pressure and drawdown. These authors also opine that well test analysis provides a means of quantifying these variables allowing for the cause(s) of non-ideal well performance to be identified. *Corapcioglu et al. (1983)* suggested that analytical solutions can sometimes be used as a partial check of numerical solutions for large-scale problems.

The primary objective of this study is to recognize and evaluate the importance of considering the contrasts of rock and fluid properties in a compartmentalized system by using analytical models that are able to provide useful information about such a system. These transient-pressure models for compartmentalized reservoirs are developed analytically in a generalized way. Closed-form solutions are obtained for compartmentalized systems with one-, two- and three-dimensional flow systems. The interface-boundaries between adjoining compartments, due to vertical barriers of low-permeability or partially-communicating faults, are modeled as thin skins. The production rate at each producing well and conditions at the extreme boundaries of the reservoir are considered to be time-dependent to deal with any changing production and changing situations at these boundaries, respectively. An integral-transform technique for finite, composite domains has been used to derive the solutions for dimensionless pressure in terms of dimensionless time and space. The new analytical solutions have been validated by comparing simplified cases with those available in the literature. A number of practical applications of the new model are also discussed.

1.2 Geology of Compartmentalized Reservoirs

Due to geologic processes, most hydrocarbon reservoirs are heterogeneous. Some of the reservoirs are compartmentalized (*Junkin et al.*, 1992). A compartmentalized reservoir is considered to have a number of hydraulically-connected compartments. The interfaces between adjoining compartments are usually partially communicating due to the presence of faults or low-permeability barriers (*Fox et al.*, 1988). According to *Stewart and Whaballa* (1989), the discontinuities in pressure occur over both horizontal events such as shales, micaceous streaks, stylolites etc. and near vertical events such as partially-communicating faults, turbidite lobe interfaces, etc.

Levorsen (1967) mentioned that the extent of a reservoir boundary may be sharp or it may be gradational as is more often the case. This heterogeneous character in a reservoir makes it difficult to model. However, to alleviate the mathematical difficulties of modeling such a system, the concept of compartmentalization may be used. Using this concept, a heterogeneous system is assumed to be comprised of a number of homogeneous compartments. The communication of fluid between adjoining compartments may be hindered due to the presence of faults, permeability pinch-outs or any other flow barriers.

Cant (1982) has opined that fluvial sediments are deposited by activities of rivers and that they are common in geologic record. This author has also mentioned that river sediments are highly variable in many aspects and cannot be characterized by any single facies model. This is so because of the fact that different types of rivers occur in nature and, although a continuous spectrum of river types exists, they can be categorized into discrete types - straight, anastomosing, meandering and sandy or pebbly braided. According to this author, in braided river deposits, lateral migration coupled with aggradation leads to sheet sandstones or conglomerates with thin, impersistent shales enclosed within coarser sediments. Meandering rivers are generally more laterally-stable than braided rivers because they have thicker, more vegetated, cohesive floodplain deposits which are difficult to erode; they occur in areas of lower slope; and they show more regular discharge pattern. These rivers are also confined laterally by abandoned mud-filled meander loops, known as oxbow lakes, which are common on the floodplains of most meandering rivers. *Cant* (1982) also notes that anastomosing rivers have semi-

permanent islands dividing the flow and well developed floodplain and backswamp areas extending away from the river. Because of the coarse-grained nature of fluvial sediments, they may form potentially good reservoir rocks for oil or gas. This author also pointed out that ancient fluvial sediments with up to 30% porosity and thousands of millidarcys permeability have been reported.

Kerr and Jirik (1990) have given a good description of reservoir compartmentalization in the middle Frio (Oligocene) formation, South Texas. This formation is composed of sand-rich channel-fill and splay deposits interstratified with floodplain mudstones, all forming part of the Gueydan fluvial system. Channel-fill and associated splay sandstones are reservoir facies while levee sandy mudstones obstruct flow and separate individual reservoirs and compartments both laterally and vertically. These authors also observe that laterally-stacked sandstone bodies lead to separate but potentially-leaky reservoir compartments while vertically-stacked sandstone bodies favor more isolated reservoir compartments. This means that in situations with vertically-stacked sandstone bodies, there is a high potential for reserve growth through the identification of untapped, poorly drained and by-passed reservoir compartments.

Chilingarian et al. (1992) and *Mazzullo and Chilingarian (1992)* have given an account of geologic and engineering aspects of compartmentalization in carbonate reservoirs and reservoir heterogeneity. These authors have pointed out that reservoir compartmentalization may result not only from vertical and lateral lithofacies changes, but also from spatial variations in those processes of postdepositional diagenesis that have created secondary porosity in the rocks. In a number of reservoirs, the interbedding of originally-permeable and relatively non-permeable rock units is further accentuated by subsequent modifications, or is reversed, such that the originally-impermeable units become porous and permeable, and vice versa.

Bradley and Powley (1994) have presented various aspects of a compartmentalized system. These authors point out that a sealing boundary restricts the flow of both hydrocarbon and brine and is formed where the pore throats become effectively closed

(that is, the permeability approaches zero). However, a hydraulically-communicating boundary occurs when the pressure difference caused by subsidence-sedimentation or uplift-erosion or other pressure sources is greater than the leakage pressure for that seal.

Qin and Ortoleva (1994) review the structure, mechanisms of formation and key role of diagenetically-banded pressure seals. These authors mention that layered rock may make a very efficient barrier to flow normal to the layering plane. If a few layers are of very low permeability, the flow of fluid across the layering is repressed. These authors also point out, as an example, that if 1% of the rock is occupied by 10^{-9} darcy material and the rest is milli-darcy materials, the effective permeability is about 10^{-7} darcy. This shows how the effective permeability is dominated by the presence of a few low-permeability domains. According to *Qin and Ortoleva (1994)*, intense layering can arise through diagenesis even in the absence of appreciable textural contrast from sedimentary bedding or lamination. They also mention that observed layered seals involve hundreds or thousands of individual layers.

Meehan and Verma (1995) have pointed out that the lateral heterogeneities in a reservoir appear to be diagenetic permeability alterations that result in partial compartmentalization of the many individual sands.

1.3 Literature Review

The interfaces between adjoining compartments in a compartmentalized system are usually partially-communicating due to the presence of faults or low-permeability barriers (*Fox et al., 1988*). This kind of compartmentalized behavior becomes prominent in the pressure history at late times when the other hydraulically-connected compartments start contributing. For understanding the long term behavior of a compartmentalized reservoir, it is important to characterize the inter-compartment fluid flow as a function of time. Running a reservoir simulator to understand the behavior of a compartmentalized

reservoir is not a realistic approach before identifying and quantifying the major flow units and barrier resistance (*Stewart and Whaballa, 1989*).

Presently, as described in the literature, a compartmentalized reservoir is analyzed by using models, called tank models, that are based on material balance techniques that ignore reservoir geometry (*Junkin et al., 1992; Fox et al., 1988; Stewart and Whaballa, 1989; Payne, 1996*). The amount of fluid that communicates between any two neighboring compartments is estimated using the difference in average pressures of the compartments. However, the amount of communicating fluid can be estimated more accurately if the reservoir is modeled using transient-pressure responses. The tank models are used to quantify the volumes of each compartment of a reservoir and the barrier transmissibilities through history matching and later to predict the future performance of the reservoir using the already established information.

The mathematical formulation developed by *Fox et al. (1988)* is based on the assumption that the fluid flow between adjoining compartments occurs under steady-state conditions. Therefore, this model can be used when the hydraulic diffusivity is very high so that transient effects dissipate very quickly. An analytical model has been developed by *Stewart and Whaballa (1989)* based on single-phase material balance equations. Here, the concepts of boundary-pressure time delay and desuperposition are used to predict bottom-hole pressures over different flow regimes.

Diagnostic techniques are presented by *Hower and Collins (1989)*, for detecting and quantifying poorly drained compartments, which use material balance equations and a numerical simulator based on the finite element technique. But these techniques are valid only if the reservoir is producing at pseudosteady state because they involve inflow performance relationships.

Lord et al. (1992) show the usefulness of tank models for areal and stacked channel realizations with the help of a simulator as developed by *Kocberber and Collins (1991)*. *Lord et al. (1992)* have observed that the tank models work reasonably well for gas

reservoirs having permeabilities in the range of moderate to high (greater than 5 md). They have also concluded that these tank models are not appropriate for formation permeabilities less than 5 md. Therefore, it is obvious that the above-mentioned criterion will be much more restrictive for oil reservoirs.

Ehlig-Economides (1994) presents the material balance equations due to multi-phase fluid production from a compartmentalized system with both areal and vertical extent. Here she uses the formulation in terms of potential, rather than pressure, with a view to dealing with the importance of gravity in vertical compartmentalization. This author argues that the material balance technique provides an estimation of the volume of fluid in place underground as a means independent of other sources like geophysical and geological analyses.

1.4 Statement of the Problem

From the above literature review, it has been demonstrated that the models available in the literature ignore the shape of the reservoir and the contrasts of rock and fluid properties of a compartmentalized system. This leaves an obvious choice of running a numerical simulator which can be very expensive. Therefore, it is very important to have transient-pressure models that are capable of providing useful information about compartmentalized systems with areal and vertical extent. These analytical models should also be general enough to be applicable to a number of complicated cases of practical interest. Compartmentalization of reservoirs with both areal and vertical extent is evident in the field (*Stewart and Whaballa, 1989; Ehlig-Economides, 1994*). *Stewart and Whaballa* (1989) have shown a cellular system as an example of areally-compartmentalized systems and a stacked channel realization as an example of vertically-compartmentalized systems. In the literature, it is evident that studies on compartmentalized reservoirs ignored the variations of rock and fluid properties and the resistance to fluid flow within compartments. There has been no analytical transient-pressure model available in the literature that could lead to detailed information about rock and fluid properties and its

effect on long-term production performance of a compartmentalized reservoir. Therefore, this study proposes new analytical solutions for transient responses in both areally and vertically compartmentalized systems. Throughout this study, the Cartesian coordinate system is used to formulate the problems. Moreover, for the sake of simplicity, rock and fluid properties in a compartment are considered to be homogeneous. Here, a one-dimensional flow system and also a two-dimensional flow system are considered to simulate areally-compartmentalized reservoirs and a three-dimensional flow system is considered to simulate vertically-compartmentalized reservoirs. For the convenience of analysis, transient-pressure models for compartmentalized reservoirs need to be developed analytically for the following three separate cases:

- one-dimensional flow system,
- two-dimensional flow system, and
- three dimensional flow system.

The model for a one-dimensional flow system is the simplest of the cases considered in this study. This model applies to a situation where the fluid flow in narrow reservoirs or aquifers is predominantly linear. Because of geological processes, the rock and/or fluid properties in these linear systems may be non-uniform. Such systems can be considered as one-dimensional, linear compartmentalized systems.

The model for a two-dimensional compartmentalized system is an extension of that for a linear, one-dimensional flow model. This model is capable of dealing, in a general way, with a compartmentalized system having areal extent. In this case, the flow of fluid in each compartment, neglecting gravity effects, may be described with a two-dimensional, Cartesian coordinate system. A cellular system is an example where this solution is applicable.

In the event of the presence of reservoir compartmentalization in the vertical direction, the models for areal compartmentalization cannot describe the transient-flow situation properly (*Rahman and Ambastha, 1997b*). Therefore, the model for a three-dimensional

compartmentalized system is an extension of and more general than that for a two-dimensional compartmentalized system. This model is capable of dealing with a compartmentalized system of both areal and vertical extent in a general way. In this case, the flow of fluid taking into account the effects of gravity in each compartment may be described with a three-dimensional, Cartesian coordinate system. A system of stacked channels (two sand bodies crossing over each other having hydraulic communication through an interface) is an example where this model is applicable.

1.5 Objectives of the Study

Based on the preceding discussion, the objectives of this study are:

1. To develop analytical solutions for transient pressure (or potential) for compartmentalized reservoirs with areal and vertical extent. These solutions should be capable of dealing with a number of complicated scenarios of reservoir compartmentalization. The new solutions are to be validated by comparing a number of simplified cases with those available in the literature.
2. To find a way to characterize a compartmentalized system in terms of a simple equivalent system like a homogeneous one.
3. To develop the necessary type-curves for the purpose of recognizing and analyzing various aspects of reservoir compartmentalization using well-test data.
4. To develop a method for identifying a compartmentalized reservoir based on recognizing different flow regimes with the use of the derivative analysis.
5. To use extended drawdown analysis for evaluating the parameters of a compartmentalized system.

1.6 Formulation of the Problem

A compartmentalized system is considered to have a number of parallelepiped compartments. Each compartment may have distinct rock and fluid properties and may produce through a number of wells. The pattern of compartments and type of wells dictate how many dimensions need to be considered in the Cartesian coordinate system.

The difference in formulation between areal and vertical systems of compartmentalized reservoirs is due to the fact that the effects of gravity are neglected in areal arrangements of one- and two-dimensional flow systems. In vertical systems, that is, in three-dimensional flow systems, a mathematical formulation with *potential*, as defined by *Hubbert* (1940), rather than with pressure, is developed to take into account the gravity effects of the flowing fluids. This idea is consistent with that of *Ehlig-Economides* (1994).

In two- and three-dimensional flow systems, anisotropy of formation permeability in each compartment is considered. The geometric axes (x and y in a two-dimensional or x , y and z in a three-dimensional system) are parallel to the principal axes of permeability. *Ramey* (1975) developed a method for interference analysis to determine the permeabilities along the principal axes in a two-dimensional system using a set of injection data. However, if in a case where the principal axes of permeability are not along the geometric axes, then the necessary coordinate transformations can be made to have the equivalent system conform to the geometric axes following the method described by *Chao* (1964). According to *Ramey* (1975), many formations, such as channel sands, appear to exhibit anisotropy in horizontal planes. *Lake* (1988) points out that geologic features like crossbedding and shales are responsible for causing high anisotropy of a formation. This author has also shown that heterogeneity is the major source of anisotropy at the large scale. *Streltsova* (1988) has mentioned that massive faulting, for example, can cause such preferential or directional permeability. She also points out that braided stream deposits show highly directional permeability. Since some compartmentalized reservoirs were subject to braided stream deposition in geologic periods (*Malavazos and McDonough*,

1991), it is very likely that these would show directional permeability and the consideration of anisotropy is, therefore, justified. *Link* (1987) observes that the grains oriented in one direction can increase rock permeability parallel to their long axes and reduce it normal to their long axes.

The interface-boundaries between adjoining compartments are due to low-permeability barriers or partially-communicating faults and are modeled as thin skins following the ideas of *van Everdingen* (1953) and *Hurst* (1953). The presence of such a thin skin at an interface is meant to cause an extra pressure-drop due to fluid flow across a low-permeability barrier or partially-communicating fault. However, this extra pressure-drop is directly proportional to the rate of fluid crossing the interface as will be illustrated later in this Section. The representation of the resistance to flow at an interface as a thin skin is a technique commonly used in the literature (*Carslaw and Jaeger*, 1959; *Ambastha and Sageev*, 1987; *Ambastha et al.*, 1989; *Acosta and Ambastha*, 1994). *Stewart et al.* (1984) developed a method for interference-test analysis using a two-dimensional simulator to determine the transmissibility of a partially-communicating fault. *Yaxley* (1987) modeled the communication of fluid through a partially-communicating fault separating two-regions of a composite system in terms of fault permeability and thickness. *Lord et al.* (1992) have adopted the use of transmissibility as a function of barrier dimensions and permeability in their model for compartmentalized reservoirs taking a similar approach of *Yaxley* (1987). But *Kuchuk and Habashy* (1992) mention that this approach exhibits computational difficulties in cases where the permeability of the fault is lower than the permeability of adjoining formations. *Abbaszadeh and Cinco-Ley* (1995) have modeled a partially-communicating fault analytically allowing for linear flow along the fault plane in addition to a pressure-drop across the fault plane during communication of fluid through it. These authors have pointed out that this model is appropriate when the fault-permeability is larger than that of the adjoining formations.

In this study, the skin factor at an interface boundary between adjoining compartments is defined as the dimensionless pressure drop across the interface boundary (boundary skin or thin skin) due to the flow of fluid. However, the mathematical definition of the skin

factor is slightly different in the cases of one-, two- and three-dimensional flow systems because of the distinctness of the pattern of fluid flow in each case. This is illustrated with the corresponding definitions of skin factors as follows:

One-dimensional flow (Figure 1.1):

$$s_{ij} = \frac{k_p h_p [p_j - p_i]_{\partial R_{ij}}}{q_{ij} B_p \mu_p} \dots\dots\dots(1.1)$$

Here, at any elapsed time, the rate of flow, q_{ij} , is constant over the entire interface, ∂R_{ij} , in linear, one-dimensional systems.

Two-dimensional flow (Figure 1.2):

$$s_{ij} = \frac{k_p [p_j - p_i]_{\partial R_{ij}}}{q_{ij}^* B_p \mu_p} \dots\dots\dots(1.2)$$

At any elapsed time, the rate of flow per unit width, q_{ij}^* , is constant along the pay thickness on the interface, ∂R_{ij} .

Three-dimensional flow (Figure 1.3):

$$s_{ij} = \frac{k_p [\Phi_j - \Phi_i]_{\partial R_{ij}}}{q_{ij}^{**} B_p \mu_p X_p} \dots\dots\dots(1.3)$$

Here, at any elapsed time, the rate of flow per unit area, q_{ij}^{**} , is not necessarily constant at any position on the interface, ∂R_{ij} .

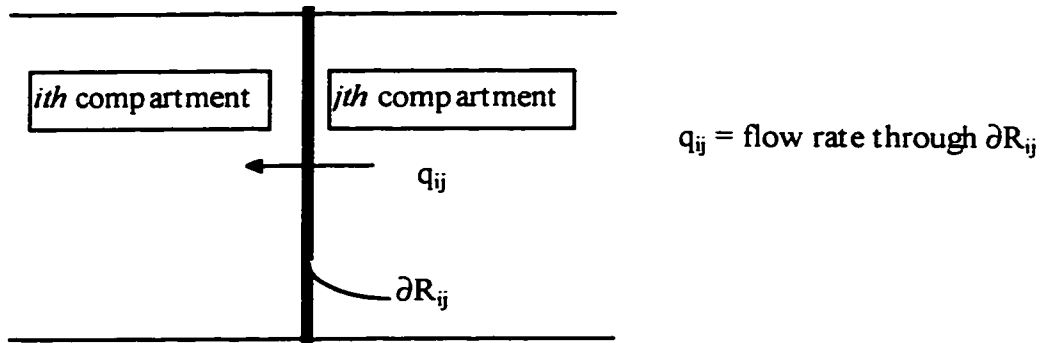


Figure 1.1: Linear, one-dimensional flow system with skin boundary.

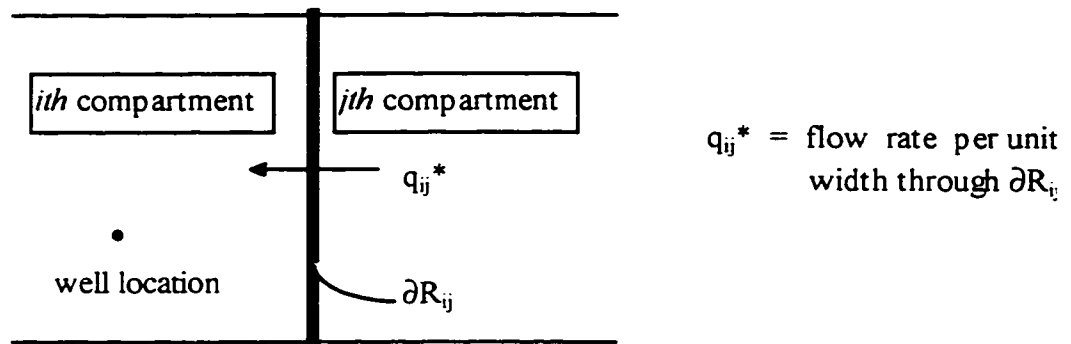


Figure 1.2: Two-dimensional flow system with skin boundary.

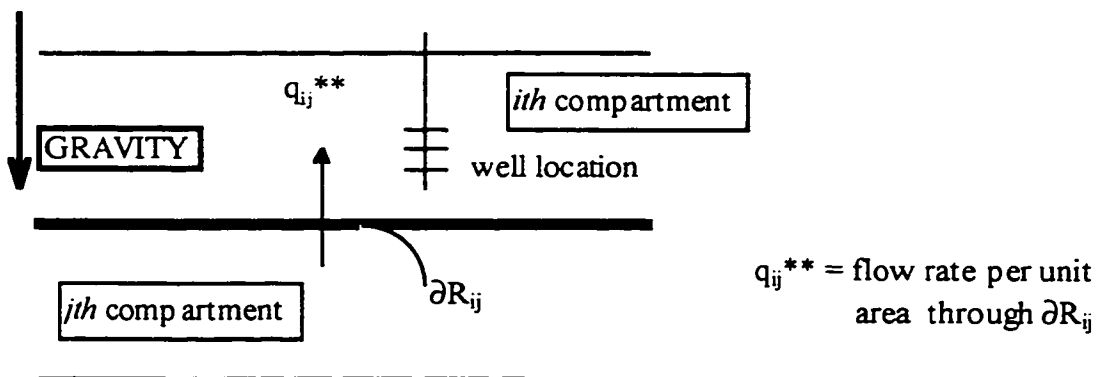


Figure 1.3: Three-dimensional flow system with skin boundary.

In Eqs. (1.1) through (1.3), the subscript, p , indicates reference parameters for rock and fluid properties. The skin factor defined in these equations cannot be negative, because a negative value of skin factor implies flow across an interface in the positive direction of pressure (or potential) gradient, violating a natural principle. This paradox, which arises when a negative skin factor is used, can be observed in the interface conditions presented in Chapters 2, 3 and 4. *Ambastha* (1988) examined a few cases of negative skin factor in radial, composite systems and reported that the corresponding solutions do not converge in those cases.

When the conditions at the extreme boundaries of the reservoir are considered to be time-dependent, Cauchy-type conditions are needed to deal with any changing situations at these boundaries. The non-homogeneous, Cauchy-type boundary conditions can be modified to any form of the boundary conditions that is encountered in the field (*Corapcioglu et al.*, 1983). This means that Cauchy-type boundary conditions can be changed to form Dirichlet-type or Neumann-type boundary conditions as special cases. This type of boundary condition (Cauchy-type) is applicable to confined or phreatic aquifers in contact with a clogged bed (*Bear*, 1972) and also when a linear system communicates hydraulically with an adjoining region through a partially-communicating fault. *Fox et al.* (1988) and *Stewart and Whaballa* (1989) have given a practical example of reservoir compartmentalization where the producing compartment is in hydraulic communication with another compartment of bigger size through a low-permeability barrier. These authors have assumed that the pressure in the bigger compartment remains unchanged during production through a well in the smaller compartment. In this particular example, the Cauchy-type boundary condition is applicable at the interface between the two compartments (*Rahman and Ambastha*, 1997a). However, in this study, the boundary conditions at an interface between a pair of adjoining compartments are meant to ensure continuity of flow rate and discontinuity of pressure (or potential) due to the presence of a thin skin, if there is any. However, continuity of pressure (or potential) at an interface prevails for the case of perfect communication between the compartments (no fault or low-permeability barrier).

Time-dependent situations can arise if the production rate in a well is varying and/or the conditions at a boundary change with time. An example of a changing boundary condition would be a situation where an aquifer that has been providing pressure-support at a boundary due to compaction of aquifer-rock is no longer able to maintain the same level of pressure-support; rather, the pressure support declines with time. Any changing pattern of the production rate from a well or of the condition at a boundary may occur over a period of time, rather than being abrupt. But similar time-dependent situations are taken care of in the literature by the use of the principle of superposition in time (Lee, 1982; Dake, 1994) or Duhamel's theorem (Collins, 1961; Thompson and Reynolds, 1986; Rahman and Ambastha, 1996a; Moser, 1996). In this study, any kind of time-dependent situation is handled through a direct approach that can be highlighted with:

- a production rate as a function of time in the source-term of the corresponding diffusivity equation;
- a Cauchy-type boundary condition as a non-homogeneous and time-dependent one.

A time-dependent changeover can be taken care of with proper formulation. Two such methods are outlined briefly as follows:

A. Linear-Segment Approximation Method

McEdwards (1981), Stewart *et al.* (1983) and Meunier *et al.* (1985) proposed this method for representing a time-dependent production rate. These authors suggest that a time-dependent function be approximated by a series of linear segments connecting the nodes of intervals. For example, a variable production rate, $q(t)$, is approximated by a series of linear segments as illustrated in Fig. 1.4. The rate within the i th interval is mathematically represented as:

$$q(t) = q_{i-1} + \frac{q_i - q_{i-1}}{t_i - t_{i-1}} (t - t_{i-1}) \dots \dots \dots (1.4)$$

where, $t_{i-1} \leq t \leq t_i$.

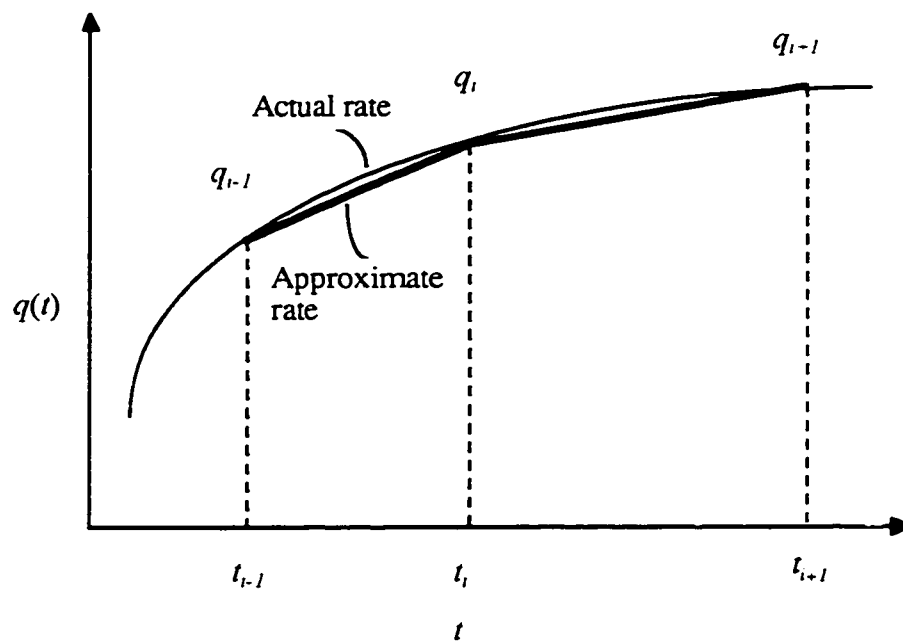


Figure 1.4: Schematic illustrating Linear-Segment Approximation Method.

This method is appropriate and widely used in convolution and deconvolution problems related to afterflow analysis where the production rate at the sand face can be better represented as illustrated above. As modern downhole instruments are capable of measuring flow rates reliably, this method is particularly useful in incorporating variable flow rate data (*Kuchuk and Avestaran, 1985; Mendes et al., 1989*).

B. Heaviside Unit-Step Function Method

The idea of representing a variable (pressure or flow rate) as a stair-step distribution has been used in the Petroleum Engineering literature for a long time. *van Everdingen and Hurst (1949)* and *Horner (1951)* suggested the use of stair-step representation of variable terminal pressures and variable production rates for subsequent use with the principle of superposition. *Odeh and Jones (1965)* and *Jargon and van Poolen (1965)* used this idea in multi-rate well test analysis. Later, *Guillot and Horne (1986)* used this idea in developing computer-based techniques for well-test interpretation using simultaneously measured flow rate and pressure data. *Latinopoulos (1984)* also used a similar approach to solve analytically a groundwater flow problem of recharging for two rates. *Horne (1990)* has suggested that a continuously-varying production rate with time can be dealt with by treating each data point as a small stair-step of constant rate. However, this idea can be extended to any case of time-dependent conditions at the extreme boundaries, including the case of time-dependent pressure at a boundary. When the production rate or extreme boundary condition is represented as a stair-step variation, its mathematical representation becomes very convenient with the use of the Heaviside unit-step function. Figure 1.5 illustrates this idea where it shows a stair-step representation of an arbitrary, time-dependent function, $\psi(t)$. A mathematical expression for $\psi(t)$ being represented as a stair-step function within the domain of t is given by:

$$\psi(t) = \psi_1[H(t - T_1) - H(t - T_2)] + \psi_2[H(t - T_2) - H(t - T_3)] + \psi_3[H(t - T_3) - H(t - T_4)]$$

.....(1.5)

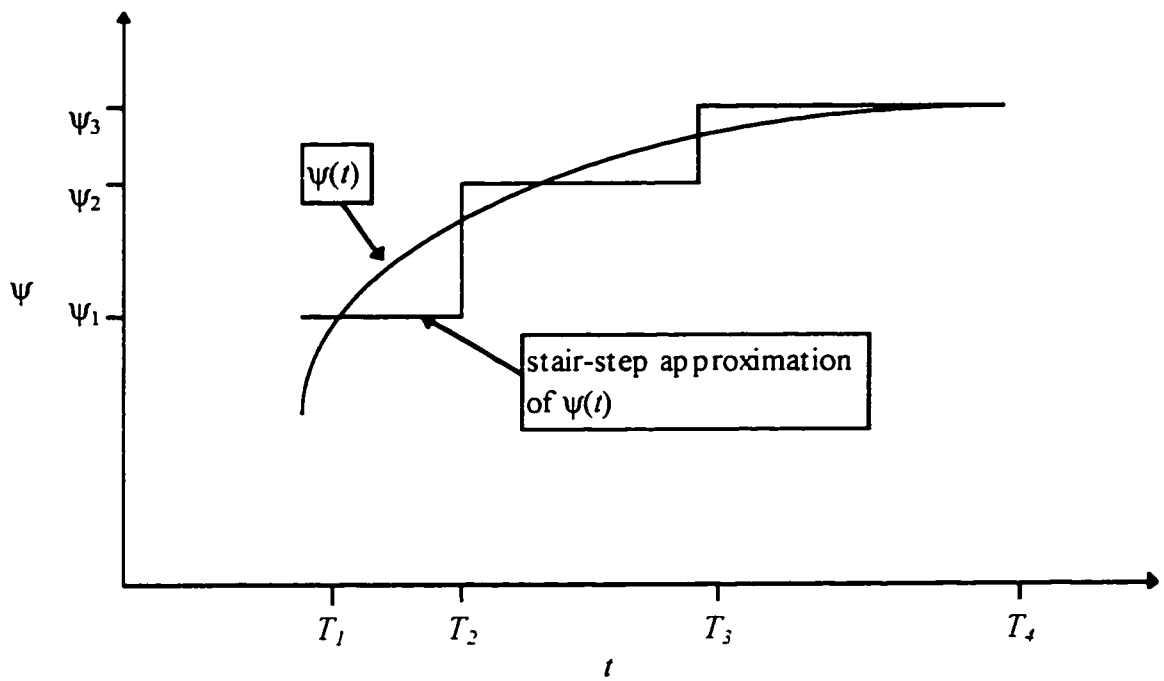


Figure 1.5: Schematic illustrating use of the Heaviside unit-step function.

The subsequent mathematical operations with the above representation is quite straightforward as explained by *Correa and Ramey* (1988).

The mathematical models of this study have been developed in such a way that the production rates and extreme boundary conditions are expressed as general functions of the time variable. Therefore, both of the simplification techniques discussed above are applicable in these models. However, the idea of a Heaviside unit-step function will be used in this study for the purpose of illustrating the use of time-dependent production rates and boundary conditions.

1.7 Solution Methodology

In developing the solutions for transient pressure of compartmentalized reservoirs, an integral-transform technique for finite, composite domains has been used following the theory as developed by *Title* (1965) and *Title and Robinson* (1965). This technique allows the solution to be derived in terms of independent variables (time and space variables) with eigenvalues as parameters. *Lockwood and Mulholland* (1973) argue the superiority of the integral-transform technique over Laplace-transform technique based on the fact that the inversion of Laplace transforms becomes difficult when the number of compartments is more than two. In this study, a closed-form solution is obtained in terms of dimensionless time and space variables with eigenvalues as parameters. *Raghavan* (1993) notes the probable difficulties that are encountered while inverting a solution in Laplace space numerically into real space (for example, the time variable) using *Stehfest's* algorithm (1970). However, the integral-transform technique used in this study has been found to converge rapidly while computing the numerical values of the solutions. *Almeida and Cotta* (1995) have discussed a number of simple applications of the integral-transform technique illustrating examples of steady-state flow and time-dependent diffusion problems. In the groundwater hydrology literature, a number of investigators (*Chan et al.*, 1976; *Case and Peck*, 1977; *Gill*, 1981; *Mustafa*, 1984) used the finite Fourier transforms

for solving the problems of unsteady flow through rectangular, homogeneous porous media. In fact, the Fourier transforms are special cases of the integral transforms for finite domains as used in this study (*Mikhailov, 1997*).

In this study, the governing equations are partial differential equations (diffusivity equations) with specified initial, interface and extreme boundary conditions. An integral-transform technique for finite, composite domains is used to solve these equations. The procedure for this technique is illustrated in Fig. 1.6. This includes the following steps:

1. Development of the integral-transform pair (transformation and inversion formulas) solving the homogeneous version of a given set of partial differential equations (diffusivity equations) and boundary conditions.
2. Integral transformation of the given set of partial differential equations (diffusivity equations) resulting in an initial value problem with dimensionless time as the independent variable.
3. Solution to the initial value problem for the transformed solution.
4. Calculation of the eigenvalues using all the prescribed interface and boundary conditions.
5. Inversion of the transformed solution for dimensionless pressure (or potential) in terms of dimensionless time and space variables.

The details of this procedure will be discussed later while developing solutions for one-, two- and three-dimensional flow systems in Chapters 2, 3 and 4, respectively.

1.8 Summary of the Following Chapters

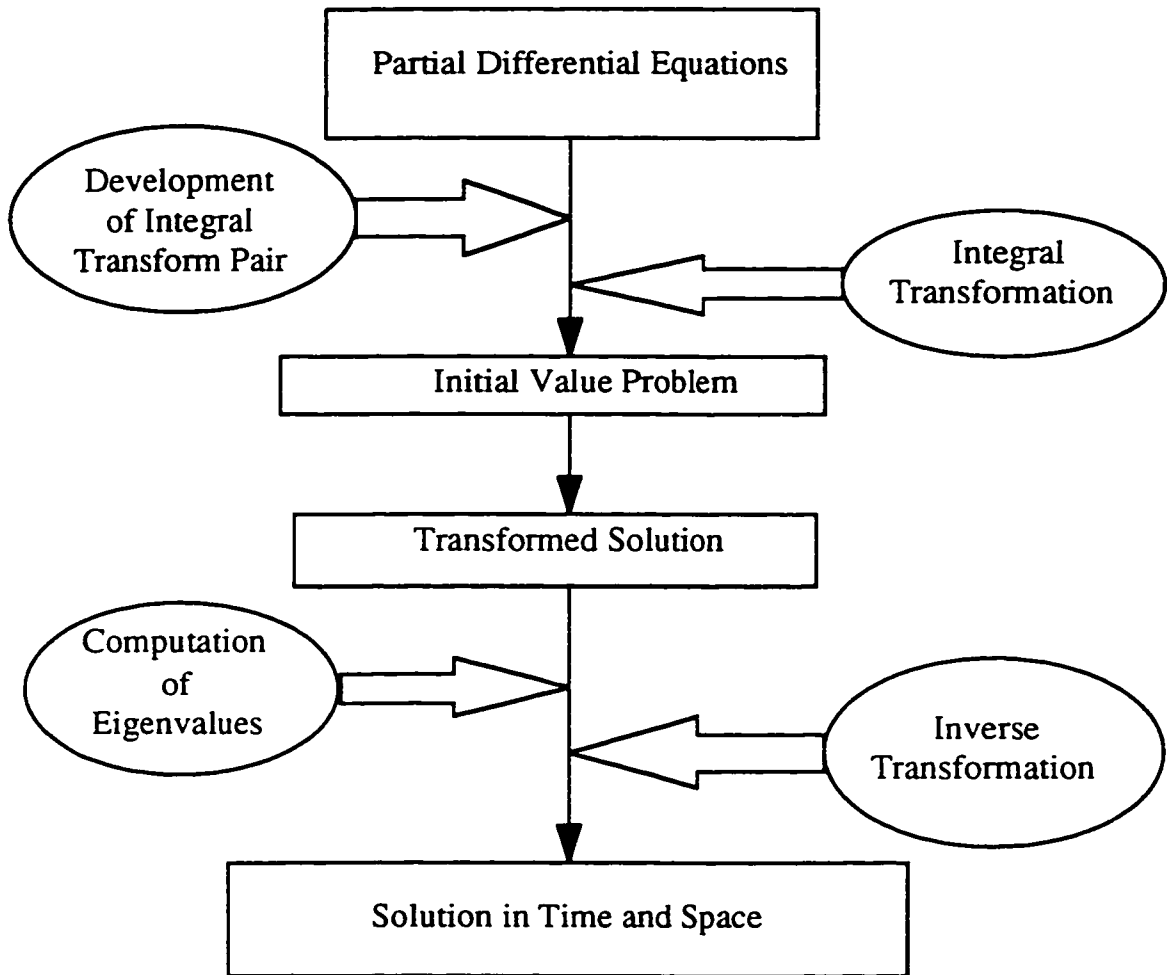


Figure 1.6: Schematic illustrating steps of the integral transform technique for finite, composite domains.

This study has taken a new approach to understand the behavior of a compartmentalized reservoir by modeling the transient fluid flow analytically.

In Chapters 2, 3 and 4, the analytical solutions for transient pressure (or potential) for compartmentalized reservoirs in one-, two-, and three- dimensional flow systems, respectively, are developed and validated by comparing their simplified cases with the solutions available in the literature. Practical applications of these solutions are also discussed. Chapter 5 deals with the interference of wells and proposes a method to unify the effects of all the wells in a compartmentalized system. Also an approach is taken to find an equivalent production rate with respect to a homogeneous system which subsequently leads to the use of the type-curves of homogeneous system for a compartmentalized system. Chapter 6 studies the transient behavior of compartmentalized reservoirs. Different flow regimes have been identified taking advantage of the derivative analysis. A number of compartmentalized systems that are often encountered in the field will be considered. These include a linear system, a system of a small producing compartment in communication with a big one, a two-compartment system and a stacked channel realization. The effects of the contrasts of rock and fluid properties in the compartments and of the presence of the boundary skins at the interfaces between compartments are shown. Where possible, different time criteria to the start or end of different flow regimes and late-time solutions are also presented. Chapter 7 deals with the extended drawdown analysis for compartmentalized reservoirs. Methods are proposed for detecting the poor communication between adjoining compartments and for estimating the hydrocarbon pore-volume in each compartment and the average reservoir pressure. Chapter 8 presents a general discussion, conclusions of the work presented in this study and recommendations for future work.

Computer programs in FORTRAN 77 have been developed to compute the numerical values from the analytical solutions for one-, two- and three-dimensional flow systems. Appendices A, B and C present the respective source codes of these programs. Appendix D presents the analytical solutions for transient potential as a function of dimensionless time and space variables in a rectangular parallelepiped due to production at a constant

rate through a partially-penetrating well. These solutions are used to validate the solutions for the three-dimensional flow system in Chapter 4 and to study the interference of wells in Chapter 5. Appendix E presents a proof of the applicability of the principle of reciprocity with the new solutions of this study.

CHAPTER 2

LINEAR, ONE-DIMENSIONAL FLOW SYSTEM

2.1 Introduction

Flow of fluid through narrow reservoirs or aquifers is predominantly linear. However, this linear-flow system may possess variations in rock and fluid properties and/or faults due to geological phenomena. *Ehlig-Economides* and *Economides* (1985) have pointed out that there are several depositional environments showing possible oil- and gas-reservoir geometries that result in predominantly linear flow. These formations, which generally have long, narrow shapes, may be the result of river meander point bars, oxbow lakes, river channels, or tectonic breccias. However, such systems may also be compartmentalized due to variations of rock and fluid properties and the presence of faults and, therefore, can be modeled as linear, compartmentalized systems.

In the literature, a number of studies of linear, one-dimensional flow systems are related to homogeneous reservoirs or aquifers (*Miller*, 1962; *Nabor and Barham*, 1964; *Bear*, 1972). *Nutakki and Mattar* (1982) generated transient pressure responses using the line-source solution with the principle of superposition for an infinitely long, narrow, homogeneous channel. They also developed a method to determine the time to the end of the radial-flow period and the beginning of the linear-flow period. *Ehlig-Economides* and *Economides* (1985) have presented the techniques for interference, drawdown and buildup analysis for an elongated linear flow system. They also provided an example illustrating the estimation of permeability, porosity, channel width and the extent of the well drainage area from those analyses.

However, few studies on composite systems with or without a linear discontinuity have been reported. *Carslaw and Jaeger* (1959) used the Laplace-transform technique to solve heat transfer problems in composite media. *Bixel et al.* (1963) developed a mathematical

model for a composite system with two regions having a fully-communicating interface with the well located near it.

Ambastha and *Sageev* (1987) obtained an analytical solution using the Laplace-transform technique for a linear, composite system composed of a finite region and an infinite region being separated by a boundary skin. *Poon* and *Chhina* (1989) developed a two-region linear, composite model in the Laplace-space domain for the purpose of investigating the transient-pressure behavior in an in-situ combustion pilot. *Larsen* (1993 and 1996) developed analytical solutions in the Laplace-space domain for systems of intersecting linear reservoirs.

In this Chapter, a linear, compartmentalized system with n parallelepiped compartments is considered (Fig. 2.1). Any irregularity of the size of individual compartments in the transverse direction is acceptable, provided the assumption that this will not affect the linear character of the flow holds. The presence of a thin skin or boundary skin at the interface of adjoining compartments is considered to represent an extra resistance to flow following the ideas of *van Everdingen* (1953) and *Hurst* (1953). The rate of fluid communication between any two neighboring compartments depends on a specified skin factor at the interface. The presence of such a boundary skin at an interface causes a discontinuity in pressure at the interface separating the two neighboring compartments. A detailed illustration of this skin factor has been presented in Section 1.6, Chapter 1.

In this study, the governing partial differential equations with appropriate initial and boundary conditions are set up starting with the diffusivity equations describing the one-dimensional, single-phase flow of a slightly-compressible fluid with constant compressibility through a compartmentalized system. The partial differential equations with initial and boundary conditions are solved using an integral-transform technique for finite domains following the steps of *Mulholland* and *Cobble* (1972) which are based on the theory of *Title* (1965) and *Title* and *Robinson* (1965). The kernel function for this integral transformation is found by solving an eigenvalue problem which has been

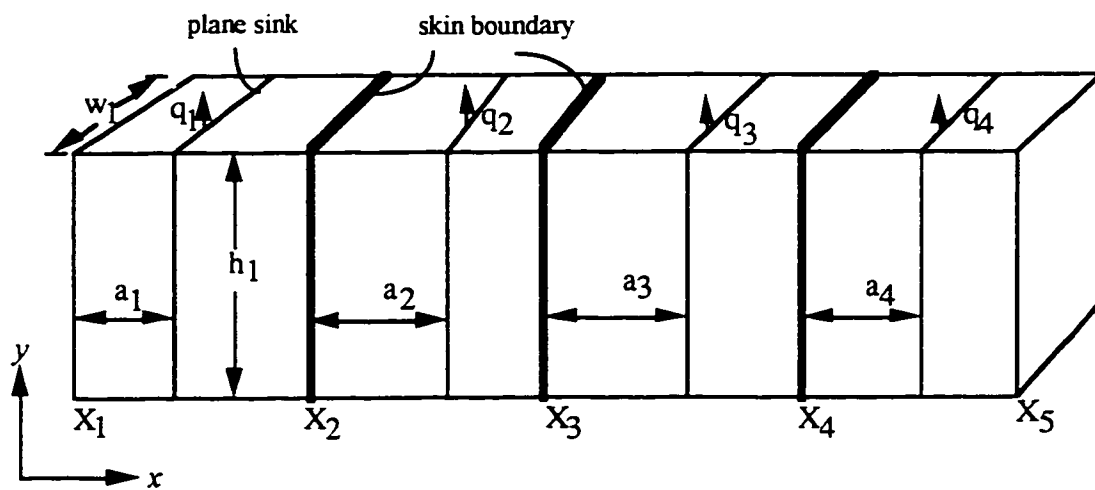


Figure 2.1: Schematic of a linear, compartmentalized system ($n = 4$).

developed from the homogeneous version of the given set of partial differential equations along with the corresponding initial and boundary conditions. An integral-transform technique with respect to the space-variable removes the spatial dependence of the partial differential equations. Thus, a partial differential equation is transformed into an ordinary differential equation with time as the only independent variable and the eigenvalues as the parameters. Non-homogeneous, Cauchy-type boundary conditions at the extreme boundaries are considered which allow for any possible situation of partial communication at those locations. However, these conditions can be modified easily by specifying the Dirichlet-type condition, as in a specified pressure case or by specifying the Neumann-type condition as in a specified rate case. In the following section, this method of solution is illustrated.

2.2 Development of the Analytical Solution

Let us consider a system of n linear compartments. In the following subsections, the solution for transient-pressure responses is developed step by step:

2.2.1 Setting up Governing Differential Equations

A dimensionless form of the diffusivity equation for a single-phase, slightly-compressible fluid with constant compressibility for the m th compartment, producing through a plane-sink, is given by:

$$\frac{\partial^2 p_{mD}}{\partial x_D^2} + \frac{q_{mD}(t_D)}{\alpha_m} \delta(x_D - a_{mD}) = \eta_m \frac{\partial p_{mD}}{\partial t_D} \dots\dots\dots(2.1)$$

where the dimensionless variables are defined as:

$$p_{mD} = \frac{k_p h_p}{q_p \mu_p B_p} (p_p - p_m) \dots\dots\dots(2.2)$$

$$x_D = \frac{x}{X_{n+1}} \dots\dots\dots(2.3)$$

$$a_{mD} = \frac{X_m + a_m}{X_{n+1}} \dots\dots\dots(2.4)$$

$$t_D = \frac{k_p t}{\Phi_p \mu_p c_{tp} X_{n+1}^2} \dots\dots\dots(2.5)$$

$$\eta_m = \frac{\Phi_m \mu_m c_{tm}}{k_m} \frac{k_p}{\Phi_p \mu_p c_{tp}} \dots\dots\dots(2.6)$$

$$\alpha_m = \frac{\mu_p B_p k_m h_m w_m}{\mu_m B_m k_p h_p X_{n+1}} \dots\dots\dots(2.7)$$

$$q_{mD}(t_D) = \frac{q_m(t)}{q_p} \dots\dots\dots(2.8)$$

where the subscript, p , refers to a reference compartment or a reference parameter.

The corresponding dimensionless forms of the initial and boundary conditions associated with Eq. (2.1) are given as follows:

(a) Initial condition:

$$p_{mD}(x_D, 0) = p_{omD} = \frac{k_p h_p}{q_p \mu_p B_p} (p_p - p_{om}) \dots\dots\dots(2.9)$$

(b) Boundary conditions:

(i) at the extreme boundaries

$$\left[\gamma_0 \frac{\partial p_{1D}}{\partial x_D} + \zeta_0 p_{1D} \right]_{x_{1D}} = f_0(t_D) \dots \dots \dots (2.10)$$

$$\left[\gamma_n \frac{\partial p_{nD}}{\partial x_D} + \zeta_n p_{nD} \right]_{x_{n+1D}} = f_n(t_D) \dots \dots \dots (2.11)$$

(ii) at the interfaces

$$u_{i-1} [p_{iD} - p_{i-1D}]_{x_{iD}} = \alpha_{i-1} \left[\frac{\partial p_{i-1D}}{\partial x_D} \right]_{x_{iD}} \dots \dots \dots (2.12)$$

$$\alpha_{i-1} \left[\frac{\partial p_{i-1D}}{\partial x_D} \right]_{x_{iD}} = \alpha_i \left[\frac{\partial p_{iD}}{\partial x_D} \right]_{x_{iD}} \dots \dots \dots (2.13)$$

with

$$u_{i-1} = \frac{l}{s_{i-1}} \dots \dots \dots (2.14)$$

for $i = 2$ to n .

The parameters, γ_0 , ζ_0 , γ_n and ζ_n , in Eqs. (2.10) and (2.11), can be chosen in such a way that these equations would take care of appropriate conditions due to partial communication or the presence of skin at the extreme boundaries. However, these parameters can also be set to either 1 or 0 if the extreme boundary conditions are of the Dirichlet- or of the Neumann-type. Also, the time-dependent functions, $f_0(t_D)$ and $f_n(t_D)$,

in Eqs. (2.10) and (2.11), respectively, allow specification of any time-dependent conditions at the extreme boundaries. However, these functions can be replaced by suitable constant numbers if there is no time-dependent condition existing there. The interface conditions, expressed by Eqs. (2.12) and (2.13), take into account the discontinuity of pressure due to the presence of a skin and also continuity of the amount of fluid crossing an interface between two compartments.

2.2.2 Solving the Differential Equations

The system of differential equations, given by Eq. (2.1), is solved with the set of initial and boundary conditions, Eqs. (2.9) through (2.13), following the steps outlined by *Mulholland and Cobble* (1972). The procedure is explained in the following steps:

(a) Obtaining Homogeneous Conditions at the Extreme Boundaries:

The conditions at the extreme boundaries, given by Eqs. (2.10) and (2.11), are non-homogeneous. However, the system of equations, expressed by Eqs. (2.1) and (2.9) through (2.13), is analytically solvable. *Mikhailov* (1977) mentioned that this system is not always uniformly convergent and needs to be split to obtain uniformly-convergent systems. The following substitution is made into Eqs. (2.1) and (2.9) through (2.13) to make the conditions at the extreme boundaries, given by Eqs. (2.10) and (2.11), homogeneous:

$$p_{mD}(x_D, t_D) = L_{0m}(x_D) f_0(t_D) + L_{nm}(x_D) f_n(t_D) + \Theta_m(x_D, t_D) \dots \dots \dots (2.15)$$

This results in three sets of simpler problems in L_{0m} , L_{nm} and Θ_m that are expressed in Eqs. (2.16), (2.17) and (2.18), respectively, as follows:

$$\frac{d^2 L_{0m}(x_D)}{dx_D^2} = 0 \dots\dots\dots(2.16a)$$

subject to the boundary conditions,

$$\left[\gamma_0 \frac{dL_{01}}{dx_D} + \zeta_0 L_{01} \right]_{x_{1,D}} = 1 \dots\dots\dots(2.16b)$$

$$\left[\gamma_n \frac{dL_{0n}}{dx_D} + \zeta_n L_{0n} \right]_{x_{n+1,D}} = 0 \dots\dots\dots(2.16c)$$

$$u_{i-1} [L_{0i} - L_{0i-1}]_{x_{i,D}} = \alpha_{i-1} \left[\frac{dL_{0i-1}}{dx_D} \right]_{x_{i,D}} \dots\dots\dots(2.16d)$$

$$\alpha_{i-1} \left[\frac{dL_{0i-1}}{dx_D} \right]_{x_{i,D}} = \alpha_i \left[\frac{dL_{0i}}{dx_D} \right]_{x_{i,D}} \dots\dots\dots(2.16e)$$

for $i = 2$ to n .

$$\frac{d^2 L_{nm}(x_D)}{dx_D^2} = 0 \dots\dots\dots(2.17a)$$

subject to the boundary conditions,

$$\left[\gamma_0 \frac{dL_{n1}}{dx_D} + \zeta_0 L_{n1} \right]_{x_{1,D}} = 0 \dots\dots\dots(2.17b)$$

$$\left[\gamma_n \frac{dL_{nn}}{dx_D} + \zeta_n L_{nn} \right]_{x_{n+1,D}} = 1 \dots\dots\dots(2.17c)$$

$$u_{i-1} [L_{n_i} - L_{n_{i-1}}]_{x_{i,D}} = \alpha_{i-1} \left[\frac{dL_{n_{i-1}}}{dx_D} \right]_{x_{i,D}} \dots\dots\dots(2.17d)$$

$$\alpha_{i-1} \left[\frac{dL_{n_{i-1}}}{dx_D} \right]_{x_{i,D}} = \alpha_i \left[\frac{dL_{n_i}}{dx_D} \right]_{x_{i,D}} \dots\dots\dots(2.17e)$$

for $i = 2$ to n .

and

$$\frac{\partial^2 \Theta_m}{\partial x_D^2} + G_m = \eta_m \frac{\partial \Theta_m}{\partial t_D} \dots\dots\dots(2.18a)$$

where,

$$G_m = \frac{1}{\alpha_m} q_{mD}(t_D) \delta(x_D - a_{mD}) - \eta_m [L_{0m}(x_D) \frac{df_0(t_D)}{dt_D} - L_{nm}(x_D) \frac{df_n(t_D)}{dt_D}] \dots\dots\dots(2.18b)$$

subject to the boundary conditions,

$$\left[\gamma_0 \frac{\partial \Theta_l}{\partial x_D} + \zeta_0 \Theta_l \right]_{x_{1,D}} = 0 \dots\dots\dots(2.18c)$$

$$\left[\gamma_n \frac{\partial \Theta_n}{\partial x_D} + \zeta_n \Theta_n \right]_{x_{n+1,D}} = 0 \dots\dots\dots(2.18d)$$

$$u_{i-1} [\Theta_i - \Theta_{i-1}]_{x_{i,D}} = \alpha_{i-1} \left[\frac{\partial \Theta_{i-1}}{\partial x_D} \right]_{x_{i,D}} \dots\dots\dots(2.18e)$$

$$\alpha_{i-1} \left[\frac{\partial \Theta_{i-1}}{\partial x_D} \right]_{x_{i,D}} = \alpha_i \left[\frac{\partial \Theta_i}{\partial x_D} \right]_{x_{i,D}} \dots\dots\dots (2.18f)$$

for $i = 2$ to n .

and the initial condition,

$$\Theta_m(x_D, 0) = p_{omD} - L_{0m}(x_D) f_0(0) - L_{nm}(x_D) f_n(0) \dots\dots\dots (2.18g)$$

The extreme boundary conditions in $\Theta_m(x_D, t_D)$, expressed by Eqs. (2.18c) and (2.18d), are homogeneous. This development has made the system in $\Theta_m(x_D, t_D)$, expressed by Eqs. (2.18a) through (2.18g), simpler than the system in $p_{mD}(x_D, t_D)$, expressed by Eqs. (2.1) and (2.9) through (2.13), from the solution point of view.

(b) Solution of Sets of Equations

Solution of L_{om}

The general solution to Eq. (2.16a) is given by:

$$L_{0m}(x_D) = A_{0m} x_D - B_{0m} \dots\dots\dots (2.19)$$

Substituting Eq. (2.19) into the boundary and interface conditions, given by Eqs. (2.16b) through (2.16e), it follows that,

$$[R_{Lo}] \{S_{Lo}\} = \{W_{Lo}\} \dots\dots\dots (2.20)$$

where,

$$[R_{L0}] = \begin{bmatrix} \gamma_0 + \zeta_0 X_{1D} & \zeta_0 & 0 & 0 & 0 & 0 \\ u_1 X_{2D} - \alpha_1 & -u_1 & X_{2D} u_1 & u_1 & 0 & 0 \\ \alpha_1 & 0 & -\alpha_2 & 0 & 0 & 0 \\ \dots & \dots & \dots & \dots & \dots & \dots \\ \dots & \dots & \dots & \dots & \dots & \dots \\ 0 & 0 & 0 & 0 & \gamma_n + \zeta_n X_{n+1D} & \zeta_n \end{bmatrix} \dots\dots\dots(2.21a)$$

$$\{S_{L0}\}^T = \{A_{01} \ B_{01} \ A_{02} \ B_{02} \ \dots \ \dots \ A_{0n} \ B_{0n}\} \dots\dots\dots(2.21b)$$

$$\{W_{L0}\}^T = \{1 \ 0 \ 0 \ \dots \ \dots \ 0\} \dots\dots\dots(2.21c)$$

The coefficient vector, $\{S_{L0}\}$, is computed from the solution of the linear system of equations, given by Eq. (2.20).

Solution of L_{nm}

The general solution to Eq. (2.17a) is given by:

$$L_{nm}(x_D) = A_{nm} x_D + B_{nm} \dots\dots\dots(2.22)$$

Substituting Eq. (2.22) into the boundary and interface conditions, given by Eqs. (2.17b) through (2.17e), it follows that,

$$[R_{Ln}] \{S_{Ln}\} = \{W_{Ln}\} \dots\dots\dots(2.23)$$

where,

$$[R_{L_n}] = \begin{bmatrix} \gamma_0 + \zeta_0 X_{1D} & \zeta_0 & 0 & 0 & 0 & 0 & 0 \\ -u_1 X_{2D} - \alpha_1 & -u_1 & u_1 X_{2D} & u_1 & 0 & 0 & 0 \\ \alpha_1 & 0 & -\alpha_2 & 0 & 0 & 0 & 0 \\ \dots & \dots & \dots & \dots & \dots & \dots & \dots \\ \dots & \dots & \dots & \dots & \dots & \dots & \dots \\ 0 & 0 & 0 & 0 & \gamma_n + \zeta_n X_{n+1D} & \zeta_n & 0 \end{bmatrix} \dots\dots\dots(2.24a)$$

$$\{S_{L_n}\}^T = \{A_{n1} \quad B_{n1} \quad A_{n2} \quad B_{n2} \quad \dots \quad \dots \quad A_{nn} \quad B_{nn}\} \dots\dots\dots(2.24b)$$

$$\{W_{L_n}\}^T = \{0 \quad 0 \quad 0 \quad \dots \quad \dots \quad I\} \dots\dots\dots(2.24c)$$

The coefficient vector, $\{S_{L_n}\}$, is computed from the solution of the linear system of equations, given by Eq. (2.23).

Solution of Θ_m

The procedure for solving for Θ_m involves the use of an integral-transform technique and will be explained in the following steps:

(i) Development of an integral-transform pair

Let us represent $\Theta_m(x_D, t_D)$, as defined in the region within the *m*th compartment, R_m , in terms of the eigenfunctions, $\psi_m(x_D, \lambda_l)$, in the form as follows:

$$\Theta_m = \sum_{l=1}^{\infty} z_l \psi_{ml} \dots\dots\dots(2.25)$$

The eigenvalue problem corresponding to the set of differential equations, given by Eqs. (2.18a) through (2.18g), is developed upon separating the space and time variables in the homogeneous version of these equations. Therefore, the set of separated equations in terms of the space variable is referred to as the eigenvalue problem with an eigenvalue as a parameter and is given as follows:

$$\frac{d^2 \psi_m}{dx_D^2} = -\eta_m \lambda^2 \psi_m \dots \dots \dots (2.26)$$

with the following boundary conditions:

$$\left[\gamma_0 \frac{\partial \psi_1}{\partial x_D} - \zeta_0 \psi_1 \right]_{x_{1,D}} = 0 \dots \dots \dots (2.27)$$

$$\left[\gamma_n \frac{\partial \psi_n}{\partial x_D} - \zeta_n \psi_n \right]_{x_{n+1,D}} = 0 \dots \dots \dots (2.28)$$

$$u_{i-1} [\psi_i - \psi_{i-1}]_{x_{i,D}} = \alpha_{i-1} \left[\frac{d\psi_{i-1}}{dx_D} \right]_{x_{i,D}} \dots \dots \dots (2.29)$$

$$\alpha_{i-1} \left[\frac{d\psi_{i-1}}{dx_D} \right]_{x_{i,D}} = \alpha_i \left[\frac{d\psi_i}{dx_D} \right]_{x_{i,D}} \dots \dots \dots (2.30)$$

where λ is an eigenvalue and ψ_m is an eigenfunction at the *m*th compartment for $i = 2$ to n . The eigenfunction, ψ_m , of this eigenvalue problem should satisfy the following condition of orthogonality:

$$\sum_{m=1}^n \alpha_m \eta_m \int_{R_m} \psi_{m1} \psi_{m1'} dx_D = \delta_{u'} N_l \dots \dots \dots (2.31)$$

where the norm, N_l , is defined as:

$$N_l = \sum_{m=1}^n \alpha_m \eta_m \int_{R_m} \psi_{m,l}^2 dx_D \dots\dots\dots(2.32)$$

Multiplying both sides of Eq. (2.25) by $\alpha_m \eta_m \psi_{m,l} dx_D$ and integrating over R_m , then summing up the resulting expressions over all the compartments, it follows,

$$\sum_{m=1}^n \alpha_m \eta_m \int_{R_m} \Theta_m \psi_{m,l} dx_D = \sum_{m=1}^n \alpha_m \eta_m \sum_{l=1}^{\bar{m}} \int_{R_m} z_l \psi_{m,l} \psi_{m,l} dx_D \dots\dots\dots(2.33)$$

With Eqs. (2.31), (2.32) and (2.33), it can be shown that,

$$z_l = \frac{l}{N_l} \sum_{m=1}^n \alpha_m \eta_m \int_{R_m} \Theta_m \psi_{m,l} dx_D \dots\dots\dots(2.34)$$

From Eqs. (2.25) and (2.34), one finds,

$$\Theta_m = \sum_{l=1}^{\bar{m}} \left[\frac{l}{N_l} \sum_{m=1}^n \alpha_m \eta_m \int_{R_m} \Theta_m \psi_{m,l} dx_D \right] \psi_{m,l} \dots\dots\dots(2.35)$$

From Eq. (2.35), the integral-transform pair is written as:

Inversion formula:

$$\Theta_m = \sum_{l=1}^{\bar{m}} \frac{\bar{\Theta}_l \psi_{m,l}}{N_l} \dots\dots\dots(2.36)$$

Transformation formula:

$$\bar{\Theta}_l = \sum_{m=1}^n \alpha_m \eta_m \int_{R_m} \Theta_m \Psi_{ml} dx_D \dots\dots\dots(2.37)$$

(ii) Integral transformation of differential equations along with associated conditions

Multiplying both sides of Eq. (2.18a) by $\alpha_m \Psi_{ml} dx_D$ and integrating over R_m , then summing up the resulting expressions over all the compartments, one finds,

$$\sum_{m=1}^n \alpha_m \int_{R_m} \frac{\partial^2 \Theta_m}{\partial x_D^2} \Psi_{ml} dx_D + \sum_{m=1}^n \alpha_m \int_{R_m} G_m(x_D, t_D) \Psi_{ml} dx_D = \sum_{m=1}^n \alpha_m \eta_m \int_{R_m} \frac{\partial \Theta_m}{\partial t_D} \Psi_{ml} dx_D \dots\dots\dots(2.38)$$

The first term in Eq. (2.38) is expanded using Green's theorem, and then the values from Eqs. (2.18c) through (2.18f) and (2.26) through (2.29) are substituted into it. The second term is simplified with the substitution of Eq. (2.18b). Then, Eq. (2.37) is substituted on both sides of the simplified Eq. (2.38) which follows as:

$$-\lambda_l^2 \bar{\Theta}_l - g_l(t_D) = \frac{d\bar{\Theta}_l}{dt_D} \dots\dots\dots(2.39)$$

where,

$$g_l(t_D) = \sum_{m=1}^n \left\{ [\Psi_{ml}]_{a_{mD}} q_{mD}(t_D) - \int_{R_m} \alpha_m \eta_m [L_{0m}(x_D) \frac{df_0(t_D)}{dt_D} + L_{nm}(x_D) \frac{df_n(t_D)}{dt_D}] \Psi_{ml} dx_D \right\} \dots\dots\dots(2.40)$$

Taking the integral transformation of the initial condition, given by Eq. (2.18g), one gets,

$$\bar{\Theta}_l(t_D = 0) = \sum_{m=1}^n \alpha_m \eta_m \int_{R_m} [p_{omD} - L_{om}(x_D) f_o(0) - L_{nm}(x_D) f_n(0)] \Psi_{ml} dx_D \dots\dots\dots(2.41)$$

At this point in time, we have an initial-value problem with an ordinary differential equation, given by Eq. (2.39), and an initial condition, given by Eq. (2.41). The solution to this initial-value problem is given by,

$$\bar{\Theta}_l(t_D) = e^{-\lambda_l^2 t_D} \left[\bar{\Theta}_l(t_D = 0) + \int_0^{t_D} g_l(\tau) e^{\lambda_l^2 \tau} d\tau \right] \dots\dots\dots(2.42)$$

where, τ is a dummy variable and $g_l(\tau)$ is the same as $g_l(t_D)$, defined in Eq. (2.40), except that t_D is replaced by τ . $\bar{\Theta}_l$ in Eq. (2.42) is inverted into $\Theta_m(x_D, t_D)$ with the inversion formula, given by Eq. (2.36), as follows:

$$\Theta_m = \sum_{l=1}^{\infty} \left[\bar{\Theta}_l(t_D = 0) + \int_0^{t_D} g_l(\tau) e^{\lambda_l^2 \tau} d\tau \right] \frac{\Psi_{ml} e^{-\lambda_l^2 t_D}}{N_l} \dots\dots\dots(2.43)$$

(iii) Computation of eigenvalues and eigenfunctions

The general solution to Eq. (2.26) for the l th eigenvalue is given by (Mikhailov and Vulchanov, 1983; Cotta, 1993),

$$\Psi_{ml} = \Psi_{ml}^* U_{ml} + \Psi_{ml}^{\bullet} V_{ml} \dots\dots\dots(2.44)$$

where,

$$U_{ml}(\lambda_l, x_D) = \frac{\sin(\sqrt{\eta_m} \lambda_l (X_{m+1D} - x_D))}{\sin(\sqrt{\eta_m} \lambda_l (X_{m+1D} - X_{mD}))} \dots\dots\dots(2.45a)$$

$$V_{m_l}(\lambda_l, x_D) = \frac{\sin(\sqrt{\eta_m} \lambda_l (x_D - X_{mD}))}{\sin(\sqrt{\eta_m} \lambda_l (X_{m+1D} - X_{mD}))} \dots\dots\dots (2.45b)$$

Equations (2.44), (2.45a) and (2.45b) have been set up in such a way that $\psi_{m_l}^{\bullet}$ and $\psi_{m_l}^{\bullet\bullet}$ represent the values of ψ_{m_l} at X_{mD} and X_{m-1D} , respectively. The derivative of both sides of Eq. (2.44) with respect to x_D is written as:

$$\frac{d\psi_{m_l}}{dx_D} = \psi_{m_l}^{\bullet} P_{m_l} + \psi_{m_l}^{\bullet\bullet} T_{m_l} \dots\dots\dots (2.46)$$

where,

$$P_{m_l}(\lambda_l, x_D) = - \frac{\sqrt{\eta_m} \lambda_l \cos(\sqrt{\eta_m} \lambda_l (X_{m+1D} - x_D))}{\sin(\sqrt{\eta_m} \lambda_l (X_{m+1D} - X_{mD}))} \dots\dots\dots (2.47a)$$

$$T_{m_l}(\lambda_l, x_D) = \frac{\sqrt{\eta_m} \lambda_l \cos(\sqrt{\eta_m} \lambda_l (x_D - X_{mD}))}{\sin(\sqrt{\eta_m} \lambda_l (X_{m+1D} - X_{mD}))} \dots\dots\dots (2.47b)$$

Substitution of Eqs. (2.44) and (2.46) in the boundary conditions, expressed by Eqs. (2.26) through (2.29), results in a system of homogeneous, linear equations in $\psi_{m_l}^{\bullet}$ and $\psi_{m_l}^{\bullet\bullet}$. This system of equations is written in matrix notation as:

$$[D] \{Y\} = \{0\} \dots\dots\dots (2.48)$$

where,

$$[D] = \begin{bmatrix} D(1, 1) & D(1, 2) & 0 & 0 & 0 & 0 \\ D(2, 1) & D(2, 2) & D(2, 3) & D(2, 4) & 0 & 0 \\ D(3, 1) & D(3, 2) & D(3, 3) & D(3, 4) & 0 & 0 \\ \dots & \dots & \dots & \dots & \dots & \dots \\ & & & & D(2n, 2n-1) & D(2n, 2n) \end{bmatrix} \dots (2.49a)$$

with

$$D(1, 1) = \zeta_0 + \gamma_0 P_{11}(\lambda_1, X_{1D}) \dots (2.49b)$$

$$D(1, 2) = \gamma_0 T_{11}(\lambda_1, X_{1D}) \dots (2.49c)$$

$$D(2, 1) = -\alpha_1 P_{11}(\lambda_1, X_{2D}) \dots (2.49d)$$

$$D(2, 2) = -u_1 - \alpha_1 T_{11}(\lambda_1, X_{2D}) \dots (2.49e)$$

$$D(2, 3) = u_1 \dots (2.49f)$$

$$D(2, 4) = 0 \dots (2.49g)$$

$$D(3, 1) = \alpha_1 P_{21}(\lambda_1, X_{2D}) \dots (2.49h)$$

$$D(3, 2) = \alpha_1 T_{21}(\lambda_1, X_{2D}) \dots (2.49i)$$

$$D(3, 3) = -\alpha_2 P_{21}(\lambda_1, X_{2D}) \dots (2.49j)$$

$$D(3, \neq) = -\alpha_2 T_{2l}(\lambda_l, X_{2D}) \dots \dots \dots (2.49k)$$

$$D(2n, 2n - 1) = \gamma_n P_{nl}(\lambda_l, X_{n+1D}) \dots \dots \dots (2.49l)$$

$$D(2n, 2n) = \zeta_n + \gamma_n T_{nl}(\lambda_l, X_{n+1D}) \dots \dots \dots (2.49m)$$

$$\{Y\}^T = \{\psi_{1l}^{\cdot} \ \psi_{1l}^{\bar{\cdot}} \ \psi_{2l}^{\cdot} \ \psi_{2l}^{\bar{\cdot}} \ \dots \ \psi_{2nl}^{\cdot} \ \psi_{2nl}^{\bar{\cdot}}\} \dots \dots \dots (2.49n)$$

and $\{0\}$ is a $(2n \times 1)$ -null vector.

To get a nontrivial set of the coefficients, ψ_{ml}^{\cdot} and $\psi_{ml}^{\bar{\cdot}}$, the corresponding coefficient matrix, described by Eq. (2.49a), has to be singular. That means,

$$|D| = 0 \dots \dots \dots (2.50)$$

Equation (2.50) results in a transcendental equation which can be solved for positive eigenvalues, λ_l , by a suitable method. However, in this study, the modified regula falsi method has been used to get a good estimation of the eigenvalues which are later used as an initial guess to compute the corresponding eigenvalues with more accuracy using Newton's method (Borse, 1985). The number of eigenvalues to be calculated is dependent on the desired level of accuracy of the computed solution. Then, with each of these eigenvalues, the system of homogeneous, linear equation, given by Eq. (2.48), is solved for the coefficient vector, $\{Y\}$. From these known coefficients, the eigenfunctions are computed from Eq. (2.44).

Substituting Eqs. (2.19), (2.22) and (2.42) in Eq. (2.15), the expression for dimensionless pressure at the m th compartment takes the form as follows:

$$\begin{aligned}
p_{mD}(x_D, t_D) = & [A_{0m}x_D + B_{0m}] f_0(t_D) + [A_{nm}x_D + B_{nm}] f_n(t_D) + \sum_{l=1}^{\infty} [\bar{\Theta}_l(t_D = 0) \\
& + \int_0^{t_D} g_l(\tau) e^{\lambda_l \tau} d\tau] \frac{\Psi_{ml} e^{-\lambda_l t_D}}{N_l} \dots\dots\dots(2.51)
\end{aligned}$$

2.2.3 Summary of the Solution Procedure

The following is a summary of the solution procedure:

- (i) Solve for the coefficient vectors, $\{S_{L0}\}$ and $\{S_{Ln}\}$ from Eqs. (2.20) and (2.23), respectively. Thus, the coefficients, A_{0m} , B_{0m} , A_{nm} and B_{nm} , become known;
- (ii) Determine the first available positive eigenvalue, λ_1 , from the transcendental equation (2.50);
- (iii) Determine the coefficient vector, $\{Y\}$, from Eq. (2.48) and the norm from Eq. (2.31) corresponding to a calculated eigenvalue;
- (iv) For a given set of x_D and t_D , evaluate p_{mD} (or its derivative as the case may be) from Eq. (2.51);
- (v) Determine higher positive eigenvalues from Eq. (2.50) and include their resulting contributions to p_{mD} (or its derivative) in Eq. (2.51) following steps (iii) and (iv). Also keep comparing the contribution to p_{mD} (or its derivative) due to each additional eigenvalue with the desired level of accuracy;
- (vi) When the desired level of accuracy is met, stop calculating eigenvalue and report the value of p_{mD} (or its derivative).

2.2.4 Computer Program for Numerical Values

A computer program incorporating the solution scheme described in Section 2.2.3 has been developed in FORTRAN 77 for the purpose of generating numerical values from the solution developed in this Chapter. The complete source code and a sample data file are

presented in Appendix A. This program has a number of Subroutines and Subroutine-Subfunctions which are coordinated by the Main Program. Typically, it takes less than 30 seconds to run the program for a 4-compartment system in the "Numerical Server" (RS/6000 Model 59Hs, 66.7 MHz) at the University of Alberta.

2.2.5 Determination of Cumulative Flux at an Interface

The dimensionless influx rate, $q''_{i,D}$ at the i th interface, between two compartments as a function of t_D can be evaluated by substituting Eq. (2.51) into Darcy's equation for one-dimensional, linear flow through porous media. It follows as:

$$q''_{i,D}(t_D) = -\alpha_i [A_{o,i} f_o(t_D) - A_{n,i} f_n(t_D) + \sum_{l=i}^{\infty} \frac{[\bar{\Theta}_l(t_D = 0) - \int_0^{t_D} g_l(\tau) e^{\lambda_i \tau} d\tau] \left[\frac{d\psi_{i,l}}{dx_D} \right]_{x_{i,D}} e^{-\lambda_i^2 t_D}}{N_l}] \quad (2.52)$$

The dimensionless cumulative influx, $Q_{c,i,D}(t_D)$, over a dimensionless period of t_D is given by,

$$Q_{c,i,D}(t_D) = \int_0^{t_D} q''_{i,D}(\tau) d\tau \quad (2.53)$$

Substituting the value of $q''_{i,D}(\tau)$ from Eq. (2.52) into Eq. (2.53) and evaluating the integral, one gets,

$$Q_{c,i,D}(t_D) = -\alpha_i \left[\int_0^{t_D} \{A_{o,i} f_o(\tau) + A_{n,i} f_n(\tau)\} d\tau + \sum_{l=i}^{\infty} \frac{\left[\frac{d\psi_{i,l}}{dx_D} \right]_{x_{i,D}}}{\lambda_l^2 N_l} \left\{ \bar{\Theta}_l(t_D = 0) (1 - e^{-\lambda_l^2 t_D}) + \int_0^{t_D} g_l(\tau) d\tau - e^{-\lambda_l^2 t_D} \int_0^{t_D} g_l(\tau) e^{\lambda_l \tau} d\tau \right\} \right] \quad (2.54)$$

2.2.6 Special Cases

The general solution for dimensionless pressure, given by Eq. (2.51), needs modification for some particular cases. These are discussed below:

(a) Neumann-type Boundary Conditions:

Ozisik (1980) mentions that when the conditions at both extreme boundaries are of the Neumann-type, $\lambda_0 = 0$ is also an eigenvalue. This kind of situation would arise when both extreme boundaries are closed or when one boundary is closed and the other is producing at a specified rate. In this case, we have, $\zeta_0 = \zeta_n = 0$. But the expression for Θ_m in Eq. (2.43) is valid for positive, non-zero eigenvalues. Therefore, Equation (2.43) needs to include an additional term due to the zero-eigenvalue. The zero-eigenvalue corresponds to an eigenfunction, ψ_{m0} , which is equal to E_m , a non-zero constant.

Multiplying both sides of Eq. (2.18a) by $\alpha_m E_m dx_D$ and integrating over R_m , then summing up the resulting expressions over all the compartments, one finds,

$$\sum_{m=1}^n \alpha_m \int_{R_m} \frac{\partial^2 \Theta_m}{\partial x_D^2} E_m dx_D + \sum_{m=1}^n \alpha_m \int_{R_m} E_m G_m dx_D = \sum_{m=1}^n \alpha_m \eta_m \int_{R_m} \frac{\partial \Theta_m}{\partial t_D} E_m dx_D \dots\dots\dots(2.55)$$

Substitution of the values from Eqs. (2.18c) through (2.18f), (2.26) through (2.29) and (2.37) in an expanded form of Eq. (2.53) results in an ordinary differential equation. The initial condition to this ordinary differential equation is set up by taking the integral transformation of the initial condition, given by Eq. (2.18g). The solution to this initial-value problem is given by,

$$\bar{\Theta}_o(t_D) = \bar{\Theta}_o(t_D = 0) + \int_0^{t_D} g_o(\tau) d\tau \dots\dots\dots(2.56)$$

where,

$$\bar{\Theta}_o(t_D = 0) = \sum_{m=1}^n \alpha_m \eta_m \int_{R_m} E_m [p_{omD} - L_{om}(x_D) f_o(0) - L_{nm}(x_D) f_n(0)] dx_D \dots\dots\dots(2.57)$$

$$g_o(\tau) = \sum_{m=1}^n \{q_{mD}(\tau) E_m - \int_{R_m} \alpha_m \eta_m [L_{om}(x_D) \frac{df_o(\tau)}{d\tau} + L_{nm}(x_D) \frac{df_n(\tau)}{d\tau}] E_m dx_D\} \dots\dots\dots(2.58)$$

Therefore, a final form of Θ_m that includes the zero-eigenvalue condition becomes,

$$\Theta_m = \frac{I}{N_o} \left[\bar{\Theta}_o(t_D = 0) + \int_0^{t_D} g_o(\tau) d\tau \right] + \sum_{l=1}^m \frac{\Psi_{ml} e^{-\lambda_l t_D}}{N_l} \left[\bar{\Theta}_l(t_D = 0) + \int_0^{t_D} g_l(\tau) d\tau \right] \dots\dots\dots(2.59)$$

where,

$$N_o = \sum_{m=1}^n \alpha_m \eta_m \int_{R_m} dx_D \dots\dots\dots(2.60)$$

$$\bar{\Theta}_o(t_D = 0) = \sum_{m=1}^n \alpha_m \int_{R_m} [p_{omD} - L_{om}(x_D) f_o(0) - L_{nm}(x_D) f_n(0)] dx_D \dots\dots\dots(2.61)$$

$$g_o(\tau) = \sum_{m=1}^n \left\{ q_{mD}(\tau) - \int_{R_m} \alpha_m \eta_m [L_{om}(x_D) \frac{df_o(\tau)}{d\tau} + L_{nm}(x_D) \frac{df_n(\tau)}{d\tau}] dx_D \right\} \dots\dots\dots(2.62)$$

The evaluation of the integral in Eqs. (2.43) and (2.59) requires prior knowledge of the functional dependence of q_m on t (that is, q_{mD} on t_D). *Horne* (1990) suggested that a continuously varying flow rate can be dealt with by treating each data point as a small

stair-step of constant rate. However, this idea can be extended to any other time-dependent extreme boundary conditions including time-dependent pressure at a boundary. Mathematically, this stair-step variation of a variable can be treated conveniently when represented by a Heaviside unit-step function as illustrated in Section 1.6, Chapter 1.

(b) Perfect Communication at an Interface:

In the absence of a skin at the *i*th interface, the adjoining compartments become perfectly communicating. Thus, we should consider the limiting condition as $s_i \rightarrow 0$. This modifies the interface boundary conditions, given by Eqs. (2.12) and (2.13), to the following form:

$$[p_{i,D}]_{x_{i,D}} = [p_{i-1,D}]_{x_{i,D}} \dots\dots\dots(2.63a)$$

and

$$\alpha_{i-1} \left[\frac{\partial p_{i-1,D}}{\partial x_D} \right]_{x_{i,D}} = \alpha_i \left[\frac{\partial p_{i,D}}{\partial x_D} \right]_{x_{i,D}} \dots\dots\dots(2.63b)$$

This also changes the other equations related to interface conditions. Thus,

Equations (2.16d) and (2.16e) are modified to:

$$[L_{0,i-1}]_{x_{i,D}} = [L_{0,i}]_{x_{i,D}} \dots\dots\dots(2.64a)$$

and

$$\alpha_{i-1} \left[\frac{dL_{0,i-1}}{dx_D} \right]_{x_{i,D}} = \alpha_i \left[\frac{dL_{0,i}}{dx_D} \right]_{x_{i,D}} \dots\dots\dots(2.64b)$$

Equations (2.17d) and (2.17e) are modified to:

$$[L_{n,i-l}]_{X_i,D} = [L_{n,i}]_{X_i,D} \dots\dots\dots(2.65a)$$

and

$$\alpha_{i-l} \left[\frac{dL_{n,i-l}}{dx_D} \right]_{X_i,D} = \alpha_i \left[\frac{dL_{n,i}}{dx_D} \right]_{X_i,D} \dots\dots\dots(2.65b)$$

Equations (2.18e) and (2.18f) are modified to:

$$[\Theta_i]_{X_i,D} = [\Theta_{i-l}]_{X_i,D} \dots\dots\dots(2.66a)$$

and

$$\alpha_{i-l} \left[\frac{\partial \Theta_{i-l}}{\partial x_D} \right]_{X_i,D} = \alpha_i \left[\frac{\partial \Theta_i}{\partial x_D} \right]_{X_i,D} \dots\dots\dots(2.66b)$$

and Equations (2.29) and (2.30) are modified to:

$$[\Psi_{i-l}]_{X_i,D} = [\Psi_i]_{X_i,D} \dots\dots\dots(2.67a)$$

and

$$\alpha_{i-l} \left[\frac{d\Psi_{i-l}}{dx_D} \right]_{X_i,D} = \alpha_i \left[\frac{d\Psi_i}{dx_D} \right]_{X_i,D} \dots\dots\dots(2.67b)$$

Accommodating the above changes into the solution would simulate the situation of no skin at an interface.

(c) Presence of a Non-communicating Fault at an Interface:

If there is a non-communicating fault present at an interface, we take the limit as $s_j \rightarrow \infty$ in the interface conditions. Hence, the condition at the i th interface, given by Eq. (2.13) takes the following form:

$$\left[\frac{\partial p_{i-1,D}}{\partial x_D} \right]_{x_{i,D}} = \left[\frac{\partial p_{i,D}}{\partial x_D} \right]_{x_{i,D}} = 0 \dots\dots\dots (2.68)$$

The above condition forces the corresponding interface conditions in L_{0i} , L_{ni} , Θ_i and ψ_i to change into homogeneous, Neumann-type conditions. Accommodating the above changes into the solution would simulate the situation of a non-communicating fault at an interface.

2.3 Validation of New Solution

The new analytical solution developed in this study has been validated by comparing the transient data for homogeneous and composite systems with those generated from the solutions available in the literature. In all the solutions generated in this study, each compartment has been assumed to have a distinct and uniform initial pressure. The dimensions of each compartment along the planes perpendicular to the direction of flow have been considered uniform. Also the dimensionless parameters are based on the first compartment as the reference compartment, and the initial pressure as the reference pressure (p_p). In all cases of model validation, the inner boundary is located at $x_D = 0$ and the outer boundary is located at $x_D = 1$. Transient data for a homogeneous system from the new solution have been generated by considering identical rock and fluid properties in each compartment of a compartmentalized system. Time-dependent, stair-step varying

conditions are considered in this solution using the Heaviside unit-step function following the approach illustrated in Section 1.6, Chapter 1.

Figure 2.2 illustrates a comparison of the solution of this study with that of *Nabor and Barham* (1964) for a homogeneous system with no skin present at the interfaces. An excellent match for a two-rate flow condition at the inner boundary and a closed outer boundary has been obtained. The *Nabor and Barham* (1964) solution was used in conjunction with the application of the principle of superposition to deal with this variable rate situation.

Figure 2.3 shows a comparison of dimensionless cumulative influx due to a constant, dimensionless pressure at the inner boundary while the outer boundary is closed for a homogeneous system with no skin at the interfaces. The definition of dimensionless pressure used in this study has been modified to the following form to have it comparable with that of *Nabor and Barham* (1964) for the case of a constant pressure at the inner boundary:

$$p_D(x_D, t_D) = \frac{p_{om} - p_m(x, t)}{p_{om} - p_i(0, t)} \dots\dots\dots(2.69)$$

where, $p_i(0, t)$ is the pressure maintained at the inner boundary for $t > 0$. For this particular case, the definition for dimensionless cumulative influx, Q_{cD} , at the inner boundary, $x_D = 0$, becomes,

$$Q_{cD} = \frac{Q_c}{w_p h_p \phi_p c_{tp} X_{\pi-1}} \dots\dots\dots(2.70)$$

where Q_c is defined in the same way as Q_{cm} in the Nomenclature. The above definition is used for both the new solution and that of *Nabor and Barham* (1964). The comparison in Fig. 2.3 also shows an excellent match.

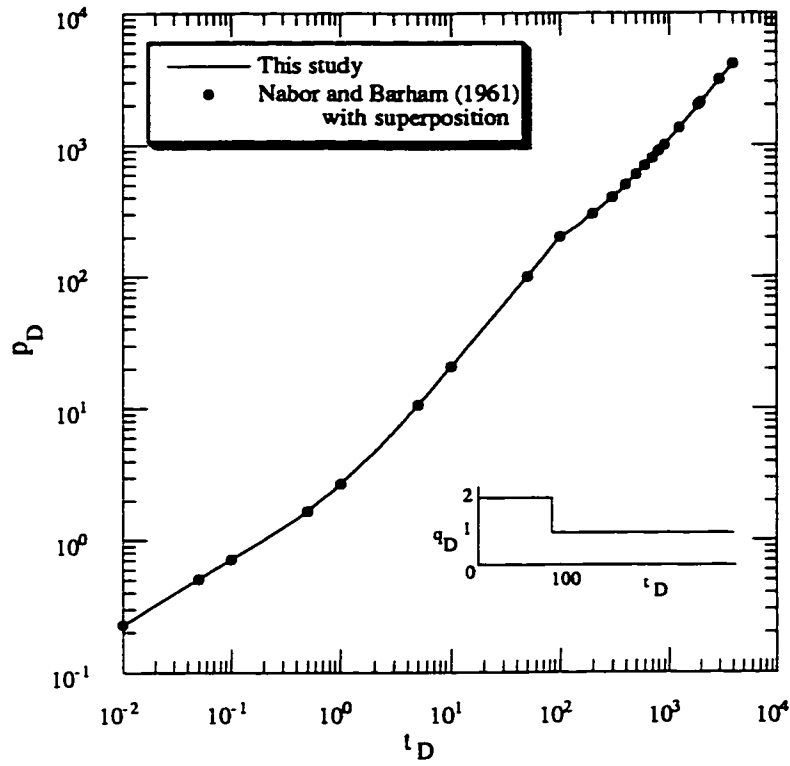


Figure 2.2: Two-rate flow condition at the inner boundary and closed outer boundary in a homogeneous system.

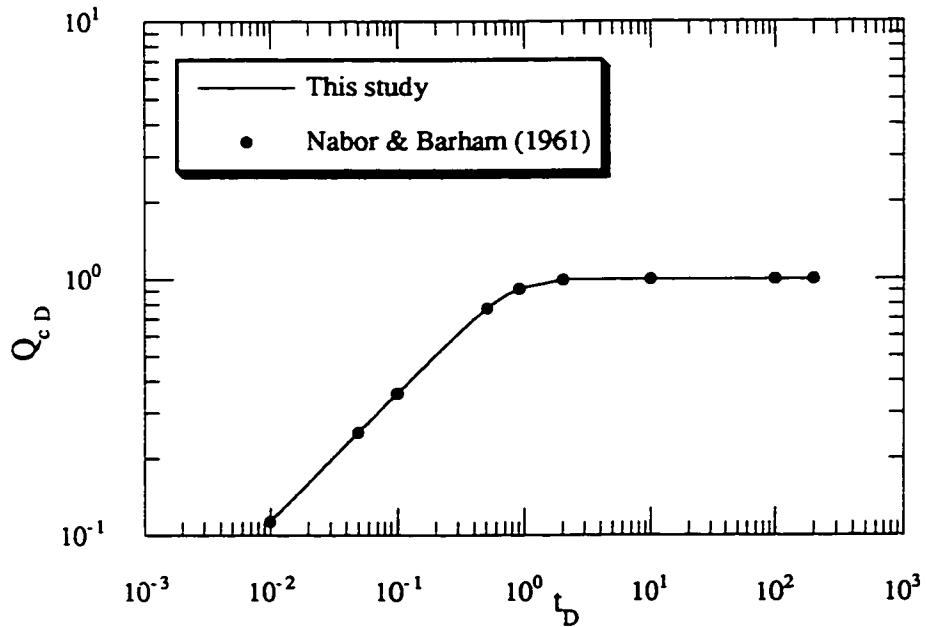


Figure 2.3: Comparison of dimensionless cumulative influx at the constant pressure inner boundary while the outer boundary is closed.

Figure 2.4 shows a comparison of buildup behavior of a homogeneous system with no skin at the interfaces. In this case, a period of production is followed by a shut-in period while the outer boundary is maintained at a constant, dimensionless pressure. This also shows an excellent match of the data from *Nabor and Barham* (1964) with the data from the new solution. As before, the solution of *Nabor and Barham* (1964) has been used with the application of the principle of superposition.

Figures 2.5 and 2.6 show comparisons of the solution from this study with that of a modified form of the work of *Ambastha and Sageev* (1987). The solution of this study belongs to the case of constant dimensionless-rate production at the inner boundary and constant dimensionless-pressure at the outer boundary. The solution of *Ambastha and Sageev* (1987) has been modified to consider the outer boundary at a finite distance and to keep this at a constant pressure. Figure 2.5 shows the transient-pressure responses for a homogeneous, two-compartment system with a skin boundary located at $x_D = 0.1$ for skin-factors, $s_l = 100, 1000$ and 10000 . This shows an excellent match. Figure 2.6 compares the dimensionless transient-pressure responses for a two-region, composite system with a skin boundary located at $x_D = 0.1$ for skin-factors, $s_l = 100, 1000$ and 10000 . Two distinct mobility ratios, $M_1 = 1$ and $M_2 = 5$ have been used for the two regions. Each of these comparisons also shows an excellent match.

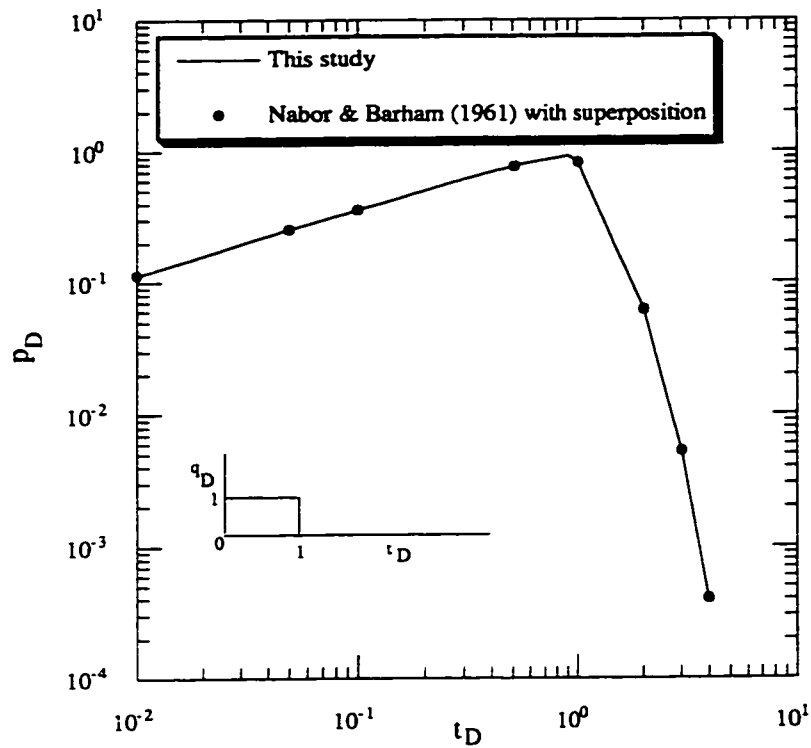


Figure 2.4: Shut-in followed by production at the inner boundary and constant pressure at the outer boundary.

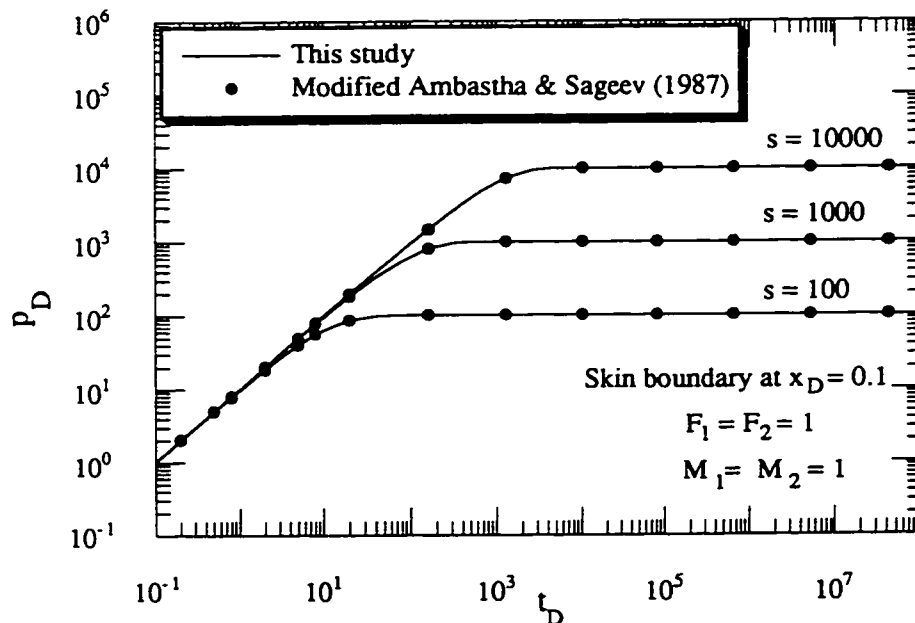


Figure 2.5: Comparison of the dimensionless pressure at the producing boundary of a homogeneous system with the modified solution of Ambastha and Sageev (1987).

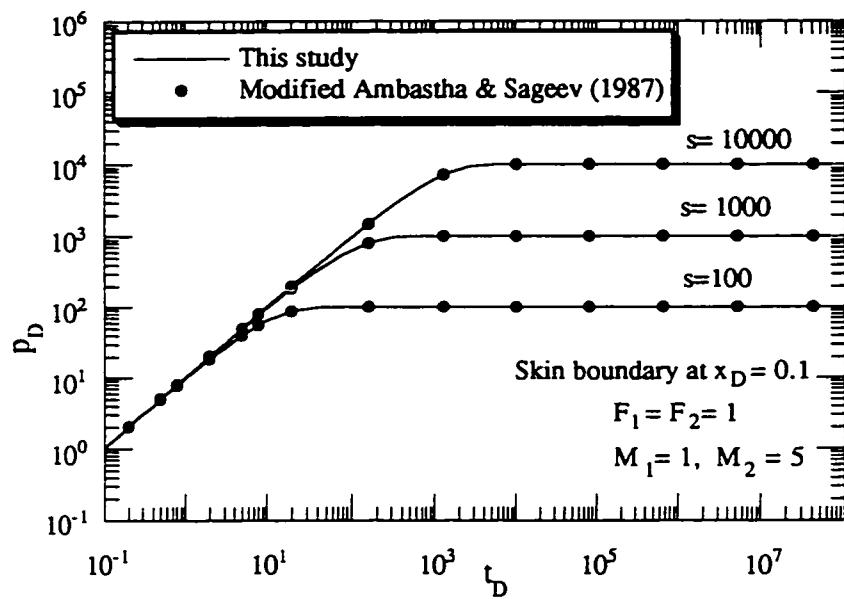


Figure 2.6: Comparison of the dimensionless pressure at the producing boundary of a composite system with the modified solution of Ambastha and Sageev (1987).

2.4 Scope of the Model

In this study, a generalized transient solution for an n region linear, compartmentalized system has been developed. Each compartment is allowed to have distinct rock and/or fluid properties. Also, each compartment may have distinct physical dimensions provided it still maintains the linear character of flow. The conditions at the extreme boundaries may need adjustment with time as a result of the way a compartmentalized system produces. In addition, the production rate from a compartment may not be kept at a constant value. The proposed solution has been generalized by allowing the extreme boundary conditions and the production rate through a line-sink in each compartment to be time-dependent. Thus, this solution is capable of dealing with a time-dependent situation directly. Conventionally, this kind of time-dependent situation is dealt with by the use of the principle of superposition and/or Duhamel's theorem. *Corapcioglu et al.* (1983) mention that various types of boundary conditions can be encountered in the field, depending on the geological conditions. Considering the extreme boundary conditions as the Cauchy-type for the new solution has a number of advantages. This type of boundary condition is applicable in confined or phreatic aquifers in contact with a clogged bed (*Bear*, 1972) and also when a linear system communicates fluid with an adjoining region through a partially-communicating fault. Also, the Cauchy-type boundary condition can easily be modified to the Dirichlet- or the Neumann-type boundary condition as a special case. The Dirichlet-type condition applies to specifying the pressure at a boundary while the Neumann-type applies to specifying rate and to the condition of no-flow. Therefore, the Cauchy-type boundary condition that has been adopted in this study is general in nature and can be modified easily to conform with various types of problems encountered in the field.

The inclusion of property contrasts in the compartments and skin factors at the interfaces permits one to investigate complicated scenarios of heterogeneity in a linear system. Conventionally, transient responses of an aquifer are studied based on the assumption that the reservoir-aquifer interface is either at a constant pressure or producing at a

constant rate. In this kind of analysis, the transient behavior of the reservoir is neglected. However, the new solution can be used to study the transient behavior of an entire reservoir-aquifer system which predominantly maintains a linear character of flow.

2.5 Example Problems

It is very important to estimate the cumulative water influx into a reservoir from an adjoining aquifer for material balance purposes. Any error in the cumulative water influx will result in an error in the estimation of the initial oil in-place and in the projected future performance of the reservoir. In this section, a number of example problems are studied with the new analytical solution to check on the validity of certain conventionally-accepted simplifying assumptions in the calculation of cumulative water influx. In these assumptions the transients and compressibilities in the reservoir are neglected while calculating the cumulative water influx through the reservoir-aquifer interface (*Craft et al.*, 1991). These assumptions lead to a situation where the pressure responses at the reservoir-aquifer interface are the same as those at the producing boundary of the reservoir. Thus, the transient-pressure behavior of an aquifer is analyzed assuming that the reservoir-aquifer interface is at a constant pressure or that the aquifer is replenishing the reservoir at a constant rate. *Earlougher* (1977) pointed out that the reservoir-aquifer interface, in practice, is generally neither at a constant pressure nor replenishing the reservoir at a constant rate. However, with the use of the new solution of this study, it is possible to include the transients and compressibilities of the reservoir to calculate the cumulative water influx.

Figure 2.7 shows a schematic of a reservoir-aquifer system. The reservoir-aquifer interface is located at $x_D = X_{2D}$. The adjoining aquifer is considered to have two regions with different rock and fluid properties. For all the example problems discussed in this section, it is considered that the inner boundary is located at $x_D = 0$ and that the outer boundary is located at $x_D = 1$.

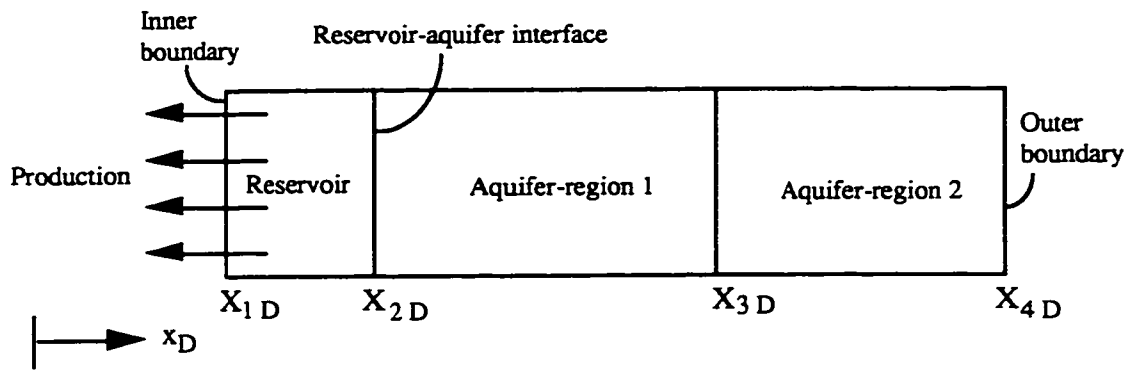


Figure 2.7: Schematic of a reservoir-aquifer system.

First, a reservoir-aquifer system is considered with the following properties or parameters:

$$M_1 = 1, M_2 = 10, M_3 = 6, F_1 = 1, F_2 = 0.64, F_3 = 0.55, X_{2D} = 0.05, X_{3D} = 0.7, B_2/B_1 = B_3/B_1 = 0.895.$$

Here, multiple, dimensionless production-rates at the inner boundary and a constant, dimensionless pressure at the outer boundary are considered. Figure 2.8 shows a stair-step variation of dimensionless rate at the inner boundary with dimensionless time. The outer boundary always maintains the initial pressure. The finite aquifer is considered to have two compartments with contrasts in rock and fluid properties. The dimensionless cumulative influxes, Q_{c1D} at the inner boundary and Q_{c2D} at the reservoir-aquifer interface are computed and are shown in Fig. 2.9. Conventionally, the cumulative influx through the reservoir-aquifer interface in this kind of situation is computed assuming that the water-influx rate is equal to the production rate at the inner boundary neglecting any possibility of the effects of transients and compressibilities in the reservoir. However, the coincidence of Q_{c1D} with Q_{c2D} in Fig. 2.9 within 1% demonstrates the validity of this assumption despite the presence of transients at the reservoir-aquifer interface due to the variable dimensionless production rate at the inner boundary.

Another reservoir-aquifer system is considered with the following properties:

$$M_1 = 1, M_2 = 10, M_3 = 6, F_1 = 1, F_2 = 0.64, F_3 = 0.62, X_{2D} = 0.05, X_{3D} = 0.7, B_2/B_1 = B_3/B_1 = 0.895.$$

In this case, the inner boundary is producing at a variable dimensionless pressure and the outer boundary is closed. Figure 2.10 shows the comparison of the stair-step variation of dimensionless pressure at the inner boundary due to production and the corresponding dimensionless-pressure response at the reservoir-aquifer interface. Also the dimensionless cumulative influxes are calculated at the inner boundary and at the reservoir-aquifer interface with dimensionless time and then plotted in Fig. 2.11. Conventionally, the

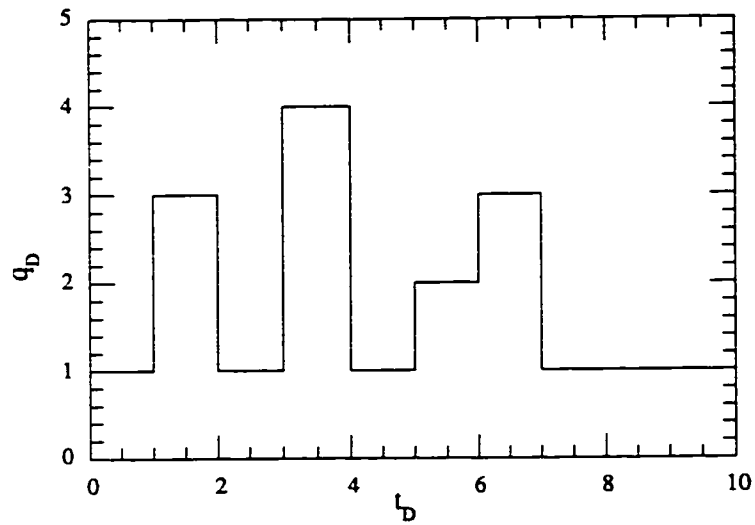


Figure 2.8: The variation of flow rate at the inner boundary.

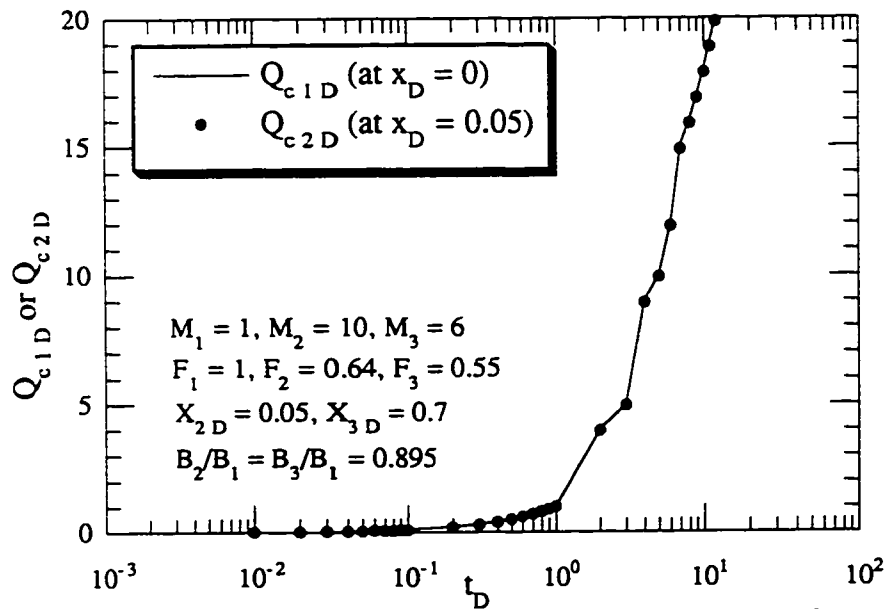


Figure 2.9: Comparison of dimensionless cumulative influxes at the inner boundary and the reservoir-aquifer interface.

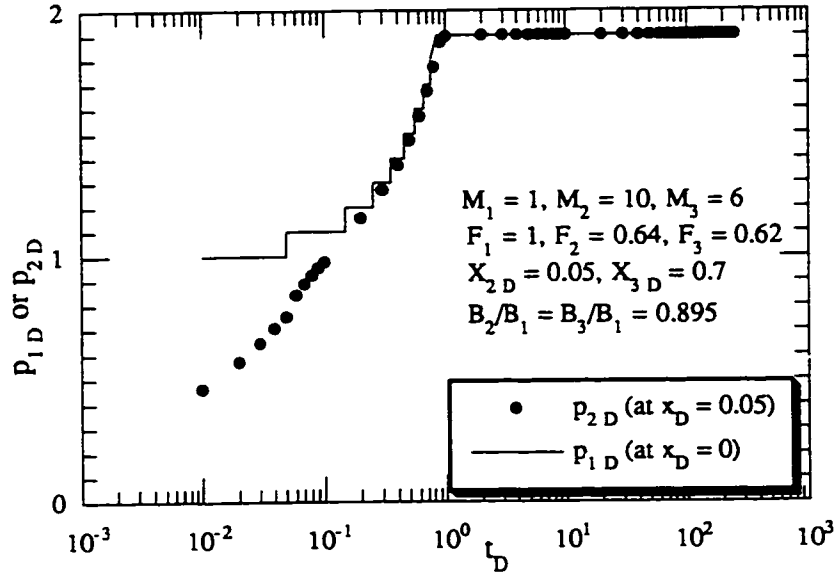


Figure 2.10: Comparison of dimensionless pressures at the inner boundary and reservoir-aquifer interface.

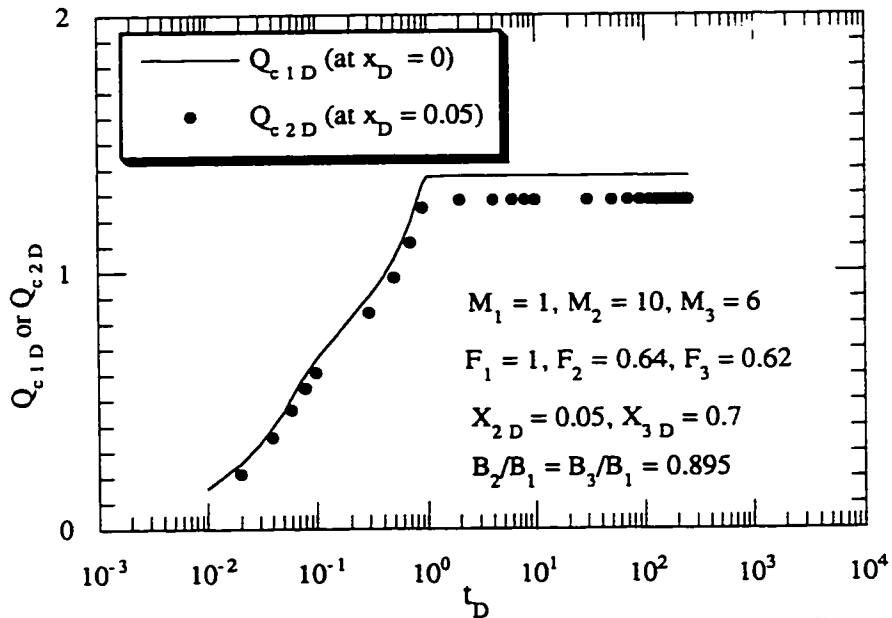


Figure 2.11: Comparison of dimensionless cumulative influxes at the inner boundary and the reservoir-aquifer interface.

cumulative influx at the reservoir-aquifer interface in this kind of situation is considered to be equal to the cumulative production at the inner boundary, neglecting the effects of transients and compressibilities in the reservoir. Fig. 2.11 shows that there will be an error of 8.4% near $t_D = 1$, if the transient and compressibility effects in the reservoir are neglected.

Finally, homogeneous rock and fluid properties, and dimensions in a reservoir-aquifer system are considered. The inner boundary is considered to be producing at a constant dimensionless pressure of $p_{iD}(0, t_D) = 1$. The corresponding dimensionless-pressure response at the reservoir-aquifer interface is shown in Fig. 2.12. The dimensionless cumulative influxes at the inner boundary and at the reservoir-aquifer interface are compared in Fig. 2.13. This plot shows that at the flow cut-off point (near $t_D = 1$), there will be a 5% error if the transient and compressibility effects of the reservoir are neglected.

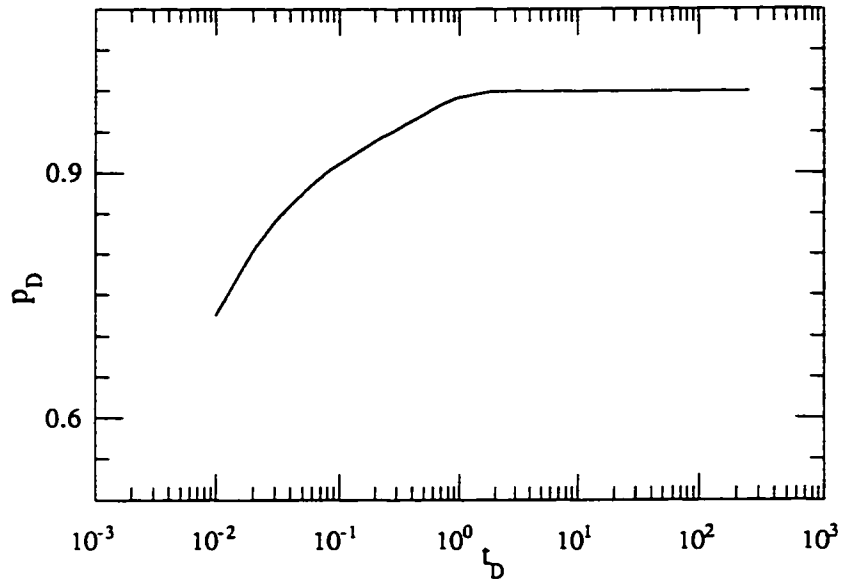


Figure 2.12: Dimensionless pressure response at the reservoir-aquifer interface for a homogeneous system.

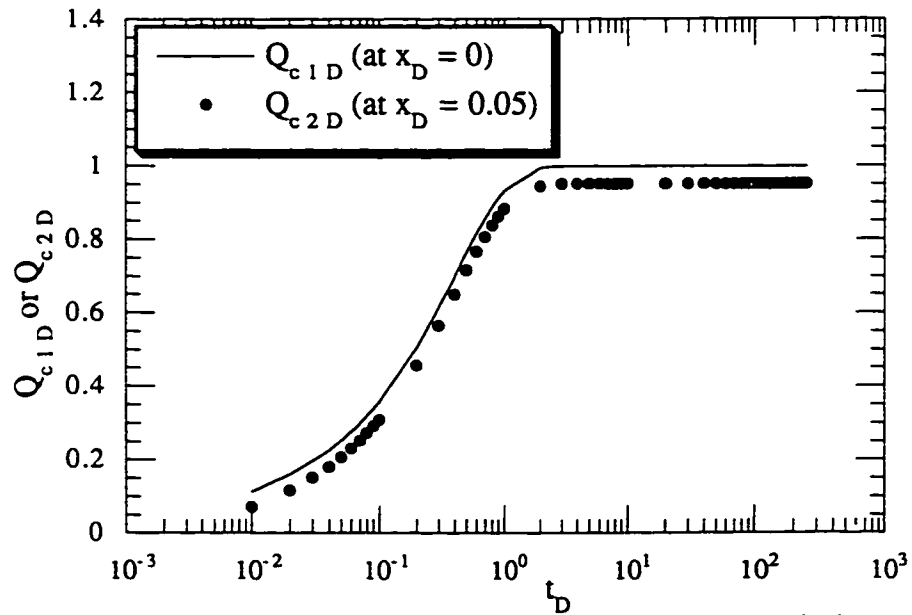


Figure 2.13: Comparison of dimensionless cumulative influxes at the inner boundary and the reservoir-aquifer interface for a homogeneous system.

CHAPTER 3

TWO-DIMENSIONAL FLOW SYSTEM

3.1 Introduction

The model for a linear, one-dimensional flow system developed in Chapter 2 may not be able to describe an areally-compartmentalized system adequately. This can happen when an areal system is not narrow enough to have predominantly linear flow of fluid. An areal compartmentalization is observed due to the presence of partially-communicating faults and turbidite lobe interfaces (*Stewart and Whaballa, 1989*). Such a system may be dominated by two-dimensional flow. In this Chapter, an analytical transient-pressure model for two-dimensional compartmentalized systems will be developed.

There are a number of papers available in the literature on the transient-pressure behavior of rectangular reservoirs. *Earlougher et al. (1968)* generated the pressure responses at different locations for various rectangular systems and well locations. *Ramey and Cobb (1971)* developed a general pressure buildup theory for a well in closed drainage areas of any shape. *Kumar and Ramey (1974)* presented the methods for drawdown and buildup analysis for a well inside a square with constant-pressure boundaries. These authors also showed how to measure the average pressure at any time during shut-in when the reservoir boundaries are maintained at a constant pressure.

There are a few studies reported on two-dimensional composite systems. Of these, *Yaxley (1987)* presented a mathematical model for a homogeneous system with a linear, partially-communicating fault of finite thickness and finite conductivity. *Ambastha et al. (1989)* extended the work of *Yaxley (1987)* and developed a more generalized, analytical, mathematical model for a composite system of two regions with property contrasts and separated by a boundary skin. These authors developed the solutions for transient-

pressure behavior for a line-sink well producing at a constant rate using a Fourier transformation in one space-variable and Laplace transformations in the other space-variable and time-variable. *Kuchuk and Habashy (1992)* obtained analytical solutions for transient-pressure responses in the Laplace-space domain for a laterally-composite system with a finite number of fully-communicating zones, each of which is of a constant cross-sectional area and parallel to the interfaces. In these solutions, these authors considered the property contrasts and that the production is through a single well located in one of the zones. *Butler and Liu (1991)* developed a semi-analytical solution for a three-region composite system to study aquifers with property contrasts using the Laplace-transform technique. These authors also generated both drawdown and drawdown-derivative responses for aquifer systems with different rock and fluid property contrasts.

3.2 Development of the Analytical Solution

An analytical solution for transient pressure will be developed here. The resistance to fluid communication between any two neighboring compartments is specified by a skin factor. The presence of this skin is meant to cause an extra pressure drop at an interface between two compartments simulating the effect of the presence of a low-permeability barrier or a partially-communicating fault in between two hydraulically-communicating compartments. Partial differential equations with appropriate initial and boundary conditions are set up starting from diffusivity equations describing two-dimensional flow through porous media. The partial differential equations are solved by an integral-transform technique for finite, composite domains, following the ideas of *Title (1965)*, *Title and Robinson (1965)* and *Padovan (1974)*. The kernel functions of the integral transformation are developed by solving an eigenvalue problem which has been developed from the homogeneous version of the partial differential equation in hand. The governing partial differential equation for a compartment has three independent variables: two space

variables and one time variable. Integral transformation with respect to the space-variables removes the spatial dependence of the partial differential equations. Thus, a partial differential equation transforms into an ordinary differential equation with time as the only independent variable with the eigenvalues as the parameters.

Let us suppose that there are n compartments in a compartmentalized system. The amount of fluid communication between any two neighboring compartments is specified by a skin factor. Definition of this skin factor has been illustrated in Section 1.6, Chapter 1. In the following Sub-Sections, an analytical solution will be developed step by step.

3.2.1 Setting up Governing Differential Equations

We consider a compartmentalized reservoir in a finite region, R , bounded by a surface, ∂R_o , and divided into n finite subregions or compartments, R_i with $i = 1, 2, 3, \dots, n$. Each compartment may have distinct rock or fluid properties. There are N_w , fully-penetrating, line-sink wells in R_i producing at time-dependent rates. *Kamal and Hegeman* (1988) pointed out that the multiple-well tests provide information about reservoir characteristics such as permeability, porosity, communication between wells, and reservoir heterogeneity. Any compartment, R_i , is hydraulically communicating with at most four adjacent compartments. A general configuration like this is shown in Fig. 3.1. However, for the sake of mathematical generality, let us suppose that compartment R_i is communicating with adjacent (along the x -axis) compartment R_j , through the interface boundary, ∂R_{ij} , and with another adjacent (along the y -axis) compartment, R_n , through the interface boundary, ∂R_{in} . Compartment R_i may have extreme boundaries, ∂R_{ox} , and ∂R_{oy} . A dimensionless form of the diffusivity equation for the flow of a single-phase, slightly-compressible fluid with a constant compressibility through an anisotropic and

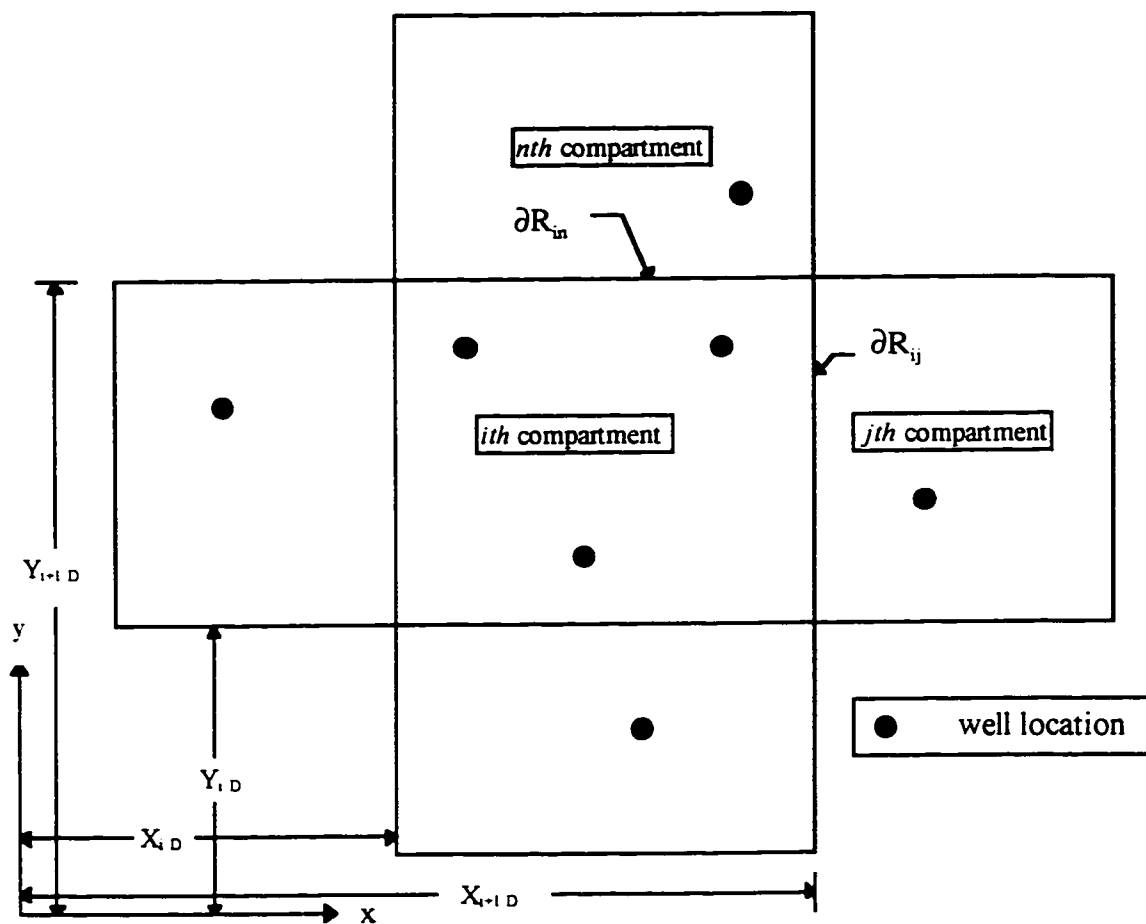


Figure 3.1: Schematic illustrating the geometry of a two-dimensional, areally-compartmentalized system.

homogeneous porous medium in the i th compartment which is producing through N_w , fully-penetrating line-sink wells is given by:

$$\alpha_{x_i} \frac{\partial^2 p_{i,D}}{\partial x_D^2} + \alpha_{y_i} \frac{\partial^2 p_{i,D}}{\partial y_D^2} + h_{p,D} \sum_{m=1}^{N_{w_i}} q_{i,D}^{(m)}(t_D) \delta(x_D - a_{i,D}^{(m)}) \delta(y_D - b_{i,D}^{(m)}) = e_i \frac{\partial p_{i,D}}{\partial t_D} \dots\dots\dots(3.1)$$

The initial and boundary conditions are prescribed as:

(a) initial condition:

$$p_{i,D}(x_D, y_D, 0) = p_{\alpha i,D} = \frac{k_p h_p}{q_p \mu_p B_p} (p_p - p_\alpha) \dots\dots\dots(3.2)$$

(b) boundary conditions:

(i) at an extreme boundary parallel to the y -axis, $\partial R_{\alpha y_i}$,

$$\left[\gamma_{\alpha y_i} \frac{\partial p_{i,D}}{\partial x_D} - \xi_{\alpha y_i} p_{i,D} \right]_{\partial R_{\alpha y_i}} = f_{\alpha y_i}(t_D) \dots\dots\dots(3.3)$$

(ii) at an extreme boundary parallel to the x -axis, $\partial R_{\alpha x_i}$,

$$\left[\gamma_{\alpha x_i} \frac{\partial p_{i,D}}{\partial y_D} + \xi_{\alpha x_i} p_{i,D} \right]_{\partial R_{\alpha x_i}} = f_{\alpha x_i}(t_D) \dots\dots\dots(3.4)$$

(iii) at an interface parallel to the y -axis, ∂R_{γ_i}

$$-\frac{l}{s_y} [p_{i,D} - p_{j,D}]_{\partial R_y} = \alpha_{x_i} \left[\frac{\partial p_{i,D}}{\partial x_D} \right]_{\partial R_y} \dots\dots\dots(3.5)$$

$$\alpha_{x_i} \left[\frac{\partial p_{i,D}}{\partial x_D} \right]_{\partial R_y} = \alpha_{x_j} \left[\frac{\partial p_{j,D}}{\partial x_D} \right]_{\partial R_y} \dots\dots\dots(3.6)$$

(iv) at an interface parallel to the x-axis, ∂R_m ,

$$-\frac{l}{s_m} [p_{i,D} - p_{n,D}]_{\partial R_m} = \alpha_{y_i} \left[\frac{\partial p_{i,D}}{\partial y_D} \right]_{\partial R_m} \dots\dots\dots(3.7)$$

$$\alpha_{y_i} \left[\frac{\partial p_{i,D}}{\partial y_D} \right]_{\partial R_m} = \alpha_{y_n} \left[\frac{\partial p_{n,D}}{\partial y_D} \right]_{\partial R_m} \dots\dots\dots(3.8)$$

where the dimensionless variables are defined as:

$$p_{i,D} = \frac{k_p h_p}{q_p \mu_p B_p} (p_p - p_i) \dots\dots\dots(3.9)$$

$$x_D = x/X_p \dots\dots\dots(3.10)$$

$$y_D = y/X_p \dots\dots\dots(3.11)$$

$$t_D = \frac{k_p t}{\phi_p \mu_p c_{tp} X_p^2} \dots\dots\dots(3.12)$$

$$\alpha_{i,D}^{(m)} = \alpha_i^{(m)} / X_p \dots\dots\dots(3.13)$$

$$b_{iD}^{(m)} = b_i^{(m)} / X_p \dots\dots\dots(3.14)$$

$$h_{pD} = h_p / X_p \dots\dots\dots(3.15)$$

$$\alpha_{xi} = \frac{k_{xi} h_i \mu_p B_p}{\mu_i B_i k_p X_p} \dots\dots\dots(3.16)$$

$$\alpha_{yi} = \frac{k_{yi} h_i \mu_p B_p}{\mu_i B_i k_p X_p} \dots\dots\dots(3.17)$$

$$e_i = \frac{\phi_i c_{i1} h_i B_p}{B_i \phi_p c_{ip} X_p} \dots\dots\dots(3.18)$$

$$q_{iD}^{(m)}(t_D) = q_i^{(m)}(t) / q_p \dots\dots\dots(3.19)$$

where the subscript, p , refers to a reference compartment or a reference parameter.

The mathematical formulation described above has considered variations of dimensionless pay thickness. In this case, there is an underlying simplification that assumes that the variation of dimensionless pay thickness does not lead to predominantly three-dimensional flow. Specifying a uniform pay thickness for each compartment would guarantee two-dimensional flow. The conditions at the extreme boundaries expressed in Eqs. (3.3) and (3.4) are of the non-homogeneous, Cauchy-type which allow for any possible situation of partial communication at those locations. However, the parameters for the conditions at the extreme boundaries, γ_{axi} , ζ_{axi} , γ_{oyi} and ζ_{oyi} in Eqs. (3.3) and (3.4), can be chosen in such a way that these equations take care of the appropriate conditions

due to partial communication or the presence of skin at the extreme boundaries. These parameters can also be set to 0 or 1 to obtain the conditions at the extreme boundaries as the Dirichlet- or the Neumann-type. Also, the time-dependent functions, $f_{\alpha x}(t_D)$ and $f_{\alpha y}(t_D)$ in Eqs. (3.3) and (3.4), respectively, allow for specifying any time-dependent conditions at the extreme boundaries. Thus, the mathematical formulation described by Eqs. (3.1) through (3.8) deals with time-dependent variations of production rates and extreme boundary conditions directly.

3.2.2 Solution of Differential Equations

An integral-transform technique for finite, composite domains, based on the theory and technique as developed by *Title* (1965), *Title and Robinson* (1965), and *Padovan* (1974), will be used to develop an analytical solution of the set of equations in the following steps:

(i) Development of integral-transform pair

To develop the integral-transform pair, it is necessary to define the corresponding eigenvalue problems. Following the similar procedure for one-dimensional flow described in Chapter 2, and also by *Padovan* (1974), two sets of eigenvalue problems with the *lth* eigenvalue as a parameter can be developed by separating variables of the homogeneous version of the set of governing differential equations listed above as follows:

x-direction eigenvalue problem

$$\frac{d^2 U_{i,l}(x_D)}{dx_D^2} = -\theta_{i,l}^2 \eta_{x,l} U_{i,l}(x_D) \dots \dots \dots (3.20)$$

where,

$$\eta_{x_i} = e_i / \alpha_{x_i} \dots \dots \dots (3.21)$$

with the boundary conditions:

$$\left[\gamma_{\alpha_i} \frac{dU_{i,l}}{dx_D} - \xi_{\alpha_i} U_{i,l} \right]_{\partial R_{\alpha_i}} = 0 \dots \dots \dots (3.22)$$

$$- \frac{1}{s_y} [U_{i,l} - U_{j,l}]_{\partial R_y} = \alpha_{x_i} \left[\frac{dU_{i,l}}{dx_D} \right]_{\partial R_y} \dots \dots \dots (3.23)$$

$$\alpha_{x_i} \left[\frac{dU_{i,l}}{dx_D} \right]_{\partial R_y} = \alpha_{x_j} \left[\frac{dU_{j,l}}{dx_D} \right]_{\partial R_y} \dots \dots \dots (3.24)$$

y-direction eigenvalue problem

$$\frac{d^2 V_{i,l}(y_D)}{dy_D^2} = - \sigma_{i,l}^2 \eta_{y_i} V_{i,l}(y_D) \dots \dots \dots (3.25)$$

where,

$$\eta_{y_i} = e_i / \alpha_{y_i} \dots \dots \dots (3.26)$$

with the boundary conditions:

$$\left[\gamma_{\alpha_i} \frac{dV_{i,l}}{dy_D} + \xi_{\alpha_i} V_{i,l} \right]_{\partial R_{\alpha_i}} = 0 \dots \dots \dots (3.27)$$

$$-\frac{l}{s_{in}} [V_{i,l} - V_{n,l}]_{\partial R_{in}} = \alpha_{y,l} \left[\frac{dV_{i,l}}{dy_D} \right]_{\partial R_{in}} \dots\dots\dots(3.28)$$

$$\alpha_{y,l} \left[\frac{dV_{i,l}}{dy_D} \right]_{\partial R_{in}} = \alpha_{y,n} \left[\frac{dV_{n,l}}{dy_D} \right]_{\partial R_{in}} \dots\dots\dots(3.29)$$

The functions, $U_i(x_D)$ and $V_i(y_D)$ are *lth* eigenfunctions for the *ith* compartment in the *x* and *y* directions, respectively. *Title* (1965) and *Title and Robinson* (1965) mention that the eigenvalue problems for the *x*- and *y*-directions described above are related by the condition of identical time-behavior of dimensionless pressure on both sides of an interface which is given as follows:

$$\theta_{i,l}^2 - \sigma_{i,l}^2 = \theta_{j,l}^2 - \sigma_{j,l}^2 \dots\dots\dots(3.30)$$

Salt (1983 a and b) also endorsed the above relationship (Eq. (3.30)) between eigenvalues in the *x*- and *y*-directions. Following the similar procedure described by *Padovan* (1974), one has the following integral-transform pair:

Inversion formula:

$$p_{i,D} = \sum_{l=1}^{\infty} \frac{\bar{p}_{Dl} U_{i,l} V_{i,l}}{N_l} \dots\dots\dots(3.31)$$

Transformation formula:

$$\bar{p}_{Dl} = \sum_{i=1}^n e_i \iint_{R_i} p_{i,D} U_{i,l} V_{i,l} dx_D dy_D \dots\dots\dots(3.32)$$

where,

$$N_i = \sum_{i=1}^n e_i \iint_{R_i} U_{i1}^2 V_{i1}^2 dx_D dy_D \dots \dots \dots (3.33)$$

(ii) Integral transformation of differential equations along with their conditions

Multiplying both sides of Eq. (3.1) by $U_{i1} V_{i1} dx_D dy_D$ and integrating over R_i and then summing up the resulting expressions over all compartments, one gets,

$$\sum_{i=1}^n \left[\alpha_{x_i} \iint_{R_i} \frac{\partial^2 p_{iD}}{\partial x_D^2} U_{i1} V_{i1} dx_D dy_D + \alpha_{y_i} \iint_{R_i} \frac{\partial^2 p_{iD}}{\partial y_D^2} U_{i1} V_{i1} dx_D dy_D \right] + h_{pD} \sum_{i=1}^n \left\{ \sum_{m=1}^{N_{w_i}} q_{iD}^{(m)}(t_D) \right. \\ \left. \cdot \iint_{R_i} U_{i1} V_{i1} \delta(x_D - a_{iD}^{(m)}) \delta(y_D - b_{iD}^{(m)}) dx_D dy_D \right\} = \sum_{i=1}^n e_i \iint_{R_i} \frac{\partial p_{iD}}{\partial t_D} U_{i1} V_{i1} dx_D dy_D \dots \dots \dots (3.34)$$

The first two terms of the above equation are simplified by using Green's theorem. Then substituting the values from Eqs. (3.3) through (3.8), (3.20), (3.22) through (3.25), (3.27) through (3.30) and (3.32) in Eq. (3.34), it can be shown that,

$$-\lambda_i^2 \bar{p}_{Di} + g_i = \frac{d\bar{p}_{Di}}{dt_D} \dots \dots \dots (3.35)$$

where,

$$\lambda_i^2 = \theta_i^2 + \sigma_i^2 \dots \dots \dots (3.36)$$

$$g_i(t_D) = \sum_{i=1}^n \left\{ \sum_{m=1}^{N_{w_i}} h_{pD} q_{iD}^{(m)}(t_D) U_{i1}(a_{iD}^{(m)}) V_{i1}(b_{iD}^{(m)}) + \left[\frac{\alpha_{x_i} U_{i1} f_{\alpha x_i}}{\gamma_{\alpha x_i}} \right]_{\partial R_{y_i}} \int_{\partial R_{y_i}} V_{i1} dy_D + \left[\frac{\alpha_{y_i} V_{i1} f_{\alpha y_i}}{\gamma_{\alpha y_i}} \right]_{\partial R_{x_i}} \int_{\partial R_{x_i}} U_{i1} dx_D \right\} \dots \dots \dots (3.37)$$

A detailed procedure for the above step that leads to the development of an initial value problem upon integral transformation is described in Chapter 2. The parameter λ_l in Eq. (3.36) is the same for each compartment; therefore, Eqs. (3.30) and (3.36) are identical. Both of these equations ensure that the time-behavior of the dimensionless pressure at either side of an interface is identical on the assumption that the skin boundary does not have any storage.

Taking the integral transformation of the initial condition, Eq. (3.2), one gets,

$$\bar{p}_{Di}(t_D = 0) = \sum_{i=1}^n p_{\alpha D} \iint_{R_i} U_{i,l} V_{i,l} dx_D dy_D \dots\dots\dots(3.38)$$

We now have an initial-value problem with an ordinary differential equation, given by Eq. (3.35), with an initial condition, given by Eq. (3.38), as a result of an integral transformation of the space variables. The solution of this initial-value problem is given by,

$$\bar{p}_{Di}(t_D) = \left[\bar{p}_{Di}(0) - \int_0^{t_D} g_i(\tau) e^{\lambda_i \tau} d\tau \right] e^{-\lambda_i t_D} \dots\dots\dots(3.39)$$

(iii) Inversion

$\bar{p}_{Di}(t_D)$ from Eq. (3.39) is inverted into $p_{D,i}(x_D, y_D, t_D)$ using the inversion formula, Eq. (3.31), as follows:

$$p_{D,i}(x_D, y_D, t_D) = \sum_{i=1}^n \left[\bar{p}_{Di}(t_D = 0) + \int_0^{t_D} g_i(\tau) e^{\lambda_i \tau} d\tau \right] \frac{U_{i,l}(x_D) V_{i,l}(y_D) e^{-\lambda_i t_D}}{N_i} \dots\dots\dots(3.40)$$

Before carrying out the above inversion process, it is required to have calculated a number of eigenvalues of the system. Computation of eigenvalues is discussed in the next step. In general, the rate of convergence for summing up the series in Eq. (3.40) is very high. The number of eigenvalues or the number of terms required in the series is dependent on the desired level of accuracy.

(iv) Computation of eigenvalues and eigenfunctions

First we need to evaluate the *l*th eigenvalues, θ_{il} and σ_{il} , for each compartment ($i = 1, 2, 3, 4, \dots, n$) in order to determine the corresponding eigenfunctions, U_{il} and V_{il} . According to *Mikhailov and Vulchanov (1983)* and *Cotta (1993)*, the general expressions for these eigenfunctions are the general solutions to Eqs. (3.20) and (3.25), respectively, as follows:

$$U_{il}(x_D) = U_{il}^* U_{1il} - U_{il}^{**} U_{2il} \dots \dots \dots (3.41)$$

$$V_{il}(y_D) = V_{il}^* V_{1il} - V_{il}^{**} V_{2il} \dots \dots \dots (3.42)$$

where,

$$U_{1il}(\theta_{il}, x_D) = \frac{\sin(\theta_{il} \sqrt{\eta_{x_i}} (X_{i+1D} - x_D))}{\sin(\theta_{il} \sqrt{\eta_{x_i}} (X_{i+1D} - X_{iD}))} \dots \dots \dots (3.43)$$

$$U_{2il}(\theta_{il}, x_D) = \frac{\sin(\theta_{il} \sqrt{\eta_{x_i}} (x_D - X_{iD}))}{\sin(\theta_{il} \sqrt{\eta_{x_i}} (X_{i+1D} - X_{iD}))} \dots \dots \dots (3.44)$$

$$V_{1,l}(\sigma_{il}, y_D) = \frac{\sin(\sigma_{il} \sqrt{\eta_{y_l}} (Y_{i+1D} - y_D))}{\sin(\sigma_{il} \sqrt{\eta_{y_l}} (Y_{i+1D} - Y_{iD}))} \dots\dots\dots (3.45)$$

$$V_{2,l}(\sigma_{il}, y_D) = \frac{\sin(\sigma_{il} \sqrt{\eta_{y_l}} (y_D - Y_{iD}))}{\sin(\sigma_{il} \sqrt{\eta_{y_l}} (Y_{i+1D} - Y_{iD}))} \dots\dots\dots (3.46)$$

Also, $U_{i,l}^*$ and $U_{i,l}^{**}$ are the values of $U_i(x_D)$ at $x_D = X_{iD}$ and X_{i+1D} , respectively, and, $V_{i,l}^*$ and $V_{i,l}^{**}$ are the values of $V_i(y_D)$ at $y_D = Y_{iD}$ and Y_{i+1D} , respectively.

The substitution of Eqs. (3.41) and (3.42) in the boundary conditions for the x -direction eigenvalue problem (Eqs. (3.22) through (3.24)) and for the y -direction eigenvalue problem (Eqs. (3.27) through (3.29)) results in two systems of linear, homogeneous algebraic equations in $U_{i,l}^*$ and $U_{i,l}^{**}$, and $V_{i,l}^*$ and $V_{i,l}^{**}$, respectively, with the eigenvalues as parameters. Thus, a two-dimensional eigenvalue problem in this study has been converted into two one-dimensional eigenvalue problems related by the condition expressed by Eq. (3.30). For n compartments, there are $2n$ of the l th eigenvalues to be calculated. There are also $2n$ non-linear equations available for the purpose of calculating the $2n$ eigenvalues. Of these $2n$ equations, there are $(n - 1)$ equations due to the continuity of the time-independent behavior at an interface-boundary and the other $(n + 1)$ equations are from the conditions of non-trivial values of eigenfunctions (*Rahman and Ambastha, 1996a*). *Padovan (1974)* mentions that the positive roots of this simultaneous system of equations are the eigenvalues and that they can be computed by using a suitable method. In this study, a modified regula falsi method has been used to get a good estimation of the eigenvalues which are later used as an initial guess to compute the corresponding eigenvalues with an assigned accuracy by using Newton's method (*Borse, 1985*). Since the mathematical model developed in this study is an extension of that for the one-

dimensional flow situation described in Chapter 2, a similar procedure has been followed here to calculate the eigenvalues and eigenfunctions.

The formal solution to the set of Eqs. (3.1) through (3.8) is given by Eq. (3.40). This solution is subject to accommodation of changes corresponding to certain special cases which will be discussed later in Section 3.2.7.

3.2.3 Computer Program for Numerical Values

A computer program incorporating the solution scheme described in Section 3.2.2 has been developed in FORTRAN 77 for the purpose of generating numerical values of the solution developed in this Chapter. The complete source code and a sample data file are presented in Appendix B. This program has a number of Subroutines and Subroutine-Subfunctions which are coordinated by the Main Program. Typically, it takes about 5 minutes to run the program for a 4-compartment system in the "Numerical Server" (RS/6000 Model 59Hs, 66.7 MHz) at the University of Alberta.

3.2.4 Average Compartment Pressure

The expression for the volumetric average dimensionless pressure in the *i*th compartment as a function of dimensionless time is given by:

$$P_{iD,ave}(t_D) = (1/A_i) \iint_{R_i} P_{iD}(x_D, y_D, t_D) dx_D dy_D \dots\dots\dots(3.47)$$

where,

$$A_i = (X_{i+1D} - X_{iD}) (Y_{i+1D} - Y_{iD}) \dots\dots\dots(3.48)$$

Substituting the expression for $p_{i,D}$ from Eq. (3.40) in Eq. (3.47) results in the following expression,

$$p_{i,D \text{ ave}}(t_D) = \sum_{i=1}^{\bar{n}} \left[\bar{p}_{Di}(t_D = 0) + \int_0^{t_D} g_i(\tau) e^{\lambda_i^* \tau} d\tau \right] \frac{\bar{U}_{i,i} \bar{V}_{i,i} e^{-\lambda_i^* t_D}}{A_i N_i} \dots\dots\dots(3.49)$$

where,

$$\bar{U}_{i,i} = \int_{x_{i,D}}^{x_{r,i,D}} U_{i,i}(x_D) dx_D \dots\dots\dots(3.50)$$

$$\bar{V}_{i,i} = \int_{y_{i,D}}^{y_{r,i,D}} V_{i,i}(y_D) dy_D \dots\dots\dots(3.51)$$

The expression for dimensionless average pressure in the *i*th compartment shown in Eq. (3.49) has considered dimensionless pressure in that compartment based on extreme boundary conditions of the Cauchy-type. However, similar expressions for average dimensionless pressure with any other type of conditions at the extreme boundaries can be shown by taking care of the appropriate changes in the expression for dimensionless pressure which will be discussed later.

3.2.5 Cumulative Influx through an Interface

Following a similar approach to that described in Chapter 2, the expression for the dimensionless cumulative influx through an interface at ∂R_j as a function of dimensionless time is given by:

$$Q_{ijD}(t_D) = \int_0^{t_D} q_{ijD}(\tau) d\tau \dots\dots\dots (3.52)$$

where,

$$q_{ijD} = - \frac{\alpha_{xi}}{h_{pD}} \int_{Y_{iD}}^{Y_{i-1D}} \left[\frac{\partial p_{iD}}{\partial x_D} \right]_{\partial R_{ij}} dy_D \dots\dots\dots (3.53)$$

In Eq. (3.53), the flow of fluid from the *j*th compartment to the *i*th compartment has been considered positive. Therefore, a positive value of the cumulative influx, $Q_{ijD}(t_D)$, will mean that the net flow has been from the *j*th compartment to the *i*th compartment.

It is also assumed that all compartments have been at a uniform, initial pressure prior to going on production. Substituting Eqs. (3.40) and (3.53) into Eq. (3.52), one gets,

$$Q_{ijD}(t_D) = - \frac{\alpha_{xi}}{h_{pD}} \sum_{l=1}^i \left\{ \left[\frac{dU_{l,l}}{dx_D} \right]_{X_{l-1D}} \frac{\bar{V}_{l,l}}{N_l} \int_0^{t_D} F(\tau) e^{-\lambda_i \tau} d\tau \right\} \dots\dots\dots (3.54)$$

where,

$$F_l(\tau) = \int_0^{\tau} g_l(\tau') e^{-\lambda_i \tau'} d\tau' \dots\dots\dots (3.55)$$

An expression similar to Eq. (3.54) can be shown for the dimensionless cumulative influx, Q_{inD} , through an interface parallel to the *x*-axis, ∂R_{in} .

3.2.6 Relationship between Skin Factor and Barrier Transmissibility

Fox *et al.* (1988) and Stewart and Whaballa (1989) gave the expression for the rate of fluid that communicates between *ith* and *jth* compartments as:

$$q_{ij} = T_{ij} (\bar{p}_i - \bar{p}_j) \dots \dots \dots (3.56)$$

The above definition neglects the internal resistance to flow in each compartment (Stewart and Whaballa, 1989). But the barrier resistance in the form of a skin factor as used in this study does not impose any limitation on the internal resistance to flow within any compartment (Rahman and Ambastha, 1996b). However, there is a relationship between the skin factor at an interface as used in this study and the barrier transmissibility defined by Fox *et al.* (1988) and Stewart and Whaballa (1989). This relationship is given by:

$$s_{ij} = [k_p / \{\mu_p B_p T_{ij} (\bar{p}_i - \bar{p}_j)\}] \int_{r_i}^{r_{i+1}} [p_i - p_j]_{\partial R_{ij}} dy \dots \dots \dots (3.57)$$

where $[p_i - p_j]_{\partial R_{ij}}$ defines the difference in pressures between the *ith* and *jth* compartments across an interface parallel to the *y*-axis, ∂R_{ij} . Equation (3.57) can be rearranged to obtain the following dimensionless form:

$$s_{ij} = \frac{v_{ij}}{T_{ijD}} \dots \dots \dots (3.58)$$

where,

$$T_{ijD} = \frac{\mu_p B_p T_{ij}}{k_p X_p} \dots \dots \dots (3.59)$$

$$u_{ij} = [1/(\bar{p}_{i,D} - \bar{p}_{j,D})] \int_{y_{i,D}}^{y_{i+1,D}} [p_{i,D} - p_{j,D}]_{\partial R_{ij}} dy_D \dots\dots\dots(3.60)$$

Expressions similar to Eqs. (3.57) and (3.58) can be obtained for the relationship between T_{in} and s_{in} due to fluid communication through an interface parallel to the x -axis, ∂R_{in} .

3.2.7 Modification of Solution for Special Cases

The general solution developed above needs modification in some special cases. These are discussed below:

(i) Perfect communication at an interface

If there is a perfect communication at an interface, ∂R_{ij} , we can write, $s_{ij} \rightarrow 0$. This establishes the condition of continuity of pressure. Thus, the corresponding interface conditions described in Eqs. (3.5) and (3.6) take the following form:

$$[p_{i,D}]_{\partial R_{ij}} = [p_{j,D}]_{\partial R_{ij}} \dots\dots\dots(3.61)$$

$$\alpha_{x_i} \left[\frac{\partial p_{i,D}}{\partial x_D} \right]_{\partial R_{ij}} = \alpha_{x_j} \left[\frac{\partial p_{j,D}}{\partial x_D} \right]_{\partial R_{ij}} \dots\dots\dots(3.62)$$

Subsequent interface conditions for the corresponding eigenvalue problem should be updated also to reflect the conditions expressed by Eqs. (3.61) and (3.62).

(ii) Dirichlet-type condition at an extreme boundary

When the condition at an extreme boundary is of the Dirichlet-type, the solution as given by Eq. (3.40) remains the same (Ozisik, 1980). But the expression for g_i in Eq. (3.37) needs to be modified. For example, if an extreme boundary parallel to the y -axis in the i th compartment has the dimensionless pressure specified, then the following changes should be introduced:

Here, $\gamma_{\alpha i} = 0$, therefore,

$$\text{replace } \frac{U_{i1}}{\gamma_{\alpha i}} \text{ by } \frac{1}{\xi_{\alpha i}} \frac{dU_{i1}}{dx_D}.$$

(iii) Neumann-type condition at extreme boundaries

When the conditions at the extreme boundaries are of both the Cauchy- and the Neumann-type, then the expression for p_{iD} in Eq. (3.40) remains unchanged (Ozisik, 1980). But when the conditions at the extreme boundaries are all of the Neumann-type, the solution given by Eq. (3.40) needs to be augmented by an amount $p_{D\text{ add}}$, due to the fact that $\lambda_0 = 0$ is an eigenvalue of the system. This means that an additional term corresponding to the zero-eigenvalue has to be added to the solution presented in Eq. (3.40). Here all $\xi_{\alpha i}$'s and $\xi_{\beta i}$'s are equal to 0. The additional term corresponding to the zero-eigenvalue has been derived following the procedure discussed in Chapter 2 and is presented below:

$$p_{D\text{ add}} = \frac{1}{N_0} \left[\bar{p}_{D\text{ add}}(t_D = 0) + \int_0^{t_D} g_0(\tau) d\tau \right] \dots\dots\dots(3.63)$$

where,

$$g_o(\tau) = \sum_{i=1}^n \left\{ \sum_{m=1}^{N_{oi}} h_{p,D} q_{i,D}^{(m)}(\tau) + \left[\frac{\alpha_{x_i} f_{\alpha_i}}{\gamma_{\alpha_i}} \right]_{BR_{oy_i}} \int_{\partial R_{oy_i}} dy_D + \left[\frac{\alpha_{y_i} f_{\alpha_i}}{\gamma_{\alpha_i}} \right]_{BR_{ox_i}} \int_{\partial R_{ox_i}} dx_D \right\} \dots (3.64)$$

$$N_o = \sum_{i=1}^n e_i \iint_{R_i} dx_D dy_D \dots (3.65)$$

$$\bar{p}_{D\text{ add}}(t_D = 0) = \sum_{i=1}^n p_{oi,D} \iint_{R_i} dx_D dy_D \dots (3.66)$$

3.3 Validation of New Solution

It is necessary to validate the new solution to check its arithmetic reliability. Here, the new solution developed in this study has been validated by comparing a number of its simplified forms with those available in the literature.

Figure 3.2 shows the comparison of dimensionless pressure responses at $x_D = 0.553$, $y_D = 0.553$ due to a constant dimensionless production rate of $q_D = 1$ from a well located at $a_D = 0.52$, $b_D = 0.434$. The comparison has been made between the analytical solution for a closed, homogeneous rectangular reservoir as developed by *Hovanessian* (1961) and that from this study. To generate responses for a homogeneous reservoir from this study, a three-compartment system with each compartment having identical rock and fluid properties and the presence of no skin at the interfaces is considered. This comparison shows an excellent match.

Figure 3.3 shows a comparison of the dimensionless pressure responses using the solution of *Hovanessian* (1961) with the principle of superposition and that of this study at $x_D = 0.5$, $y_D = 0.5$ of a closed homogeneous reservoir. The well is located at $a_D = 0.2$, $b_D = 0.7$ producing at three different rates:

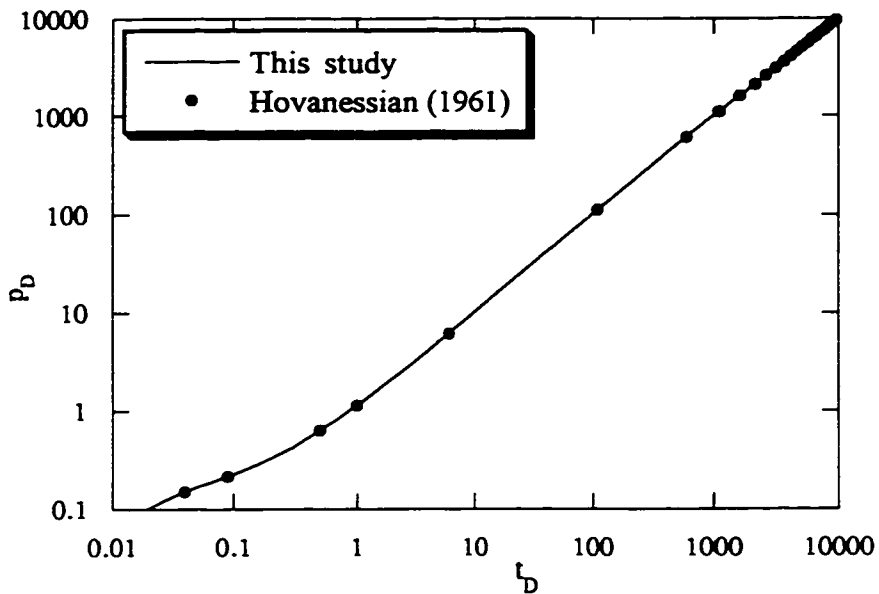


Figure 3.2: Comparison of dimensionless pressure responses in a closed homogeneous reservoir.

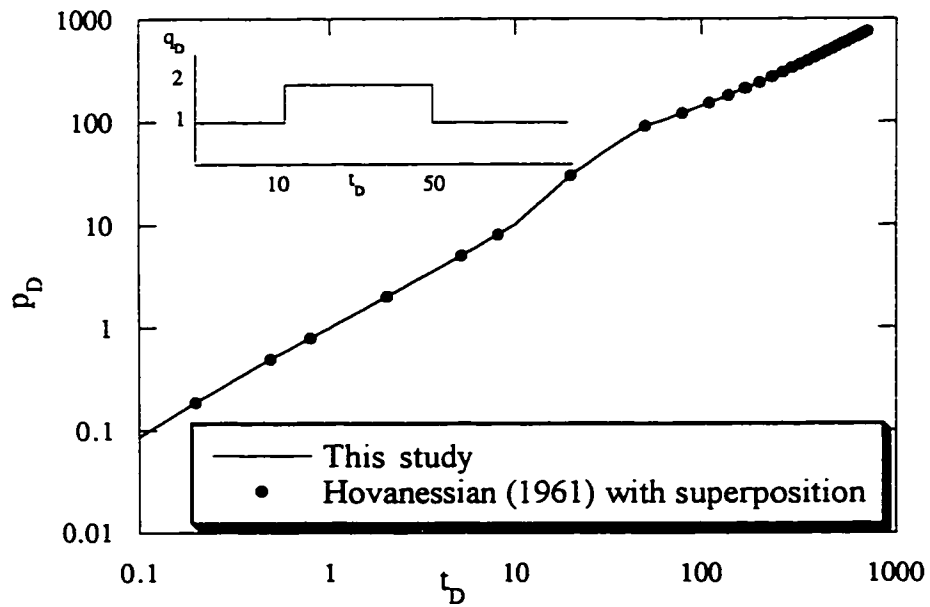


Figure 3.3: Comparison of dimensionless pressure responses for a 3-rate situation in a closed homogeneous system.

$q_{1D} = 1$, while $0 < t_D \leq 10$;

$q_{2D} = 2$, while $10 < t_D \leq 50$; and

$q_{3D} = 1$, while $t_D > 50$.

The multiple-flow rate situation for this study has been dealt with directly by the use of the Heaviside unit-step function while the solution of *Hovanessian* (1961) is used in conjunction with the principle of superposition. This shows an excellent match.

Figure 3.4 shows a comparison of responses at $x_D = 0.5$, $y_D = 0.5$ where a shut-in period is followed by a flow period in a closed homogeneous reservoir. The well located at $a_D = 0.2$, $b_D = 0.7$ produces at the rate of $q_D = 1$, while $0 < t_D \leq 10$. This situation has been dealt with as two-rate flow situation and the principle of superposition is used with the solution of *Hovanessian* (1961). The comparison made in this plot shows an excellent match.

Figure 3.5 shows a comparison of dimensionless pressure responses at $x_D = 0.4$, $y_D = 0.6$ due to a constant dimensionless production rate of $q_D = 1$ from a well located at $a_D = 0.3$, $b_D = 0.7$. The comparison has been made between the analytical solution for a homogeneous rectangular reservoir with constant-pressure boundaries as developed by *Hovanessian* (1961) and that from this study. To generate responses for a homogeneous reservoir from this study, a three-compartment system with each compartment having identical rock and fluid properties and presence of no skin at the interfaces is considered. This comparison shows an excellent match.

Figure 3.6 shows a comparison of the dimensionless pressure responses using the solution of *Hovanessian* (1961) with the principle of superposition and that of this study at $x_D = 0.4$, $y_D = 0.6$ of a homogeneous reservoir with constant-pressure boundaries. The well is located at $a_D = 0.3$, $b_D = 0.7$ and produces at three different rates:

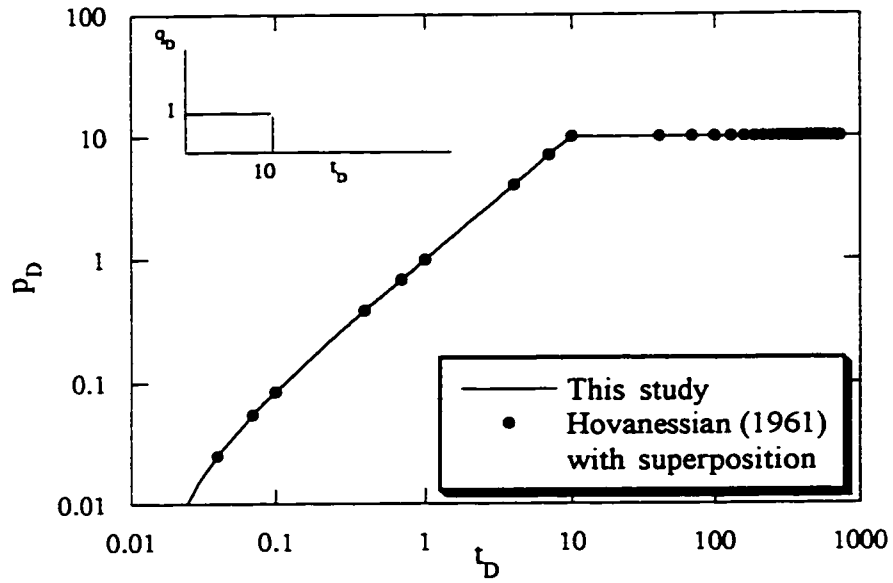


Figure 3.4: Comparison of buildup responses in a closed homogeneous system.

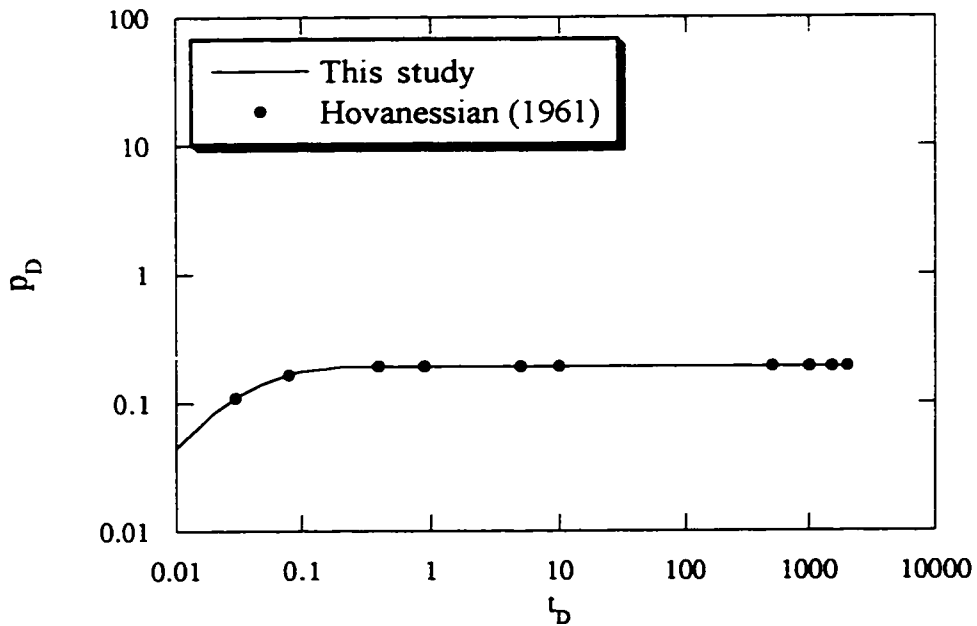


Figure 3.5: Comparison of dimensionless pressure responses in a homogeneous reservoir with constant-pressure boundaries.

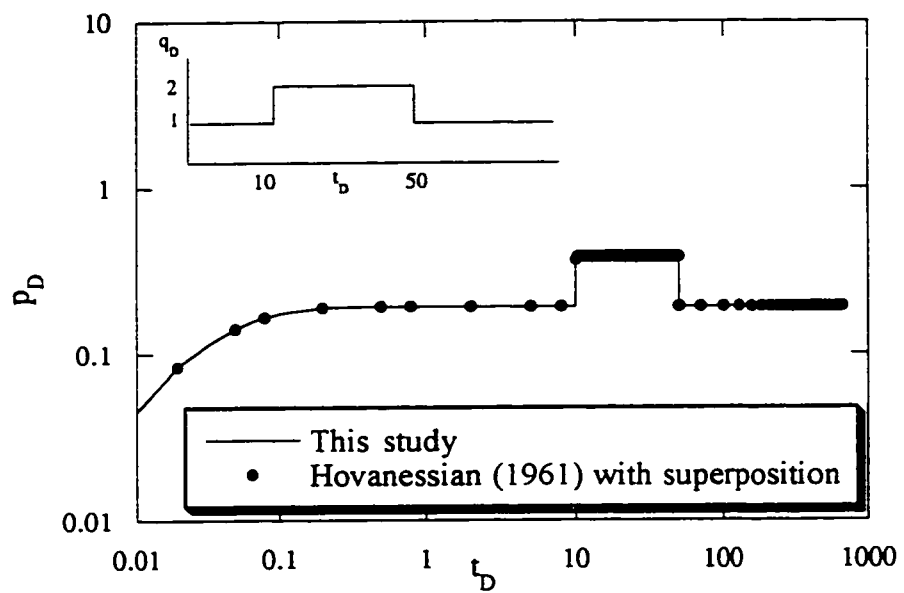


Figure 3.6: Comparison of dimensionless pressure responses for a 3-rate situation in a homogeneous system with constant-pressure boundaries.

$q_{1D} = 1$, while $0 < t_D \leq 10$;

$q_{2D} = 2$, while $10 < t_D \leq 50$; and

$q_{3D} = 1$, while $t_D > 50$.

The multiple-flow rate situation for this study has been dealt with directly by the use of the Heaviside unit-step function while the solution of *Hovanessian* (1961) is used in conjunction with the principle of superposition. This shows an excellent match.

Figure 3.7 shows a comparison of responses at $x_D = 0.4$, $y_D = 0.6$ where a shut-in period is followed by a flow period in a homogeneous reservoir with constant-pressure boundaries. The well located at $a_D = 0.3$, $b_D = 0.7$ produces at the rate of $q_D = 1$, while $0 < t_D \leq 1$. For this situation, the principle of superposition is used with the corresponding solution of *Hovanessian* (1961) for the two-rate flow condition. This comparison shows an excellent match.

Figure 3.8 shows the semilog derivative and the Cartesian derivative responses due to production through a well located at the center of a closed square reservoir. This shows an excellent match of the semilog derivative responses with those generated using the solution of *Hovanessian* (1961). From observation of the end of the zero-slope line of the semilog derivative responses (that is, end of the infinite-acting period), as computed using the new solution, it is inferred that the pseudosteady-state flow starts when $t_D > 0.1$. This is confirmed here by the observation that the Cartesian derivative line with zero slope begins around $t_D = 0.1$. The study of *Ramey and Cobb* (1971) observes the onset of pseudosteady-state flow at the same dimensionless time based on the area for a closed rectangular system. Therefore, this comparison of semilog derivative responses and the start of pseudosteady-state period confirms the validity of the solution developed earlier in this Chapter.

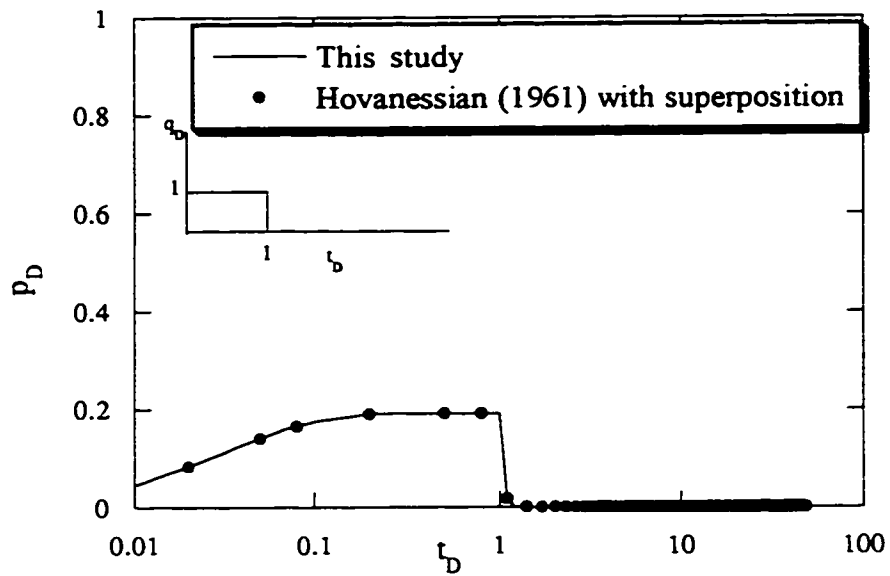


Figure 3.7: Comparison of buildup responses in a homogeneous system with constant-pressure boundaries.

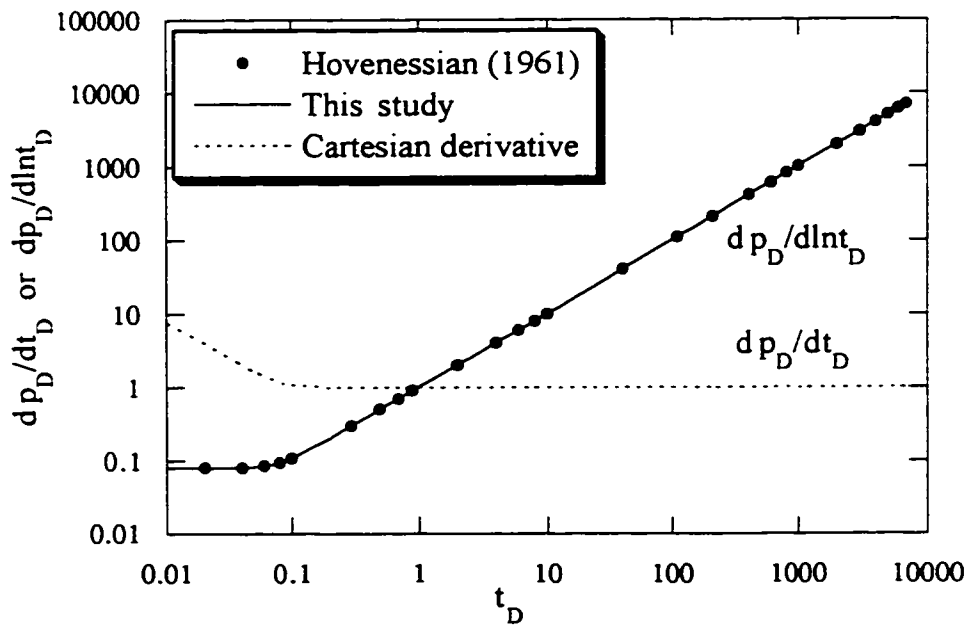


Figure 3.8: Comparison of semilog derivative responses with those from Hovanessian (1961).

In the preceding discussion, a number of simplified cases leading to homogeneous systems have been compared with the corresponding homogeneous systems. The solution presented in this Chapter corresponds to an extension of the solution for the linear, one-dimensional system presented in Chapter 2. The system of partial differential equations for a two-dimensional system is essentially similar to that for a one-dimensional system. Both systems of equations are solved using the same theory for an integral-transform technique. As shown in Chapter 2, the solution for a one-dimensional system was validated with a number of cases involving distinct rock and fluid properties in the compartments, with or without skin at the interfaces. Therefore the comparison of the solution for two-dimensional system with the cases of distinct rock and fluid properties in the compartments, with or without skin at the interfaces, would obviously lead to the same conclusion of good matching.

3.4 Application of New Model

The new analytical solution developed in this study may be used for understanding the transient-pressure behavior of an areally-compartmentalized system. Detecting and quantifying the flow units and flow barriers in a compartmentalized system is very important for designing development schemes. The new analytical solution is capable of providing useful information for this purpose. It is also possible to generate type-curves of transient-pressure responses for diagnostic identification of compartmentalized behavior in a reservoir.

The ability to consider the time-dependence of production rates and extreme boundary conditions directly makes this model more flexible from a practical point of view. Also, the Cauchy-type boundary condition is a general way of specifying conditions at an extreme boundary which can be modified to the Dirichlet- or the Neumann-type as special cases. Since this model considers contrasts of rock and fluid properties, including

anisotropy in compartments, it can be used for studying reservoir heterogeneity. *Bourgeois et al.* (1993) underline the importance of using analytical solutions for understanding the pressure behavior of channel-levee complexes. These complexes are modeled as a main channel bounded laterally by finite or infinite width levees with distinct rock and fluid properties. The solution developed earlier can be used to study the transient-pressure behavior of channel-levee complexes. A number of applications of this solution will be illustrated in Chapter 6.

CHAPTER 4

THREE-DIMENSIONAL FLOW SYSTEM

4.1 Introduction

In the case of vertical compartmentalization of reservoirs, the models presented for areal compartmentalization are not able to describe the transient-flow behavior adequately because the effects of gravity have been neglected in these models. Therefore, an analytical solution will be developed in this Chapter that accounts for the effects of gravity by formulating the problem in terms of potential, rather than pressure. The solution to the problem will be of a general nature, but it degenerates to the solutions for areal compartmentalization when the effects of gravity and the flow in the vertical direction are neglected. This kind of formulation is considered as an appropriate description of the flow of fluid in complex geological structures of compartmentalized systems including cellular systems, stacked channel realizations, and aeolian dune sand realizations. *Smalley and Hale* (1996) have pointed out that the identification of stratigraphic (vertical) compartmentalization is very important for the purpose of assessing the effectiveness of a production strategy. In these kinds of geological structures, the areal models, as developed in Chapters 2 and 3, are able to describe the mechanics of flow adequately because of the high degree of compartmentalization in the vertical direction. Here, we consider that there are n compartments that might be arranged vertically and areally for the purpose of developing the solution.

In this analytical solution, the resistance to fluid communication between any two neighboring compartments is specified by a skin factor to take into account the poor hydraulic communication between these compartments. The reason for the presence of such probable poor communication and the implication of representing this with a skin

boundary have already been discussed in Section 1.6, Chapter 1. Partial differential equations with appropriate initial and boundary conditions are set up starting from diffusivity equations describing three-dimensional flow through porous media. Due to the importance of gravity, the governing equations are considered in terms of potential, instead of pressure. *Ehlig-Economides* (1994) emphasized the importance of considering the formulation in terms of potential for compartmentalized systems. *Collins* (1961) used the force potential, as described by *Hubbert* (1940), in the form of energy per unit volume to formulate Darcy's equation for incompressible flow. In this study, a similar approach is taken with the transient potential, $\Phi(x, y, z, t)$, defining it at a point, (x, y, z) , in the Cartesian coordinate system, within the domain under consideration, as:

$$\Phi(x, y, z, t) = p(x, y, z, t) - \rho g z \dots\dots\dots(4.1)$$

where $p(x, y, z, t)$ is the pore pressure at the point, (x, y, z) , at time t , and z is the distance from a reference plane (x - y plane as in this case) which is taken positive in the direction of gravity. A similar approach with potential in the form of the energy per unit volume has also been taken by *Papatzacos* (1987) in formulating an analytical model for a partially-penetrating well. The introduction of potential in the diffusivity equation means that the flow of fluid at a point occurs only if there a potential gradient at that point.

4.2 Development of the Analytical Solution

The partial differential equations describing the flow of each compartment are solved by a integral-transform technique for finite, composite domains, following the ideas of *Title* (1965), *Title and Robinson* (1965) and *Padovan* (1974). The kernel functions for the integral transformation are developed by solving an eigenvalue problem which has been developed from separating the variables of the homogeneous version of the partial

differential equations. The governing partial differential equation for a compartment has four independent variables: three space variables and the time variable. Therefore, the integral transformation of the partial differential equations and associated conditions with respect to the space-variables removes the spatial dependence of the partial differential equations and associated conditions. Thus, a partial differential equation is transformed into an ordinary differential equation with time as the only independent variable with the eigenvalues as the parameters. In the following Sub-Sections, an analytical solution will be developed step by step.

4.2.1 Setting up Governing Differential Equations

We consider a compartmentalized reservoir in a finite region, R , bounded by a surface, ∂R_o , and divided into n finite sub-regions or compartments, R_i , with $i = 1, 2, 3, \dots, n$. Each compartment may have distinct rock or fluid properties. There are N_w , partially-penetrating, line-sink wells in R , producing at time-dependent rates. Any compartment, R_i , is hydraulically communicating with at most six adjacent compartments. A general configuration like this is shown in Fig. 4.1. Here, for the sake of mathematical generality, let us consider that the compartment, R_i , is communicating with the compartment, R_j , adjacent along the x -axis, through the interface boundary, ∂R_{ip} with compartment, R_k , adjacent along the y -axis through the interface boundary, ∂R_{ik} , and with another compartment, R_m , adjacent along the z -axis, through the interface boundary, ∂R_{im} . The compartment, R_i , may have extreme boundaries, $\partial R_{\alpha i}$, $\partial R_{\beta i}$, and $\partial R_{\gamma i}$. A dimensionless form of the diffusivity equation for the flow of a single-phase, slightly-compressible fluid with constant compressibility through an anisotropic and homogeneous porous medium in the i th compartment which is producing through N_w , partially-penetrating, line-sink wells, as illustrated in Fig. 4.2, is given by:

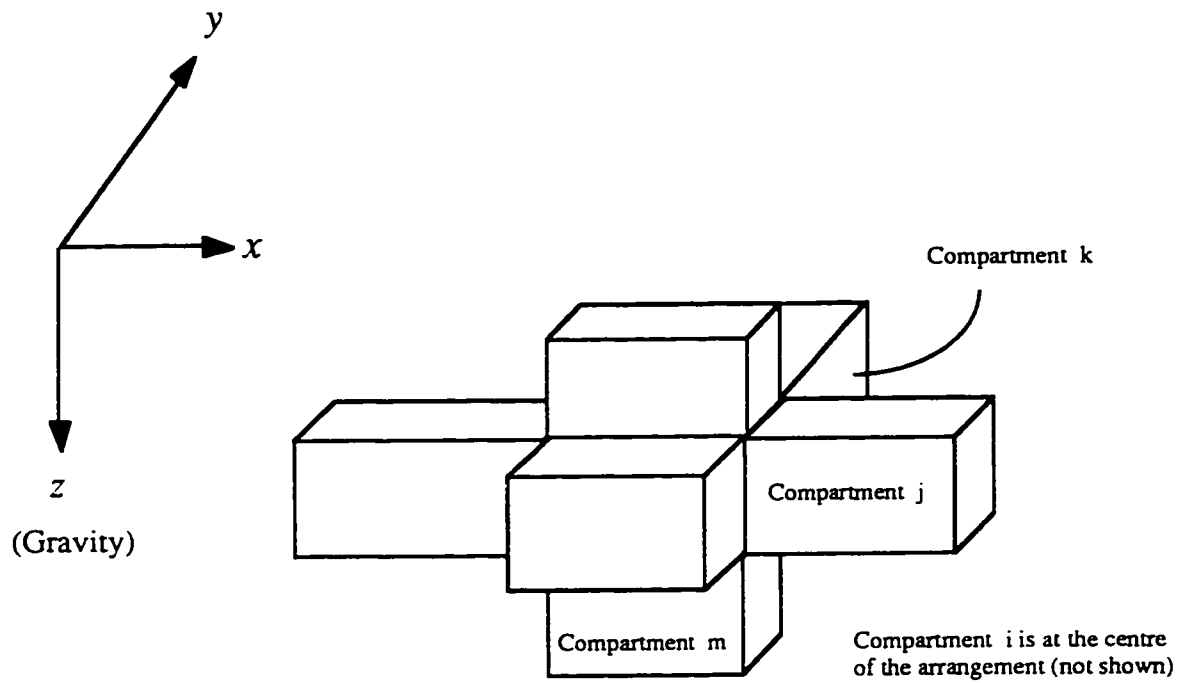


Figure 4.1: Schematic of a general arrangement in a three-dimensional compartmentalized system.

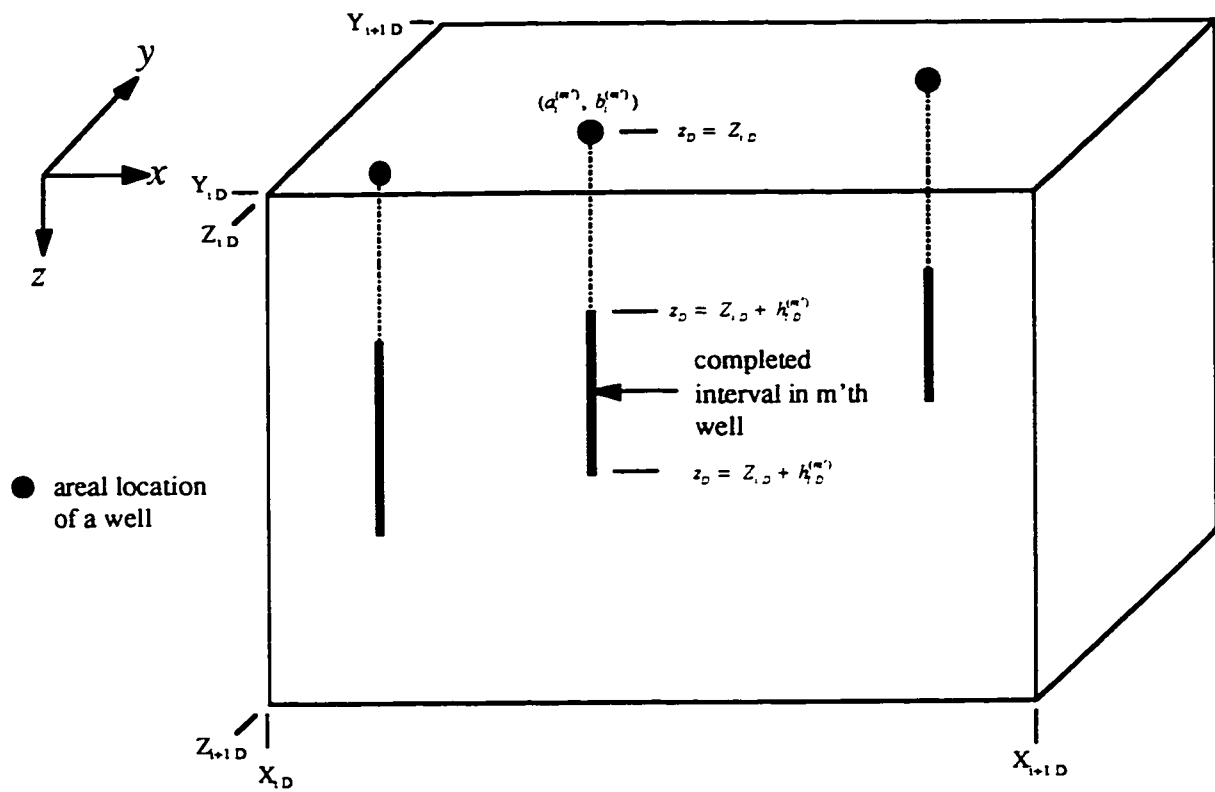


Figure 4.2: Schematic showing location of wells in *i*th compartment.

$$\alpha_{x_i} \frac{\partial^2 \Phi_{i,D}}{\partial x_D^2} + \alpha_{y_i} \frac{\partial^2 \Phi_{i,D}}{\partial y_D^2} + \alpha_{z_i} \frac{\partial^2 \Phi_{i,D}}{\partial z_D^2} + \sum_{m'=1}^{N_{\alpha_i}} \frac{q_{i,D}^{(m')}(t_D)}{h_{2i,D}^{(m')} - h_{1i,D}^{(m')}} \delta(x_D - a_{i,D}^{(m')}) \delta(y_D - b_{i,D}^{(m')}) = e_i \frac{\partial \Phi_{i,D}}{\partial t_D} \dots (4.2)$$

The initial and boundary conditions are prescribed as:

(a) initial condition:

$$\Phi_{i,D}(x_D, y_D, z_D, 0) = \Phi_{oi,D} = \frac{k_p h_p}{q_p \mu_p B_p} (\Phi_p - \Phi_{oi}) \dots (4.3)$$

(b) boundary conditions:

(i) at an extreme boundary parallel to the y - z -plane, $\partial R_{\alpha_{yz}}$,

$$\left[\gamma_{\alpha_{yz}} \frac{\partial \Phi_{i,D}}{\partial x_D} + \xi_{\alpha_{yz}} \Phi_{i,D} \right]_{\partial R_{\alpha_{yz}}} = f_{\alpha_{yz}}(t_D) \dots (4.4)$$

(ii) at an extreme boundary parallel to the x - z -plane, $\partial R_{\alpha_{xz}}$,

$$\left[\gamma_{\alpha_{xz}} \frac{\partial \Phi_{i,D}}{\partial y_D} + \xi_{\alpha_{xz}} \Phi_{i,D} \right]_{\partial R_{\alpha_{xz}}} = f_{\alpha_{xz}}(t_D) \dots (4.5)$$

(iii) at an extreme boundary parallel to the x - y -plane, $\partial R_{\alpha_{xy}}$,

$$\left[\gamma_{\alpha_{xy}} \frac{\partial \Phi_{i,D}}{\partial z_D} + \xi_{\alpha_{xy}} \Phi_{i,D} \right]_{\partial R_{\alpha_{xy}}} = f_{\alpha_{xy}}(t_D) \dots (4.6)$$

(iv) at an interface parallel to the y - z -plane, ∂R_y ,

$$-\frac{l}{s_{ij}} [\Phi_{iD} - \Phi_{jD}]_{\partial R_y} = \alpha_{xi} \left[\frac{\partial \Phi_{iD}}{\partial x_D} \right]_{\partial R_y} \dots \dots \dots (4.7)$$

$$\alpha_{xi} \left[\frac{\partial \Phi_{iD}}{\partial x_D} \right]_{\partial R_y} = \alpha_{xj} \left[\frac{\partial \Phi_{jD}}{\partial x_D} \right]_{\partial R_y} \dots \dots \dots (4.8)$$

(v) at an interface parallel to the x - z -plane, ∂R_k ,

$$-\frac{l}{s_{ik}} [\Phi_{iD} - \Phi_{kD}]_{\partial R_k} = \alpha_{yi} \left[\frac{\partial \Phi_{iD}}{\partial y_D} \right]_{\partial R_k} \dots \dots \dots (4.9)$$

$$\alpha_{yi} \left[\frac{\partial \Phi_{iD}}{\partial y_D} \right]_{\partial R_k} = \alpha_{yk} \left[\frac{\partial \Phi_{kD}}{\partial y_D} \right]_{\partial R_k} \dots \dots \dots (4.10)$$

(vi) at an interface parallel to the x - y -plane, ∂R_m ,

$$-\frac{l}{s_{im}} [\Phi_{iD} - \Phi_{mD}]_{\partial R_m} = \alpha_{zi} \left[\frac{\partial \Phi_{iD}}{\partial z_D} \right]_{\partial R_m} \dots \dots \dots (4.11)$$

$$\alpha_{zi} \left[\frac{\partial \Phi_{iD}}{\partial z_D} \right]_{\partial R_m} = \alpha_{zm} \left[\frac{\partial \Phi_{mD}}{\partial z_D} \right]_{\partial R_m} \dots \dots \dots (4.12)$$

where the dimensionless variables are defined as:

$$\Phi_{iD} = \frac{k_p h_p}{q_p \mu_p B_p} (\Phi_p - \Phi_i) \dots \dots \dots (4.13)$$

$$x_D = x/X_p \dots \dots \dots (4.14)$$

$$y_D = y/X_p \dots \dots \dots (4.15)$$

$$z_D = z/X_p \dots \dots \dots (4.16)$$

$$t_D = \frac{k_p t}{\Phi_p \mu_p c_{tp} X_p^2} \dots \dots \dots (4.17)$$

$$\alpha_{iD}^{(m')} = \alpha_i^{(m')} / X_p \dots \dots \dots (4.18)$$

$$b_{iD}^{(m')} = b_i^{(m')} X_p \dots \dots \dots (4.19)$$

$$h_{iD}^{(m')} = \frac{h_{i1}^{(m')}}{h_p} \dots \dots \dots (4.20)$$

$$h_{2iD}^{(m')} = \frac{h_{2i}^{(m')}}{h_p} \dots \dots \dots (4.21)$$

$$\alpha_{xi} = \frac{k_{xi} \mu_p B_p}{\mu_i B_i k_p} \dots \dots \dots (4.22)$$

$$\alpha_{yi} = \frac{k_{yi} \mu_p B_p}{\mu_i B_i k_p} \dots \dots \dots (4.23)$$

$$\alpha_{z_i} = \frac{k_{z_i} \mu_p B_p}{\mu_i B_i k_p} \dots\dots\dots(4.24)$$

$$e_i = \frac{\phi_i c_{t_i} B_p}{B_i \phi_p c_{t_i p}} \dots\dots\dots(4.25)$$

$$q_{iD}^{(m)}(t_D) = q_i^{(m)}(t) / q_p \dots\dots\dots(4.26)$$

where the subscript, p , refers to a reference compartment or a reference parameter.

The conditions at extreme boundaries expressed in Eqs. (4.4) through (4.6) are of the non-homogeneous, Cauchy-type which allow for any possible situation of partial communication at those locations. However, the parameters for the conditions at extreme boundaries, γ_{ox_i} , ζ_{ox_i} , γ_{oy_i} , ζ_{oy_i} , γ_{oz_i} and ζ_{oz_i} , in Eqs. (4.4) through (4.6), respectively, can be chosen in such a way that these equations would take care of the appropriate conditions due to partial communication or presence of skin at the extreme boundaries. These parameters can also be set to 0 or 1 to obtain the conditions at the extreme boundaries of the Dirichlet- or the Neumann-type. The time-dependent functions, $f_{ox_i}(t_D)$, $f_{oy_i}(t_D)$ and $f_{oz_i}(t_D)$ in Eqs. (4.4) through (4.6), respectively, allow for specifying any time-dependent conditions at the extreme boundaries. Thus, the mathematical formulation, described by Eqs. (4.2) through (4.12), deals with time-dependent variations of production rates and extreme boundary conditions directly.

4.2.2 Solution of Differential Equations

An integral-transform technique for finite, composite domains, based on the theory and technique as developed by *Title* (1965), *Title and Robinson* (1965) and *Padovan* (1974) will be used to develop an analytical solution to the set of governing differential equations, as developed in the previous Section, in the following steps:

(i) Development of integral-transform pair

To develop an integral-transform pair, it is necessary to define the corresponding eigenvalue problems. Following the similar procedure for one-dimensional flow described in Chapter 2 and also by *Padovan* (1974), three sets of eigenvalue problems with the *l*th eigenvalue as a parameter can be developed by separating variables of the homogeneous version of the set of governing differential equations listed above as follows:

x-direction eigenvalue problem

$$\frac{d^2 U_{,l}(x_D)}{dx_D^2} = -\theta_{,l}^2 \eta_{x,l} U_{,l}(x_D) \dots\dots\dots (4.27)$$

where,

$$\eta_{x,l} = e_l / \alpha_{x,l} \dots\dots\dots (4.28)$$

with the boundary conditions:

$$\left[\gamma_{\alpha,l} \frac{dU_{,l}}{dx_D} + \xi_{\alpha,l} U_{,l} \right]_{\partial R_{\alpha,l}} = 0 \dots\dots\dots (4.29)$$

$$-\frac{I}{s_{ij}} [U_{,l} - U_{,l}]_{\partial R_{ij}} = \alpha_{x,l} \left[\frac{dU_{,l}}{dx_D} \right]_{\partial R_{ij}} \dots\dots\dots (4.30)$$

$$\alpha_{x_i} \left[\frac{dU_{i,l}}{dx_D} \right]_{\partial R_y} = \alpha_{x_j} \left[\frac{dU_{j,l}}{dx_D} \right]_{\partial R_y} \dots\dots\dots(4.31)$$

y-direction eigenvalue problem

$$\frac{d^2V_{i,l}(y_D)}{dy_D^2} = -\sigma_{i,l}^2 \eta_{y_i} V_{i,l}(y_D) \dots\dots\dots(4.32)$$

where,

$$\eta_{y_i} = e_i / \alpha_{y_i} \dots\dots\dots(4.33)$$

with the boundary conditions:

$$\left[\gamma_{\alpha_i} \frac{dV_{i,l}}{dy_D} - \xi_{\alpha_i} V_{i,l} \right]_{\partial R_{\alpha_i}} = 0 \dots\dots\dots(4.34)$$

$$-\frac{l}{s_{in}} [V_{i,l} - V_{n,l}]_{\partial R_{in}} = \alpha_{y_i} \left[\frac{dV_{i,l}}{dy_D} \right]_{\partial R_{in}} \dots\dots\dots(4.35)$$

$$\alpha_{y_i} \left[\frac{dV_{i,l}}{dy_D} \right]_{\partial R_{in}} = \alpha_{y_n} \left[\frac{dV_{n,l}}{dy_D} \right]_{\partial R_{in}} \dots\dots\dots(4.36)$$

z-direction eigenvalue problem

$$\frac{d^2W_{i,l}(z_D)}{dz_D^2} = -\epsilon_{i,l}^2 \eta_{z_i} W_{i,l}(z_D) \dots\dots\dots(4.37)$$

where,

$$\eta_{z,i} = e_i / \alpha_{z,i} \dots\dots\dots(4.38)$$

with the boundary conditions:

$$\left[\gamma_{\alpha,i} \frac{dW_{i,l}}{dz_D} + \xi_{\alpha,i} W_{i,l} \right]_{\partial R_{\alpha,i}} = 0 \dots\dots\dots(4.39)$$

$$- \frac{l}{s_{in}} [W_{i,l} - W_{n,l}]_{\partial R_{in}} = \alpha_{z,i} \left[\frac{dW_{i,l}}{dz_D} \right]_{\partial R_{in}} \dots\dots\dots(4.40)$$

$$\alpha_{z,i} \left[\frac{dW_{i,l}}{dz_D} \right]_{\partial R_{in}} = \alpha_{z,n} \left[\frac{dW_{n,l}}{dz_D} \right]_{\partial R_{in}} \dots\dots\dots(4.41)$$

The functions $U_{i,l}(x_D)$, $V_{i,l}(y_D)$ and $W_{i,l}(z_D)$ are the l th eigenfunctions for the i th compartment in the x -, y - and z -directions, respectively. *Title* (1965) and *Title and Robinson* (1965) mentioned that the eigenvalue problems with the x -, y - and z -directions described above are related by the condition of identical time-behavior of the dimensionless potential on both sides of an interface boundary which is given as follows:

$$\theta_{i,l}^2 + \sigma_{i,l}^2 + \epsilon_{i,l}^2 = \theta_{j,l}^2 + \sigma_{j,l}^2 + \epsilon_{j,l}^2 \dots\dots\dots(4.42)$$

Salt (1983 a and b) and *Mikhailov and Ozisik* (1986) also endorsed the above relationship between eigenvalues in the x -, y - and z -directions, respectively. Following a similar procedure described by *Padovan* (1974), one has the following integral-transform pair as:

Inversion formula:

$$\Phi_{i,D} = \sum_{i=1}^n \frac{\bar{\Phi}_{D,i} U_{i,l} V_{i,l} W_{i,l}}{N_i} \dots\dots\dots(4.43)$$

Transformation formula:

$$\bar{\Phi}_{D,i} = \sum_{i=1}^n e_i \iiint_{R_i} \Phi_{i,D} U_{i,l} V_{i,l} W_{i,l} dx_D dy_D dz_D \dots\dots\dots(4.44)$$

where,

$$N_i = \sum_{i=1}^n e_i \iiint_{R_i} U_{i,l}^2 V_{i,l}^2 W_{i,l}^2 dx_D dy_D dz_D \dots\dots\dots(4.45)$$

(ii) Integral transformation of differential equations along with their conditions

Multiplying both sides of Eq. (4.2) by $U_{i,l} V_{i,l} W_{i,l} dx_D dy_D dz_D$ and integrating over R_i and then summing up the resulting expressions over all compartments, one gets,

$$\begin{aligned} & \sum_{i=1}^n \left[\alpha_{x_i} \iiint_{R_i} \frac{\partial^2 \Phi_{i,D}}{\partial x_D^2} U_{i,l} V_{i,l} W_{i,l} dx_D dy_D dz_D - \alpha_{y_i} \iiint_{R_i} \frac{\partial^2 \Phi_{i,D}}{\partial y_D^2} U_{i,l} V_{i,l} W_{i,l} dx_D dy_D dz_D \right. \\ & \left. + \alpha_{z_i} \iiint_{R_i} \frac{\partial^2 \Phi_{i,D}}{\partial z_D^2} U_{i,l} V_{i,l} W_{i,l} dx_D dy_D dz_D \right] + \sum_{i=1}^n \sum_{m=1}^{N_i} \frac{q_{i,D}^{(m)}(t_D)}{h_{2i,D}^{(m)} - h_{1i,D}^{(m)}} \iiint_{R_i} U_{i,l} V_{i,l} W_{i,l} \\ & \cdot \delta(x_D - a_{i,D}^{(m)}) \delta(y_D - b_{i,D}^{(m)}) dx_D dy_D dz_D = \sum_{i=1}^n e_i \iiint_{R_i} \frac{\partial \Phi_{i,D}}{\partial t_D} U_{i,l} V_{i,l} W_{i,l} dx_D dy_D dz_D \dots\dots(4.46) \end{aligned}$$

The first three terms of the above equation are simplified by using Green's theorem. Then substituting the values from Eqs. (4.4) through (4.12), (4.27), (4.29) through (4.32), (4.34) through (4.37), (4.39) through (4.41), (4.44) and (4.45) in Eq. (4.35), it can be shown that,

$$-\lambda_l^2 \bar{\Phi}_{Dl} + g_l = \frac{d\bar{\Phi}_{Dl}}{dt_D} \dots\dots\dots(4.47)$$

where,

$$\lambda_l^2 = \theta_l^2 + \sigma_l^2 + \varepsilon_l^2 \dots\dots\dots(4.48)$$

$$g_l(t_D) = \sum_{i=1}^n \left[\sum_{m=1}^{N_{oi}} \frac{q_{iD}^{(m)}(t_D) U_{i1}(\alpha_{iD}^{(m)}) V_{i1}(b_{iD}^{(m)})}{h_{2iD}^{(m)} - h_{1iD}^{(m)}} \int_{\kappa_{1i}^{(m)}}^{\kappa_{2i}^{(m)}} W_{i1}(z_D) dz_D \right. \\ \left. + \left[\frac{\alpha_{x1} U_{i1} f_{\alpha x1}}{\gamma_{\alpha x1}} \right]_{\partial R_{\alpha x1}} \iint_{\partial R_{\alpha x1}} V_{i1} W_{i1} dy_D dz_D + \left[\frac{\alpha_{y1} V_{i1} f_{\alpha y1}}{\gamma_{\alpha y1}} \right]_{\partial R_{\alpha y1}} \iint_{\partial R_{\alpha y1}} U_{i1} W_{i1} dx_D dz_D \right. \\ \left. - \left[\frac{\alpha_{z1} W_{i1} f_{\alpha z1}}{\gamma_{\alpha z1}} \right]_{\partial R_{\alpha y1}} \iint_{\partial R_{\alpha y1}} U_{i1} V_{i1} dx_D dy_D \right] \dots\dots\dots(4.49)$$

$$\kappa_{1i}^{(m)} = Z_{iD} + \frac{h_p}{X_p} h_{1iD}^{(m)} \dots\dots\dots(4.50)$$

$$\kappa_{2i}^{(m)} = Z_{iD} + \frac{h_p}{X_p} h_{2iD}^{(m)} \dots\dots\dots(4.51)$$

A detailed procedure of the above step that leads to the development of an ordinary differential equation, given by Eq. (4.47), upon integral transformation is described in Chapter 2. The parameter λ_l in Eq. (4.48) is the same for each compartment. Therefore, Eqs. (4.42) and (4.48) are identical. Both of these equations ensure that the time-behavior of the dimensionless potential at either side of an interface is identical on the assumption that the skin boundary does not have any storage.

Taking the integral transformation of the initial condition, Eq. (4.3), we get,

$$\bar{\Phi}_{Dl}(t_D = 0) = \sum_{i=1}^n \Phi_{\alpha D} \iiint_{R_i} U_{i,l} V_{i,l} W_{i,l} dx_D dy_D dz_D \dots \dots \dots (4.52)$$

One now has an initial-value problem with an ordinary differential equation, given by Eq. (4.47) and with an initial condition, given by Eq. (4.52), as a result of the integral transformation of the space variables. The solution to this initial-value problem is given by,

$$\bar{\Phi}_{Dl}(t_D) = \left[\bar{\Phi}_{Dl}(0) + \int_0^{t_D} g_l(\tau) e^{\lambda_i \tau} d\tau \right] e^{-\lambda_i t_D} \dots \dots \dots (4.53)$$

(iii) Inversion

$\bar{\Phi}_{Dl}(t_D)$ from Eq. (4.53) is inverted into $\Phi_{Dl}(x_D, y_D, z_D, t_D)$ using the inversion formula, Eq. (4.43), as follows:

$$\Phi_{Dl}(x_D, y_D, z_D, t_D) = \sum_{i=1}^n \left[\bar{\Phi}_{Dl}(t_D = 0) + \int_0^{t_D} g_l(\tau) e^{\lambda_i \tau} d\tau \right] \frac{U_{i,l}(x_D) V_{i,l}(y_D) W_{i,l}(z_D) e^{-\lambda_i t_D}}{N_i} \dots \dots \dots (4.54)$$

Before carrying out the above inversion process, it is required to have calculated a number of eigenvalues of the system. Computation of eigenvalues is discussed in the next step. In general, the rate of convergence for summing the series in Eq. (4.54) is very high. The number of eigenvalues or the number of terms required in the series is dependent on the

desired level of accuracy. For example, in a 6-compartment system, it requires about 100 sets of eigenvalues for a level of accuracy of 10^{-9} .

(iv) Computation of eigenvalues and eigenfunctions

First one needs to evaluate the l th set of eigenvalues, $\theta_{i,l}$, $\sigma_{i,l}$, and $\epsilon_{i,l}$ for each compartment ($i = 1, 2, 3, 4, \dots, n$) in order to determine the corresponding eigenfunctions, $U_{i,l}$, $V_{i,l}$ and $W_{i,l}$. According to *Mikhailov and Vulchanov (1983)*, *Mikhailov and Ozisik (1984)* and *Cotta (1993)*, the general expressions for these eigenfunctions are the general solutions to Eqs. (4.27), (4.32) and (4.37), respectively, as follows:

$$U_{i,l}(x_D) = U_{i,l}^* U_{1,i,l} + U_{i,l}^{**} U_{2,i,l} \dots \dots \dots (4.56)$$

$$V_{i,l}(y_D) = V_{i,l}^* V_{1,i,l} + V_{i,l}^{**} V_{2,i,l} \dots \dots \dots (4.57)$$

$$W_{i,l}(z_D) = W_{i,l}^* W_{1,i,l} + W_{i,l}^{**} W_{2,i,l} \dots \dots \dots (4.58)$$

where,

$$U_{1,i,l}(\theta_{i,l}, x_D) = \frac{\sin(\theta_{i,l} \sqrt{\eta_{x_i}} (X_{i+1,D} - x_D))}{\sin(\theta_{i,l} \sqrt{\eta_{x_i}} (X_{i+1,D} - X_{i,D}))} \dots \dots \dots (4.59)$$

$$U_{2,i,l}(\theta_{i,l}, x_D) = \frac{\sin(\theta_{i,l} \sqrt{\eta_{x_i}} (x_D - X_{i,D}))}{\sin(\theta_{i,l} \sqrt{\eta_{x_i}} (X_{i+1,D} - X_{i,D}))} \dots \dots \dots (4.60)$$

$$V_{1,l}(\sigma_{il}, y_D) = \frac{\sin(\sigma_{il} \sqrt{\eta_{y_l}} (Y_{i+1,D} - y_D))}{\sin(\sigma_{il} \sqrt{\eta_{y_l}} (Y_{i+1,D} - Y_{i,D}))} \dots (4.61)$$

$$V_{2,l}(\sigma_{il}, y_D) = \frac{\sin(\sigma_{il} \sqrt{\eta_{y_l}} (y_D - Y_{i,D}))}{\sin(\sigma_{il} \sqrt{\eta_{y_l}} (Y_{i+1,D} - Y_{i,D}))} \dots (4.62)$$

$$W_{1,l}(\epsilon_{il}, z_D) = \frac{\sin(\epsilon_{il} \sqrt{\eta_{z_l}} (Z_{i+1,D} - z_D))}{\sin(\epsilon_{il} \sqrt{\eta_{z_l}} (Z_{i+1,D} - Z_{i,D}))} \dots (4.63)$$

$$W_{2,l}(\epsilon_{il}, z_D) = \frac{\sin(\epsilon_{il} \sqrt{\eta_{z_l}} (z_D - Z_{i,D}))}{\sin(\epsilon_{il} \sqrt{\eta_{z_l}} (Z_{i+1,D} - Z_{i,D}))} \dots (4.64)$$

Also, $U_{i,l}^*$ and $U_{i,l}^{**}$ are the values of $U_{i,l}(x_D)$ at $x_D = X_{i,D}$ and $X_{i-1,D}$, respectively; $V_{i,l}^*$ and $V_{i,l}^{**}$ are the values of $V_{i,l}(y_D)$ at $y_D = Y_{i,D}$ and $Y_{i-1,D}$, respectively; and $W_{i,l}^*$ and $W_{i,l}^{**}$ are the values of $W_{i,l}(z_D)$ at $z_D = Z_{i,D}$ and $Z_{i-1,D}$, respectively.

Substituting Eq. (4.56) in the boundary conditions in the x -direction eigenvalue problem (Eqs. (4.29) through (4.31)), Eq. (4.57) in the y -direction eigenvalue problem (Eqs. (4.34) through (4.36)), and also Eq. (4.58) in the z -direction eigenvalue problem (Eqs. (4.39) through (4.41)) results in three systems of linear, homogeneous algebraic equations in $U_{i,l}^*$ and $U_{i,l}^{**}$, $V_{i,l}^*$ and $V_{i,l}^{**}$, and $W_{i,l}^*$ and $W_{i,l}^{**}$, respectively, with eigenvalues as parameters. Thus, a three-dimensional eigenvalue problem in this study has been converted into three one-dimensional eigenvalue problems related by the condition expressed by Eq. (4.42). For n compartments, there are $3n$ of l th eigenvalues to be calculated. There are also $3n$ non-linear equations available for the purpose of calculating $3n$ eigenvalues. Of these $3n$ equations, there are $(n - 1)$ equations due to the continuity of time-independent behavior at an interface-boundary and the other $(2n + 1)$ equations are from the conditions of non-

trivial values of eigenfunctions (*Rahman and Ambastha, 1996a*). *Padovan (1974)* mentions that the positive roots of this simultaneous system of equations are the eigenvalues and that they can be computed by using a suitable method. In this study, each set of eigenvalues is computed by using Newton's method (*Scarborough, 1966*). Since the mathematical model developed in this Chapter is an extension of that for the one-dimensional flow situation described in Chapter 2, a similar procedure has been followed here to calculate the eigenvalues and eigenfunctions.

The formal solution to the set of Eqs. (4.2) through (4.12) is given by Eq. (4.54). This solution is subject to changes corresponding to certain special cases which will be discussed later in Section 4.2.7.

4.2.3 Computer Program for Numerical Values

A computer program incorporating the solution scheme described in Section 4.2.2 has been developed in FORTRAN 77 for the purpose of generating numerical values of the solution developed in this Chapter. The complete source code and a sample data file are presented in Appendix C. This program has a number of Subroutines and Subroutine-Subfunctions which are coordinated by the Main Program. Typically, it takes about 14 minutes to run the program for a 6-compartment system in the "Numerical Server" (RS/6000 Model 59Hs, 66.7 MHz) at the University of Alberta.

4.2.4 Average Compartment Potential

An average compartment potential at a given time is a measure of the available driving force to produce hydrocarbon from that compartment. Knowing this value also helps to prepare a production schedule that avoids producing from a compartment below the

bubble-point pressure. *Ehlig-Economides* (1994) has presented an expression for the average compartment pressure based on the assumption that the system has already reached pseudosteady state. The expression for the volumetric average dimensionless potential in the *i*th compartment as a function of dimensionless time is given by:

$$\Phi_{i,D,ave}(t_D) = (1/A_i) \iiint_{R_i} \Phi_{i,D}(x_D, y_D, z_D, t_D) dx_D dy_D dz_D \dots\dots\dots(4.65)$$

where,

$$A_i = (X_{m,D} - X_{i,D}) (Y_{m,D} - Y_{i,D}) (Z_{m,D} - Z_{i,D}) \dots\dots\dots(4.66)$$

Substituting the expression for $\Phi_{i,D}$ from Eq. (4.54) in Eq. (4.65) results in the following expression,

$$\Phi_{i,D,ave}(t_D) = \sum_{l=1}^{\infty} \left[\bar{\Phi}_{D,l}(t_D = 0) - \int_0^{t_D} g_l(\tau) e^{\lambda_l^i \tau} d\tau \right] \frac{\bar{U}_{i,l} \bar{V}_{i,l} \bar{W}_{i,l} e^{-\lambda_l^i t_D}}{A_i N_i} \dots\dots\dots(4.67)$$

where,

$$\bar{U}_{i,l} = \int_{X_{i,D}}^{X_{m,D}} U_{i,l}(x_D) dx_D \dots\dots\dots(4.68)$$

$$\bar{V}_{i,l} = \int_{Y_{i,D}}^{Y_{m,D}} V_{i,l}(y_D) dy_D \dots\dots\dots(4.69)$$

$$\bar{W}_{i,l} = \int_{Z_{i,D}}^{Z_{m,D}} W_{i,l}(z_D) dz_D \dots\dots\dots(4.70)$$

The expression for the average dimensionless potential in the *i*th compartment shown in Eq. (4.67) has considered the dimensionless potential in that compartment based on extreme boundary conditions of the Cauchy-type. However, similar expressions for the average dimensionless potential with any other type of conditions at the extreme boundaries can be developed by taking care of the appropriate changes in the expression for dimensionless potential which will be discussed later.

4.2.5 Cumulative Influx through an Interface

Following a similar approach to that taken in Chapter 2, the expression for the dimensionless cumulative influx through an interface at ∂R_{ij} (parallel to the *y-z*-plane) as a function of dimensionless time is given by:

$$Q_{ijD}(t_D) = \int_0^{t_D} q_{ijD}(\tau) d\tau \dots \dots \dots (4.71)$$

where,

$$q_{ijD} = -\alpha_{x_i} C_{h_p} \int_{Y_{iD}}^{Y_{j+1D}} \int_{Z_{iD}}^{Z_{j+1D}} \left[\frac{\partial \Phi_{iD}}{\partial x_D} \right]_{\partial R_{ij}} dy_D dz_D \dots \dots \dots (4.72)$$

$$C_{h_p} = X_p / h_p \dots \dots \dots (4.73)$$

In Eq. (4.72), the flow from the *j*th compartment to the *i*th compartment is considered to be positive. Therefore a positive value of cumulative influx, $Q_{ijD}(t_D)$, implies that the net flow has been from the *j*th compartment to the *i*th compartment.

Substituting Eqs. (4.54) and (4.72) into Eq. (4.71), one gets,

$$Q_{ijD}(t_D) = -\alpha_{x_i} C_{h_p} \sum_{l=1}^{\infty} \left\{ \left[\frac{dU_{i,l}}{dx_D} \right]_{x_{i-1,D}} \frac{\bar{V}_{i,l} \bar{W}_{i,l}}{N_i} \int_0^{t_D} F(\tau) e^{-\lambda^i \tau} d\tau \right\} \dots\dots\dots (4.74)$$

where,

$$F_i(\tau) = \int_0^{\tau} g_i(\tau') e^{\lambda^i \tau'} d\tau' \dots\dots\dots (4.75)$$

Expressions, similar to that in Eq. (4.74), for the dimensionless cumulative influxes, Q_{ikD} , through an interface parallel to the x - z -plane, ∂R_{ik} , and Q_{imD} , through an interface parallel to the x - y -plane, ∂R_{im} , can be derived.

4.2.6 Relationship between Skin Factor and Barrier Transmissibility

Fox et al. (1988) and *Stewart and Whaballa* (1989) gave the expression for the rate of fluid that communicates between the i th and j th compartments as:

$$q_{ij} = T_{ij} (\bar{\Phi}_i - \bar{\Phi}_j) \dots\dots\dots (4.76)$$

The relationship between the skin factor at an interface as used in this study and the barrier transmissibility as defined by *Fox et al.* (1988) and *Stewart and Whaballa* (1989) is given by:

$$s_{ij} = [k_p / B_p \mu_p T_y (\bar{\Phi}_i - \bar{\Phi}_j)] \int_{y_i}^{y_{i+1}} \int_{z_i}^{z_{i+1}} [\Phi_i - \Phi_j]_{\partial R_y} dy dz \dots\dots\dots(4.77)$$

where $[\Phi_i - \Phi_j]_{\partial R_y}$ implies the difference in potentials between the *i*th and *j*th compartments on an interface parallel to the *y*-axis, ∂R_y . Equation (4.77) can be written in dimensionless form as follows:

$$s_{ij} = \frac{v_{ij}}{T_{yD}} \dots\dots\dots(4.78)$$

where,

$$T_{yD} = \frac{\mu_p B_p T_y}{k_p X_p} \dots\dots\dots(4.79)$$

$$v_{ij} = [1/(\bar{\Phi}_{iD} - \bar{\Phi}_{jD})] \int_{y_{iD}}^{y_{i+1D}} \int_{z_{iD}}^{z_{i+1D}} [\Phi_{iD} - \Phi_{jD}]_{\partial R_y} dy_D dz_D \dots\dots\dots(4.80)$$

Expressions, similar to Eqs. (4.77) and (4.78), can be developed for the relationships between T_{ik} and s_{ik} due to fluid communication through an interface parallel to the *x-z*-plane, ∂R_{ik} , and between T_{im} and s_{im} due to fluid communication through an interface parallel to the *x-y*-plane, ∂R_{im} .

4.2.7 Modification of Solution for Special Cases

The general solution developed above needs modification in some special cases. These are discussed below:

(i) Perfect communication at an interface

If there is a perfect communication at an interface, ∂R_{ij} , one can write, $s_{ij} \rightarrow 0$. This establishes the condition of continuity of potential. Thus, the corresponding interface conditions described in Eqs. (4.7) and (4.8) take the following form:

$$[\Phi_{i,D}]_{\partial R_{ij}} = [\Phi_{j,D}]_{\partial R_{ij}} \dots\dots\dots(4.81)$$

$$\alpha_{x_i} \left[\frac{\partial \Phi_{i,D}}{\partial x_D} \right]_{\partial R_{ij}} = \alpha_{x_j} \left[\frac{\partial \Phi_{j,D}}{\partial x_D} \right]_{\partial R_{ij}} \dots\dots\dots(4.82)$$

Subsequent interface conditions for the corresponding eigenvalue problem should also be updated reflecting the conditions expressed by Eqs. (4.81) and (4.82).

(ii) Dirichlet-type condition at an extreme boundary

When the condition at an extreme boundary is of the Dirichlet-type, the solution as given by Eq. (4.54) remains the same (Ozisik, 1980). But the expression for g_l in Eq. (4.49) needs to be modified. For example, if an extreme boundary, ∂R_{oyz} , is parallel to the y - z -plane in the i th compartment has the dimensionless potential specified, then the following changes should be introduced:

Here, $\gamma_{\alpha_i} = 0$, therefore,

$$\text{replace } \frac{U_{i,l}}{\gamma_{\alpha_i}} \text{ by } \frac{1}{\xi_{\alpha_i}} \frac{dU_{i,l}}{dx_D}.$$

(iii) Neumann-type condition at extreme boundaries

When the conditions at the extreme boundaries are mixed with both the Cauchy- and the Neumann-types, then the expression for Φ_{iD} in Eq. (4.54) remains unchanged (Ozisik, 1980). But when the conditions at all the extreme boundaries are of the Neumann-type, the solution given by Eq. (4.54) needs to be augmented by an amount $\Phi_{D\text{ add}}$, due to the fact that $\lambda_0 = 0$ is an eigenvalue of the system. This means that an additional term corresponding to the zero-eigenvalue has to be added to the solution presented in Eq. (4.54). Here all $\xi_{\alpha x_i}$'s, $\xi_{\alpha y_i}$'s and $\xi_{\alpha z_i}$'s are equal to 0. The additional term corresponding to the zero-eigenvalue has been derived following the procedure discussed in Chapter 2 and is presented below:

$$\Phi_{D\text{ add}} = \frac{l}{N_o} [\bar{\Phi}_{D\text{ add}}(t_D = 0) + \int_0^{t_D} g_o(\tau) d\tau] \dots\dots\dots (4.83)$$

where,

$$g_o(\tau) = \sum_{i=1}^n \left[\sum_{m'=1}^{N_{w_i}} \frac{q_{iD}^{(m')}(\tau)}{C_{hp}} d\tau - \left[\frac{\alpha_{x_i} f_{\alpha x_i}}{\gamma_{\alpha x_i}} \right]_{R_{\alpha x_i}} \iint_{\partial R_{\alpha x_i}} dy_D dz_D \right. \\ \left. - \left[\frac{\alpha_{y_i} f_{\alpha y_i}}{\gamma_{\alpha y_i}} \right]_{R_{\alpha y_i}} \iint_{\partial R_{\alpha y_i}} dx_D dz_D - \left[\frac{\alpha_{z_i} f_{\alpha z_i}}{\gamma_{\alpha z_i}} \right]_{R_{\alpha z_i}} \iint_{\partial R_{\alpha z_i}} dx_D dy_D \right] \dots\dots\dots (4.84)$$

$$N_o = \sum_{i=1}^n e_i \iiint_{R_i} dx_D dy_D dz_D \dots\dots\dots (4.85)$$

$$\bar{\Phi}_{D\text{ add}}(t_D = 0) = \sum_{i=1}^n \Phi_{oiD} \iiint_{R_i} dx_D dy_D dz_D \dots\dots\dots (4.86)$$

and C_{hp} has already been defined in Eq. (4.73).

4.3 Validation of New Solution

It is necessary to validate the new solution to check its arithmetic reliability. Here, the new solution for a compartmentalized system developed in this Chapter is validated by comparing a number of its simplified forms with those of homogeneous systems. Analytical solutions for a homogeneous and isotropic, rectangular parallelepiped producing through a partially-penetrating well are presented in Appendix D following the ideas of *Hovanessian* (1961). The solutions for a homogeneous system for special cases of the compartmentalized system are compared with the solutions for the homogeneous system.

A homogeneous, isotropic parallelepiped ($X_{0D} = Y_{0D} = Z_{0D} = 1$) is considered to be producing through a partially-penetrating well for validation purposes. The corresponding solution for the compartmentalized system is generated by considering three compartments with identical rock and fluid properties and no skins at the interfaces. Two cases of the extreme boundary conditions are considered below.

All Boundaries Closed

Here all the extreme boundaries are considered closed. Figure 4.3 shows the comparison of the dimensionless potential responses, the Cartesian derivative, $d\Phi_D/dt_D$, and the particular derivative, $(t_D)^{1.5} d\Phi_D/dt_D$, for spherical flow with dimensionless time at $x_D = 0.51$, $y_D = 0.51$ and $z_D = 0.5$ for systems with closed boundaries. The well is located areally at $x_D = 0.5$ and $y_D = 0.5$, and vertically between $h_{1D} = 0.45$ and $h_{2D} = 0.55$, and is producing at a dimensionless rate of $q_D = 1$. According to *Issaka and Ambastha* (1996), an infinite-acting spherical flow period is characterized by a zero-slope line of this particular derivative. Therefore, the transient period (up to $t_D = 0.1$, approximately) for this particular case is dominated by the infinite-acting spherical flow pattern due to a very

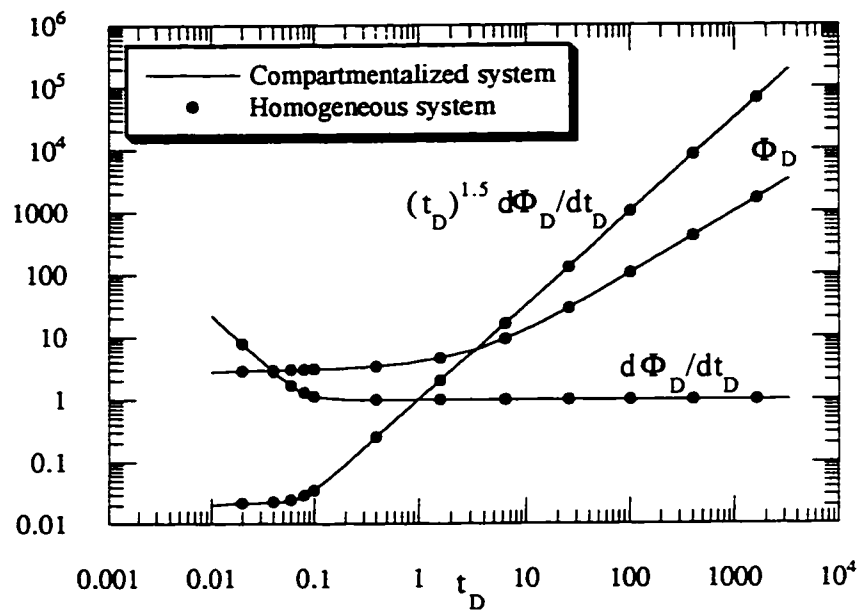


Figure 4.3: Comparison of the dimensionless potential response and its derivatives from the solution of a compartmentalized system with those from a closed, homogeneous system.

small producing interval (10% of total pay). It is also observed that the pseudosteady-state flow period starts approximately at $t_D = 0.1$ which is characterized by a zero-slope line of the Cartesian derivative (Proano and Lilley, 1986). This plot shows an excellent match of all profiles.

Figure 4.4 shows the comparison of the dimensionless potential responses, its Cartesian and semilog derivatives with dimensionless time at $x_D = 0.5$, $y_D = 0.5$ and $z_D = 0.5$ for systems with closed boundaries. The well is located areally at $x_D = 0.5$ and $y_D = 0.5$ and vertically between $h_{1D} = 0.0$ and $h_{2D} = 1.0$ (fully-penetrating interval), and is producing at a constant dimensionless rate of $q_D = 1$. As a result of the presence of the fully-penetrating interval, the flow of fluid degenerates to the two-dimensional flow system and therefore is comparable with the solution of Hovanessian (1961). This graph shows an excellent match of the dimensionless potential responses generated from the solutions of a compartmentalized system, a homogeneous parallelepiped system and a homogeneous, rectangular system as developed by Hovanessian (1961).

All Boundaries at Constant Potential

Here all the extreme boundaries are maintained at a constant potential (initial potential). Figure 4.5 shows the comparison of the dimensionless potential responses and its Cartesian derivative, $d\Phi_D/dt_D$, with dimensionless time at $x_D = 0.51$, $y_D = 0.51$ and $z_D = 0.5$ for systems with constant-potential boundaries. The well is located areally at $x_D = 0.5$ and $y_D = 0.5$, and vertically between $h_{1D} = 0.45$ and $h_{2D} = 0.55$, and is producing at a dimensionless rate of $q_D = 1$. This shows an excellent match of the dimensionless potential responses and its Cartesian derivative. This graph also shows that the transient period ends approximately at $t_D = 0.1$. Also, the steady-state flow starts approximately at $t_D = 0.1$ which is characterized by a zero-slope line with zero-intercept of the Cartesian

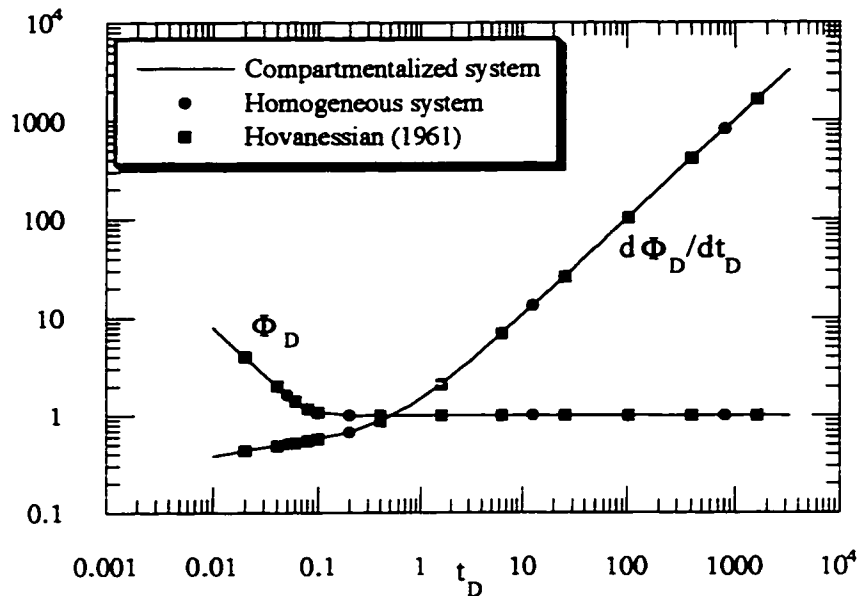


Figure 4.4: Comparison of the dimensionless potential response and its Cartesian derivative from the solution of a compartmentalized system with those from a closed, homogeneous system and Hovanessian (1961).

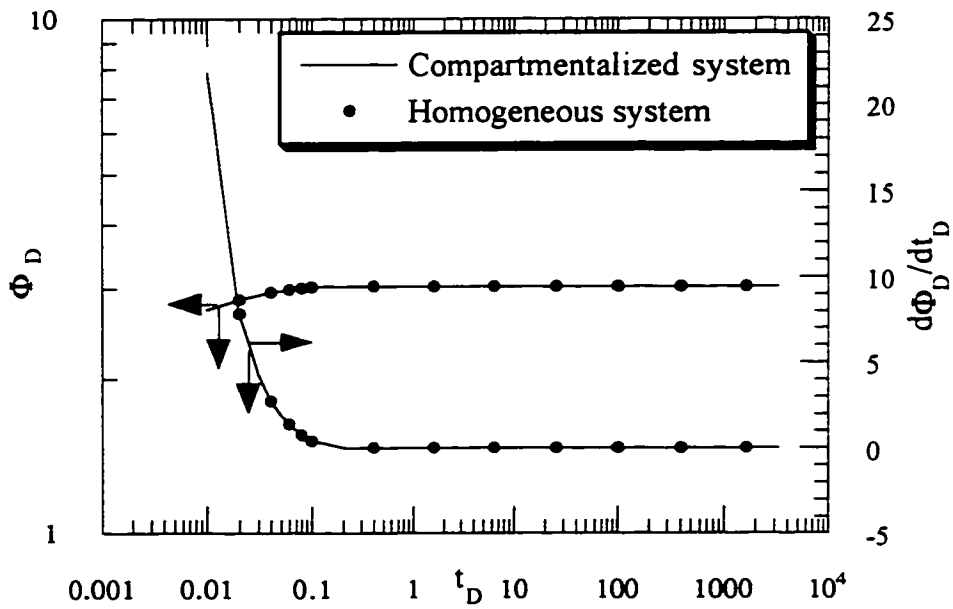


Figure 4.5: Comparison of the dimensionless potential response and its Cartesian derivative from the solution of a compartmentalized system with those from a homogeneous system.

derivative (*Proano and Lilley, 1986*). Moreover, the comparison of the potential responses and its derivative shows an excellent match.

Figure 4.6 shows the comparison of the dimensionless potential responses with dimensionless time at $x_D = 0.51$, $y_D = 0.51$ and $z_D = 0.5$ for systems with closed boundaries. The well is located areally at $x_D = 0.5$ and $y_D = 0.5$, and vertically between $h_{1D} = 0.0$ and $h_{2D} = 1.0$ (fully-penetrating interval), and is producing at a dimensionless rate of $q_D = 1$. As a result of the presence of the fully-penetrating interval, unlike the case of closed boundaries, the flow of fluid in this case does not degenerate to the two-dimensional flow system. This plot shows an excellent match of the profiles.

In the preceding discussion, a number of simplified cases leading to homogeneous systems have been compared with the corresponding homogeneous systems. The solution presented in this Chapter corresponds to an extension of the solution for the linear, one-dimensional system presented in Chapter 2. The system of partial differential equations for a three-dimensional system is essentially similar to that for a one-dimensional system. Both systems of equations are solved using an integral-transform technique. As shown in Chapter 2, the solution for a one-dimensional system was validated with a number of cases involving distinct rock and fluid properties in the compartments with or without skin at the interfaces. Therefore, the comparison of the solution for a three-dimensional system from this Chapter with the cases of distinct rock and fluid properties in the compartments with or without skin at the interfaces would lead to the same conclusion with respect to the quality of the match.

4.4 Application of New Model

The new analytical solution developed in this study may be used for understanding the transient behavior of a compartmentalized system with vertical extent. Detecting and

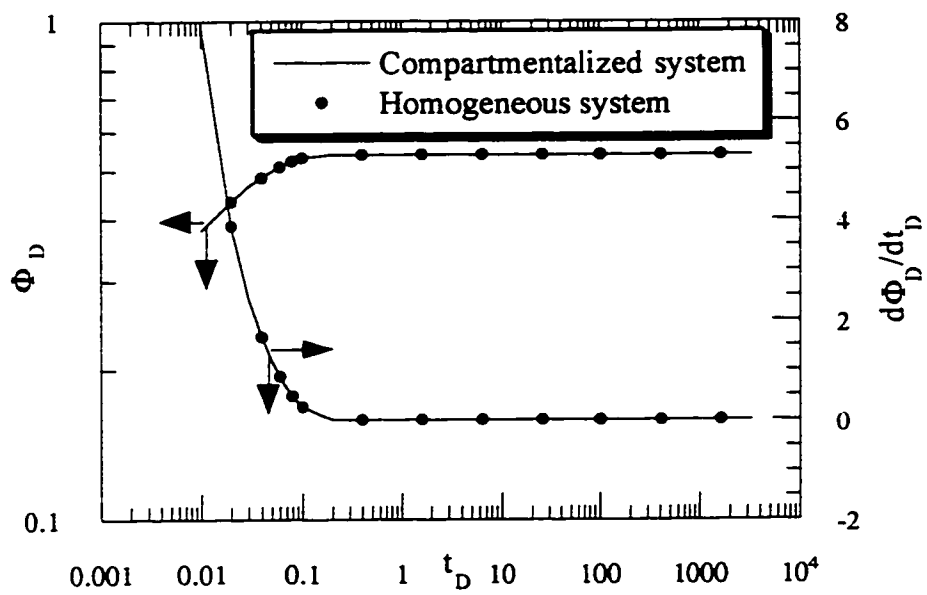


Figure 4.6: Comparison of the dimensionless potential response and its Cartesian derivative generated from the solution of a compartmentalized system with those from a homogeneous system.

quantifying the flow units and flow barriers in a compartmentalized system are very important for designing development schemes. The new analytical solution is capable of providing useful information for this purpose. It is also possible to generate type-curves of transient responses at the wellbore for diagnostic identification of compartmentalized behavior in a reservoir. This possibility will be illustrated with an example in Chapter 6.

The ability to consider the time-dependence of production rates and extreme boundary conditions directly makes this model more flexible from a practical point of view. Also, the Cauchy-type boundary condition is a general way of specifying condition at an extreme boundary which can be modified to the Dirichlet- or the Neumann-type, as special cases.

Since this model considers contrasts of rock and fluid properties including anisotropy in compartments, it can be used for studying computationally the reservoir heterogeneity.

CHAPTER 5

INTERFERENCE OF WELLS DUE TO PRODUCTION

5.1 Introduction

Interference in the pressure behavior of a well is inherent due to production through the other wells located in the same compartment or in other hydraulically-communicating compartments of the same reservoir. *Ramey et al.* (1973) have defined interference as the effect of a production well that causes a detectable pressure drop at an adjacent well. The system becomes particularly complicated when each well has a distinct production schedule. However, in this Chapter, it is intended to integrate the interference of wells due to production and to express this in terms of an equivalent parameter. Interference becomes very simple to deal with if the effects of all the wells in each compartment can be lumped into the behavior of a single well. In that case, studying with a single producing well would give the desired transient pressure effects of multiple wells with different production schedules. This Chapter shows the development of an equivalent dimensionless production rate with respect to a corresponding equivalent system as a function of dimensionless time. In this development, the advantage of the fact that the eigenvalues are not functions of time has been utilized. This means that an equivalent dimensionless production rate as a function of dimensionless time can be computed for a compartmentalized system with a multi-well and a multi-rate configuration. The primary objective of computing such equivalent production rates is to characterize a compartmentalized system with a plausible parameter, rather than in terms of a series of eigenvalues. This would also facilitate the use of solutions of homogeneous systems in a compartmentalized system under the condition of equivalence which will be illustrated later.

Hurst (1960) and *Mortada* (1960) developed analytical solutions for studying interference in radial systems with distinct rock and fluid properties. *Hurst* (1960) examined the interference pressure drop due to a point sink located in an infinite system consisting of two regions in series where the permeability has changed at some distance from the point sink. However, *Mortada* (1960) has considered a line-sink well producing from a two-region system and showed the effects of such variations of properties by comparing the transient responses with those of a homogeneous system.

Ramey et al. (1973) used the principle of superposition to generate the transient-pressure responses in rectangular reservoirs producing with multiple wells under water-drive conditions. *Dake* (1994) suggests the use of the principle of superposition in time and space to generate pressure responses in the case of multi-well and multi-rate situations. *Earlougher and Ramey* (1973) computed the dimensionless pressure responses as a function of dimensionless time at different locations within bounded rectangular reservoirs for selected locations of a producing well using the principle of superposition for the purpose of using it in interference test analysis. However, this method of superposition is not applicable in a compartmentalized system because of the presence of partially-communicating faults and the variations of rock and fluid properties. As shown in Chapters 3 and 4, multi-well and multi-rate situations are dealt with directly in the source term of the diffusivity equation for each compartment in this study. *Duong* (1989) develops the expressions for equivalent time in a multi-rate production situation with a view to applying it with type-curves based on constant-rate production incorporating the variation of production rate. These expressions are derived for both drawdown and buildup analyses. In this Chapter, a similar attempt will be made to derive an equivalent flow-rate for a compartmentalized system.

By observing the respective solutions, it has been found that the eigenvalues calculated for two- and three-dimensional flow systems represent the characteristics of a

compartmentalized system. A set of these eigenvalues *is* dependent on the following properties of a compartmentalized system:

- Geometry of the system including all the boundaries
- Location of the boundaries
- Extreme boundary conditions (homogeneous form)
- Interface conditions due to the presence of skins, if any.

However, these eigenvalues are *not* dependent on the following properties of a compartmentalized system:

- Number and location of wells in any compartment
- Production rate from a well, even as a function of time.

5.2 Mathematical Consideration

For a one-to-one correspondence of the dimensionless pressure (or potential) at a point in a compartmentalized system with that in a simpler system, one has to equate dimensionless pressures (or potentials) to find the necessary relationship. The original system is considered to have n compartments, where the i th compartment has $N_{w,i}$ ($i = 1, 2, 3, \dots, n$) wells and the m' th well in the i th compartment is producing at a dimensionless rate of $q_{i,D}^{(m')}$ (t_D) (with the $m' = 1, 2, 3, \dots, N_{w,i}$). We also consider that both original and equivalent systems have been subject to uniform pressure (or potential) initially which leads to the homogeneous initial conditions in dimensionless form for both systems with the reference pressure (or potential) taken as the initial pressure (or potential) in the definition for dimensionless pressures (or potentials) as in Eqs. (3.9) and (4.10). Also it is considered that the extreme boundaries are all closed. The source terms (g_i) that consider

the locations of wells and the production rates as a function of dimensionless time are within the diffusivity equations, expressed by Eqs. (3.1) and (4.2). In the following Sub-Sections, the equivalent systems are developed for two- and three-dimensional flow systems:

5.2.1 Two-Dimensional System

Here the solutions developed in Section 3.2, Chapter 3, are considered. The dimensionless pressure, p_{ED} , at (x_D, y_D) of an equivalent system for the original system is defined as:

$$p_{ED}(x_D, y_D, t_D) = h_{pD} \sum_{i=1}^n \sum_{m=1}^{N_{wi}} \left\{ \frac{1}{N_0} \int_0^{t_D} q_{iD}^{(m)}(\tau) d\tau \right. \\ \left. - \left[\sum_{i=1}^n U_{i,i}(a_{iD}^{(m)}) V_{i,i}(b_{iD}^{(m)}) \int_0^{t_D} q_{iD}^{(m)}(\tau) e^{\lambda_i \tau} d\tau \right] \frac{U_{i,i}(x_D) V_{i,i}(y_D) e^{-\lambda_i t_D}}{N_i} \right\} \dots \dots \dots (5.1)$$

Equivalence to Compartmentalized System with a Single Well

If an equivalent system refers to the same compartmentalized system but which is producing through a single well located at (a_{0D}, b_{0D}) in the *i*th compartment at a constant rate of $q_{ECD}(t_D)$ until the elapsed dimensionless time of t_D , then Eq. (5.1) reduces to the following relationship:

$$q_{ECD}(t_D) = \frac{1}{D_{EC}} \sum_{i=1}^n \sum_{m=1}^{N_{wi}} \left\{ \frac{1}{N_0} \int_0^{t_D} q_{iD}^{(m)}(\tau) d\tau \right. \\ \left. + \left[\sum_{i=1}^n U_{i,i}(a_{iD}^{(m)}) V_{i,i}(b_{iD}^{(m)}) \int_0^{t_D} q_{iD}^{(m)}(\tau) e^{\lambda_i \tau} d\tau \right] \frac{U_{i,i}(x_D) V_{i,i}(y_D) e^{-\lambda_i t_D}}{N_i} \right\} \dots \dots \dots (5.2)$$

where,

$$D_{EC} = \frac{t_D}{N_0} + \sum_{i=1}^{\infty} \frac{U_{,i}(a_{0D}) V_{,i}(b_{0D}) U_{,i}(x_D) V_{,i}(y_D) (1 - e^{-\lambda_i^2 t_D})}{\lambda_i^2 N_i} \dots\dots\dots(5.3)$$

Equivalence to Homogeneous Rectangular System with a Single Well

Here an equivalent system is defined as a closed, homogeneous rectangular system with the single well, located at (a_{0D}, b_{0D}) , as shown in Fig. 5.1, that is producing at a constant rate of $q_{EHD}(t_D)$ until the elapsed dimensionless time of t_D . By equating the dimensionless pressure responses at (x_{cD}, y_{cD}) of the compartmentalized system under consideration and at (x_D, y_D) of the homogeneous system, Eq. (5.1) leads to the following relationship:

$$q_{EHD}(t_D) = \frac{h_{pD}}{D_{EH}} \sum_{i=1}^n \sum_{m=1}^{N_{,i}} \left\{ \frac{1}{N_0} \int_0^{t_D} q_{,iD}^{(m)}(\tau) d\tau \right. \\ \left. + \left[\sum_{i=1}^{\infty} U_{,i}(a_{,iD}) V_{,i}(b_{,iD}) \int_0^{t_D} q_{,iD}^{(m)}(\tau) e^{\lambda_i^2 \tau} d\tau \right] \frac{U_{,i}(x_D) V_{,i}(y_D) e^{-\lambda_i^2 t_D}}{N_i} \right\} \dots\dots\dots(5.4)$$

where,

$$D_{EH} = t_D + \sum_{i=1}^{\infty} \frac{U_{,i}(a_{0D}) V_{,i}(b_{0D}) U_{,i}(x_D) V_{,i}(y_D) (1 - e^{-\lambda_i^2 t_D})}{\lambda_i^2 N_i} \dots\dots\dots(5.5)$$

The nomenclature for the symbols used in Eqs. (5.1) through (5.5) is the same as that for Chapter 3.

In the above development, the solution for a closed, homogeneous system has been taken from *Hovanessian* (1961).

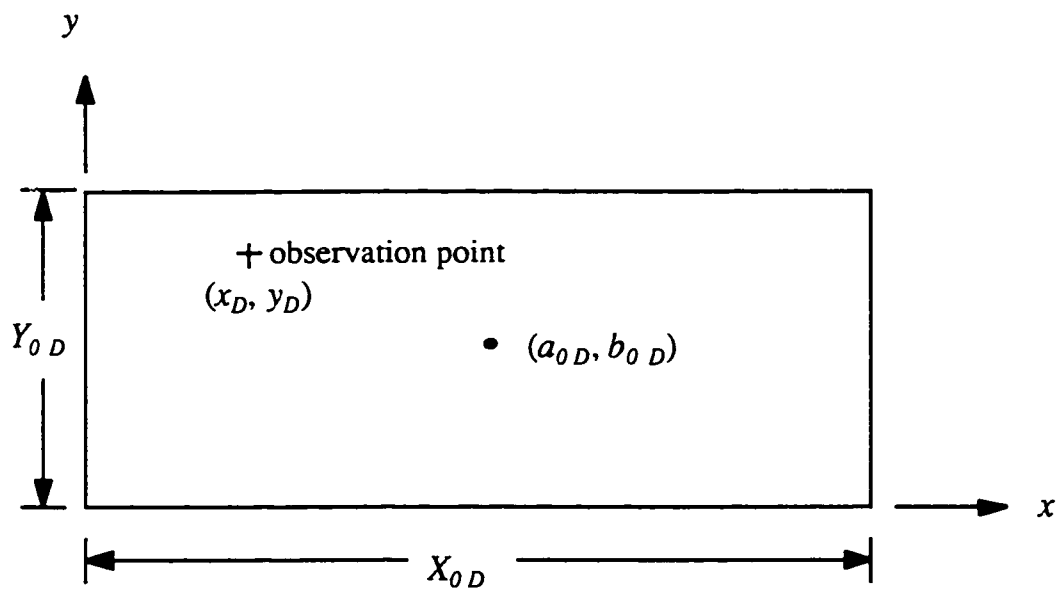


Figure 5.1: A homogeneous rectangular reservoir with a two-dimensional flow system.

5.2.2 Three-Dimensional System

Here the solutions developed in Section 4.2, Chapter 4, are considered. The dimensionless potential, Φ_{ED} , at (x_D, y_D, z_D) of an equivalent system for the original system is defined as:

$$\begin{aligned} \Phi_{ED}(x_D, y_D, z_D, t_D) = & \sum_{i=1}^n \sum_{m'=1}^{N_{wi}} \left\{ \frac{I}{C_{hp} N_0} \int_0^{t_D} q_{iD}^{(m')}(\tau) d\tau \right. \\ & + \left[\sum_{l=1}^{\infty} \frac{U_{il}(a_{iD}^{(m')}) V_{il}(b_{iD}^{(m')})}{h_{2iD}^{(m')} - h_{1iD}^{(m')}} \int_{\kappa_{li}^{(m')}}^{\kappa_{2i}^{(m')}} W_{il}(z_D) dz_D \int_0^{t_D} q_{iD}^{(m')}(\tau) e^{\lambda_i \tau} d\tau \right] \frac{U_{il}(x_D) V_{il}(y_D) W_{il}(z_D) e^{-\lambda_i t_D}}{N_l} \left. \right\} \end{aligned} \quad (5.6)$$

Equivalence to Compartmentalized System with a Single Well

If an equivalent system refers to the same compartmentalized system but which is producing through a single well located at (a_{0D}, b_{0D}, c_{0D}) in the i th compartment at a constant rate of $q_{EC D}(t_D)$ until the elapsed dimensionless time of t_D , then Eq. (5.6) reduces to the following relationship:

$$\begin{aligned} q_{EC D}(t_D) = & \frac{I}{D_{EC}} \sum_{i=1}^n \sum_{m'=1}^{N_{wi}} \left\{ \frac{I}{N_0} \int_0^{t_D} q_{iD}^{(m')}(\tau) d\tau \right. \\ & + \left[\sum_{l=1}^{\infty} \frac{U_{il}(a_{iD}^{(m')}) V_{il}(b_{iD}^{(m')})}{h_{2iD}^{(m')} - h_{1iD}^{(m')}} \int_{\kappa_{li}^{(m')}}^{\kappa_{2i}^{(m')}} W_{il}(z_D) dz_D \int_0^{t_D} q_{iD}^{(m')}(\tau) e^{\lambda_i \tau} d\tau \right] \frac{U_{il}(x_D) V_{il}(y_D) W_{il}(z_D) e^{-\lambda_i t_D}}{N_l} \left. \right\} \end{aligned} \quad (5.7)$$

where,

$$D_{EC} = \frac{t_D}{N_0} + \sum_{i=1}^n \frac{U_{i1}(a_{0D}) V_{i1}(b_{0D}) U_{i1}(x_D) V_{i1}(y_D) (1 - e^{-\lambda_i^2 t_D})}{\lambda_i^2 N_i} \dots\dots\dots(5.8)$$

The nomenclature for the symbols used in Eqs. (5.6) through (5.8) is the same as that for Chapter 4.

Equivalence to Homogeneous Parallelepiped with a Single Well

Here, an equivalent system is defined as a closed, homogeneous parallelepiped with a single well, located at (a_{0D}, b_{0D}) and completed between the interval h_{1D} and h_{2D} , as shown in Fig. 5.2, that is producing at a constant rate of $q_{EHD}(t_D)$ until the elapsed dimensionless time of t_D . By equating the dimensionless potential responses at (x_{cD}, y_{cD}, z_{cD}) of the compartmentalized system under consideration and at (x_D, y_D, z_D) of the homogeneous system, Eq. (5.6) leads to the following relationship as:

$$q_{EHD}(t_D) = \frac{l}{D_{EH}} \sum_{i=1}^n \sum_{m=1}^{N_{i1}} \left\{ \frac{l}{N_0} \int_0^{t_D} q_{iD}^{(m')}(\tau) d\tau \right. \\ \left. + \left[\sum_{i=1}^n \frac{U_{i1}(a_{iD}^{(m')}) V_{i1}(b_{iD}^{(m')})}{h_{2D}^{(m')} - h_{1D}^{(m')}} \int_{\kappa_{i1}^{(m')}}^{\kappa_{i1}^{(m')}} W_{i1}(z_D) dz_D \int_0^{t_D} q_{iD}^{(m')}(\tau) e^{\lambda_i^2 \tau} d\tau \right] \frac{U_{i1}(x_D) V_{i1}(y_D) W_{i1}(z_D) e^{-\lambda_i^2 t_D}}{N_i} \right\} \\ \dots\dots\dots(5.9)$$

where,

$$D_{EH} = t_D + \sum_{i=1}^n \frac{U_{i1}(a_{0D}) V_{i1}(b_{0D}) U_{i1}(x_D) V_{i1}(y_D) (1 - e^{-\lambda_i^2 t_D})}{\lambda_i^2 N_i} \dots\dots\dots(5.10)$$

In the above development, the solution for a closed, homogeneous rectangular parallelepiped has been taken from that presented in Appendix D.

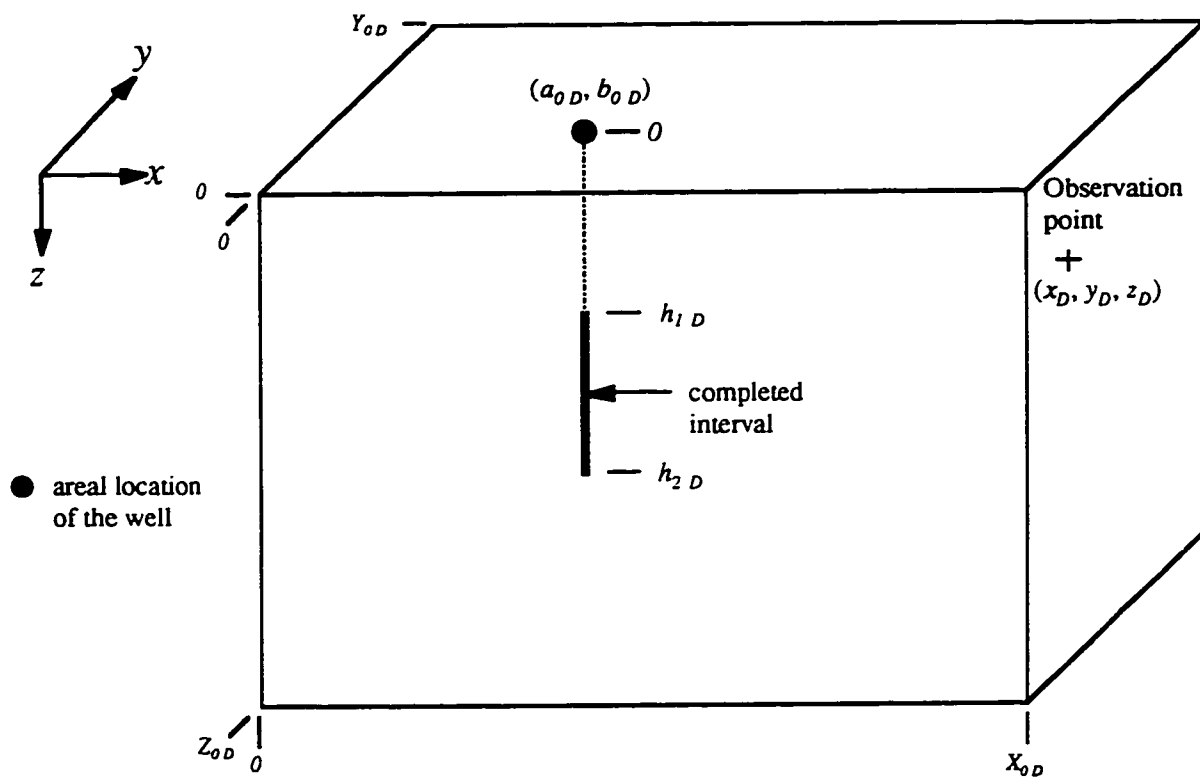


Figure 5.2: A homogeneous rectangular parallelepiped with a three-dimensional flow system.

5.3 Results and Discussion

The ideas of equivalent dimensionless production rate presented in the preceding Section are meant to help understand the effects of production rate and/or production time on the interference behavior in a compartmentalized system. Thus, the effects of all the producing and/or shut-in wells are felt through the equivalent dimensionless rate at a single well in an equivalent system. In this Section, these ideas will be illustrated by examples.

First, a two-compartment system which is subject to two-dimensional flow is considered. Wells are located at $x_D = 0.25, y_D = 0.5$ in the first compartment and at $x_D = 0.75, y_D = 0.5$ in the second compartment. Both wells are producing at a constant dimensionless rate, $q_D = 1$. Profiles for the equivalent dimensionless production rate in the same compartmentalized system with the well located at $x_D = 0.25, y_D = 0.5$ for different values of the skin factor are presented in Fig. 5.3. The periods with an equivalent dimensionless rate, $q_{E C D}$, of 2.0 signifies the fact that both the compartmentalized system with two wells and the equivalent compartmentalized system with one well have simultaneously reached pseudosteady state. But the beginning of such a period for the compartmentalized system under consideration cannot be ascertained from these profiles, because the equivalent system was late in arriving at its pseudosteady state. For instance, with $s = 100$, the system with two wells reaches pseudosteady state at $t_D = 0.08$, whereas the equivalent system with one well reaches pseudosteady state at $t_D = 14.08$; therefore, the profile in Fig. 5.3 shows the corresponding flat profile after $t_D = 14.08$. Figure 5.4 shows the profiles for the equivalent dimensionless rates for the compartmentalized system described above but with a two-rate production history having the following dimensionless rates:

From the well in the first compartment: $q_{D1} = 1.0$, while, $0 < t_D \leq 100$

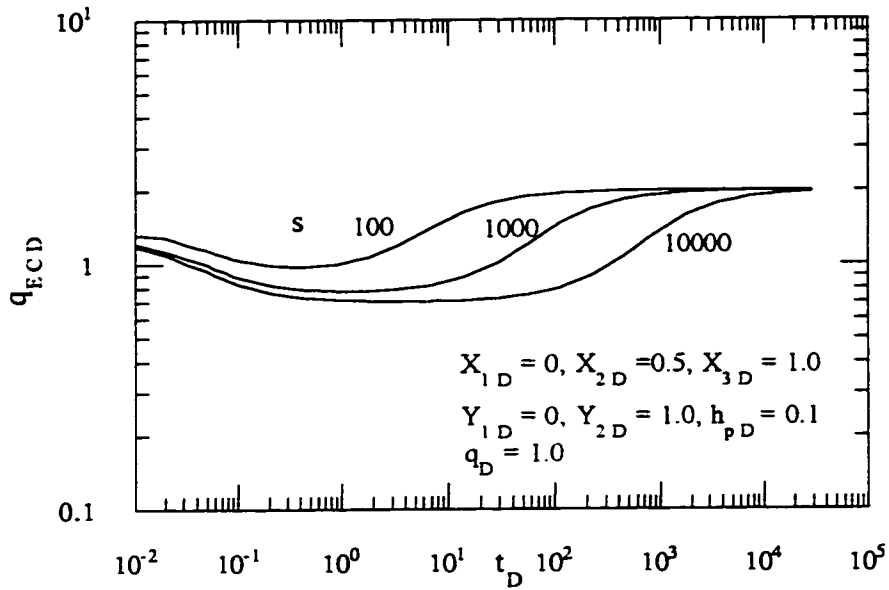


Figure 5.3: Profiles of equivalent dimensionless production rate due to interference of wells in a two-well, two-compartment system .

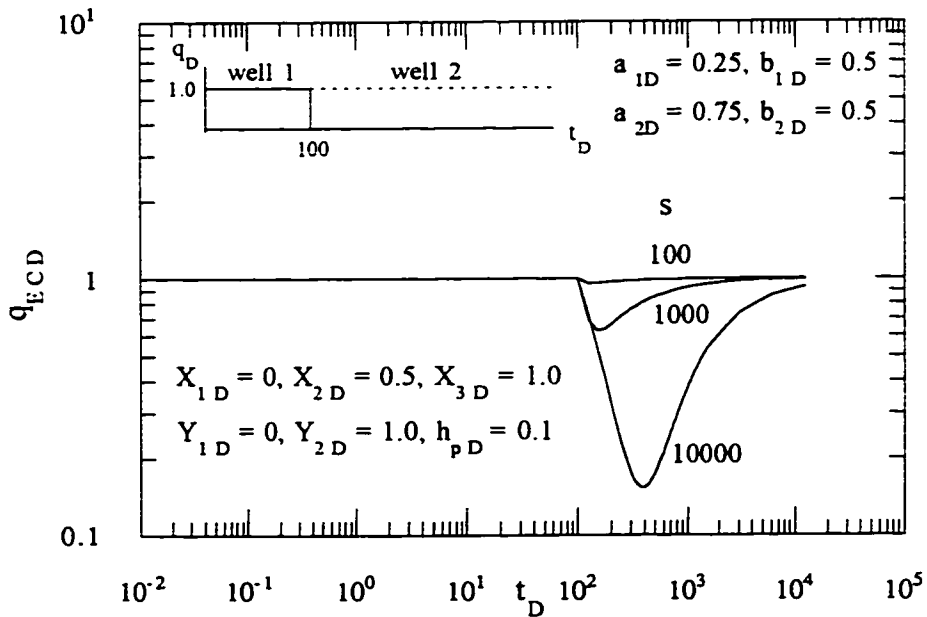


Figure 5.4: Effect of skin factor on profiles of equivalent dimensionless production rate due to interference of wells in a two-well, two-compartment system.

$$q_{D1} = 0.0, \text{ while, } t_D > 100$$

From the well in the second compartment: $q_{D2} = 0.0, \text{ while, } 0 < t_D \leq 100$

$$q_{D2} = 1.0, \text{ while, } t_D > 100$$

Since the well in the second compartment is producing before $t_D = 100$, up to this time the compartmentalized system under consideration is generating the same responses as its equivalent system, as evidenced from $q_{E c D} = 1$. After the well in the first compartment is shut in and the well in the second compartment starts producing at $t_D = 100$, the deviation of the dimensionless profile is towards a higher value of the skin factor, where it takes longer for the system to stabilize.

Figures 5.5 and 5.6 present the profiles for equivalent production rate with respect to a homogeneous system of the same systems considered in Figs. 5.3 and 5.4, respectively. Figure 5.5 shows that all profiles for the equivalent production rate, $q_{E H D}$, have merged into a single line. This is an indication of the fact that the compartmentalized system is acting like a homogeneous system. In the compartmentalized system under consideration, the skin boundary is behaving like a no-flow boundary regardless of the value of the skin factor because each of the producing wells has been placed at an equal distance from and on opposite sides of the skin boundary. Thus the dimensionless pressure responses in the first compartment would follow the pattern of a homogeneous system resulting in merging of equivalent dimensionless rates for all skin factors. Figure 5.6 shows the profiles for the equivalent production rates of the same system as described for Fig. 5.4. This shows that the interference behavior of the compartmentalized system under consideration merges with that of the homogeneous system when both systems are at pseudosteady state, resulting in $q_{E H D} = 1$. However this merging is delayed longer, after the rate change at $t_D = 100$, by a higher value of the skin factor in the compartmentalized system under consideration.

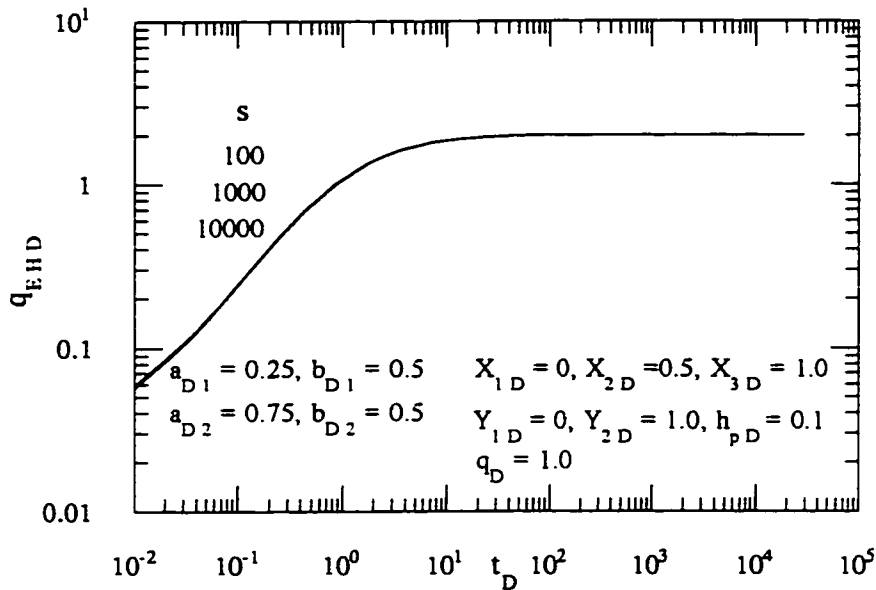


Figure 5.5: Profiles of equivalent dimensionless production rate compared with a homogeneous system due to interference of wells in a two-well, two-compartment system .

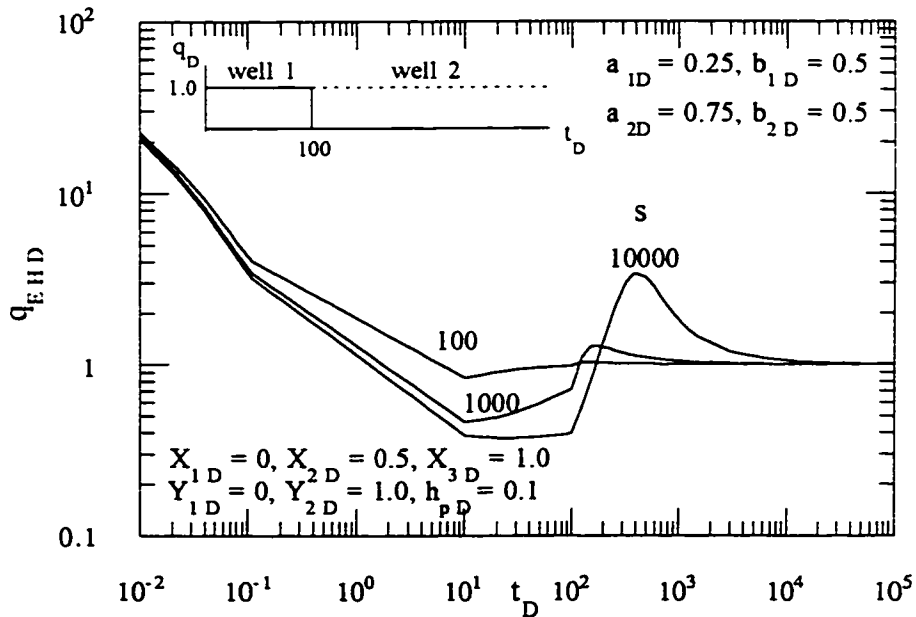


Figure 5.6: Effect of skin factor on profiles of equivalent dimensionless production rate due to interference of wells in a two-well, two-compartment system with respect to a homogeneous system.

5.4 Applicability of the Principle of Reciprocity

McKinley et al. (1968) stated the principle of reciprocity as - “The pressure response at well A, $p_{BA}(t)$, caused by injecting fluid at well B at a rate of $q(t)$ is equal to the pressure response at well B, $p_{AB}(t)$, caused by injecting fluid at well A at the same rate, $q(t)$.” They also added that this principle is applicable subject to the following conditions:

- the pressure responses must satisfy the diffusivity equation;
- the mobility and storativity of the reservoir may have arbitrary spatial variation, but these must not be pressure-sensitive.

Raghavan (1993) has pointed out the main advantage of this theorem is that the decision to choose an active well or an observation well from a pair of wells is moot because identical information is obtained in an interference test with either case. *McKinley et al.* (1968) demonstrated that this principle is applicable in the following cases:

- constant pressure on the boundary;
- no flow on the boundary;
- constant pressure on part of the boundary and no flow on the rest of it;
- an infinite medium.

Ogbe and Bringham (1984) have studied the effects of the presence of wellbore storage and skin on the principle of reciprocity for infinite reservoirs. They also presented correlations for correcting the pulse response amplitude and time lag due to wellbore storage. *Deng and Horne* (1993) have provided an extension of this principle to discontinuous distributions of reservoir properties, developing analytical solutions in

terms of Green's function. These authors also found that the principle of reciprocity does not hold for non-uniform, initial pressure.

As far as the solutions of this study are concerned, the principle of reciprocity is valid, provided the initial pressure (or potential) in the compartments is uniform. From an inspection of these solutions, it is also found that the distinctness of the rock and fluid properties in each compartment and the presence of skin at an interface do not affect the validity of this principle. However, the conditions at the extreme boundaries should be of the homogeneous, Dirichlet-, Neumann-type or a combination of these. This means that the boundary condition can be constant pressure (or potential), no-flow or a combination of these, which is in agreement with the findings of *Deng and Horne* (1993) for bounded systems. Appendix E presents a proof of the applicability of the principle of reciprocity when the conditions at the extreme boundaries in a compartmentalized system are of the homogeneous, Dirichlet-type.

CHAPTER 6

TRANSIENT-PRESSURE BEHAVIOR OF COMPARTMENTALIZED SYSTEMS

6.1 Introduction

In this Chapter, the transient-pressure behavior of a number of compartmentalized systems will be studied using the analytical solutions developed in Chapters 2, 3 and 4. When a new model of transient behavior is introduced in the literature, it is important to illustrate the similarities to commonly observed trends, and to identify the distinguishing characteristics (*Ehlig-Economides et al.*, 1989). The advantage of the fact that an analysis based on pressure-derivative responses provides more definitive results than that on pressure responses will also be utilized here.

It has been demonstrated in the literature that the pressure-derivative responses show more features than the pressure responses (*Bourdet et al.*, 1983; *Proano and Lilley*, 1986; *Ehlig-Economides*, 1988). The pressure-derivative analysis requires an accurate set of pressure data which is now possible to acquire with the advent of sensitive pressure gauges (*Ehlig-Economides*, 1988; *Bourdet et al.*, 1989 and *Raghavan*, 1993). *Ramey* (1992) has pointed out that the pressure-derivative type-curves are sensitive throughout the time domain and permit identification of events not evident on either log-log or semilog pressure graphs. *Alvarado* (1994) has mentioned that the basis of pressure-derivative analysis is recognizing a pattern for each flow regime.

According to *Raghavan* (1993), the use of pressure derivatives was first discussed by *Chow* (1952) in the ground-water hydrology literature and the applications of the derivative were first discussed by *Jones* (1957) in the petroleum literature. *Chow* (1952) also formulated the basis for semilog derivative responses by introducing a similar

parameter involving logarithms to the base 10. *Tiab and Kumar* (1980) developed a pressure-derivative method for a system with a line-source well in an infinite system. Later, *Bourdet et al.* (1983) introduced the idea of the semilog pressure derivative, defined as the derivative of the well pressure with respect to the natural logarithm of time. *Wong et al.* (1986) presented Cartesian and semilog pressure-derivative responses for closed rectangular reservoirs with different well locations outlining the criteria of identifying different flow regimes. According to *Proano and Lilley* (1986), the basis for the derivative approach involves the recognition of a pattern of any departure of well test data from a reference line. *Ehlig-Economides* (1988) has discussed the use of pressure-derivative responses for diagnostic purposes in characterizing different flow regimes, adapting the examples from *Matthews and Russell* (1967). *Duong* (1989) developed a new set of type-curves using the pressure/pressure-derivative ratio which is applicable for use in computer-aided analysis. *Issaka and Ambastha* (1996) have extended the notion of a generalized pressure-derivative analysis, proposed by *Jelmert* (1993 a and b), to different flow regimes of composite systems.

In this chapter, the effect of the contrasts of rock and fluid properties on pressure (or potential) and its derivative responses for various compartmentalized configurations will be examined. The contrasts of rock and fluid properties are shown by assigning different mobility and storativity ratios to different compartments. From this pressure (or potential)-derivative analysis, it is possible to estimate the dimensionless time to the start of steady-state or pseudosteady-state flow. *Lord and Collins* (1991) used the production data in the pseudosteady-state period for evaluating the production performance of a compartmentalized system using the inflow performance relationship. This inflow performance relationship is valid only when pseudosteady-state flow has been achieved. Therefore, it is important to know the time to the end of the transient-flow period and the time to the start of the pseudosteady-state period to use the inflow performance relationship. In the next four Sections, the pressure-derivative analysis is used for

understanding the pressure behavior of different compartmentalized systems. Here a linear system, a system composed of a small compartment in communication with a big one, a two-compartment system and a stacked channel realization will be considered.

6.2 Linear System

Gringarten et al. (1974), *Ershaghi and Woodbury* (1985) and *Wong et al.* (1986) have characterized the infinite-acting linear flow period by a 1/2-slope on log-log plots of the pressure responses versus time for a homogeneous system. However, *Kamal et al.* (1995) have pointed out that this slope is less than 1/2 on a log-log plot of pressure responses versus time if the wellbore skin is non-zero. The entire flow regime in a linear, compartmentalized system of this study is linear. It would be interesting to see how the flow regimes in a compartmentalized system that may have rock and fluid properties contrasts and skins at interface boundaries would behave in comparison to the 1/2-slope criterion of infinite-acting linear flow for homogeneous systems as presented in the literature.

In this Section on a linear system, the analytical solution for linear, one-dimensional systems as developed in Chapter 2 has been used. A system with two linear compartments is considered here. The communication between the compartments is poor due to the presence of a thin skin at the interface located at $x_D = X_{2D}$. One extreme boundary of the system at $x_D = X_{1D} = 0$ is producing while the other extreme boundary at $x_D = X_{3D} = 1$ is closed. Here the variation of the value of the skin factor (s) and the rock and fluid properties is considered. The reference values of the rock and fluid properties are taken with respect to the first compartment ($X_{1D} \leq x_D \leq X_{2D}$). Initially, both compartments are considered to be at a uniform pressure.

Issaka and Ambastha (1996) have shown that the specific derivative ($t_D^{0.5} dp_{wD}/dt_D$) during an infinite-acting linear flow period has a value of $1/\sqrt{\pi}$. Therefore, the specific derivative profile along dimensionless time in infinite-acting linear flow is a zero-slope line. In this study, the criterion for the end of the infinite-acting linear flow period is taken as 2% deviation of the specific derivative from $1/\sqrt{\pi}$. Also the criterion for the dimensionless time to the start of the pseudosteady-state flow period is taken as the Cartesian derivative (dp_{wD}/dt_D) falling within 2% of unity.

Figure 6.1 shows dimensionless pressure responses at the wellbore located at $x_D = X_{1D} = 0$. The situation with $s = 0$ corresponds to a linear homogeneous system whose extreme boundaries are located at $x_D = X_{1D} = 0$ and $x_D = X_{2D} = 1$. It is also observed that the slope increases to slightly more than $1/2$ in this log-log plot of dimensionless pressure responses versus dimensionless time as the infinitely-acting linear flow ends for a non-zero value of the skin factor. Figure 6.2 shows the specific derivative profile of dimensionless pressure responses ($t_D^{0.5} dp_{wD}/dt_D$) with dimensionless time. This plot clearly demonstrates that a longer period of infinite-acting linear flow exists for $s = 0$ than for $s \neq 0$. The Cartesian derivative (dp_{wD}/dt_D) profile of dimensionless pressure responses with dimensionless time is presented in Fig. 6.3. This figure shows that with an increase in the value of the skin factor, the onset of pseudosteady-state flow is delayed. Using the criteria mentioned earlier, the end of the infinite-acting linear flow period (t_{DL}) and the start of pseudosteady-state flow period (t_{Dpsst}) for the linear compartmentalized system are presented in Table 6.1. It has also been observed that $t_{DL} = 0.054$ for $s > 0$. However, $t_{DL} = 0.22$ for $s = 0$ (homogeneous system).

Figures 6.4 and 6.5 show the effect of contrasts of rock and fluid properties on the Cartesian derivative of dimensionless pressure responses at the wellbore for $s = 100$. With low storativity in the second compartment ($F_2 = 0.01$), the flow reaches

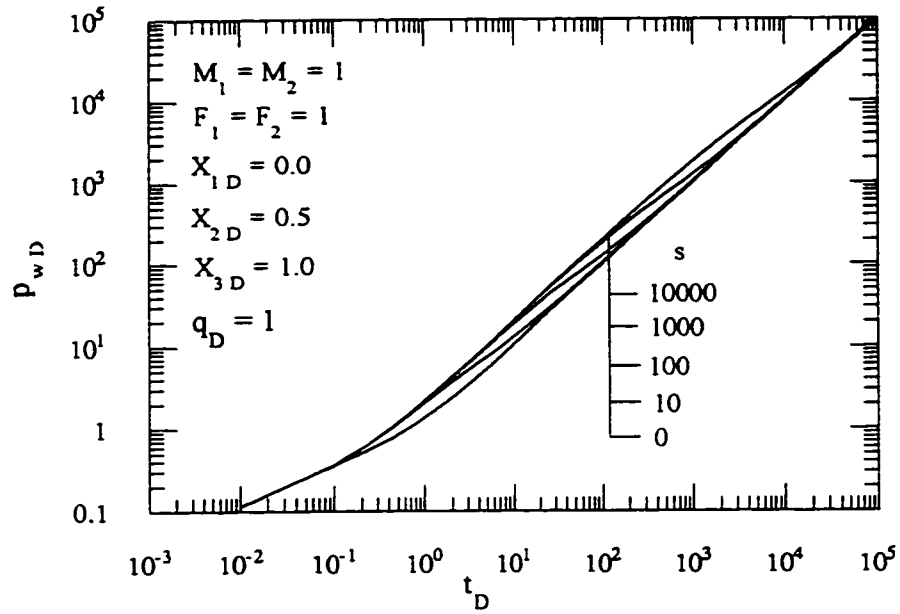


Figure 6.1: Dimensionless wellbore pressure responses in a linear system.

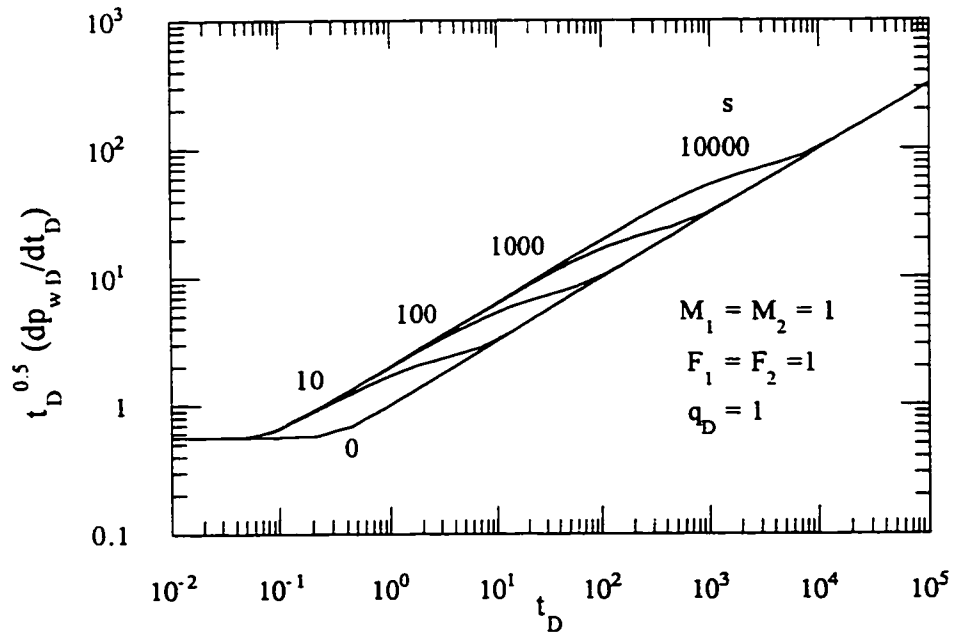


Figure 6.2: Specific derivative profile of dimensionless wellbore pressure responses for a linear system.

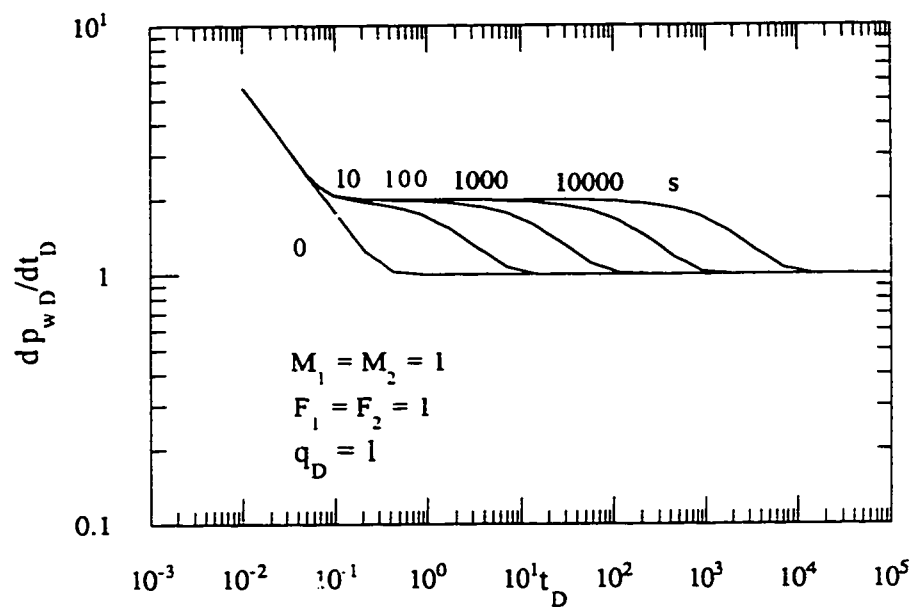


Figure 6.3: Cartesian derivative profile of dimensionless wellbore pressure responses in a linear system.

TABLE 6.1: DIMENSIONLESS TIME TO THE END OF INFINITE-ACTING LINEAR FLOW, t_{DL} , AND THE START OF PSEUDOSTEADY-STATE FLOW, $t_{D PSS}$

s	t_{DL}	$t_{D PSS}$
0	0.22	0.465
10	0.054	10.15
100	0.054	98.01
1000	0.054	980.07
10000	0.054	9795.4

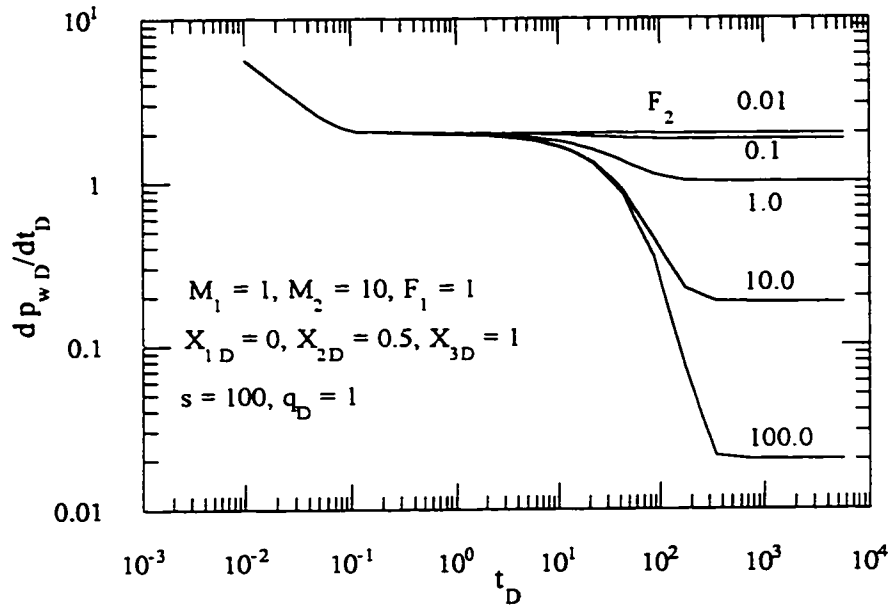


Figure 6.4: Effect of storativity ratio on the Cartesian derivative of dimensionless pressure responses in a linear system for $M_2 = 10$.

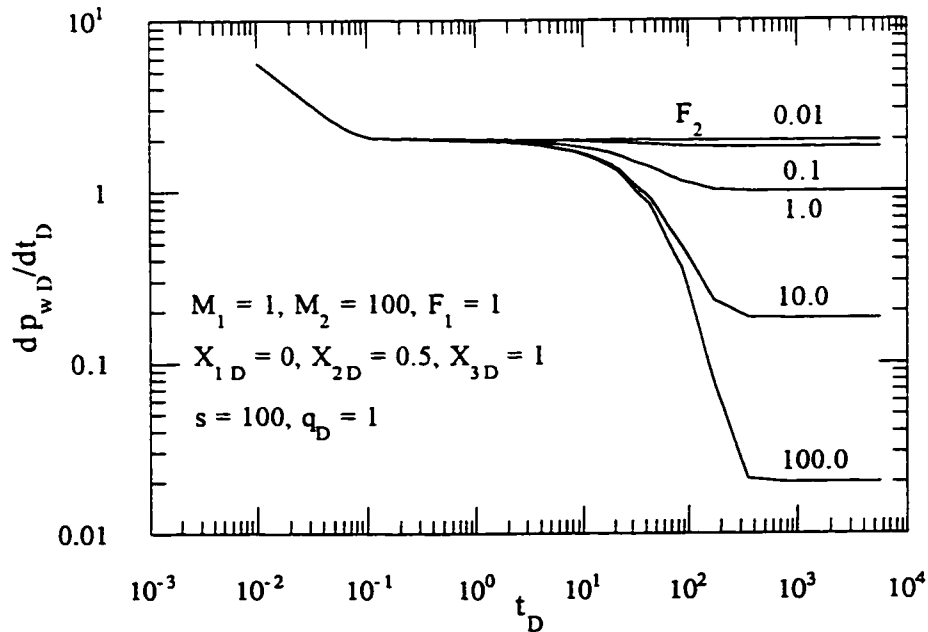


Figure 6.5: Effect of storativity ratio on the Cartesian derivative of dimensionless pressure responses in a linear system for $M_2 = 100$.

pseudosteady-state very quickly. Moreover, the Cartesian derivative of dimensionless pressure responses at late times can be approximated by,

$$\frac{dp_{wD}}{dt_D} = \frac{1}{\sum_{i=1}^n F_i (X_{iD} - X_{iD})} \dots\dots\dots(6.1)$$

where n is the total number of linear compartments and F_i is the storativity ratio in the i th compartment. For the system under consideration with $F_1 = 1$, $F_2 = 10$, we have, $dp_{wD}/dt_D = 0.1818$ at late times. Equation (6.1) shows that the Cartesian derivative of dimensionless pressure responses at late times is not a function of the mobility ratio (M_i) or the values of the skin factor. However, any higher value of F_i decreases the value of this derivative due to an increase of the pore volume and/or of the total compressibility in the system. The values of the Cartesian derivative at late times are found to be in good agreement with the respective values as found from Figs. 6.4 and 6.5. Equation (6.1) can play an important role in confirming the volume-weighted storativity from the late-time data.

6.3 A Small Compartment in Communication with a Big one

In this section, one of the very important aspects of reservoir compartmentalization will be considered. Sometimes it is discovered that a small compartment is in poor hydraulic communication with a big one (Fox *et al.*, 1988). Here the volume and hydraulic diffusivity of the supporting compartment are very large compared to the producing compartment. The big compartment has been termed the “source reservoir” by Fox *et al.* (1988). According to Stewart and Whaballa (1989), because of its large size, depletion of the supporting compartment is very slow indeed and it remains essentially at the initial pressure. Therefore, any production from the small compartment apparently would not have any effect on the pressure behavior of the neighboring big compartment in the short

term. It is apparently a situation where the condition at the extreme boundary (at the interface on the side of the big compartment) can be considered as a constant-pressure condition. As a result of such a consideration, the condition at the communicating boundary becomes a Cauchy-type boundary condition. This situation is illustrated schematically in Fig. 6.6. In this study, the small compartment is considered to be producing through a well, located at the center, at a constant rate of q_D . The region within the small compartment with a well is bounded by $0 \leq x_D \leq X_{0D}$ and $0 \leq y_D \leq Y_{0D}$ areally and has a dimensionless pay thickness of h_D . However, in this study, we consider, $X_{0D} = Y_{0D} = h_D = 1$.

Table 6.2 identifies all the boundaries in terms of location, extent and specification with a skin factor. There is a possibility that not all of the boundaries of the small compartment may be in communication with the big compartment. Hence, all possible combinations of the conditions at the boundaries of the small compartment need to be analyzed. These combinations of the values of the skin factor on the boundaries to be considered are shown in Table 6.3. "Combination 1", for example, refers to a condition where the boundary at $x_D = 1$ ($0 \leq y_D \leq 1$) of the small compartment is considered to be in communication with the big compartment while all the remaining boundaries are closed. Similarly, with "Combination 2", there are boundaries at $x_D = 1$ ($0 \leq y_D \leq 1$) and at $y_D = 1$ ($0 \leq x_D \leq 1$) of the small compartment in communication with the big compartment while the remaining boundaries are closed. With "Combination 3", the boundaries located at $x_D = 0$ ($0 \leq y_D \leq 1$) and $x_D = 1$ ($0 \leq y_D \leq 1$) of the small compartment are in communication with the big compartment while the remaining boundaries are closed. This combination possesses the same amount of surface area for fluid communication through the boundaries as "Combination 2", but has a different configuration. "Combination 3" possesses two times as much area for fluid communication on the boundaries of the small compartment as "Combination 1". "Combination 4" possesses boundaries at $x_D = 0$

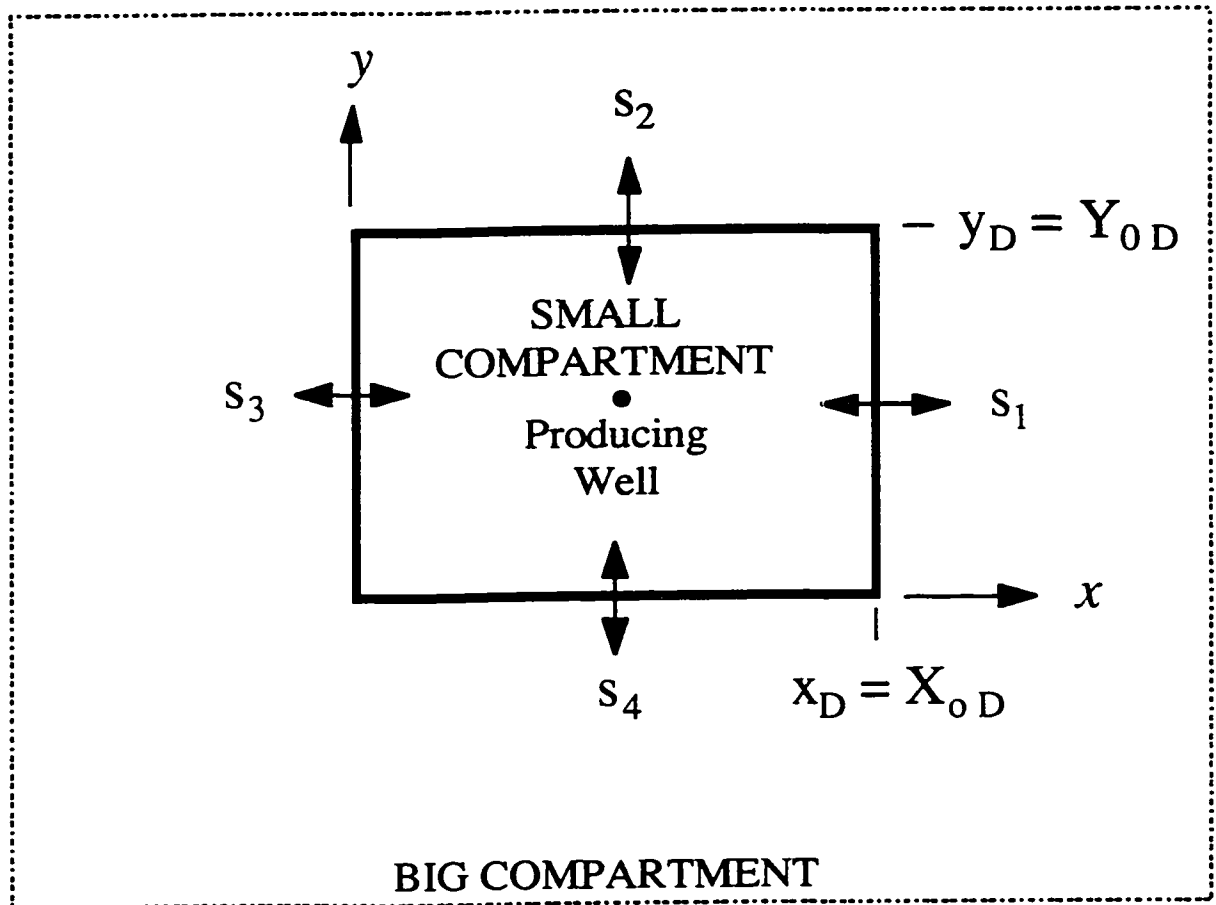


Figure 6.6: A schematic showing a small compartment in communication with a big one.

TABLE 6.2: LOCATION, EXTENT AND SPECIFICATION OF SKIN FACTOR OF COMMUNICATING BOUNDARIES

Location	Extent	Skin Factor
$x_D = 1$	$0 \leq y_D \leq 1$	s_1
$y_D = 1$	$0 \leq x_D \leq 1$	s_2
$x_D = 0$	$0 \leq y_D \leq 1$	s_3
$y_D = 0$	$0 \leq x_D \leq 1$	s_4

TABLE 6.3: COMBINATIONS OF SKIN FACTORS AT THE BOUNDARIES OF A SMALL COMPARTMENT

Combination	s_1	s_2	s_3	s_4
1	Finite	∞	∞	∞
2	Finite	Finite	∞	∞
3	Finite	∞	Finite	∞
4	Finite	Finite	Finite	∞
5	Finite	Finite	Finite	Finite

($0 \leq y_D \leq 1$), at $y_D = 1$ ($0 \leq x_D \leq 1$), and at $x_D = 1$ ($0 \leq y_D \leq 1$) of the small compartment in communication with the big compartment while the remaining boundary is closed. This combination has three times as much area for fluid communication through the boundaries of the small compartment as “Combination 1”. Finally, “Combination 5” assumes that all the boundaries of the small compartment are in communication with the big compartment. This arrangement has four times as much communicating area of the small compartment as in “Combination 1”.

For a boundary with finite values for the skin factor, skin factors of 0, 1, 10, 100, 1000, 10000 and ∞ are considered. An infinite value (∞) for the skin factor at a certain boundary of the small compartment means that the boundary is closed to fluid communication with the big compartment (boundary condition of the Neumann-type) and a zero value for the skin factor means that the boundary on the side of the small compartment is maintained at a constant pressure with the big compartment (boundary condition of the Dirichlet-type). Thus, the small compartment would tend to be closed for fluid communication altogether as the value of the skin factor at all boundaries tends to have a limiting value of infinity (∞). However, zero and infinite values for the skin factor are meant to consider the respective extreme situations that are possible as far as a boundary condition is concerned.

All the reference parameters regarding the reservoir geometry, and the rock and fluid properties, are taken with respect to the small compartment. Initially the whole reservoir is considered to be at a constant uniform pressure. In the definition of dimensionless pressure, the initial pressure of the reservoir is taken as the reference pressure, p_p . Therefore, the dimensionless initial pressure everywhere in the reservoir is zero and $p_{wD}(a_D, b_D, 0) = 0$. For all the combinations of the conditions of the communicating boundaries, as listed in Table 6.3, the dimensionless times, t_{DR} , at which infinite-acting radial flow period ends, and, t_{DS} , at which the steady-state flow period starts, will be

determined later. For all combinations, t_{DR} is determined using the criterion of 2% deviation from the intercept of the initial flat line in the semilog derivative plot and t_{DS} is determined using the criterion of the Cartesian derivative falling below 0.02 (for a perfect steady state, it is zero). The transient behavior corresponding to the combinations is discussed in detail below.

6.3.1 Drawdown

Figures 6.7 through 6.11 show the dimensionless pressure responses in drawdown at the wellbore for different values of the skin factor at the communicating boundary for “Combination 1” through “Combination 5”. The infinite-acting radial flow periods at early times are characterized by the line (up to about $t_D = 0.1$) before the effects of the boundaries are felt. However, the boundary-dominated flow regimes are characterized by the respective value of the skin factor.

At late times, the flow leads to steady state regardless of the finite value of the skin factor. The dimensionless time required to reach steady state is longer for higher values of the skin factor, in any combination. Moreover, the dimensionless pressure responses in drawdown for late times for different combinations can be estimated from the following equations:

Combination 1:

$$p_{wD} = s + 1.5 \dots\dots\dots(6.2)$$

where $s = s_I$.

Combination 2:

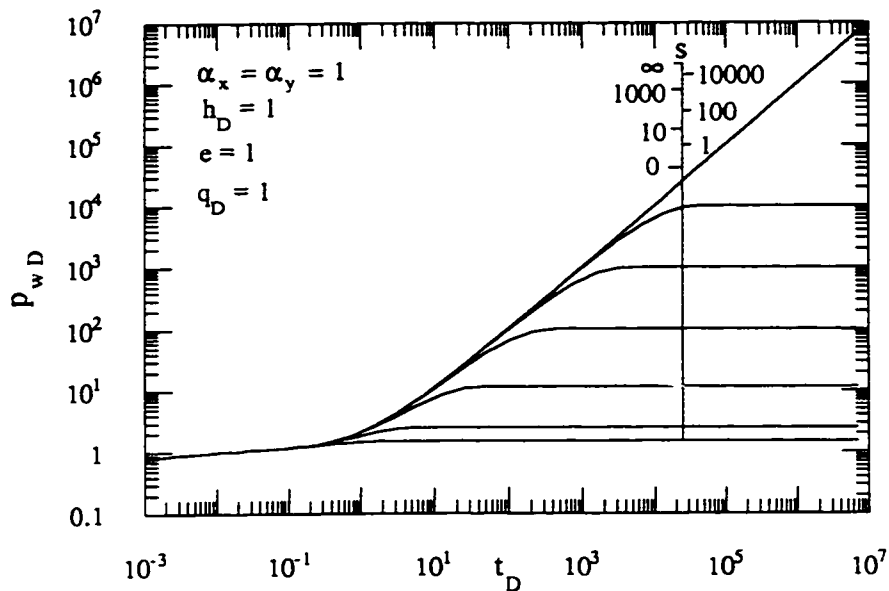


Figure 6.7: Dimensionless pressure responses in drawdown for different values of skin factor considered in "Combination 1".

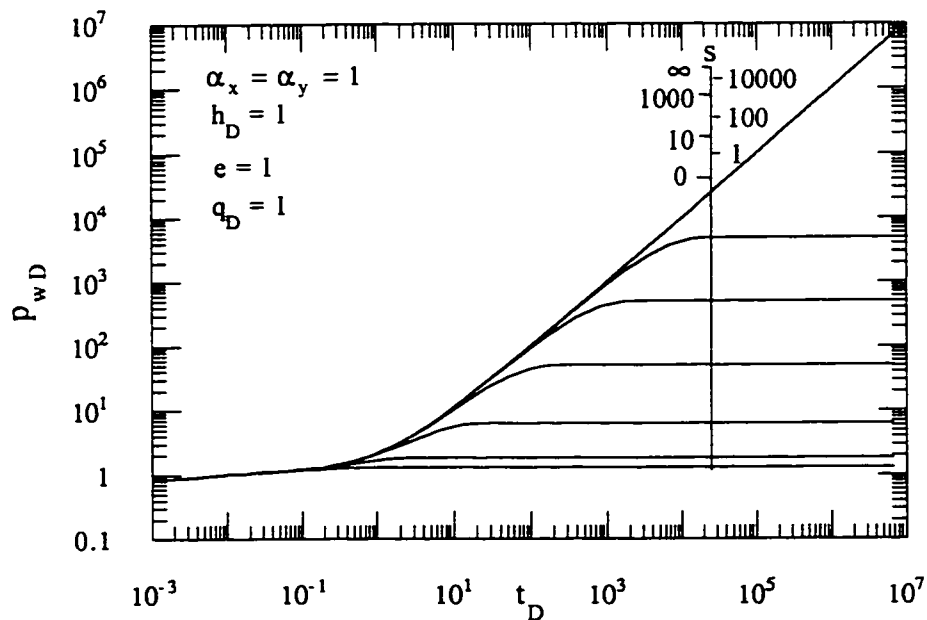


Figure 6.8: Dimensionless pressure responses in drawdown for different values of skin factor considered in "Combination 2".

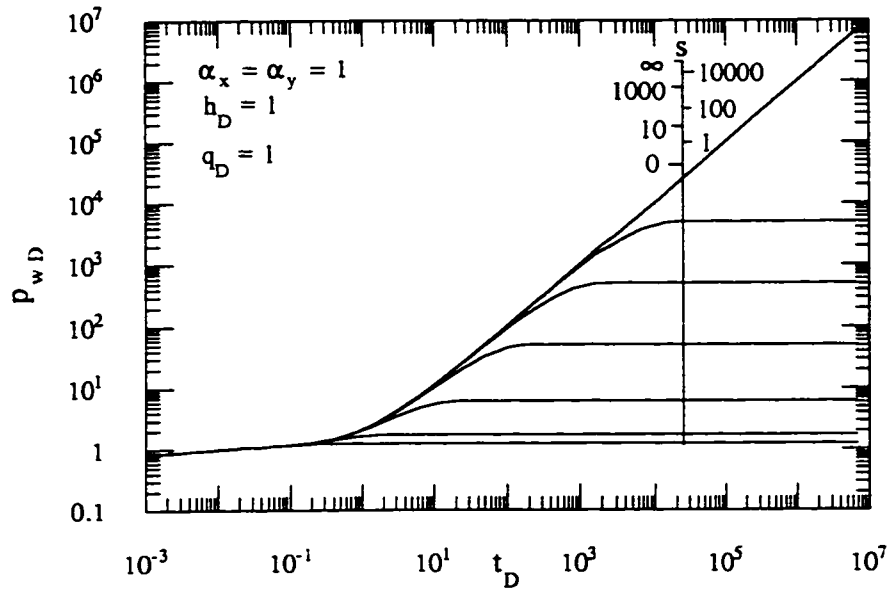


Figure 6.9: Dimensionless pressure responses in drawdown for different values of skin factor considered in "Combination 3".

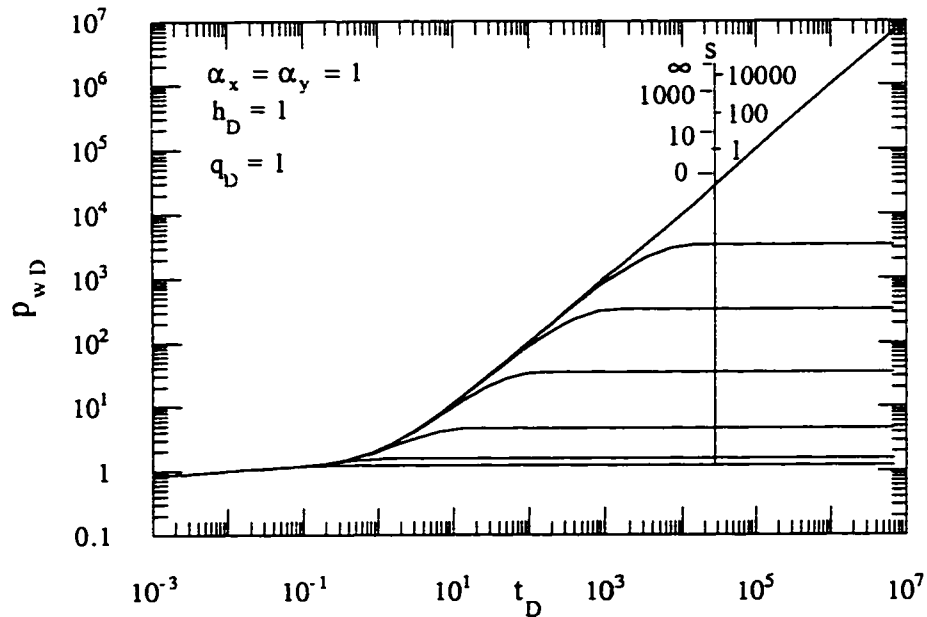


Figure 6.10: Dimensionless pressure responses in drawdown for different values of skin factor considered in "Combination 4".

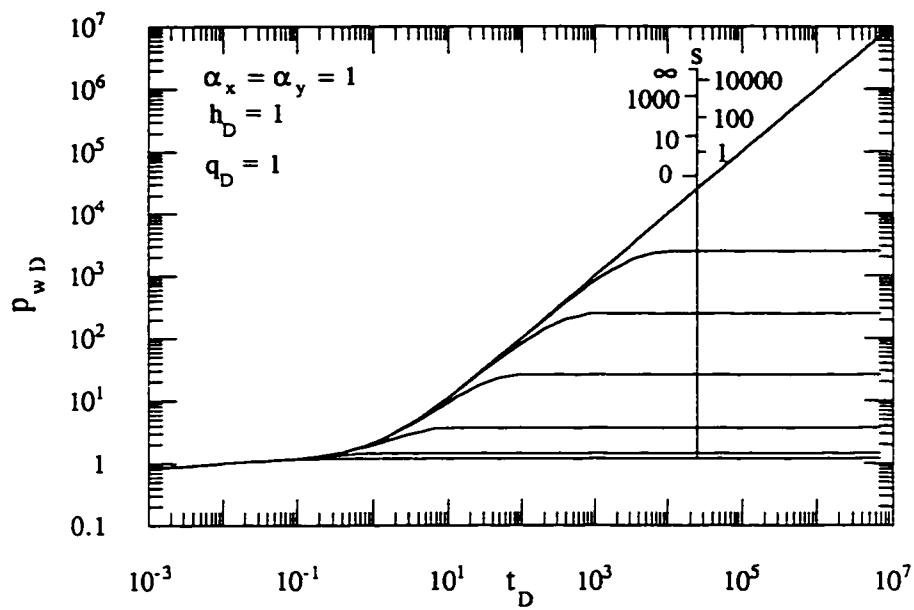


Figure 6.11: Dimensionless pressure responses in drawdown for different values of skin factor considered in "Combination 5".

$$p_{wD} = 0.5 s + 1.31 \dots\dots\dots(6.3)$$

where $s = s_1 = s_2$.

Combination 3:

$$p_{wD} = 0.5 s + 1.25 \dots\dots\dots(6.4)$$

where $s = s_1 = s_3$.

Combination 4:

$$p_{wD} = 0.33 s + 1.23 \dots\dots\dots(6.5)$$

where $s = s_1 = s_2 = s_3$.

Combination 5:

$$p_{wD} = 0.25 s + 1.21 \dots\dots\dots(6.6)$$

where $s = s_1 = s_2 = s_3 = s_4$.

For finite values of the skin factor, Eqs. (6.2) through (6.6) show linear relationships between the dimensionless wellbore pressures at late times and the values of the skin factor. These equations may be used to estimate the values of the skin factor by matching the data from an extended drawdown test. Comparison of Eq. (6.3) with Eq. (6.2) shows that “Combination 2” always leads to a lower dimensionless wellbore pressure (or lower drawdown) than “Combination 1” at steady state because of possessing a larger amount

of area for fluid communication. Also the comparison of Eqs. (6.3) and (6.4) shows that both “Combination 2” and “Combination 3” lead to about the same dimensionless pressure at late times, especially at high values of the skin factor. For example, the difference in dimensionless wellbore pressures between these two combinations is 4.8% for $s = 0$ and 0.12% for $s = 100$. Comparison of Eq. (6.5) with Eqs. (6.3) and (6.4) shows that “Combination 4” results in a lower dimensionless wellbore pressure (or lower pressure drop at the wellbore) than “Combination 2” or “Combination 3” does at steady state. This is so because this combination has one and a half times as much area open to fluid communication as “Combination 2” or “Combination 3”. Comparison of Eq. (6.6) with Eqs. (6.2) through (6.5) shows that among all the combinations, “Combination 5” results in the lowest dimensionless wellbore pressure at steady state. This is so because this combination possesses the largest amount of the area for fluid communication through the boundaries of the small compartment.

Figures 6.12 through 6.16 show the semilog derivative profiles of dimensionless pressure responses generated in drawdown for different values of the skin factor at the communicating boundary for “Combination 1” through “Combination 5”. Here the infinite-acting radial flow regimes are shown to be separated distinctly from the boundary dominated flow regimes for different values of skin factor in any combination. Figures 6.17 through 6.21 show the Cartesian derivative profiles of dimensionless pressure responses generated in drawdown for different values of the skin factor at the communicating boundary for “Combination 1” through “Combination 5”. These figures also demonstrate that effects of boundary-dominated flow on the transient behavior is distinct for different values of the skin factor. The steady-state flow regime is characterized by the flat line with a Cartesian derivative of 0, whereas, the pseudosteady-state flow period (in the case of $s = \infty$) is characterized by a flat line with a Cartesian derivative value of 1. It has been estimated that the infinite-acting radial flow period ends at $t_{DR} = 0.101$ using the criterion of 2% deviation from the intercept of the initial flat line,

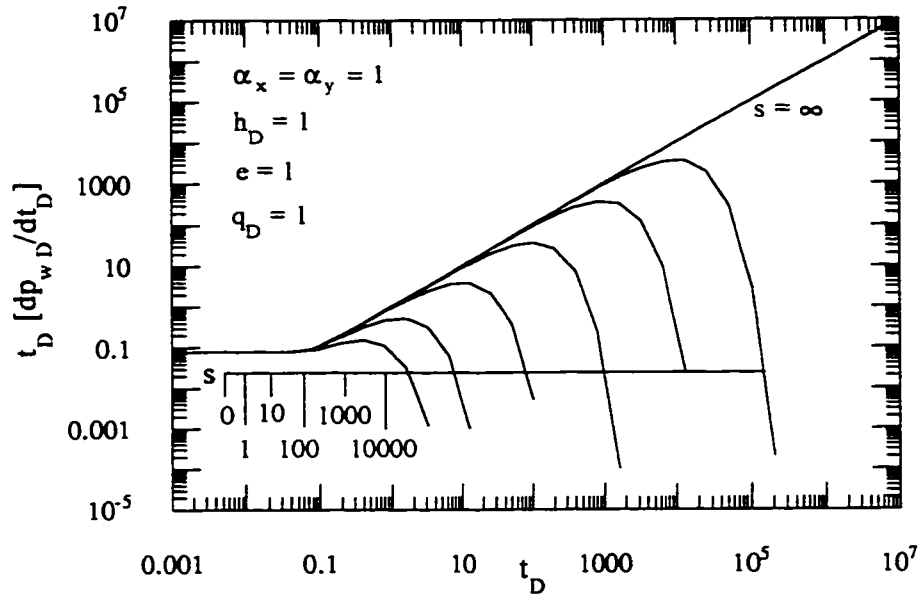


Figure 6.12: Semilog derivative of dimensionless pressure responses in drawdown for different values of skin factor considered in "Combination 1".

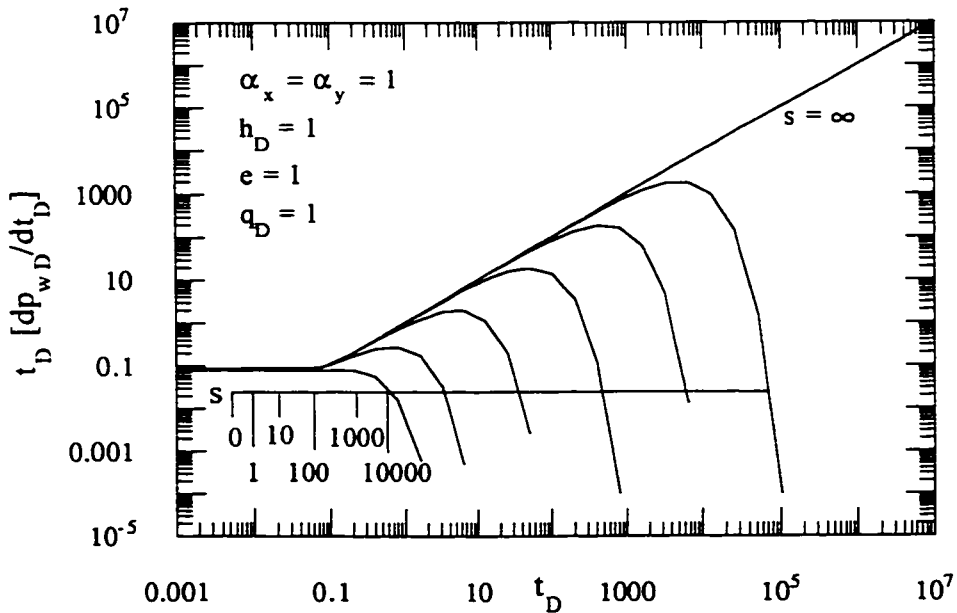


Figure 6.13: Semilog derivative of dimensionless pressure responses in drawdown for different values of skin factor considered in "Combination 2".

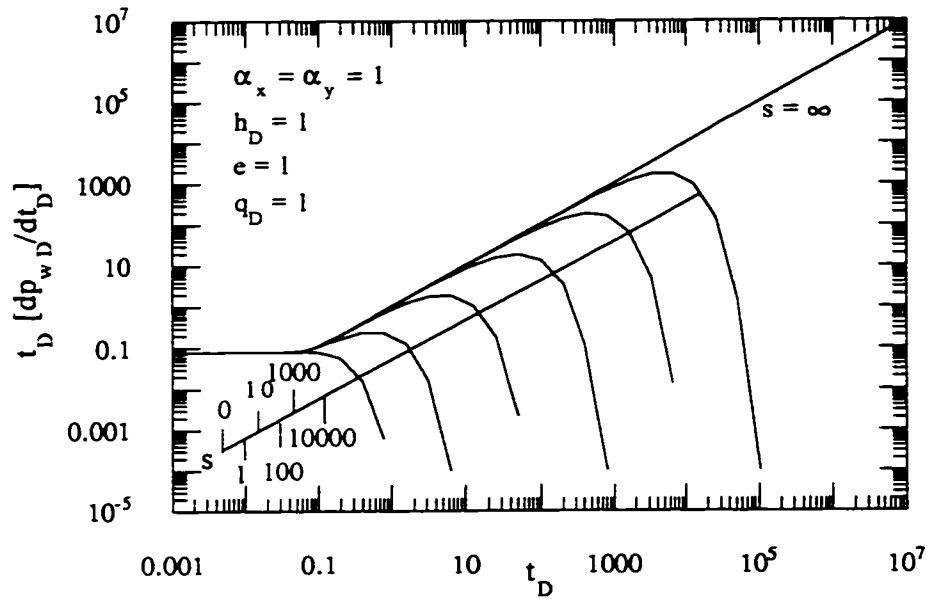


Figure 6.14: Semilog derivative of dimensionless pressure responses in drawdown for different values of skin factor considered in "Combination 3".

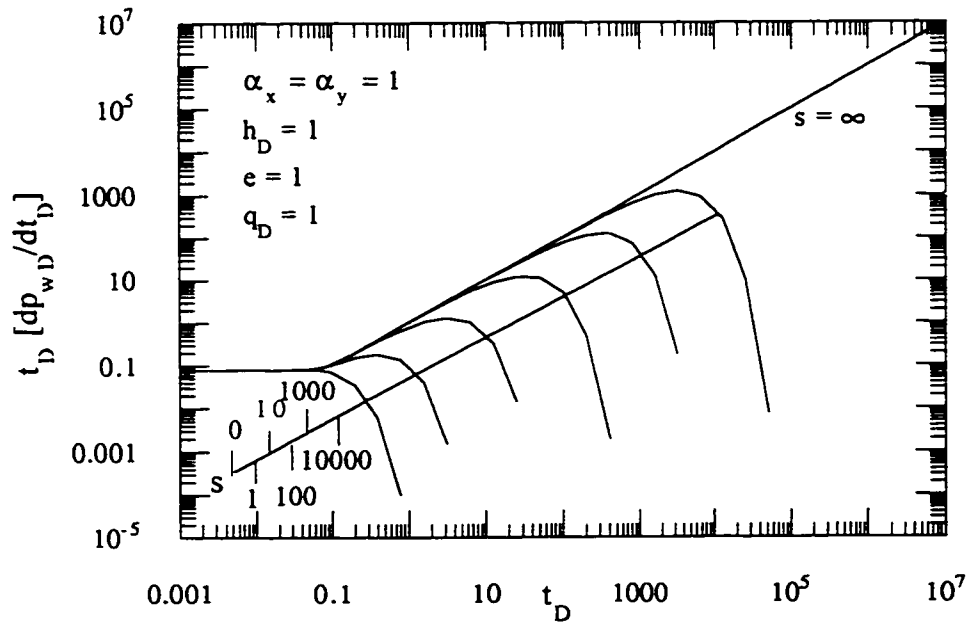


Figure 6.15: Semilog derivative of dimensionless pressure responses in drawdown for different values of skin factor considered in "Combination 4".

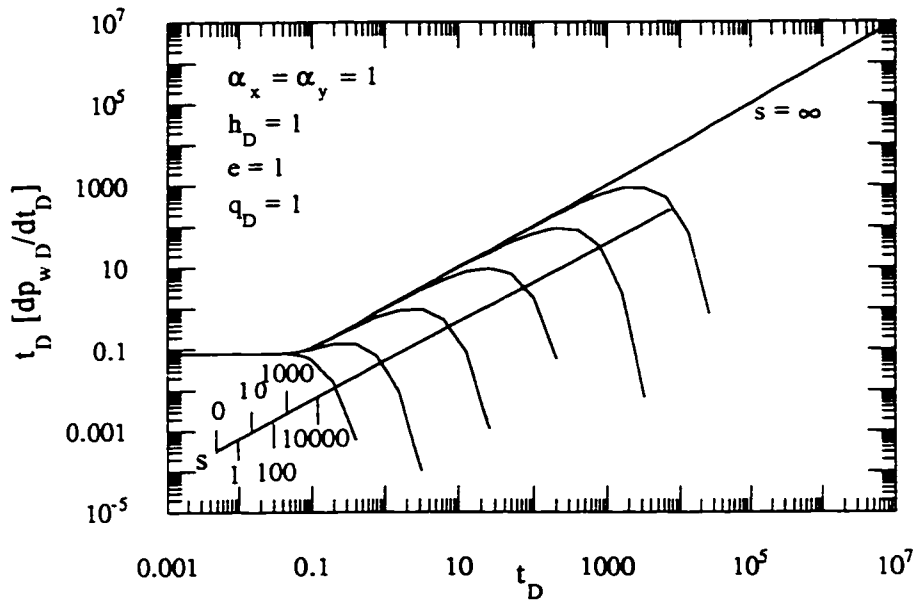


Figure 6.16: Semilog derivative of dimensionless pressure responses in drawdown for different values of skin factor considered in "Combination 5".

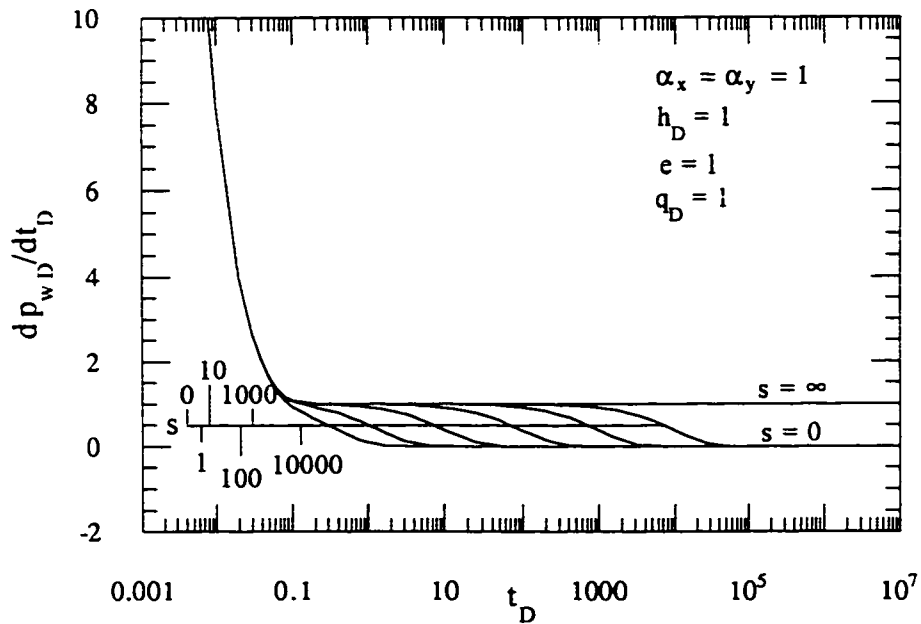


Figure 6.17: Cartesian derivative of dimensionless pressure responses in drawdown for different values of skin factor considered in "Combination 1".

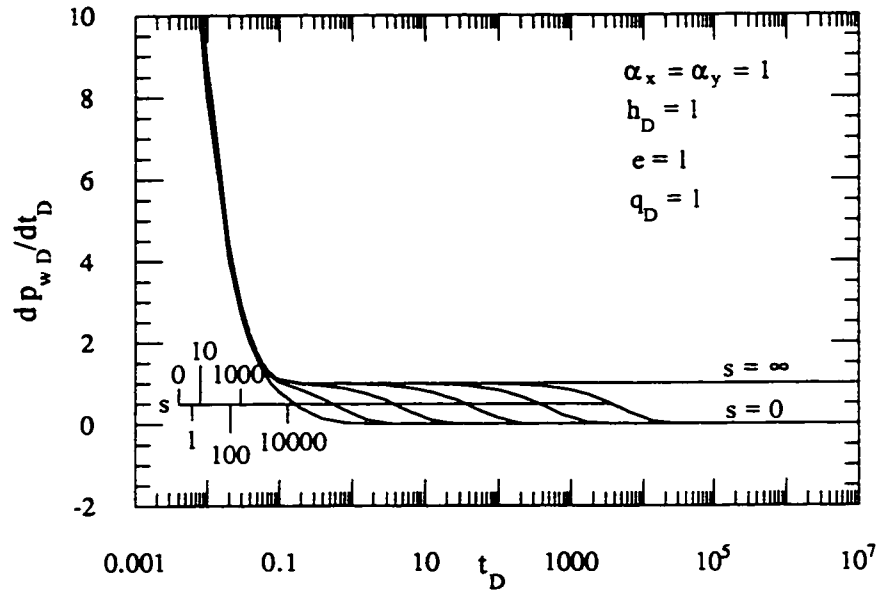


Figure 6.18: Cartesian derivative of dimensionless pressure responses in drawdown for different values of skin factor considered in "Combination 2".

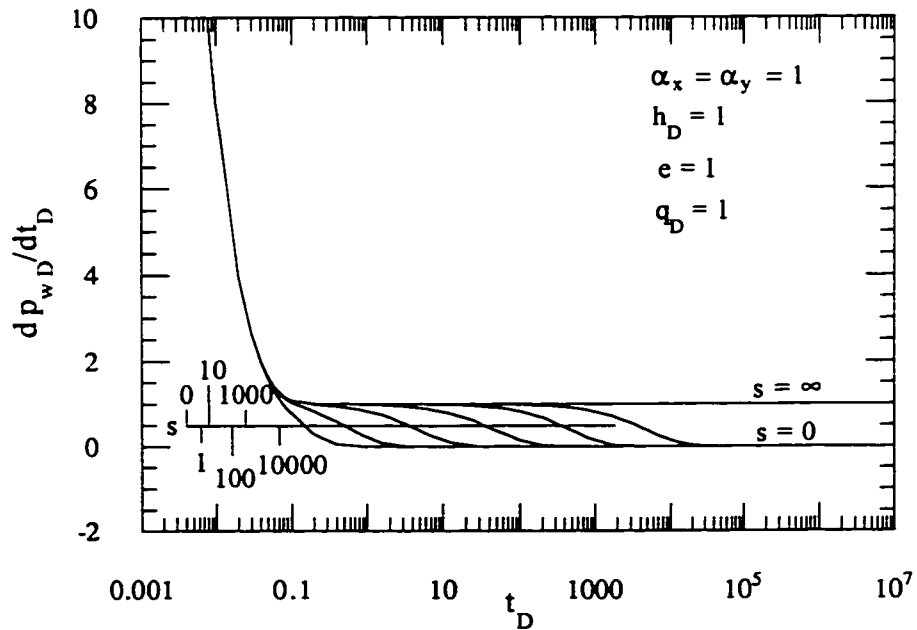


Figure 6.19: Cartesian derivative of dimensionless pressure responses in drawdown for different values of skin factor considered in "Combination 3".

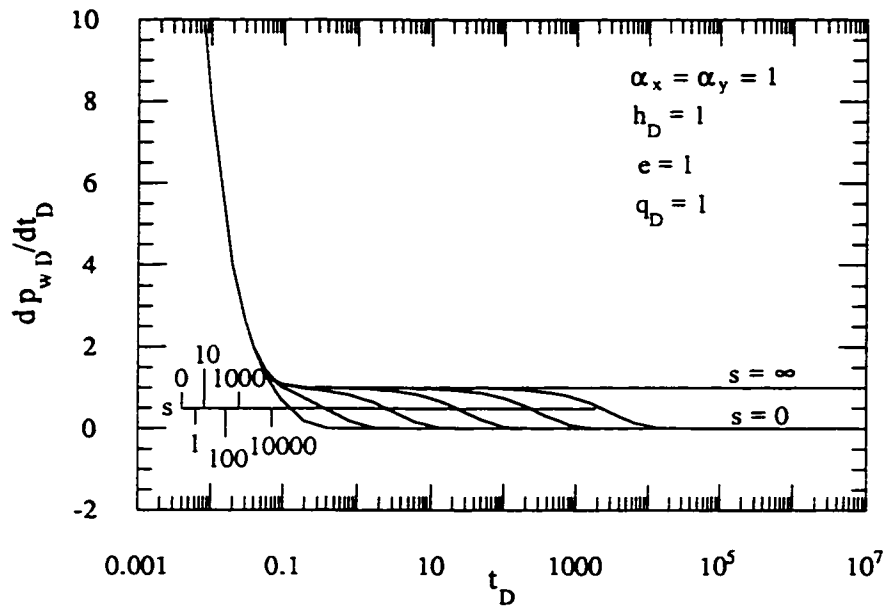


Figure 6.20: Cartesian derivative of dimensionless pressure responses in drawdown for different values of skin factor considered in "Combination 4".

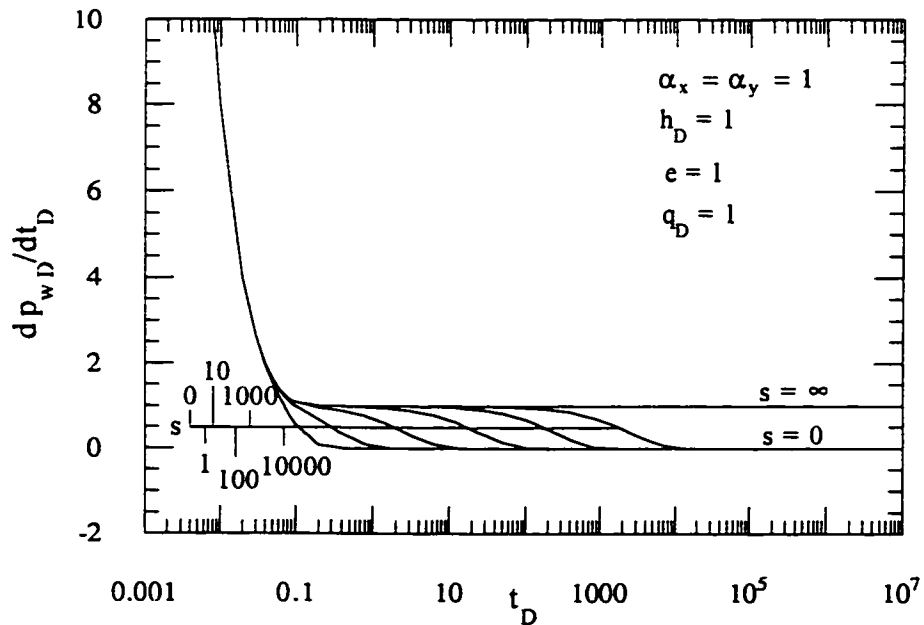


Figure 6.21: Cartesian derivative of dimensionless pressure responses in drawdown for different values of skin factor in "Combination 5".

which is $0.25/\pi$, as shown by *Proano and Lilley (1986)*, on the semilog derivative plot regardless of the values of the skin factor and combination of boundary conditions. Tables 6.4 through 6.8 show the dimensionless times, t_{DS} , at which the steady-state flow period would start for different finite values of skin factor for “Combination 1” through “Combination 5”. Comparison of t_{DS} -values from Table 6.4 with those from Table 6.5 shows that the system with “Combination 2” takes a shorter dimensionless time to reach steady state than that with “Combination 1” for identical values of the skin factor because of possessing a larger area for fluid communication at the boundaries. Comparison of the values in Tables 6.5 and 6.6 shows that “Combination 3” reaches steady state significantly earlier than “Combination 2” with low but identical values of skin factor. But this difference in dimensionless times to reach steady state dissipates to an insignificant level with high but identical values of the skin factor. Comparison of the values of t_{DS} from Table 6.7 with those from Tables 6.5 and 6.6 shows that “Combination 4” takes significantly shorter dimensionless times to reach steady state than “Combination 2” or “Combination 3” does. For example, t_{DS} for “Combination 2” is 48.8% longer and that for “Combination 3” is 51.3% longer than t_{DS} for “Combination 4” with $s = 10$. Comparison of the values of t_{DS} from Table 6.8 with those from Tables 6.4 through 6.7 shows that “Combination 5” reaches steady state earlier than any other combination. For example, t_{DS} with “Combination 3” is 99.9% longer and that with “Combination 4” is 33.4% longer than t_{DS} with “Combination 6” for $s = 100$. The criterion for the start of steady-state flow period, t_{DS} , is taken as when the Cartesian derivative falls below 0.02 (*i.e.*, $0 \leq p_{wD} \leq 0.02$). As is also evident in Figs. 6.12 through 6.21, the periods between t_{DR} and t_{DS} are dominated mostly by the effects of pseudosteady-state flow. During these periods the reservoir behaves predominantly like a closed one. However, these periods are longer for a higher value of the skin factor which is consistent with the trend shown in Figs. 6.7 through 6.11.

TABLE 6.4: DIMENSIONLESS TIME TO THE START OF STEADY-STATE FLOW, t_{DS} , IN "COMBINATION 1"

s	t_{DS}
0	1.586
1	5.437
10	40.531
100	392.601
1000	3913.429
10000	39124.2

TABLE 6.5: DIMENSIONLESS TIME TO THE START OF STEADY-STATE FLOW, t_{DS} , IN "COMBINATION 2"

s	t_{DS}
0	0.793
1	2.708
10	20.304
100	196.342
1000	1956.75
10000	19562.3

TABLE 6.6: DIMENSIONLESS TIME TO THE START OF STEADY-STATE FLOW, t_{DS} , IN "COMBINATION 3"

s	t_{DS}
0	0.699
1	2.375
10	19.97
100	196.0
1000	1956.1
10000	19560.5

**TABLE 6.7: DIMENSIONLESS TIME TO THE START OF STEADY-STATE FLOW, t_{DS} , IN
"COMBINATION 4"**

s	t_{DS}
0	0.377
1	1.678
10	13.418
100	130.825
1000	1304.44
10000	13040.1

**TABLE 6.8: DIMENSIONLESS TIME TO THE START OF STEADY-STATE FLOW, t_{DS} , IN
"COMBINATION 5"**

s	t_{DS}
0	0.274
1	1.231
10	10.029
100	98.05
1000	978.438
10000	9782.02

6.3.2 Buildup

Figures 6.22 through 6.26 show the dimensionless pressure responses at the wellbore due to a production period (ending at $t_D = 4$) followed by a buildup period for different values of the skin factor at the communicating boundary for “Combination 1” through “Combination 5”. These figures demonstrate that the well should be shut in earlier for higher values of the skin factor for any combination of the boundary conditions to avoid the well pressure falling below the bubble point pressure. The buildup responses are steeper for lower values of the skin factor for all combinations. This means that the systems with higher values of the skin factor need more dimensionless time to build up to the same level of dimensionless pressure, following a particular production period.

6.3.3 General Discussion

Stewart and Whaballa (1989) have argued that an extended drawdown test should be performed to detect the limits of the producing compartment. Thus, transient-pressure behavior has been studied in extended drawdown. From the preceding analysis, it is evident that the type-curves developed in Figs. 6.4 through 6.23 and the time-criteria presented in Tables 6.3 through 6.7 can be used for identifying the extent of faulted boundaries between small and big compartments. By matching the data from late times with Eqs. (6.1) through (6.5), it is possible to estimate the values of the skin factor, a parameter related to the resistance to flow of fluid at the boundary. It has already been mentioned earlier that quantifying the flow resistance in terms of a skin factor is very important for forecasting the long term production performance of a reservoir. A similar problem has been solved by *Fox et al.* (1988) making the assumption that the transient-effects dissipate so quickly that steady-state flow of the fluid can be considered for the sake of simplicity. The analysis presented earlier in this study has shown that with the use of the transient-pressure data, while considering the resistance to flow, it is possible

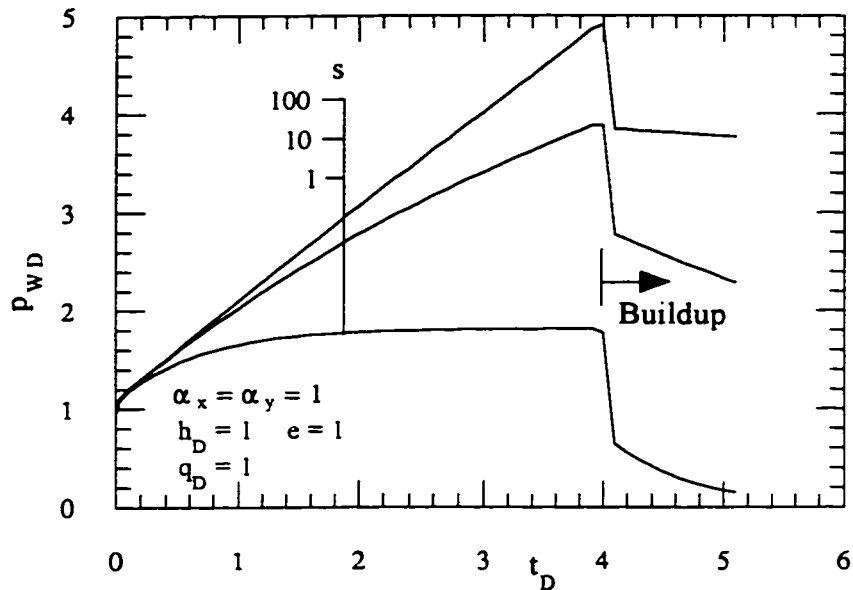


Figure 6.22: Dimensionless pressure responses at the wellbore for a shut-in period being followed by a production period where the well is shut in at $t_D = 4$ for "Combination 1".

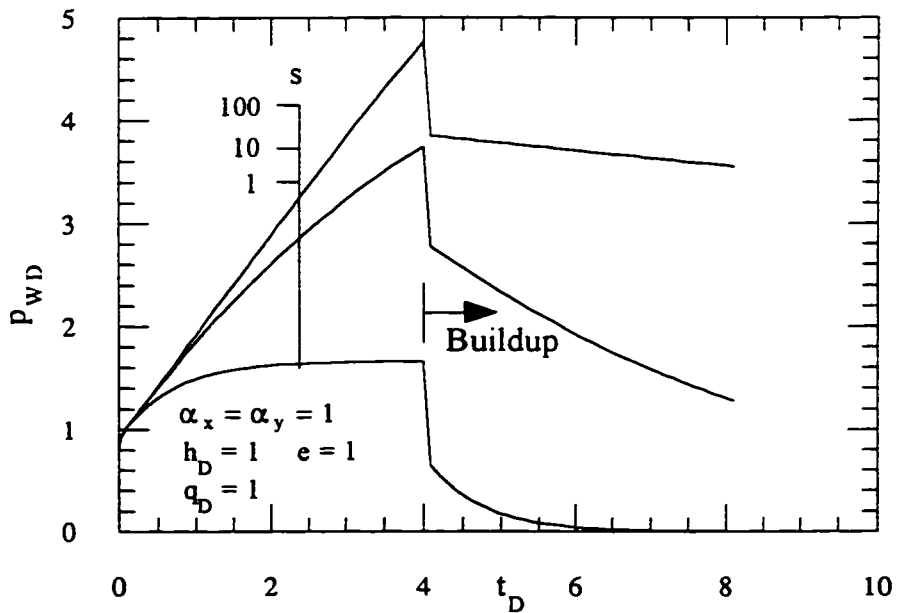


Figure 6.23: Dimensionless pressure responses at the wellbore for a shut-in period being followed by a production period where the well is shut in at $t_D = 4$ for "Combination 2".

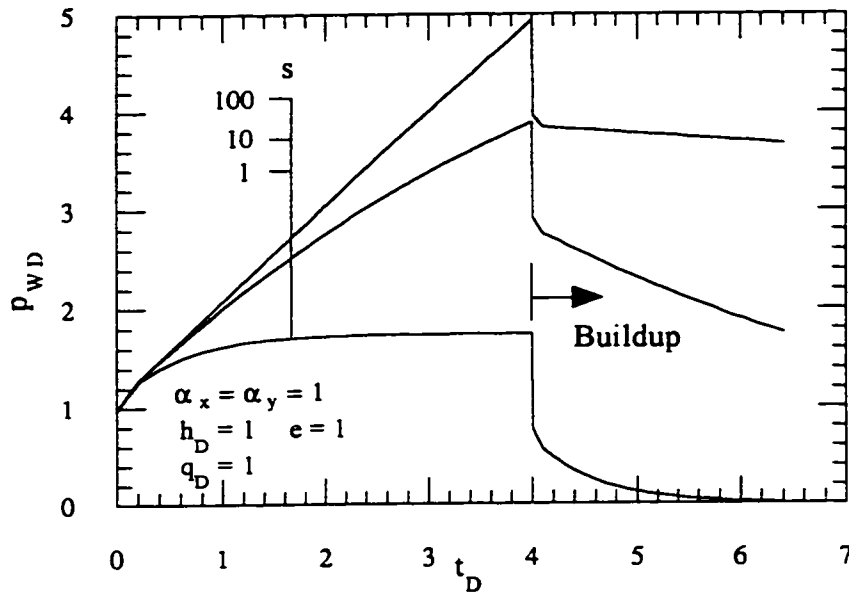


Figure 6.24: Dimensionless pressure responses at the wellbore for a shut-in period being followed by a production period where the well is shut in at $t_D = 4$ for "Combination 3".

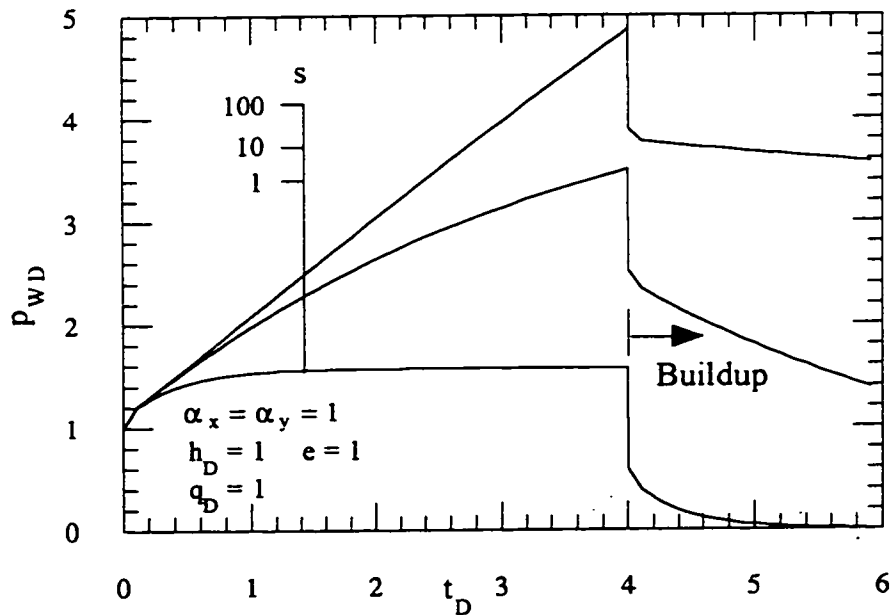


Figure 6.25: Dimensionless pressure responses at the wellbore for a shut-in period being followed by a production period where the well is shut in at $t_D = 4$ for "Combination 4".

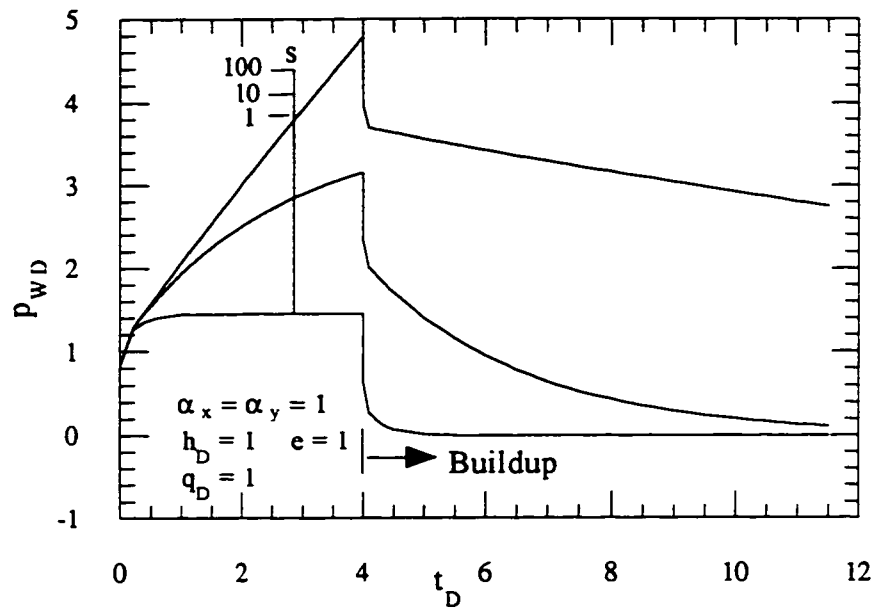


Figure 6.26: Dimensionless pressure responses at the wellbore for a shut-in period being followed by a production period where the well is shut in at $t_D = 4$ for "Combination 5".

to recognize and quantify the presence of partially-communicating faults or low-permeability barriers, if there are any. The dimensionless time at which infinite-acting radial flow ends (t_{DR}) has been estimated to be 0.101, regardless of the combination of boundary conditions. This time-criterion for the end of the infinite-acting radial flow period can be used for the semilog analysis to evaluate the rock and fluid properties of the small compartment. Also the time-criteria of Tables 6.4 through 6.8 are useful in determining the time to the start of the steady-state flow regime for the purpose of deciding the applicability of simplified analyses like the one presented in *Fox et al.* (1988). Evidence has been found in the previous Sub-Section that a pseudosteady state flow-period exists between t_{DR} and t_{DS} , that has a flattened value of the Cartesian derivative of unity. This particular period can be utilized to find the volume of the producing compartment using an extended drawdown analysis. The idea of estimating pore-volume from the extended drawdown data will be presented in Chapter 7. Therefore, the time-criteria presented earlier can help locate the pseudosteady state flow regime in a set of well test data. The onset of steady-state flow is characterized by a flattening of the Cartesian derivative profile along the intercept value of zero which signals the establishment of pressure support at the communicating boundaries of the small compartment (Figs. 6.12 through 6.16). The type-curves can also be used to design the production and shut-in schedule of the producing well ahead of time to avoid producing from the compartment below the bubble point pressure.

“Combination 2” and “Combination 3” possess the same amount of surface area for fluid communication at the boundaries. But the total area for fluid communication in “Combination 3” is split into two segments which are located at opposite sides of the small compartment. The solutions for late times of these combinations are presented in Eqs. (6.3) and (6.4), respectively, which are very close in magnitude, especially at high values of the skin factor. Dimensionless times for the start of the steady-state flow period, t_{DS} , of these combinations are tabulated in Tables 6.5 and 6.6, respectively. These

tables show that the dimensionless times in “Combination 3” are significantly shorter than those in “Combination 2” for low values of the skin factor. However, the difference in dimensionless times for these two combinations becomes insignificant for high values of the skin factor.

Dimensionless wellbore pressure at late times, as expressed by Eqs. (6.2) through (6.6), is observed to be a linear function of the finite value of the skin factor. Comparison of these equations reveals that an increase in area of the communicating boundaries for a particular value of the skin factor results in a decrease in the dimensionless wellbore pressure at steady state. An increase in area for fluid communication at the boundaries decreases the total resistance to flow which eventually causes a lower dimensionless pressure drop at the wellbore.

Comparison of Tables 6.4 through 6.8 shows a general trend of taking shorter dimensionless times for a system to reach steady-state flow with an increase in the communicating area at the boundary for identical values of the skin factor.

6.3 Two-Compartment Cellular System

Section 6.2 has dealt with a situation where a producing compartment is in hydraulic communication with a relatively big compartment having negligible internal resistance to the flow of fluid. However, in this Section the situation when the two communicating compartments are of comparable volumes having finite internal resistance to the flow of fluid is considered. *Junkin et al.* (1992) have pointed out that, in most instances, the evaluation of production data and static pressure history can be accomplished with a two-compartment system producing through a single well.

The compartmentalized system under consideration is bounded by extreme boundaries located at $x_D = X_{1D} = 0$, $x_D = X_{3D} = 1$, $y_D = Y_{1D} = 0$ and $y_D = Y_{2D} = 1$. Hydraulic communication between the compartments is poor due to the presence of a thin skin at the interface located at $x_D = X_{2D} = 0.5$ ($Y_{1D} < y_D < Y_{2D}$). The first compartment is producing at a constant rate of $q_D = 1$ through a well located areally at the center of the first compartment with coordinates ($a_D = 0.25$, $b_D = 0.5$). All the reference parameters are taken with respect to the rock and fluid properties in the first compartment ($X_{1D} \leq x_D \leq X_{2D}$). Initially the system is assumed to be at a uniform pressure. The analytical solution for a two-dimensional compartmentalized system as developed in Chapter 3 is used to generate numerical values for the system under consideration.

First, the effect of skin factor (s) on the transient responses at the wellbore is considered. The compartments with identical values of the rock and fluid properties are separated with an interface with skin. Figure 6.27 demonstrates the dimensionless pressure responses for different values of the skin factor. With increasing values of the skin factor, the elevated dimensionless pressure remains in a longer transition period before the profile merges with that of $s = 0$. Figure 6.28 shows the semilog-derivative profiles of the dimensionless pressure responses for different values of the skin factor. This plot reinforces the observations drawn from Fig. 6.27. The effects of the skin factor on the Cartesian derivative of the dimensionless pressure responses are shown in Fig. 6.29. Regardless of the value of skin factor, the flow regime eventually leads to pseudosteady-state flow where $dp_{wD}/dt_D = 1$. For instance, pseudosteady-state flow starts at $t_D = 107$ for $s = 100$ (using a criterion of the Cartesian derivative reaching within 2% of the benchmark value of 1). However, it takes longer for a higher value of the skin factor to reach the pseudosteady-state period.

Identification of the pseudosteady-state flow period is important, because one can perform an extended drawdown analysis during pseudosteady-state flow to evaluate the

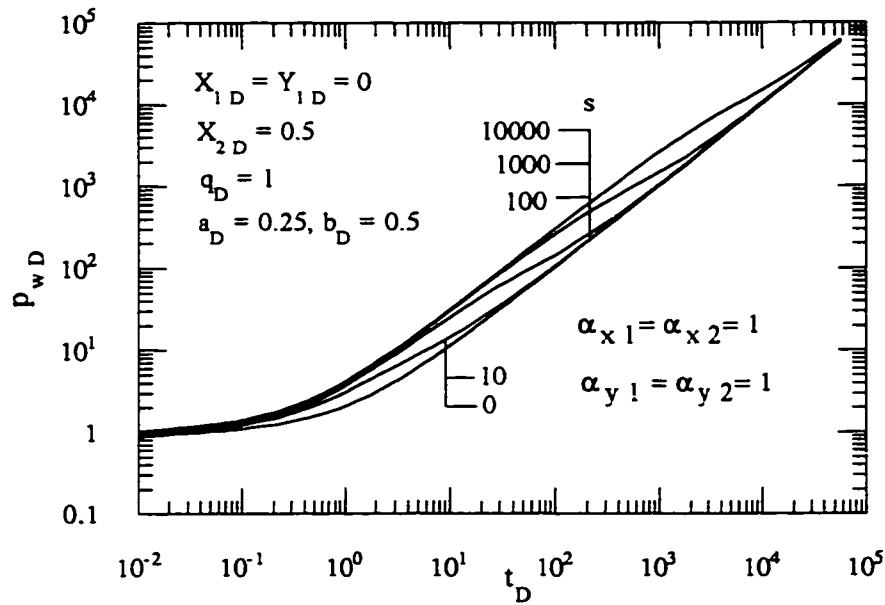


Figure 6.27: Effect of skin factor on the dimensionless pressure responses at the wellbore in a two-compartment system.

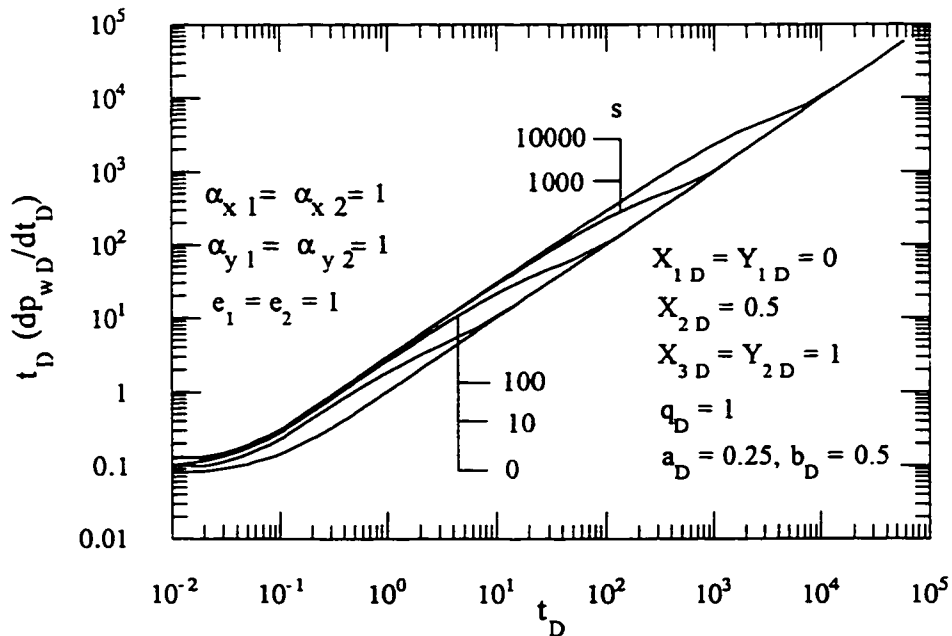


Figure 6.28: Effect of skin factor on the semilog derivative of dimensionless pressure responses at the wellbore in a two-compartment system.

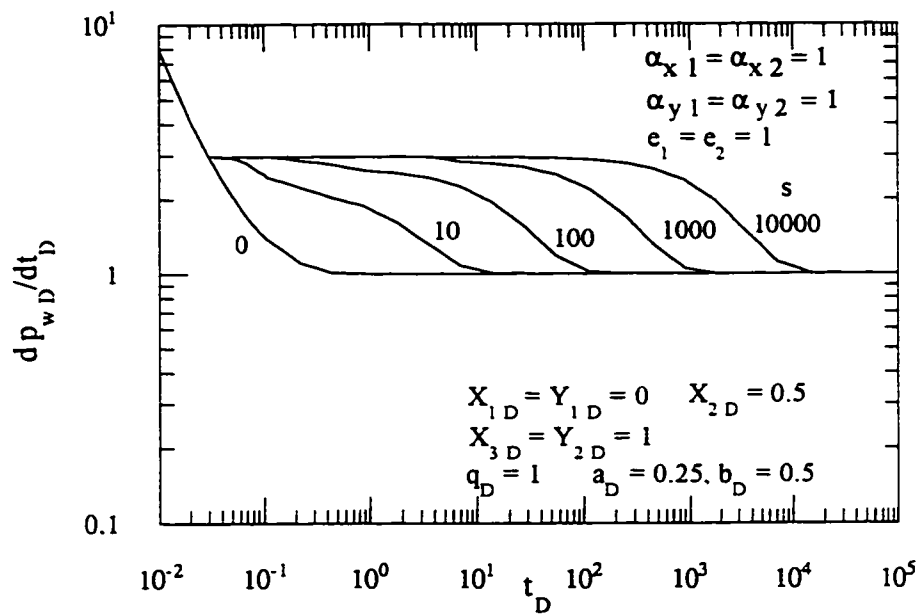


Figure 6.29: Effect of skin factor on Cartesian derivative of dimensionless pressure responses at the wellbore of a two-compartment system.

pore-volume in the producing compartment. This idea will be illustrated later in Chapter 7.

Figures 6.30 through 6.36 depict the effects of the contrasts of the values of the rock and fluid properties in the compartments on the Cartesian derivative of the dimensionless pressure responses at the wellbore. The values of $s = 100$ and 1000 are considered in these cases. A comparison of Fig. 6.30 with Fig. 6.31 shows that an increased mobility ratio in the supporting compartment (second compartment) (from $M_2 = 10$ to $M_2 = 100$) for $s = 100$ has little effect on the Cartesian derivative profiles for different storativity ratios. Moreover, a comparison of Fig. 6.30 with Fig. 6.32 demonstrates that a decreased mobility ratio in the supporting compartment (from $M_2 = 10$ to $M_2 = 0.1$) always has little effect on the Cartesian derivative. This is so because the resistance to flow due to $s = 100$ at the interface boundary is more dominant than the internal resistance in the supporting compartment. But the storativity ratio has an effect on the Cartesian derivative profiles, especially at higher values. The profiles at late times are influenced by the value of storativity ratio. A higher value of skin factor ($s = 1000$) is considered in Figs. 6.33 through 6.36. In this case, similar observations as made for $s = 100$ can be reiterated. In Figs. 6.35 and 6.36, lower mobility ratios, $M_2 = 0.01$ and 0.1 , in the supporting compartment than the producing compartment have been considered. These cases also show skin-dominated flow even after considering such low value of the mobility ratio.

The Cartesian derivative of dimensionless pressure responses at late times is approximated by the following equation:

$$\frac{dp_{wD}}{dt_D} = \frac{l}{(Y_{2D} - Y_{1D}) \sum_{i=1}^n F_i (X_{HD} - X_{iD})} \dots\dots\dots(6.7)$$

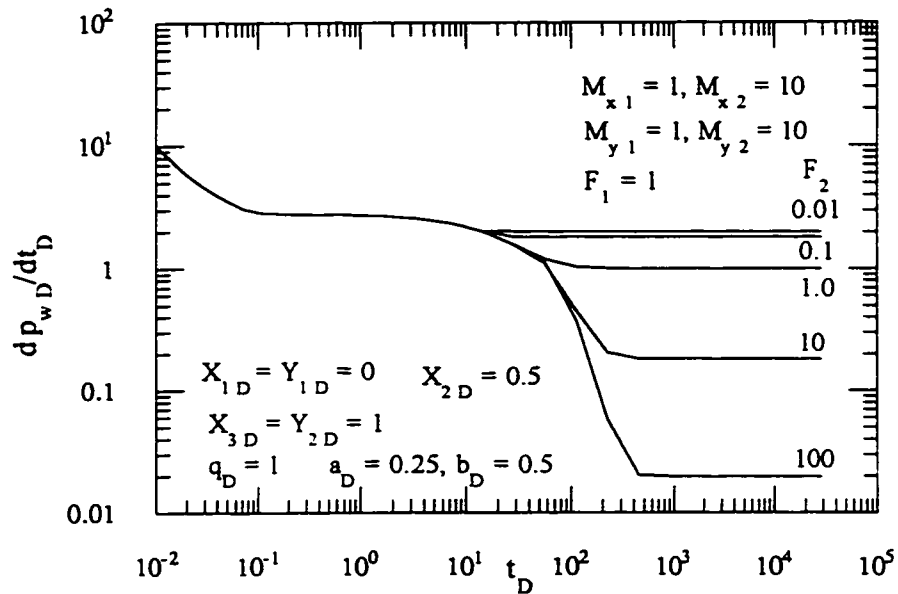


Figure 6.30: Effect of mobility and storativity ratios on Cartesian derivative of dimensionless pressure responses at the wellbore of a two-compartment system with $M_2 = 10$, $s = 100$.

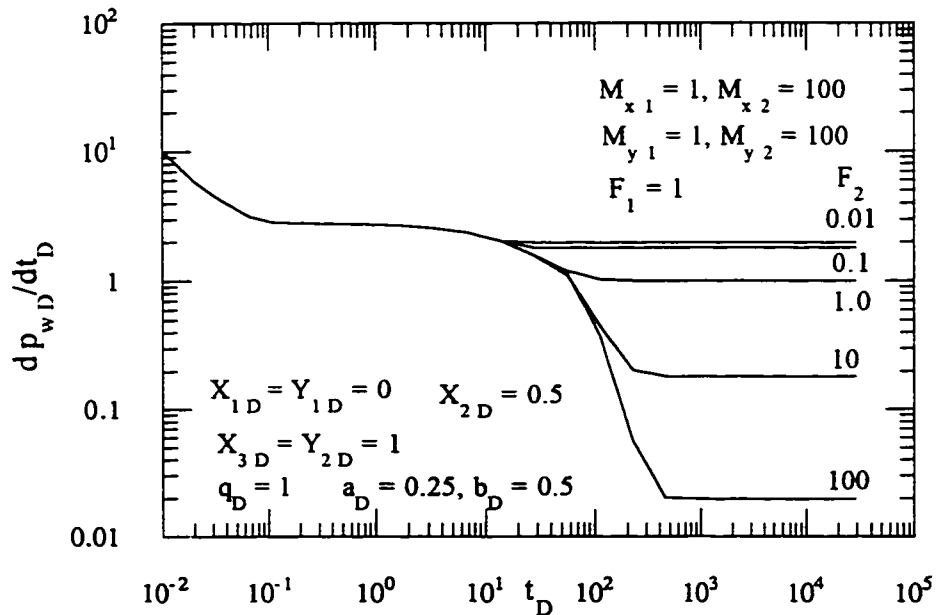


Figure 6.31: Effect of mobility and storativity ratios on Cartesian derivative of dimensionless pressure responses at the wellbore of a two-compartment system with $M_2 = 100$, $s = 100$.

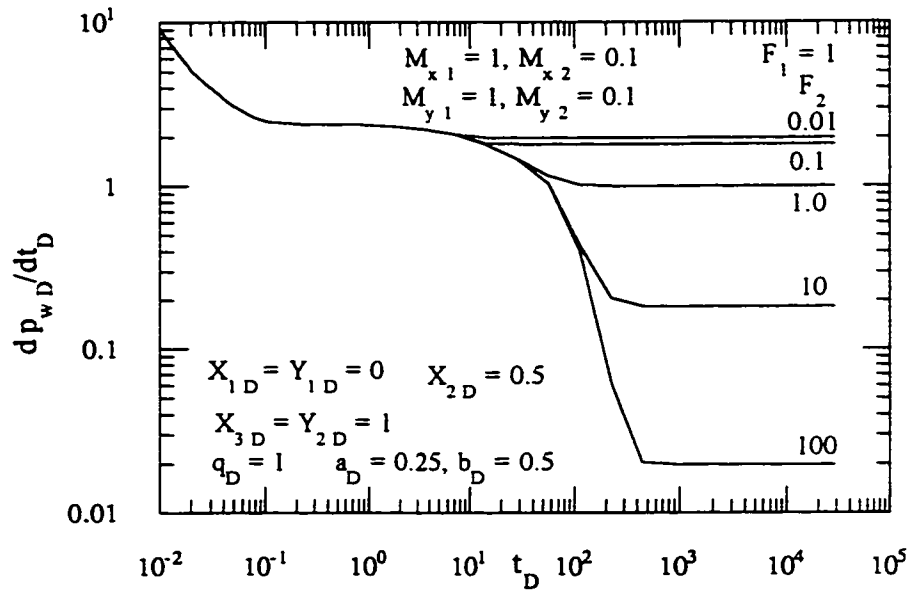


Figure 6.32: Effect of mobility and storativity ratios on Cartesian derivative of dimensionless pressure responses at the wellbore of a two-compartment system with $M_2 = 0.1$, $s = 100$.

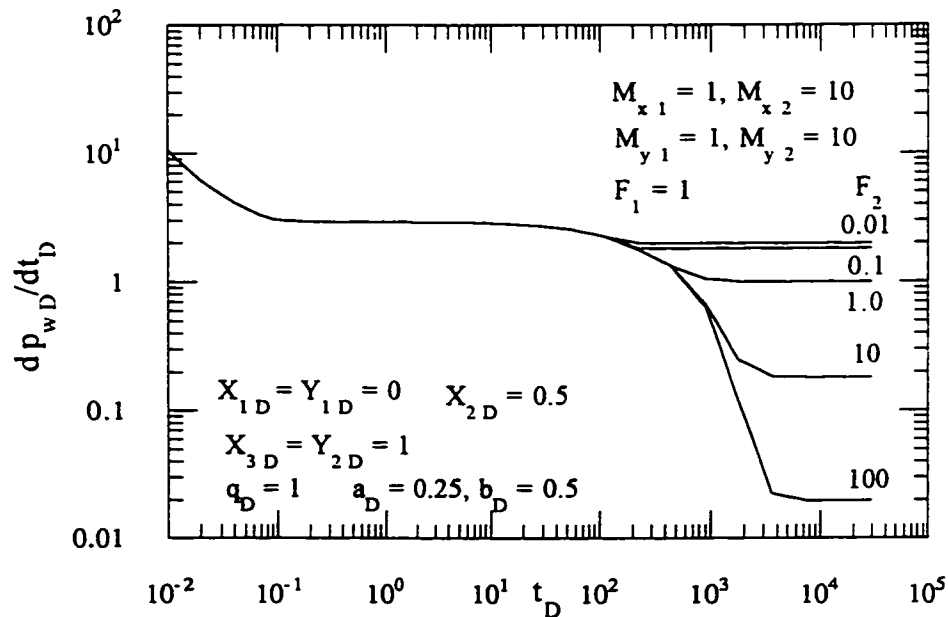


Figure 6.33: Effect of mobility and storativity ratios on Cartesian derivative of dimensionless pressure responses at the wellbore of a two-compartment system with $M_2 = 10$, $s = 1000$.

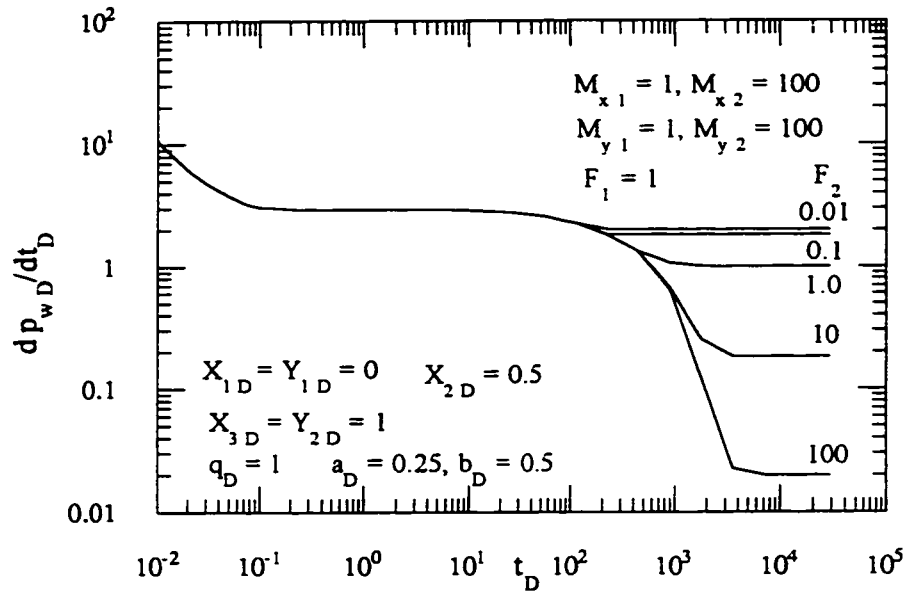


Figure 6.34: Effect of mobility and storativity ratios on Cartesian derivative of dimensionless pressure responses at the wellbore of a two-compartment system with $M_2 = 100$, $s = 1000$.

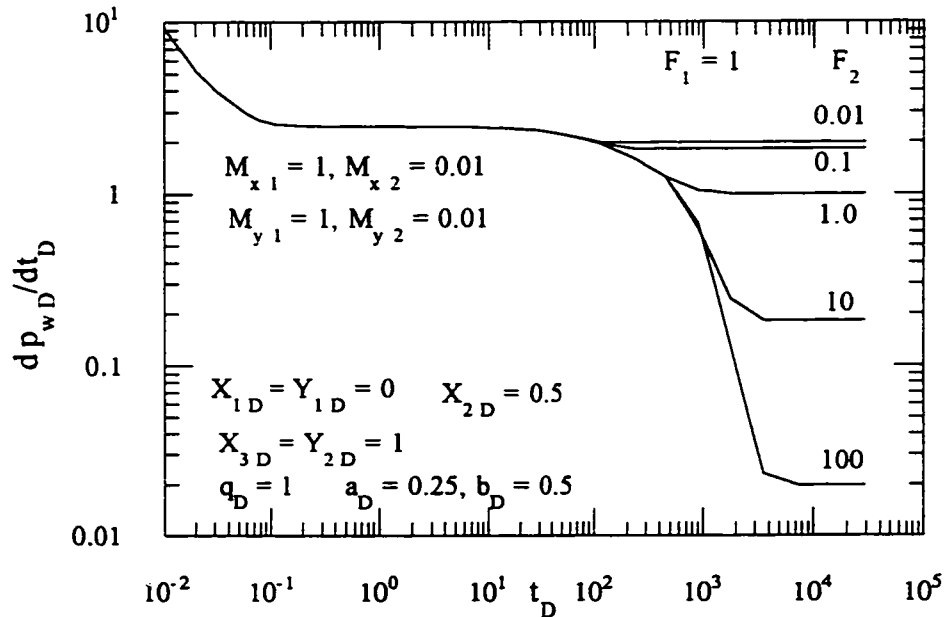


Figure 6.35: Effect of mobility and storativity ratios on Cartesian derivative of dimensionless pressure responses at the wellbore of a two-compartment system with $M_2 = 0.01$, $s = 1000$.

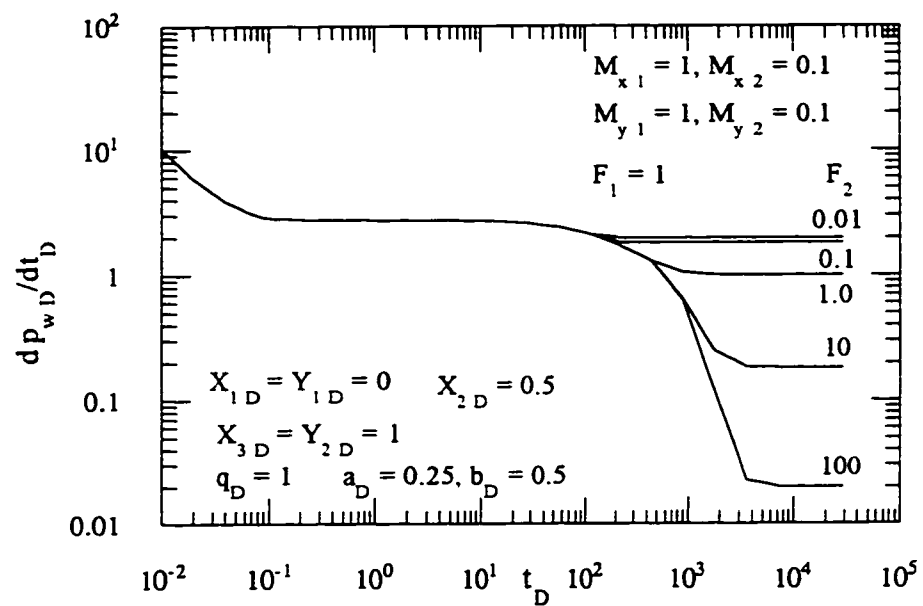


Figure 6.36: Effect of mobility and storativity ratios on Cartesian derivative of dimensionless pressure responses at the wellbore of a two-compartment system with $M_2 = 0.1$, $s = 1000$.

where n is the total number of compartments and F_i is the storativity ratio in the i th compartment. For the system under consideration with $F_1 = 1$, $F_2 = 20$, one has, $dp_w D/dt_D = 0.0952$ at late times. Equation (6.7) shows that the Cartesian derivative of dimensionless pressure responses at late times is not a function of the mobility ratio (M_i) or of the values of the skin factor. However, any higher value of F_i decreases the value of this derivative due to an increase of the pore volume and/or of total compressibility in the system. The values of the Cartesian derivative at late times are found to be in good agreement with the respective values as observed from Figs. 6.29 through 6.36. These figures also demonstrate that the value of the storativity ratio in the supporting compartment has an effect on the Cartesian derivative profile, especially at a high value during late times. However, this equation can be used in confirming the volume-weighted storativity from the late-time data or in evaluating the volume or storativity of a compartment if other parameters are known.

6.4 Stacked Channel Realization

Another important aspect of reservoir compartmentalization is a stacked channel realization where two sand bodies communicate hydraulically with each other through an overlapping area (interface). This has been illustrated schematically in Fig. 6.37. However, in this study, the poor communication between the sand bodies is taken care of by considering the presence of a thin skin at the interface. *Stewart and Whaballa (1989)* have mentioned that the sealing nature of the overlapping area would make the producing sand body behave as if it were a closed rectangular system. *Lord et al. (1992)* have pointed out that such an interface may be extensive in area, but typically consists of low-permeability shale. In this Section, the transient behavior of a stacked channel realization will be investigated.

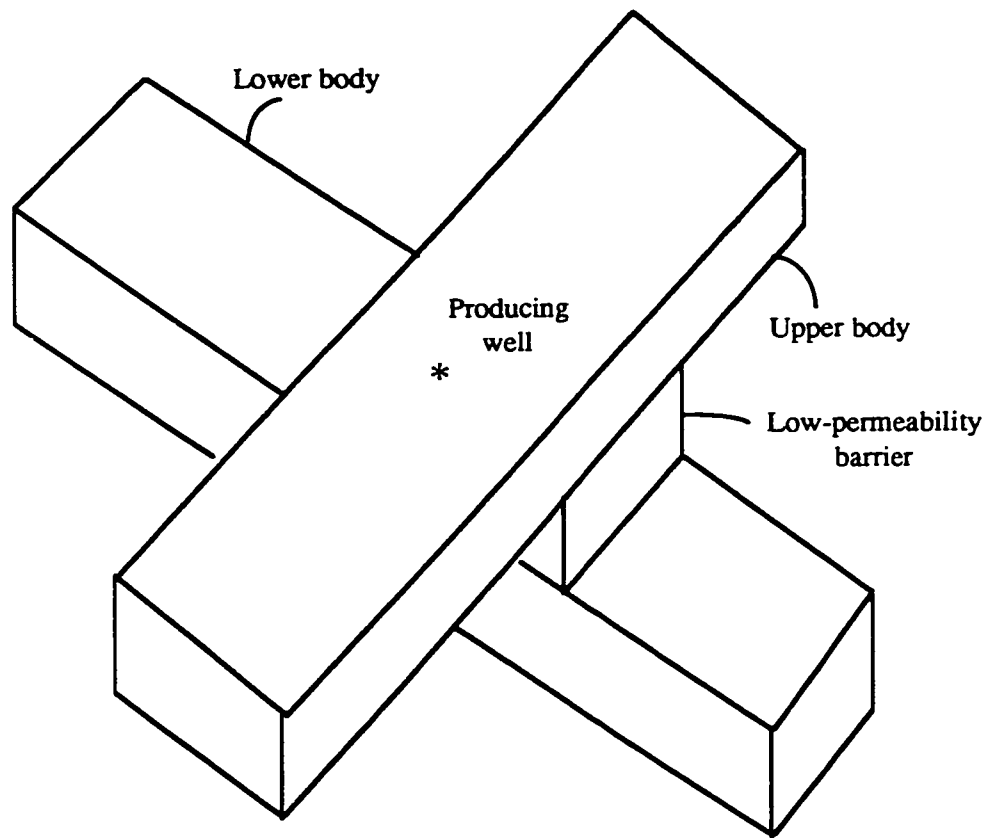


Figure 6.37: Schematic of a stacked channel realization.

Since the effects of gravity are important due to the structure of a system of stacked channels, transient-potential behavior, rather than transient-pressure, will be analyzed. The analytical solution for a three-dimensional flow system as developed in Chapter 4 will be used to generate the transient responses. The geometry of the system of stacked channels to be considered in this study is illustrated in Figs. 6.38a and 6.38b. These figures show that the upper body has a region within $X_{1D} \leq x_D \leq X_{4D}$, $Y_{2D} \leq y_D \leq Y_{3D}$ and $Z_{1D} \leq z_D \leq Z_{2D}$, and that the lower body has a region within $X_{2D} \leq x_D \leq X_{3D}$, $Y_{1D} \leq y_D \leq Y_{4D}$ and $Z_{2D} \leq z_D \leq Z_{3D}$. Also the skin surface is within the region, $X_{2D} \leq x_D \leq X_{3D}$ and $Y_{2D} \leq y_D \leq Y_{3D}$, located between the upper and lower bodies. All the extreme boundaries of this system are considered closed. All rock and fluid properties are taken with reference to those in the upper body. Initially, the entire system has been at an identical, uniform potential.

Figure 6.39 shows the effect of contrasts of rock and fluid properties in the upper and lower bodies of a stacked channel realization. Here, the upper and lower bodies are in perfect communication ($s = 0$). For a very low storativity ratio in the supporting compartment (lower body), $e_l \leq 0.1$, the producing compartment (upper body) receives very little potential support. In such cases, the Cartesian derivative responses are similar to a situation with very high communication resistance at the interface. However, for high values of the storativity ratio, $e_l > 1.0$, the upper body receives substantial potential support from the lower body. This results in low values of the Cartesian derivative at late times.

Figure 6.40 shows the effects of contrasts of rock and fluid properties when $s = 100$. The Cartesian derivative profiles for different values of e_l are presented. After the transition from infinite-acting radial flow period, there is a certain period of time where the producing compartment behaves as if it were a closed system, as indicated by flattening

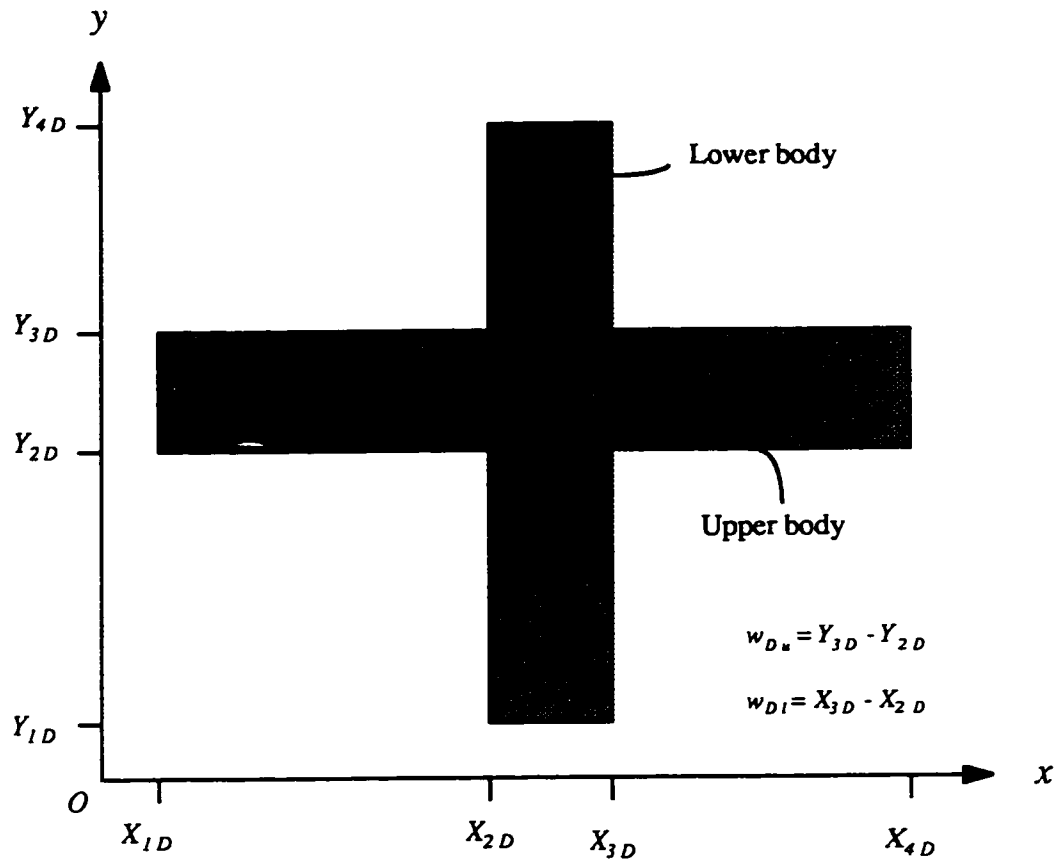


Figure 6.38a: Schematic illustrating the geometry of a stacked channel realization in areal view.

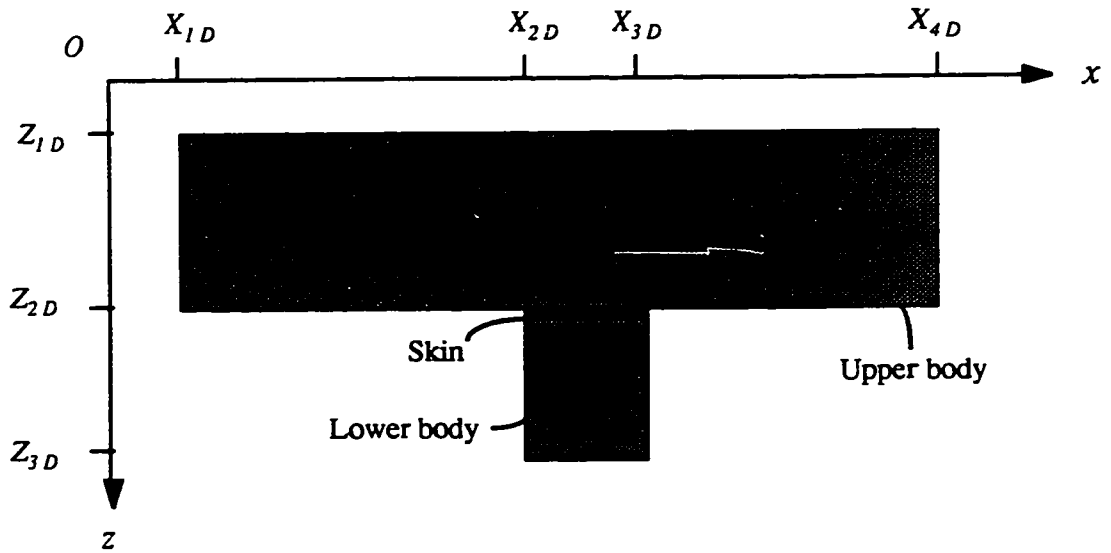


Figure 6.38b: Schematic illustrating the geometry of a stacked channel realization in plan view.

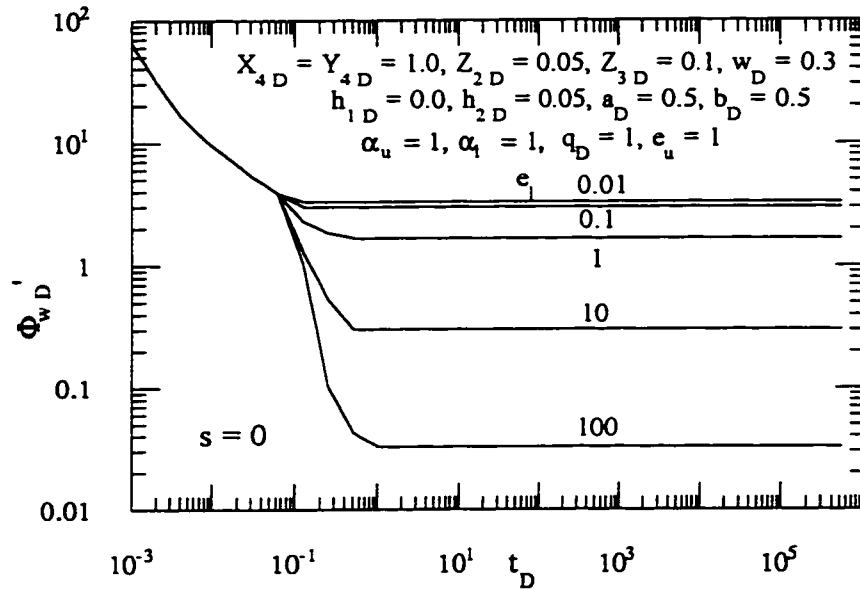


Figure 6.39: Effect of storativity ratio on the Cartesian derivative of dimensionless potential responses at a wellbore in a stacked channel realization for $s = 0$.

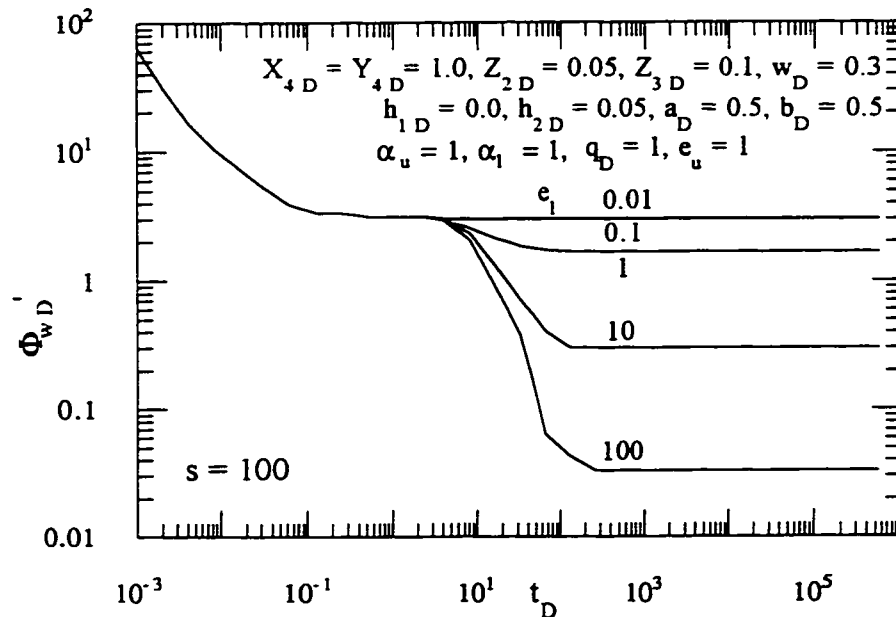


Figure 6.40: Effect of storativity ratio on the Cartesian derivative of dimensionless potential responses at a wellbore in a stacked channel realization for $s = 100$.

of the derivative values. But for $e_l \leq 0.1$, the profiles remain flat. This means that the upper body gets very little potential support from the lower body for such low storativity values for the lower body. However, this observation is identical to that for $s = 0$ in Fig. 6.39. For $e_l > 1.0$, a considerable amount of potential support is available as depicted by the lower values of the Cartesian derivative at late times. There is a time-lag for establishment of such support due to the presence of resistance at the interface between the upper and lower bodies ($s \neq 0$).

Figure 6.41 shows the Cartesian derivative profiles for the potential responses at the wellbore for different values of the skin factor in a stacked channel realization with identical rock and fluid properties in the upper and lower bodies. For $s > 0$, it is shown that the upper body (producing compartment) remains a closed system as depicted by the zero slope for some time after the infinite-acting period and the transition period after that disappear. Such an interim pseudosteady-state period is more prominent and lasts longer for a higher value of the skin factor. After this period of pseudosteady-state flow, the potential support from the lower body is established, as is depicted by the declining value of the Cartesian derivative for $s > 0$, before the entire system leads to pseudosteady-state flow. The system pseudosteady-state flow period is another flat line having a smaller value of the intercept than that during the pseudosteady-state period for the producing compartment. Recognizing these pseudosteady-state periods is important for the purpose of estimating the compartment volumes from extended drawdown data which will be discussed in the following Chapter.

The Cartesian derivative of the dimensionless potential responses at late times is approximated, from the solution presented in Chapter 4, by the following equation:

$$\frac{d\Phi_{wD}}{dt_D} = \frac{1}{e_u v_u + e_l v_l} \dots\dots\dots(6.8)$$

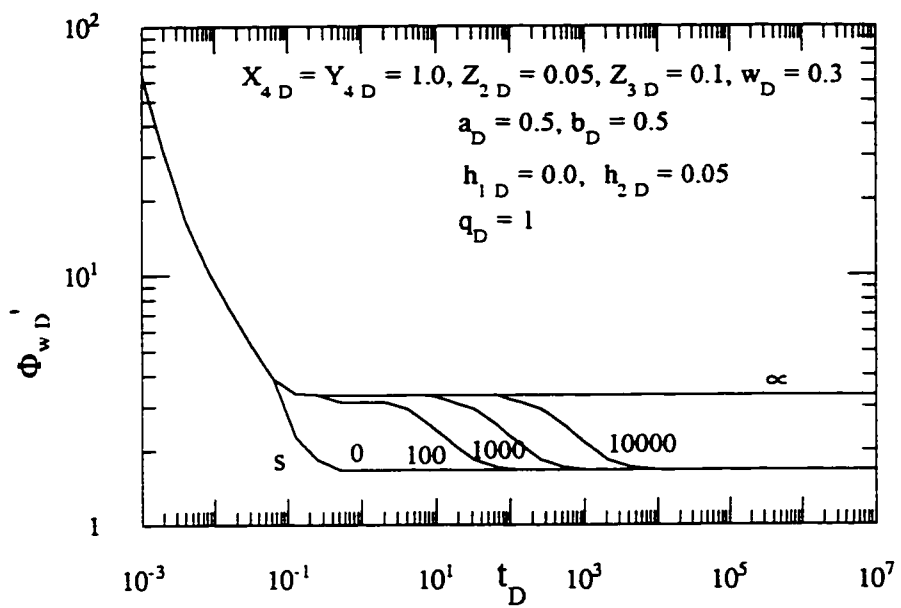


Figure 6.41: Cartesian derivative of dimensionless potential responses at a wellbore for different values of skin factor in a stacked channel realization.

where e and v stand for the storativity ratio and the dimensionless volume, respectively, and the subscripts u and l represent the upper body and the lower body, respectively. Equation (6.8) shows that the Cartesian derivative of dimensionless potential responses at late times is not a function of the mobility ratio or the skin factor. However, this equation can be used to confirm the volume-weighted storativity or to evaluate the volume or storativity of a compartment from extended drawdown data. The Cartesian derivative of the potential responses at late times, as shown in Figs. 6.39 through 6.41, is found to be in excellent agreement with that predicted by Eq. (6.8).

CHAPTER 7

EXTENDED DRAWDOWN ANALYSIS IN COMPARTMENTALIZED RESERVOIRS

7.1 Introduction

Compartmentalized models in low-permeability reservoirs are an improvement over the application of traditional volumetric analysis (material balance models). According to *Payne* (1996), this poor performance of the volumetric analysis in such reservoirs is a result of the residual pressure gradient, even after moderate shut-in periods. He also indicates that a lack of understanding of the way a number of poorly drained regions would behave in the long run could lead to a conservative estimation of reserves.

An estimation of average reservoir pressure is very important for characterizing a reservoir, computing the amount of hydrocarbons in place and predicting future reservoir behavior (*Earlougher*, 1977). Also the average reservoir pressure gives an estimation of the density of the fluids in place and the average driving force to move fluids toward the wellbore (*Raghavan*, 1993). *Dake* (1994) proposes a method for estimating the average reservoir pressure of a homogeneous system from a set of data from a two-rate flow test without any shut-in of the producing well. This method makes economic sense because any shut-in of a producing well to obtain pressure buildup data causes a loss of production. But the difficulty of establishing a second, stable production rate is mentioned as a barrier to the application of this method.

A number of well-established methods are available to measure the average reservoir pressure in homogeneous systems from pressure buildup data. These include those of *Horner* (1951), *Miller et al.* (1950), *Matthews et al.* (1954) and *Dietz* (1965).

Lord and Collins (1991) mention that the inflow relationship is valid only after a pseudosteady-state pressure distribution has evolved in the reservoir. This means that following any rate change, a time period would have to elapse before this relationship comes into effect. *Fox et al.* (1988) acknowledged the limitation of a conventional buildup test to determine the average pressure within a compartment due to uncertainty about the amount of fluid crossing a partially-communicating interface.

7.2 Relationship between Average Reservoir Pressure and Production Rate

Golan and Whitson (1986) have suggested an equation for the decline of the average reservoir pressure for constant-rate production in a closed system using material balance. To generalize the equation for the decline of the average pressure, a variable rate of production from a closed, compartmentalized system is considered. Taking a similar approach to that of *Golan and Whitson* (1986), one has the dimensionless form of this relationship as,

$$\bar{p}_D(t_D) = \frac{h_{pD} \int_0^{t_D} q_D(\tau) d\tau}{N_o} \dots\dots\dots(7.1)$$

where,

$$\bar{p}_D = \frac{k_p h_p (p_p - \bar{p})}{q_p B_p \mu_p} \dots\dots\dots(7.2)$$

$$q_D = \frac{q}{q_p} \dots\dots\dots(7.3)$$

7.3 Analysis of Extended Drawdown Data

Jones (1956) introduced the idea of analyzing the drawdown data to compute the volume of hydrocarbons from the observed rate of pressure decline due to production. *Earlougher et al.* (1968) observed that pseudosteady-state flow at the wellbore ensures that the same condition prevails at all other points in the reservoir. This has been the basis for analysis of extended drawdown data.

In the following Sub-Sections, methods will be presented to detect poor drainage between compartments and to calculate the amount of hydrocarbon reserve per unit pressure drawdown and the average reservoir pressure. Although the methods are explained in terms of a two-compartment system, they can be extended similarly to any number of compartments.

7.3.1. Detection of Poor Hydraulic Communication

Consider a two-compartment system where Compartment 1 is producing through a well at a constant rate of q , while Compartment 2 is supporting Compartment 1 hydraulically. The extreme boundaries are all closed ones. Both compartments have been subject to the same uniform, initial pressure, p_o . When the system reaches pseudosteady state, the late-time versions of the solutions from Chapters 3 and 4 are applicable.

Cartesian derivative profiles with dimensionless time for different values of the skin factor are plotted on a log-log plot in Fig. 7.1. This figure shows that the producing compartment is temporarily subject to pseudosteady-state flow after the end of the transition from infinite-acting radial flow. The responses due to this period of pseudosteady-state flow are characterized by flattening (first plateau) of the profile. A

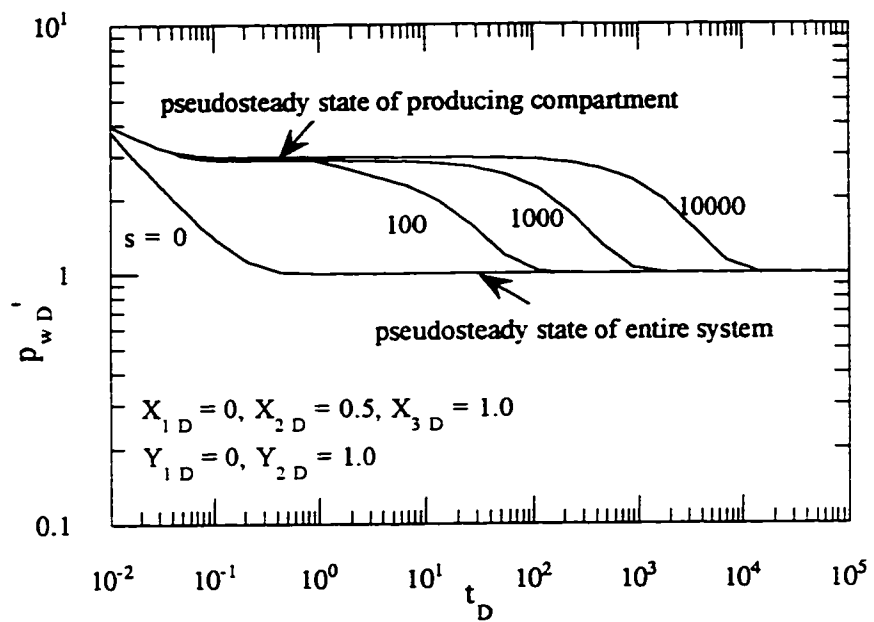


Figure 7.1: Cartesian derivative responses to detect poor hydraulic communication between compartments.

similar observation has been made in a system comprised of a small compartment in communication with a big compartment as analyzed in Section 6.3, Chapter 6. Applying pseudosteady-state analysis during this period enables estimation of the hydrocarbon pore-volume in the producing compartment. A two-compartment system possesses two plateaus: the first is due to the producing compartment and the next is due to the entire system. This observation can be extended to any number of compartments, where the number of plateaus will be equal to the number of compartments. On the other hand, for perfect communication between compartments ($s = 0$), no such plateau appears before the system reaches pseudosteady-state flow. So, the appearance of multiple plateaus in a p_w' vs. t plot is an indication of the existence of poor hydraulic communication between compartments. The order of appearance of each plateau will be in accordance with the way the compartments are arranged. However, the definition of such a plateau depends upon the value of the skin factor; a larger skin factor causes a longer plateau.

A similar approach for detecting poor communication between upper and lower sand bodies in a stacked channel realization has been shown by *Rahman and Ambastha* (1997b) by taking advantage of the fact that the partially-communicating barrier acts as a sealing barrier for some time before the entire system reaches pseudosteady state.

7.3.2 Compartment Volumes and Hydrocarbon Reserve

With the well producing at a constant rate in the first compartment, the Cartesian derivative, p_{wD}' ($= dp_{wD}/dt_D$) during the first appearance of pseudosteady-state flow is given by (from the solution in a two-dimensional system, expressed by Eq. (3.40), with a modification suggested by Eq. (3.63), Chapter 3),

$$p_{wD}'_1 = q_D h_{pD} / e_I A_I \dots \dots \dots (7.4)$$

In this analysis, the reference parameters are taken with respect to the first compartment (producing compartment). Eventually the entire system undergoes pseudosteady-state flow. Then the late-time solution for the system stated above is given by,

$$p_{wD}'_2 = q_D h_{pD} / (e_1 A_1 + e_2 A_2) \dots \dots \dots (7.5)$$

Dimensionalization of Eqs. (7.4) and (7.5) yields,

$$p_w'_1 = -q / N_{s1} \dots \dots \dots (7.6)$$

$$p_w'_2 = -q / (N_{s1} + N_{s2}) \dots \dots \dots (7.7)$$

where,

$$N_{s1} = \phi_1 c_{t1} V_1 / B_1 \dots \dots \dots (7.8)$$

$$N_{s2} = \phi_2 c_{t2} V_2 / B_2 \dots \dots \dots (7.9)$$

The values of $p_w'_1$ and $p_w'_2$ are read from the first and second flattened intercepts (plateaus), respectively, in a plot of Cartesian derivative responses at the wellbore, p_w' , versus time, t , on a Cartesian plot (or log-log plot). Figure 7.2 illustrates how these intercept values can be determined from a plot of p_w' vs. t , drawn from a set of well test data. Solving Eqs. (7.6) and (7.7) for N_{s1} and N_{s2} , one gets,

$$N_{s1} = q / |p_w'_1| \dots \dots \dots (7.10)$$

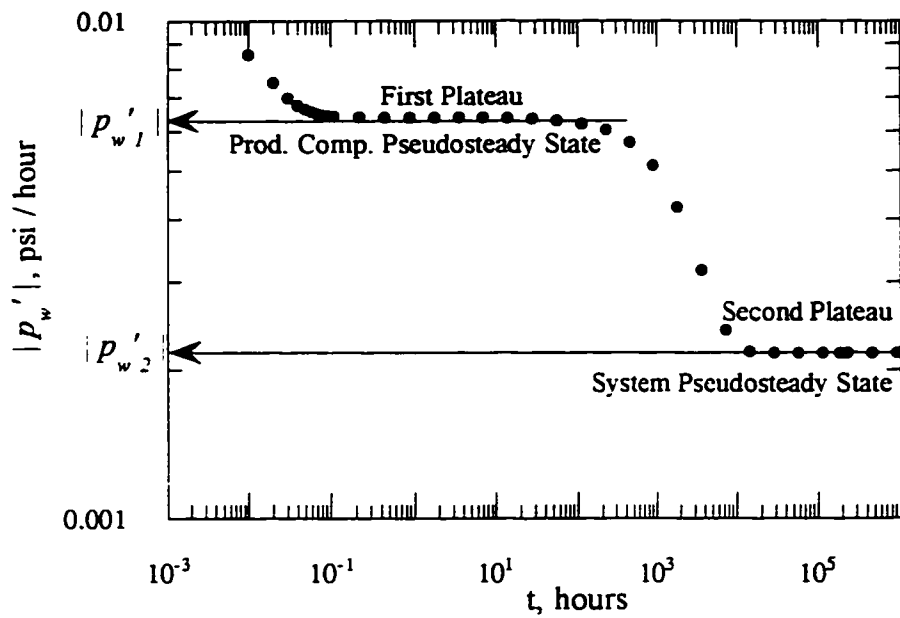


Figure 7.2: Determination of intercept values from Cartesian derivative profile plotted with well test data from a compartmentalized system.

$$N_{s,2} = q / [|p_w'_{s,2}| - |p_w'_{s,1}|] \dots\dots\dots(7.11)$$

Therefore, the hydrocarbon reserve in standard volume per unit pressure drawdown in each compartment ($N_{s,1}$ and $N_{s,2}$) is known, and the total hydrocarbon reserve in standard volume per unit pressure drawdown in the reservoir, N_S , can be computed from the following relationship,

$$N_S = N_{s,1} + N_{s,2} \dots\dots\dots(7.12)$$

This method for estimating the hydrocarbon reserve in each compartment can be extended to any number of compartments, provided the corresponding number of plateaus are available on the p_w' vs. t plot. The higher the resistance to flow at an interface (higher skin factor), the longer will be the corresponding pseudosteady-state period. If one has some prior information about formation volume factors and total compressibilities, then the respective hydrocarbon pore-volumes from Eqs. (7.8) and (7.9) can be determined. The approach taken here is based on pseudosteady-state flow. Therefore, this procedure may be extended to other compartmentalized systems regardless of the shape of the compartments.

A similar method for estimating the hydrocarbon pore-volume has been developed by *Rahman and Ambastha (1997b)*, for a stacked channel realization using extended drawdown data. In the case of a stacked channel realization, the late-time approximation of the general solution for a three-dimensional system, expressed by Eq. (4.54), has been used taking into account the proper recommendation in Section 4.3.7, Chapter 4, for having all the extreme boundaries of the closed-type. Equations for the hydrocarbon reserve in standard volume per unit potential drawdown in each compartment, similar to Eqs. (7.10) and (7.11), have been derived in terms of the intercepts of the Cartesian derivative of dimensional potential responses from a plot of Φ' vs. t .

From the drawdown data in the infinite-acting, radial-flow regime (semilog analysis), the permeability of the producing compartment can be estimated following *Tiab* (1995) as,

$$k_l = q B_l \mu_l / \{ \pi h_l (t dp_w/dt)_r \} \dots\dots\dots(7.13)$$

Subscript, *r*, refers to a data point in the infinite-acting, radial-flow regime.

7.3.3 Average Reservoir Pressure

Figure 7.3 shows the effect of the values of the skin factor at the interface on the buildup profile at the shut-in well in the first compartment. This figure shows that a longer buildup time is required to reach the average reservoir pressure for a higher value of the skin factor. Table 7.1 shows the dimensionless buildup times and the corresponding buildup times in hours with respect to a set of reference parameters for different values of *s*. For *s* > 0, the buildup times required to the average reservoir pressure are very high and such long buildup times may not always be feasible for practical reasons. As an alternative to a buildup test running for such a long time, here we will develop a method to calculate the average reservoir pressure from stabilized drawdown data.

Simplification of Eq. (7.1) into dimensional form yields,

$$p_o - \bar{p} = \frac{q t}{N_s} \dots\dots\dots(7.14)$$

The dimensionless wellbore pressure of the system under consideration at pseudosteady state can be approximated by,

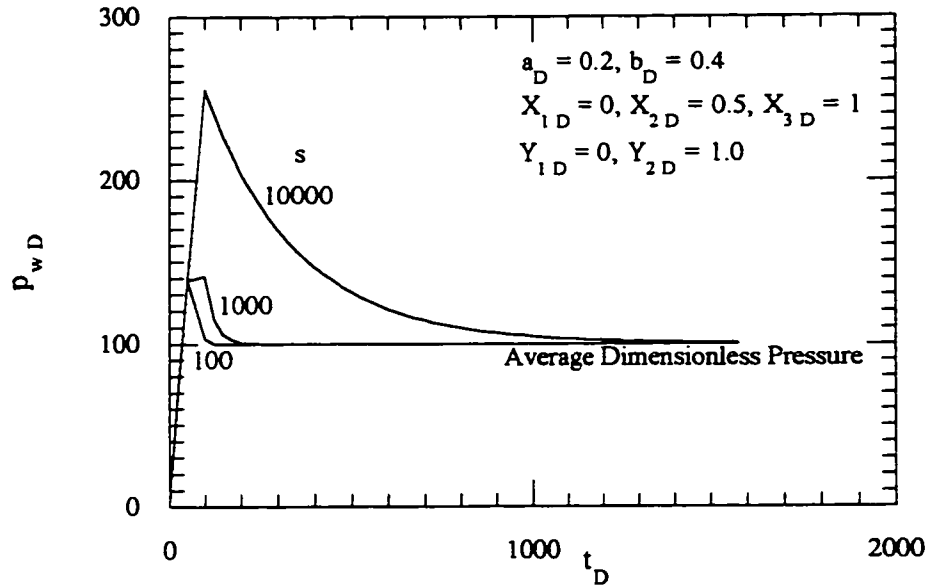


Figure 7.3: Buildup behavior at a well in the first compartment for different values of skin factor after a production period of $t_D = 100$.

TABLE 7.1: BUILDUP TIME REQUIRED FOR DIFFERENT SKIN FACTORS

Skin factor, s	Dimensionless buildup time	Buildup time*, hours
0	0.12	696.02
10	1.96	1.13×10^4
100	12.45	7.22×10^4
1000	165.2	9.58×10^5
10000	1662.0	9.64×10^6

* Based on reference parameters: $k_p = 100$ md, $\phi_p = 0.23$, $c_p = 11.4 \times 10^{-6}$ psi⁻¹, $\mu_p = 0.584$ cp, $X_p = 10000$ ft.

$$p_{wD} = C_w + q_D t_D h_{pD} / (e_1 A_1 + e_2 A_2) \dots \dots \dots (7.15)$$

where C_w is a constant. Mathematically, C_w is a function of the location of the well within the producing compartment and the skin factor, among other parameters, of a given system. To take into account the effect of well location on C_w , identical values of rock and fluid properties are considered in a compartmentalized system. Values of C_w for systems with different well locations corresponding to the aspect ratio of the producing compartment, $XY = 0.5, 1$ and 2 (Fig. 7.4) are presented in Tables 7.2 through 7.10. *Ramey and Cobb (1971)* made a similar observation with respect to pseudosteady-state flow in a closed, homogeneous square as in Eq. (7.15) where the late-time dimensionless pressure is shown to be a linear function of dimensionless time. Nevertheless, a comparison of the values of C_w in Tables 7.2 through 7.10 indicates that while C_w is a strong function of the skin factor, it is only a weak function of the well location in the producing compartment. Based on this observation, average values of C_w , calculated from those presented in Tables 7.2 through 7.10, are proposed in Table 7.11,. These values can be used for the purpose of estimating the average reservoir pressure, the procedure for which will be explained later.

Upon dimensionalization of Eq. (7.15) and substituting Eq. (7.14) in it, one gets,

$$\bar{p} = p_w + C_w q B_1 \mu_1 / k_1 h_1 \dots \dots \dots (7.16)$$

Therefore, \bar{p} can be computed from the flowing bottomhole pressure using Eq. (7.16), provided the system has reached pseudosteady state. This equation shows a linear relationship between the average reservoir pressure and the flowing bottomhole pressure at pseudosteady state in a compartmentalized system.

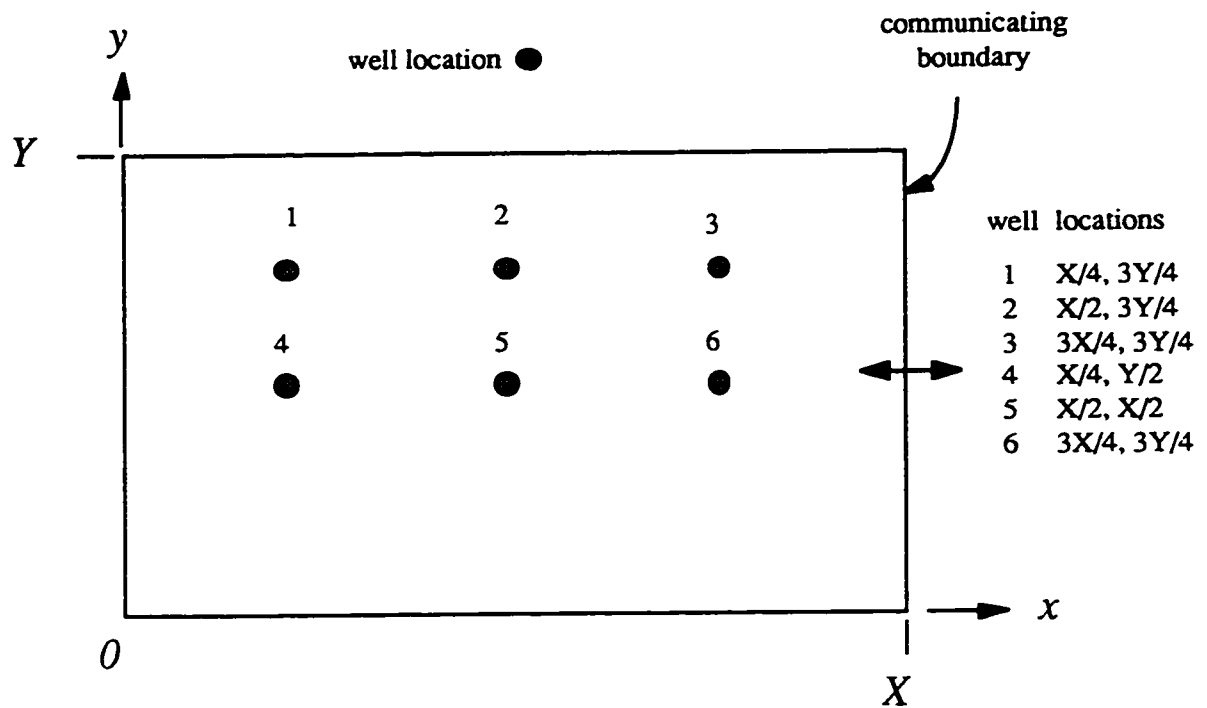


Figure 7.4: Well locations considered for determining C_w for different values of X/Y .

TABLE 7.2: VALUES OF C_w FOR WELL LOCATIONS IN A COMPARTMENTALIZED SYSTEM WITH $X/Y = 0.5, s = 100$

Well location	C_w
1	3.033
2	3.09
3	3.03
4	3.192
5	3.2
6	3.123

TABLE 7.3: VALUES OF C_w FOR WELL LOCATIONS IN A COMPARTMENTALIZED SYSTEM WITH $X/Y = 0.5, s = 1000$

Well location	C_w
1	41.53
2	41.6
3	41.53
4	41.76
5	41.65
6	41.66

TABLE 7.4: VALUES OF C_w FOR WELL LOCATIONS IN A COMPARTMENTALIZED SYSTEM WITH $X/Y = 0.5, s = 10000$

Well location	C_w
1	469.9
2	469.97
3	469.89
4	470.15
5	470.0
6	470.03

TABLE 7.5: VALUES OF C_w FOR WELL LOCATIONS IN A COMPARTMENTALIZED SYSTEM WITH $X/Y = 1, s = 100$

Well location	C_w
1	3.26
2	3.26
3	3.18
4	3.31
5	3.36
6	3.23

TABLE 7.6: VALUES OF C_w FOR WELL LOCATIONS IN A COMPARTMENTALIZED SYSTEM WITH $X/Y = 1, s = 1000$

Well location	C_w
1	41.84
2	41.83
3	41.73
4	41.93
5	41.96
6	41.82

TABLE 7.7: VALUES OF C_w FOR WELL LOCATIONS IN A COMPARTMENTALIZED SYSTEM WITH $X/Y = 1, s = 10000$

Well location	C_w
1	470.24
2	470.23
3	470.12
4	470.38
5	470.37
6	470.22

TABLE 7.8: VALUES OF C_w FOR WELL LOCATIONS IN A COMPARTMENTALIZED SYSTEM WITH $X/Y = 2, s = 100$

Well location	C_w
1	3.56
2	3.77
3	3.55
4	3.68
5	3.8
6	3.56

TABLE 7.9: VALUES OF C_w FOR WELL LOCATIONS IN A COMPARTMENTALIZED SYSTEM WITH $X/Y = 2, s = 1000$

Well location	C_w
1	42.23
2	42.07
3	42.37
4	42.37
5	42.1
6	42.69

TABLE 7.10: VALUES OF C_w FOR WELL LOCATIONS IN A COMPARTMENTALIZED SYSTEM WITH $X/Y = 2, s = 10000$

Well location	C_w
1	470.96
2	470.57
3	470.49
4	470.97
5	470.77
6	470.51

TABLE 7.11: AVERAGE VALUES OF C_w FOR DIFFERENT VALUES OF SKIN FACTOR IN A COMPARTMENTALIZED SYSTEM

Skin factor	C_w
100	3.26
1000	41.9
10000	470.7

Figures 7.5 and 7.6 show the comparison of the predicted dimensionless wellbore pressures at late time using the recommended values of C_w from Table 7.11 with those from the analytical solution. As mentioned earlier, the values of C_w are valid at pseudosteady state. The onset of pseudosteady-state flow in Figs. 7.5 and 7.6 is indicated by flattening of the Cartesian derivative corresponding to a skin factor. These figures show that the predicted values (discrete points) of dimensionless pressure at late time match well with the values from the analytical solution.

In this Chapter, a simple diagnostic technique has been developed to identify poor hydraulic-communication between compartments from p_w' vs t plots. Procedures leading to the computation of the hydrocarbon reserve in each compartment and in the entire reservoir, and the average reservoir pressure from the extended drawdown data have also been developed.

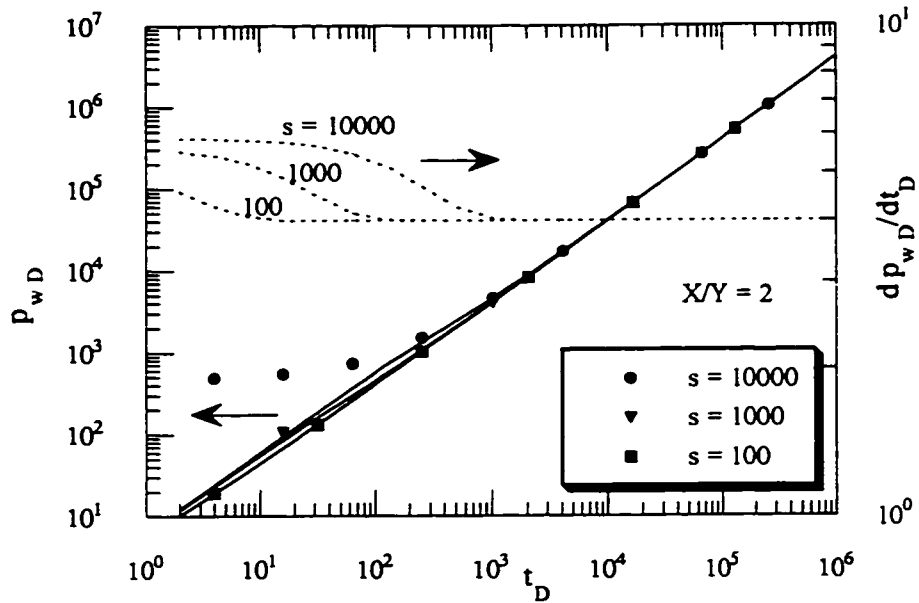


Figure 7.5: Comparison of the predicted dimensionless wellbore pressure at late time with that from the analytical solution with $X/Y = 2$.

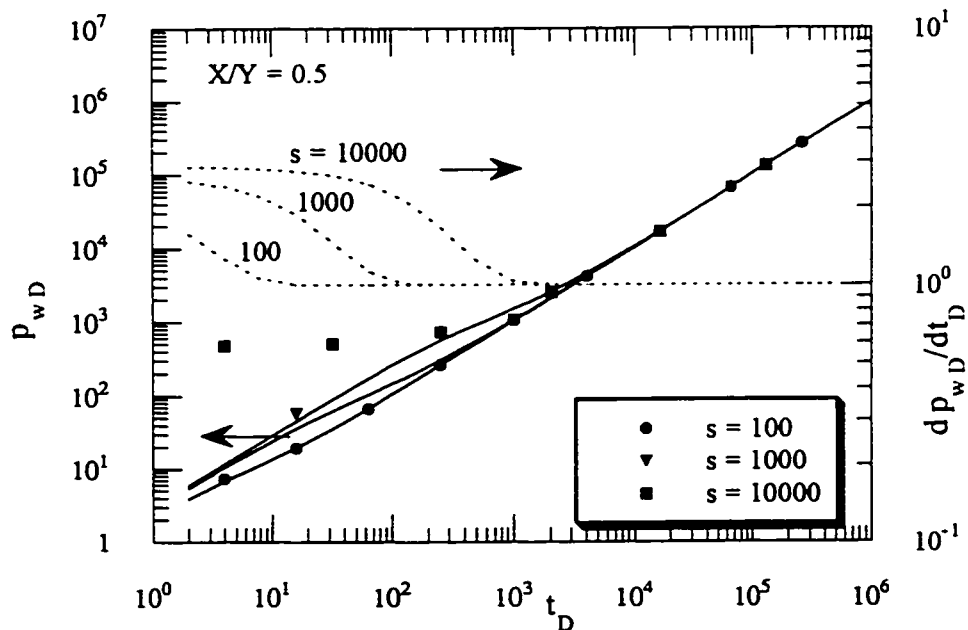


Figure 7.6: Comparison of the predicted dimensionless wellbore pressure at late time with that from the analytical solution with $X/Y = 0.5$.

CHAPTER 8

DISCUSSION, CONCLUSIONS AND RECOMMENDATIONS

8.1 General Discussion

In this study, the necessary analytical solutions have been developed to help understand the transient behavior of a number of compartmentalized systems. Poor communication between an adjoining pair of compartments has been comprehensively modeled as being due to the presence of a thin skin at the interface. As a result of this, the rate of fluid crossing the interface is primarily dependent on the amount of pressure (or potential) drop occurring across the skin. The value of the skin factor regulates the amount of pressure (or potential) drop. The higher the value of the skin factor, the higher pressure (or potential) drop that will occur across the interface, while the other parameters of the system remain the same. This approach of estimating the amount of fluid communication is more comprehensive than that which has been considered in the literature using the concept of barrier transmissibility.

New analytical solutions have been developed for transient flow in compartmentalized systems with the flow governed by one-, two- and three-dimensional Cartesian representations. Attempts have been made to include more complicated situations by extending one-dimensional to three-dimensional systems. These solutions are more rigorous than models based on the material balance technique (tank models) because of the fact that these new analytical solutions include the shape, size, internal resistance to flow and the contrasts of rock and fluid properties of a compartmentalized system. Nevertheless having more parameters with regards to rock and fluid properties and the geometry of the system in the analytical solutions makes the problem of non-uniqueness worse. This problem can be minimized when an estimation of some (if not all) of the parameters, with a high confidence level, is available. Despite the problem of non-

uniqueness, the analysis proposed in this study enables a better production (or pressure) match in compartmentalized systems. That is, this new approach is expected to overcome the shortcomings of the material balance techniques.

In order to develop the new solutions, an integral-transform technique for finite, composite domains has been used. The properties of this technique that are considered to be important include:

- it is applicable to finite, composite domains;
- it is capable of dealing with multi-dimensional variables (*e.g.*, 3 dimensional space variables);
- it has convenient transformation and inversion processes.

To the best of the author's knowledge, this method has not been used in the Petroleum Engineering literature. This integral-transform technique has proved itself to be very efficient and useful in complicated scenarios like compartmentalized reservoirs. Also, there are a lot possibilities for improvement of the simple solutions that are already known in the well-testing literature. Attempts to improve such solutions have usually failed because of the inability to deal with multiple independent variables or the process of inversion, as sometimes occurs when using the Laplace-transform technique. Application of a very powerful technique, such as the integral-transform technique, may prove to be useful when revisiting some of these simple solutions in the literature for the purpose of improving their utility. This could lead to increasing the number of tools that are currently available for analyzing and interpreting well-test data.

Equivalent production rates of compartmentalized systems with multiple wells and multiple rates have been developed with respect to the same compartmentalized system and to homogeneous systems. The ideas of equivalence have been illustrated by generating results from the mathematical expressions. The purpose of such equivalence is to integrate the interference of wells due to production into an equivalent system.

New solutions have been used for studying the transient behavior of different compartmentalized systems. The systems that have been considered include a linear system, a system with a small compartment in communication with a big one, a two-compartment system and a stacked channel realization. The effects of the inclusion of the resistance to flow and the contrast of the rock and fluid properties have been investigated. Correlations and time criteria have been proposed with the help of identifying different flow regimes.

An extended drawdown analysis for a compartmentalized system has been presented. Evidence has also been presented in Sub-Section 6.3.1, Chapter 6 and Sub-Section 7.3.1, Chapter 7, to show that a partially-communicating fault or barrier acts as a sealing fault temporarily for some time. During this period, by taking advantage of pseudosteady-state flow, it is possible to obtain information about a compartmentalized system from extended tests. A new, but simple, diagnostic technique has been developed to identify any poor hydraulic communication between compartments from drawdown data. It has been shown that estimation of the hydrocarbon pore-volume in each compartment, the total reserve and the average reservoir pressure, is possible from the late-time data.

8.2 Conclusions

Based on the study presented in the preceding Chapters, the following conclusions are drawn:

1. New generalized solutions for transient flow in one-, two- and three-dimensional coordinate systems have been developed analytically. These solutions have been validated by comparing a number of simplified cases with those available in the literature.

2. The principle of reciprocity has been found to be applicable with the new solutions, provided the conditions at the extreme boundaries of a compartmentalized system are of the homogeneous Dirichlet-, Neumann-type or a combination of these.

3. The slope of the dimensionless pressure profile with respect to dimensionless time on a log-log plot increases to slightly more than 1/2 as the infinitely-acting linear flow period ends for a non-zero value of the skin factor in a linear compartmentalized system.

4. Time criteria for the start of the pseudosteady-state flow period confirm that a higher value of the skin factor delays the onset of the pseudosteady-state flow period in a compartmentalized system.

5. The effect of the boundaries starts, or the infinite-acting radial flow ends, at $t_{DR} = 0.101$, regardless of the combination of boundary conditions or of the value of the skin factor in a system comprising a small, producing compartment in communication with a big one. In such a system, the dimensionless time required to reach steady state becomes shorter with an increase of the surface area for fluid communication with the same value of the skin factor. Dimensionless wellbore pressure at steady state decreases with an increase of the surface area for fluid communication with the same value of the skin factor. The presence of a communicating boundary with a higher value of the skin factor requires a longer time to make up the pressure drawdown in the small compartment.

6. A higher, or lower, value of the mobility ratio in the supporting compartment has little effect on the Cartesian derivative of the dimensionless pressure

responses at the wellbore in the producing compartment. This is due to the fact that the resistance to flow at the interface boundary dominates the internal resistance to flow in the supporting compartment.

7. The storativity ratio in the supporting compartment has an effect on the Cartesian derivative profiles, especially at a high value of the storativity ratio during late times.

8. For low storativity of the supporting compartment, the system behaves as if there is no communication of potential support to the producing compartment.

9. A partially-communicating barrier between a pair of adjoining compartments behaves as a sealing barrier temporarily for a certain period of time. This period lasts longer for a higher value of the resistance to fluid communication (skin factor).

10. Based on the observation made in Item 9, a simple diagnostic technique has been developed to detect any poor hydraulic communication between compartments from drawdown data. Observation of multiple plateaus in p_w' (Cartesian derivative of wellbore pressure or potential) vs. t is an indication of the presence of pressure (or potential) support through partially-communicating barrier(s).

11. The observation made in Item 9 has also been utilized to develop a method for computing the hydrocarbon reserve in each compartment and in the entire reservoir from extended drawdown data.

12. A new method has been proposed to compute the average reservoir pressure from the flowing bottomhole-pressure data.

8.3 Recommendations

Upon the conclusion of this study, the following areas are recommended for further study:

1. Developing analytical solutions of some simple problems with enhanced features to improve the current level of understanding of the transient-pressure behavior for the flow of fluids, taking advantage of the ability of the integral-transform technique to deal with multi-dimensional flow situations.
2. Developing solutions for the flow of natural gas in compartmentalized systems using the necessary transformations for pressure-sensitive gas properties. If the potential formulation is used, it must be considered in terms of energy per unit mass to make it consistent with the ideas of *Hubbert (1940)*.
3. Extending the solutions for the flow of multiphase fluids in compartmentalized systems by using the necessary transformations for pressure-sensitive fluid properties.
4. Using the solutions for transient flow developed in this study for understanding reservoir heterogeneity.

Item 1 is concerned with developing the analytical solutions for more complicated problems than the existing ones. One of the obstacles to obtaining such solutions has been the limited ability of the techniques in use (*e.g.*, Laplace transform) to deal with multiple

independent variables (*e.g.*, space coordinates). The development of such new solutions by utilizing an integral-transform technique for finite domains is expected to improve the understanding of transient-pressure behavior, as compared to that obtained using conventional techniques. With the proposed solutions in Items 2 and 3, different time criteria for compartmentalized systems should be developed for the purpose of understanding the transient behavior of the flowing fluids. Item 4 necessitates the use of an analytical solution for understanding the reservoir heterogeneity in terms of the variations of rock and fluid properties. The solutions developed in this study, and those recommended to be developed in the future, take proper account of the internal resistance to flow and the contrasts in fluid and rock properties, including anisotropy. Consequently, these solutions can be used to characterize reservoir systems wherein the compartmentalization is not as prominent as the reservoir heterogeneity.

REFERENCES

- Abbaszadeh, M. and Cinco-Ley, H.: "Pressure-Transient Behavior in a Reservoir with a Finite-Conductivity Fault," *SPE Formation Evaluation* (Mar. 1995) 26-32.
- Acosta, L.G. and Ambastha, A.K.: "Thermal Well Test Analysis Using an Analytical Multi-Region Composite Reservoir Model," paper SPE 28422 presented at the 69th Annual Technical Conference and Exhibition of the SPE of AIME, New Orleans, LA (Sept. 25-28, 1994)
- Almeida, A.R. and Cotta, R.M.: "Integral Transform Methodology for Convection-Diffusion Problems in Petroleum Reservoir Engineering," *International Journal of Heat and Mass Transfer* (1995) **38**, No. 18, 3359-3367.
- Alvarado, R.W.: "The Role of Pressure Transient Analysis in Reservoir Characterization - An Integrated Approach," *SPE Advanced Technology Series* (Mar. 1994) **2**, No. 1, 111-115.
- Ambastha, A.K.: *Pressure Transient Analysis in Composite Systems*, Ph.D. Thesis, Stanford University, CA (Oct. 1988) 193 pp.
- Ambastha, A.K., McLeroy, P.G. and Grader, A.S.: "Effect of a Partially Communicating Fault in a Composite Reservoir on Transient Pressure Testing," *SPE Formation Evaluation* (June 1989) 210-218.
- Ambastha, A.K. and Sageev, A.: "Linear Water Influx of an Infinite Aquifer through a Partially Communicating Fault," *Proceedings of the 12th Geothermal Reservoir Engineering Workshop*, Stanford, CA (Jan. 20-22, 1987).
- Badgett, K.L., Crawford, G.E., Mills, W.H., Mitchell, S.P. and Vinson, G.S., III: "Using Pressure Transient Analysis to Improve Well Performance and Optimize Field Development in Compartmentalized Shelf Margin Deltaic Reservoirs," paper SPE 36542 presented at the 71st Annual Technical Conference and Exhibition of the SPE of AIME, Denver, CO (Oct. 6-9, 1996).
- Bear, J.: *Hydraulics of Groundwater*, McGraw-Hill International Book Company (1972).
- Bixel, H.C., Larkin, B.K. and van Poolen, H.K.: "Effect of Linear Discontinuities on Pressure Build-Up and Drawdown Behavior," *Journal of Petroleum Technology* (Aug. 1963) 885-895; *Transactions of AIME*, **228**.
- Borse, G.J.: *FORTTRAN 77 and Numerical Methods for Engineers*, PWS Publishers (1985) 353-360.

- Bourdet, D., Ayoub, J.A. and Pirard, Y.M.: "Use of Pressure Derivative in Well-Test Interpretation," *SPE Formation Evaluation* (June 1989) 293-302.
- Bourdet, D., Whittle, T.M. and Pirard, Y.M.: "A New Set of Type Curves Simplifies Well Test Analysis," *World Oil* (May 1983) 95-106.
- Bourgeois, M.J., Daviau, F.H. and Boutaud de la Combe, J-L.: "Pressure Behavior in Finite Channel-Levee Complexes," paper SPE 26461 presented at the 68th Annual Technical Conference and Exhibition of the SPE of AIME, Houston, TX (Oct. 3-6 1993).
- Bradley, J.S. and Powley, D.E.: "Pressure Compartments in Sedimentary Basins: A Review," *Basin Compartments and Seals*, AAPG Memoir 61, The American Association of Petroleum Geologists, Tulsa, OK, USA (1994) 3-26.
- Butler, J.J. and Liu, W.Z.: "Pumping Tests in Non-Uniform Aquifers - the Linear Strip Case," *Journal of Hydrology* (1991) 128, 69-99.
- Cant, D.J.: "Fluvial Facies Models and Their Application," *Sandstone Depositional Environments*, AAPG Memoir 31, The American Association of Petroleum Geologists, Tulsa, OK, USA (1982) 115-137.
- Carslaw, H.S. and Jaeger, J.C.: *Conduction of Heat in Solids*, 2nd Edition, Oxford at the Clarendon Press (1959) 18-23.
- Case, C.M. and Peck, M.K.: "Transform Approach to Solution of Groundwater Flow Equations," *Journal of Hydrology* (1977) 32, 305-320.
- Chan, Y.K., Mullineux, N. and Reed, J.R.: "Analytic Solutions for Drawdowns in Rectangular Artesian Aquifers," *Journal of Hydrology* (1976) 31, 151-160.
- Chao, B.T.: "A Note on Conduction of Heat in Anisotropic Media," *Applied Scientific Research* (1964) Section A, 12, 134-138.
- Chilingarian, G.V., Mazzullo, S.J. and Rieke, H.H.: "Introduction", *Carbonate Reservoir Characterization: A Geologic-Engineering Analysis, Part I*, Developments in Petroleum Science 30, Elsevier Science Publishers B.V. (1992) 1-35 (8-12).
- Chow, V.T.: "On the Determination of Transmissibility and Storage Coefficients from Pumping Test Data," *Transactions of American Geophysical Union* (1952) 33, 397-404.

- Collins, R.E.: *Flow of Fluids through Porous Materials*, Research & Engineering Consultants Inc. (1961) 47-76.
- Corapcioglu, M.Y., Borekci, O. and Haridas, A.: "Analytical Solutions for Rectangular Aquifers with Third-Kind (Cauchy) Boundary Conditions," *Water Resources Research* (April 1983) 19, No. 2, 523-528.
- Correa, A.C. and Ramey, H.J., Jr.: "Application of the Unit Step Function to Unusual Well Test Problems," paper SPE 18156 presented at the 63rd Annual Technical Conference and Exhibition of the SPE of AIME, Houston, TX (Oct. 2-5, 1988).
- Cotta, R.M.: *Integral Transforms in Computational Heat and Fluid Flow*, CRC Press (1993) 1-31.
- Craft, B.C., Hawkins, M. and Terry, R.E.: *Applied Petroleum Reservoir Engineering*, Second Edition, Prentice-Hall, Inc. (1991) 273-334.
- Dake, L.P.: *The Practice of Reservoir Engineering*, Developments in Petroleum Science 36, Elsevier Science B.V. (1994) 137-309.
- Deng, X. and Horne, R.N.: "Well Test Analysis of Heterogeneous Reservoirs," paper SPE 26458 presented at the 68th SPE Annual Technical Conference and Exhibition of the SPE of AIME, Houston, TX (Oct. 3-6, 1993).
- Dietz, D.N.: "Determination of Average Reservoir Pressure from Build-Up Surveys," *Journal of Petroleum Technology* (Aug. 1965) 955-959.
- Duong, A.N.: "A New Set of Type Curves for Well-Test Interpretation with the Pressure/Pressure-Derivative Ratio," *SPE Formation Evaluation* (June 1989) 264-272.
- Earlougher, R.C., Jr.: *Advances in Well Test Analysis*, Monograph Volume 5 of the Henry L. Doherty Series, Society of Petroleum Engineers of AIME (1977) 69-72.
- Earlougher, R.C., Jr., Ramey, H.J., Jr.: "Interference Analysis of Bounded Systems," *The Journal of Canadian Petroleum Technology* (Oct.-Dec. 1973) 12, No. 4, 33-45.
- Earlougher, R.C., Jr., Ramey, H.J., Jr., Miller, F.G. and Mueller, T.D.: "Pressure Distributions in Rectangular Reservoirs," *Journal of Petroleum Technology* (Feb. 1968) 199-208; *Transactions of AIME* (1968) 243.
- Ehlig-Economides, C.: "Use of the Pressure Derivative for Diagnosing Pressure-Transient Behavior," *Journal of Petroleum Technology* (Oct. 1988) 1280-1282.

- Ehlig-Economides, C.A.: "Application of Multiphase Compartmentalized Material Balance," paper SPE 27999 presented at the University of Tulsa Centennial Petroleum Engineering Symposium of the SPE of AIME, Tulsa, OK (Aug. 29-31, 1994).
- Ehlig-Economides, C.A. and Economides, M.J.: "Pressure Transient Analysis in an Elongated Linear Flow System," *Society of Petroleum Engineering Journal* (Dec. 1985) 839-847.
- Ehlig-Economides, C.A., Joseph, J.A., Ambrose, R.W. and Norwood, C.: "A Modern Approach to Well Test Interpretation," paper SPE 19814 presented at the 64th SPE Annual Technical Conference and Exhibition of the SPE of AIME, San Antonio, TX (Oct. 8-11, 1989).
- Ershaghi, I. and Woodbury, J.J.: "Examples of Pitfalls in Well Test Analysis," *Journal of Petroleum Technology* (Feb. 1985) 335-341.
- Fox, M.F., Chedburn, A.C.S. and Stewart, G.: "Simple Characterization of Communication between Reservoir Regions," paper SPE 18360 presented at the European Petroleum Conference of the SPE of AIME, London, UK (Oct. 16-19, 1988).
- Gill, M.K.: "Unsteady Free Flow to a Ditch from an Artesian Aquifer," *Journal of Hydrology* (1981) 52, 39-45.
- Golan, M. and Whitson, C.H.: *Well Performance*, International Human Resources Development Corporation (1986) 178-181.
- Gringarten, A.C., Ramey, H.J., Jr. and Raghavan, R.: "Unsteady-State Pressure Distributions Created by a Well with a Single Infinite-Conductivity Vertical Fracture," *Society of Petroleum Engineers Journal* (Aug. 1974) 347-360; *Transactions of AIME*, 257.
- Guillot, A.Y. and Horne, R.N.: "Using Simultaneous Downhole Flow-Rate and Pressure Measurements to Improve Analysis of Well Tests," *SPE Formation Evaluation* (June 1986) 217-226.
- Horne, R.N.: *Modern Well Test Analysis - A computer-Aided Approach*, Petroway, Inc. (1990) 61-63.
- Homer, D.R.: "Pressure Buildup in Wells," *Proceedings of Third World Petroleum Congress*, E. J. Brill, Leiden (1951) Sec. II, 503-523; *SPE Reprint Series No. 9 - Pressure Analysis Methods*, Society of Petroleum Engineers of AIME (1967) 25-43.

- Hovanesian, S.A.: "Pressure Studies in Bounded Reservoirs," *Society of Petroleum Engineers Journal* (Dec. 1961) 223-228.
- Hower, T.L. and Collins, R.E.: "Detecting Compartmentalization in Gas Reservoirs through Production Performance," paper SPE 19790 presented at the Annual Technical Conference and Exhibition of the SPE of AIME, San Antonio, TX (Oct. 8-11, 1989).
- Hubbert, M.K.: "The Theory of Ground-Water Motion," *The Journal of Geology* (1940) 48, 785-944; (Abstract) *Transactions of American Geophysical Union* (1940), 33, No.3, 648.
- Hurst, W.: "Establishment of the Skin Effect and its Impediment to Fluid Flow into a Well Bore," *The Petroleum Engineer* (Oct. 1953) B-6 - B-16.
- Hurst, W.: "Interference between Oil Fields," *Transactions of AIME* (1960) 219, 175-190.
- Issaka, M.B. and Ambastha, A.K.: "A Generalized Pressure Derivative Analysis for Composite Reservoirs," paper CIM 96-115 presented at the 47th Annual Technical Meeting of The Petroleum Society of CIM, Calgary, AB (June 10-12, 1996).
- Jargon, J.R. and van Poolen, H.K.: "Unit Response Function from Varying-Rate Data," *Journal of Petroleum Technology* (Aug. 1965) 965-969.
- Jelmert, T.A.: "Theory and Application of Polynomial Type Curves," paper SPE 25876 presented at the Rocky Mountain Regional Meeting of the SPE of AIME, Denver, CO (April 12-14, 1993a)
- Jelmert, T.A.: "A Note on Flow-Period Diagnostics in Well-Testing," *Journal of Petroleum Science and Engineering* (1993b) 8, 329-332.
- Jones, P.: "Reservoir Limit Test," *Oil and Gas Journal* (June 1956) 184-196.
- Jones, P.: "Drawdown Exploration, Reservoir Limit, Well and Formation Evaluation," paper SPE 824-G presented at the Permian Basin Oil Recovery Conference of the SPE of AIME, Midland, TX (April 18-19, 1957).
- Junkin, J.E., Sippel, M.A. and Lord, M.E.: "Well Performance for Compartmented Geometry of Oil and Gas Reservoirs," paper SPE 24356 presented at the Rocky Mountain Regional Meeting of the SPE of AIME, Casper, WY (May 18-21, 1992).

- Kamal, M.M., Freyder, D.G. and Murray, M.A.: "Use of Transient Testing in Reservoir Management," *Journal of Petroleum Technology* (Nov. 1995) 992-999.
- Kamal, M.M. and Hegeman, P.S.: "New Developments in Multiple-Well Testing," *SPE Formation Evaluation* (Mar. 1988) 159-168; *Transactions of AIME*, 289.
- Kazemi, H. and Seth, M.S.: "Effect of Anisotropy and Stratification on Pressure Transient Analysis of Wells with Restricted Flow Entry," *Journal of Petroleum Technology* (May 1969) 639-646.
- Kerr, D.R. and Jirik, L.A.: "Fluvial Architecture and Reservoir Compartmentalization in the Oligocene Middle Frio Formation, South Texas," *Transactions of Gulf Coast Association of Geological Societies* (1990) 40, 373-380.
- Kocberber, S. and Collins, R.E.: "Gas Well Test Analysis in Complex Heterogeneous Reservoirs," paper SPE 21512 presented at the Gas Technology Symposium of the SPE of AIME, Houston, TX (Jan. 23-25, 1991).
- Kuchuk, F. and Ayestaran, L.: "Analysis of Simultaneously Measured Pressure and Sandface Flow Rate in Transient Well Testing," *Journal of Petroleum Technology* (Feb. 1985) 323-334.
- Kuchuk, F.J. and Habashy, T.M.: "Pressure Behavior of Laterally Composite Reservoirs," paper SPE 24678 presented at the 67th Annual Technical Conference and Exhibition of the SPE of AIME, Washington, DC (Oct. 4-7, 1992).
- Kumar, A. and Ramey, H.J., Jr.: "Well-Test Analysis for a Well in a Constant-Pressure Square," *Society of Petroleum Engineers Journal* (April 1974) 107-116.
- Lake, L.W.: "The Origins of Anisotropy," *Journal of Petroleum Technology* (April 1988) 395-396.
- Larsen, L.: "Pressure-Transient Behavior of Reservoirs Forming a Pattern of Coupled Linear Segments," paper SPE 26459 presented at the 68th Annual Technical Conference and Exhibition of the SPE of AIME, Houston, TX (Oct. 3-6, 1993).
- Larsen, L.: "Pressure-Transient Behavior of Wells Producing from Complex Patterns of Interconnected Linear Segments," paper SPE 36549 presented at the 71st Annual Technical Conference and Exhibition of the SPE of AIME, Denver, CO (Oct. 6-9, 1996).
- Latinopoulos, P.: "Periodic Recharge to Finite Aquifers from Rectangular Areas," *Advances in Water Resources* (Sept. 1984) 7, 137-140.

- Lee, W.J.: *Well Testing*, SPE Textbook Series - Vol. 1, Society of Petroleum Engineers of AIME (1982) 15-18.
- Levorsen, A.I.: *Geology of Petroleum*, Second Edition, W.H. Freeman and Company (1967) 634-637, 286-293.
- Link, P.K.: *Basic Petroleum Geology*, Second Edition, OGCI Publications (1987) 297-303.
- Lockwood, J.D. and Mulholland, G.P.: "Diffusion through Laminated Composite Cylinders Subjected to a Circumferentially Varying Heat Flux," *Transactions of the ASME - Journal of Heat Transfer* (Nov. 1973) 487-491.
- Lord, M.E. and Collins, R.E.: "Detecting Compartmented Gas Reservoirs Through Production Performance," paper SPE 22941 presented at the 66th Annual Technical Conference and Exhibition of the SPE of AIME, Dallas, TX (Oct. 6-9, 1991).
- Lord, M.E., Collins, R.E., Kocerber, S. and Kerr, D.R.: "A Compartmented Simulation System for Gas Reservoir Evaluation with Application to Fluvial Deposits in the Frio Formation, South Texas," paper SPE 24308 presented at the Mid-Continent Gas Symposium of the SPE of AIME, Amarillo, TX (April 13-14, 1992).
- Malavazos, M. and McDonough, R.C.M.: "Pressure-Transient Response in Compartmentalized Gas Reservoirs: A South Australian Field Example," paper SPE 23009 presented at the Asia-Pacific Conference of the SPE of AIME, Perth, Western Australia (Nov. 4-7, 1991).
- Marett, B.P., Inayat-Hussain, A.A. and Goldthorpe, W.H.: "Analytical Solutions of Three-Dimensional Flow Near a Wellbore," paper SPE 23008 presented at the Asia-Pacific Conference of the SPE of AIME, Perth, Western Australia (Nov. 4-7, 1991).
- Massonnat, G.J. and Bandiziol, D.: "Interdependence between Geology and Well Test Interpretation," paper SPE 22740 presented at the 66th Annual Technical Conference and Exhibition of the SPE of AIME, Dallas, TX (Oct. 6-9, 1991).
- Massonnat, G.J., Norris, R.J. and Chalmette, J.-C.: "Well Test Interpretation in Geologically Complex Channelized Reservoirs," paper SPE 26464 presented at the 68th Annual Technical Conference and Exhibition of the SPE of AIME, Houston, TX (Oct. 3-6, 1993).

- Matthews, C.S. and Russell, D.G.: *Pressure Buildup and Flow Tests in Wells*, Monograph Volume 1 of the Henry L. Doherty Series, Society of Petroleum Engineers of AIME (1967) 123.
- Matthews, C.S., Brons, F. and Hazebroek, P.: "A Method for Determination of Average Pressure in Bounded Reservoir," *Transactions of AIME* (1954) **201**, 181-191; *SPE Reprint Series No. 9 - Pressure Analysis Methods*, Society of Petroleum Engineers of AIME (1967) 51-60.
- Mazzullo, S.J. and Chilingarian, G.V.: "Depositional Models of Carbonate Reservoirs," *Carbonate Reservoir Characterization: A Geologic-Engineering Analysis, Part I*, Developments in Petroleum Science 30, Elsevier Science Publishers B.V. (1992) 109-198 (134-150).
- McEdwards, D.G.: "Multiwell Variable-Rate Well Test Analysis," *Society of Petroleum Engineers Journal* (Aug. 1981) 444-446.
- McKinley, R.M., Vela, S. and Carlton, L.A.: "A Field Application of Pulse-Testing for Detailed Reservoir Description," *Journal of Petroleum Technology* (Mar. 1968) 313-321.
- Meehan, D.N. and Verma, S.K.: "Improved Reservoir Characterization in Low Permeability Reservoirs with Geostatistical Models," *SPE Reservoir Engineering* (Aug. 1995).
- Mendes, L.C.C., Tygel, M. and Correa, A.C.F.: "A Deconvolution Algorithm for Analysis of Variable Rate Well Test Pressure Data," paper SPE 19815 presented at the 64th Annual Technical Conference and Exhibition of the SPE of AIME, San Antonio, TX (Oct. 8-11, 1989).
- Meunier, D., Wittmann, M.J. and Stewart, G.: "Interpretation of Pressure Buildup Test Using In-Situ Measurement of Afterflow," *Journal of Petroleum Technology* (Jan. 1985) 143-152.
- Mikhailov, M.D.: "Splitting up of Heat-Conduction Problem," *Letters in Heat and Mass Transfer* (1977) **4**, 163-166.
- Mikhailov, M.D.: *Personal Communication* (Feb. 1997).
- Mikhailov, M.D. and Ozisik, M.N.: *Unified Analysis and Solutions of Heat and Mass Diffusion*, John Wiley and Sons, Inc. (1984) 378-398.

- Mikhailov, M.D. and Ozisik, M.N.: "Transient Conduction in a Three-Dimensional Composite Slab," *International Journal of Heat and Mass Transfer* (1986) **29**, No. 2, 340-342.
- Mikhailov, M.D. and Vulchanov, N.L.: "Computational Procedure for Sturm-Liouville Problems," *Journal of Computational Physics* (1983) **50**, 323-336.
- Miller, C.C., Dyes, A.B. and Hutchinson, C.A.: "The Estimation of Permeability and Reservoir Pressure from Bottom-Hole Pressure Build-up Characteristics," *Transactions of AIME* (1950) **189**, 91-104; *SPE Reprint Series No. 9 - Pressure Analysis Methods*, Society of Petroleum Engineers of AIME (1967) 11-24.
- Miller, F.G.: "Theory of Unsteady-state Influx of Water in Linear Reservoirs," *Journal of the Institute of Petroleum* (Nov. 1962) **48**, No. 467, 365-379.
- Mortada, M.: "Oilfield Interference in Aquifers of Non-Uniform Properties," *Journal of Petroleum Technology* (Dec. 1960) 55-57.
- Moser, H.: "An Alternative to Superposition for Monotonically Changing Flow Rates," *The Journal of Canadian Petroleum Technology* (Dec. 1996) **35**, No. 10, 18-28.
- Mulholland, G.P. and Cobble, M.H.: "Diffusion Through Composite Media," *International Journal of Heat and Mass Transfer* (1972) **15**, 147-160.
- Muskat, M.: *Physical Principles of Oil Production*, McGraw-Hill Book Co., Inc. (1949) 205-214.
- Mustafa, S.: "Unsteady Flow to a Ditch from a Semi-Confined and Leaky Aquifer," *Advances in Water Resources* (June 1984) **7**, 81-84.
- Nabor, G.W. and Barham, R.H.: "Linear Aquifer Behavior," *Journal of Petroleum Technology* (May 1964) 561-563.
- Norris, R.J., Massonnat, G.J. and Alabert, F.G.: "Early Quantification of Uncertainty in the Estimation of Oil in Place in a Turbidite Reservoir," paper SPE 26490 presented at the 68th Annual Technical Conference and Exhibition of the SPE of AIME, Houston, TX (Oct. 3-6, 1993).
- Nutakki, R. and Mattar, L.: "Pressure Transient Analysis of Wells in Very Long Narrow Reservoirs," paper SPE 11221 presented at the 57th Annual Fall Technical Conference and Exhibition of the SPE of AIME, New Orleans, LA (Sept. 26-29, 1982).

- Odeh, A.S. and Jones, L.G.: "Pressure Drawdown Analysis: Variable-Rate Case," *Journal of Petroleum Technology* (Aug. 1965) 960-964; *Transactions of AIME*, 234.
- Ogbe, D.O. and Brigham, W.E.: "Pulse Testing with Wellbore Storage and Skin Effects," paper SPE 12780 presented at the California Regional Meeting of the SPE of AIME, Long Beach, CA (Apr. 11-13, 1984).
- Ozisik, M.N.: *Heat Conduction*, John Wiley and Sons, Inc. (1980) 599-600.
- Padovan, J.: "Generalized Sturm-Liouville Procedure for Composite Domain Anisotropic Transient Conduction Problems," *AIAA Journal* (Aug. 1974) 12, No.8, 1158-1160.
- Papatzacos, P.: "Exact Solutions for Infinite-Conductivity Wells," *SPE Reservoir Engineering* (May 1987) 217-226.
- Payne, D.A.: "Material-Balance Calculations in Tight-Gas Reservoirs: The Pitfalls of p/z Plots and a More Accurate Technique," *SPE Reservoir Engineering* (Nov. 1996) 260-267.
- Poon, D. and Chhina, H.: "Transient Pressure Analysis of a Linear Composite Reservoir," paper CIM 89-40-8 presented at the 40th Annual Technical Meeting of The Petroleum Society of CIM, Banff, AB (May 28-31, 1989).
- Proano, E.A. and Lilley, I.J.: "Derivative of Pressure: Application to Bounded Reservoir Interpretation," paper SPE 15861 presented at the European Petroleum Conference of the SPE of AIME, London, UK (Oct. 20-22, 1986).
- Qin, C. and Ortoleva, P.J.: "Banded Diagenetic Pressure Seals: Types, Mechanisms, and Homogenized Basin Dynamics," *Basin Compartments and Seals*, AAPG Memoir 61, The American Association of Petroleum Geologists, Tulsa, OK, USA (1994) 385-400.
- Raghavan, R.: *Well Test Analysis*, PTR Prentice-Hall, Inc. (1993).
- Raghavan, R. and Ozkan, E.: *A Method for Computing Unsteady Flows in Porous Media*, Pitman Research Notes in Mathematics Series 318, Longman Scientific & Technical (1994) 48-52.
- Rahman, N.M.A. and Ambastha, A.K.: "A Generalized Transient Flow Model for Linear, Compartmentalized Systems," paper CIM 96-50 presented at the 47th Annual Technical Meeting of The Petroleum Society of CIM, Calgary, AB (June 10-12, 1996a).

- Rahman, N.M.A. and Ambastha, A.K.: "A Generalized Transient-Pressure Model for Areally-Compartmentalized Reservoirs," paper SPE 37340 presented at the Eastern Regional Meeting of the SPE of AIME, Columbus, OH (Oct. 23-25, 1996b)
- Rahman, N.M.A. and Ambastha, A.K.: "Transient-Pressure Behaviour of Compartmentalized Reservoirs," paper SPE 38081 prepared for presentation at the Asia Pacific Oil and Gas Conference and Exhibition of the SPE of AIME, Kuala Lumpur, Malaysia (April 14-16, 1997a)
- Rahman, N.M.A. and Ambastha, A.K.: "A Generalized 3D Analytical Model for Transient Flow in Compartmentalized Reservoirs," paper SPE 38675 presented at the 72nd Annual Technical Conference and Exhibition of the SPE of AIME, San Antonio, TX (Oct. 5-8, 1997b).
- Ramey, H.J., Jr.: "Interference Analysis for Anisotropic Formations - A Case History," *Journal of Petroleum Technology* (Oct. 1975) 1290-1298.
- Ramey, H.J., Jr.: "Advances in Practical Well Test Analysis," *Journal of Petroleum Technology* (June 1992) 650-659.
- Ramey, H.J., Jr. and Cobb, W.M.: "A General Pressure Buildup Theory for a Well in a Closed Drainage Area," *Journal of Petroleum Technology* (Dec. 1971) 1493-1505; *Transactions of AIME* (1971) 251.
- Ramey, H.J., Jr., Kumar, A. and Gulati, M.S.: *Gas Well Test Analysis Under Water-Drive Conditions*, American Gas Association (1973) 9-55, 98-159.
- Salt, H.: "Transient Conduction in a Two-Dimensional Composite Slab-I. Theoretical Development of Temperature Modes," *International Journal of Heat and Mass Transfer* (1983a) 26, No. 11, 1611-1616.
- Salt, H.: "Transient Conduction in a Two-Dimensional Composite Slab-II. Physical Interpretation of Temperature Modes," *International Journal of Heat and Mass Transfer* (1983b) 26, No. 11, 1617-1623.
- Scarborough, J.B.: *Numerical Mathematical Analysis*, 6th Edition, The Johns Hopkins Press (1966) 215-223.
- Seth, M.S.: "Unsteady-State Pressure Distribution in a Finite Reservoir with Partial Wellbore Opening," *The Journal of Canadian Petroleum Technology* (Oct.-Dec. 1968) 7, 153-163.

- Smalley, P.C. and England, W.A.: "Reservoir Compartmentalization Assessed with Fluid Compositional Data," *SPE Reservoir Engineering* (Aug. 1994) 175-180.
- Smalley, P.C. and Hale, N.A.: "Early Identification of Reservoir Compartmentalization by Combining a Range of Conventional and Novel Data Types," *SPE Formation Evaluation* (Sept. 1996) 163-169.
- Sneddon, I.N.: *Fourier Transforms*, McGraw-Hill Book Co., Inc. (1951) 71-91, 202.
- Stehfest, H.: "Numerical Inversion of Laplace Transforms," *Communications of ACM* (1970) **13**, No. 1, 47-49.
- Stewart, G., Gupta, A. and Westaway, P.: "The Interpretation of Interference Tests in a Reservoir with Sealing and Communicating Faults," paper SPE 12967 presented at the European Petroleum Conference of the SPE of AIME, London, UK (Oct. 25-28, 1984).
- Stewart, G. and Whaballa, A.E.: "Pressure Behavior of Compartmentalized Reservoirs," paper SPE 19779 presented at the 64th Annual Technical Conference and Exhibition of the SPE of AIME, San Antonio, TX (Oct. 8-11, 1989).
- Stewart, G., Wittmann, M.J. and Meunier, D.: "Afterflow Measurements and Deconvolution in Well Test Analysis," paper SPE 12174 presented at the 58th Annual Technical Conference and Exhibition of the SPE of AIME, San Francisco, CA (Oct. 5-8, 1983).
- Streltsova, T.D.: *Well Testing in Heterogeneous Formations*, An Exxon Monograph, John Wiley & Sons (1988) 81-84.
- Streltsova-Adams, T.D.: "Pressure Drawdown in a Well with Limited Flow Entry," *Journal of Petroleum Technology* (Nov. 1979) 1469-1476.
- Thompson, L.G. and Reynolds, A.C.: "Analysis of Variable-Rate Well-Test Pressure Data Using Duhamel's Principle," *SPE Formation Evaluation* (Oct. 1986) 453-469.
- Tiab, D.: "Analysis of Pressure and Pressure Derivative without Type-Curve Matching - Skin and Wellbore Storage," *Journal of Petroleum Science and Engineering* (1995) **12**, 171-181.
- Tiab, D. and Kumar, A.: "Application of the p_D' Function to Interference Analysis," *Journal of Petroleum Technology* (Aug. 1980) 1465-1470.
- Title, C.W.: "Boundary Value Problems in Composite Media: Quasi-Orthogonal

Functions,” *Journal of Applied Physics* (April 1965) **36**, No.4, 1486-1488.

Title, C.W. and Robinson, V.L.: “Analytical Solution of Conduction Problems in Composite Media,” ASME paper 65-WA/HT-52 contributed by the Heat Transfer Division for presentation at the Winter Annual Meeting of The American Society of Mechanical Engineers, Chicago, IL (Nov. 7-11, 1965).

van Everdingen, A.F.: “The Skin Effect and its Influence on the Productivity Capacity of a Well,” *Journal of Petroleum Technology* (June 1953) 171-176; *Transactions of AIME*, **198**.

van Everdingen, A.F. and Hurst, W.: “The Application of the Laplace Transformation to Flow Problems in Reservoirs,” *Transactions of AIME* (1949) **186**, 305-324.

Wong, D.W., Mothersele, C.D. and Harrington, A.G.: “Pressure Transient Analysis in Finite Linear Reservoirs Using Derivative and Conventional Techniques: Field Examples,” paper SPE 15421 presented at the 61st Annual Technical Conference and Exhibition of the SPE of AIME, New Orleans, LA (Oct. 5-8, 1986).

Yaxley, L.M.: “Effect of a Partially Communicating Fault on Transient Pressure Behavior,” *SPE Formation Evaluation* (Dec. 1987) 590-598.

APPENDICES

APPENDIX A

COMPUTER PROGRAM FOR ONE-DIMENSIONAL FLOW SYSTEM

This appendix presents the computer program for computing the numerical values from the analytical solution for a one-dimensional linear, compartmentalized system as developed in Chapter 2.

A.1 Source Code

```
* Program: 1.f
.....
*   COMPARTMENTALIZED RESERVOIRS IN A 1-DIMENSIONAL SYSTEM
.....
*   Variable Identification List
.....
*   NC = Number of compartments
*   XXD(I) = Locations of boundaries along x-axis
*   F(I) = Storativity ratio in ith compartment
*   EM(I) = Mobility ratio in ith compartment
*   AL(I) = Defined in Eq. (2.7)
*   E(I) = Defined in Eq. (2.6)
*   U = 1/s (s = skin factor at an interface)
*   AD(I) = Dimensionless location of a producing well at ith compartment
*   NTS(I) = Number of variable rates that the well at ith compartment produces
*   QD(I, J) = Dimensionless production rate from ith compartment with jth rate
*   TPD(I, J) = Dimensionless time at which jth production rate commences in the
*               well at ith compartment
*   TSD(I, J) = Dimensionless time at which jth production rate ceases in the
*               well at ith compartment
*   TD = Dimensionless time
*   PD = Dimensionless pressure
*   DERL = Particular derivative for infinite-acting linear flow
*   CDER = Cartesian derivative
.....
IMPLICIT REAL*8(A-H,O-Z)
COMMON/T1/XXD(4)
COMMON/T2/AL(2)
COMMON/T3/E(2)
COMMON/T4/U
COMMON/T5/N(3)
COMMON/T6/AD(3)
COMMON/T7/NTS(3)
COMMON/T8/QD(3,2),TPD(3,2),TSD(3,2)
COMMON/T9/QDSUM
COMMON/T10/GBSUM
COMMON/T12/CO(3)
COMMON/T13/EI(2000),KK
COMMON/T16/AAL,XD
COMMON/T120/ML
OPEN(4,FILE='in1d.d')
OPEN(3,FILE='rdald.d')
OPEN(7,FILE='c.o')
NC=2
NNX=2*NC
CALL INPUT(NC)
CALL DATA(NC)
CALL RADMIN
FAL=0.1
```

```

FAL1=22.0
WRITE(7,51)
51  FORMAT(3X,'TD',15X,'PD',15X,'DERL',15X,'CDER')
    TD=0.01
    DO 5 I=1,30
    IND=0
    CALL PRIME(TD,PD,DERL,CDER)
    WRITE(7,50)TD,PD,DERL,CDER
50  FORMAT(F10.3,5X,F15.3,F10.3,F10.3)
    IF(TD.LT.FAL)THEN
        TD=TD+0.01
        IND=1
        ENDIF
        IF(IND.EQ.1)GO TO 5
        IF(TD.GT.FAL.AND.TD.LT.FAL1)THEN
            TD=TD+2.0
            IND=1
            ENDIF
            IF(IND.EQ.1)GO TO 5
            IF(TD.GT.FAL)THEN
                TD=2.0*TD
            ENDIF
5  CONTINUE
    STOP
    END
    SUBROUTINE INPUT(NX)
    * THIS SUBROUTINE READS DIMENSIONS, ROCK AND FLUID PROPERTIES
    IMPLICIT REAL*8(A-H,O-Z)
    COMMON/T1/XXD(4)
    COMMON/T2/AL(2)
    COMMON/T3/E(2)
    COMMON/T4/U
    COMMON/T5/N(3)
    COMMON/T6/AD(3)
    COMMON/T7/NTS(3)
    COMMON/T8/QD(3,2),TPD(3,2),TSD(3,2)
    COMMON/T9/QDSUM
    COMMON/T10/GBSUM
    COMMON/T12/CO(3)
    COMMON/T15/PDO(3)
    DIMENSION EM(2),F(2)
    * READING GEOMETRIC DIMENSIONS OF EACH COMPARTMENT
    READ(4,*)(XXD(I),I=1,NX+1)
    * READING DIMENSIONLESS INITIAL PRESSURE IN EACH COMPARTMENT
    READ(4,*)(PDO(I),I=1,NX)
    * READING ROCK AND FLUID PROPERTIES IN EACH COMPARTMENT
    READ(4,*)(EM(L),L=1,NX)
    READ(4,*)(F(L),L=1,NX)
    DO 81 I=1,NX
        E(I)=F(I)/EM(I)
        AL(I)=EM(I)
    WRITE(7,52)I,EM(I),F(I)
52  FORMAT('I= ',I1,5X,'EM= ',F9.3,5X,'F= ',F9.3)
81  CONTINUE
    * READING TRANSMISSIBILITY COEFFICIENT AT EACH INTER-COMPARTMENT
    * BOUNDARY
    READ(4,*)S
    WRITE(7,51)S
51  FORMAT('SKIN FACTOR = ',F7.1)
    U=1.0/S
    * READING WHETHER A COMPARTMENT HAS A WELL, N(L)=0 MEANS NO WELL
    READ(4,*)(N(L),L=1,NX)
    * READING LOCATION OF EACH WELL
    DO 4 I=1,NX
        IF(N(I).NE.0) THEN
            READ(4,*)AD(I)
        ENDIF
4  CONTINUE
    RETURN
    END
    SUBROUTINE COEFF(EVV,FA)
    * THIS SUBROUTINE CREATES A COEFFICIENT MATRIX

```

```

      IMPLICIT REAL*8(A-H,O-Z)
      COMMON/T1/XXD(4)
      COMMON/T2/AL(2)
      COMMON/T3/E(2)
      COMMON/T4/U
      COMMON/T14/AR(3)
      DIMENSION FA(3,3)
      DO 101 I=1,2
      AR(I)=EVV*DSQRT(E(I))
101  CONTINUE
      V1=DSQRT(E(1))
      V2=DSQRT(E(2))
      FA(1,1)=DCOS(AR(1)*XXD(2))-EVV*AL(1)*V1*DSIN(AR(1)*XXD(2))/U
      FA(1,2)=-V2*DSIN(AR(2)*XXD(2))
      FA(1,3)=-V2*DCOS(AR(2)*XXD(2))
      FA(2,1)=-AL(1)*V1*DSIN(AR(1)*XXD(2))
      FA(2,2)=-AL(2)*V2*DCOS(AR(2)*XXD(2))
      FA(2,3)=AL(2)*V2*DSIN(AR(2)*XXD(2))
      FA(3,1)=0.0
      FA(3,2)=DCOS(AR(2)*XXD(3))
      FA(3,3)=-DSIN(AR(2)*XXD(3))
      RETURN
      END
      SUBROUTINE DCOEFF(EV,FA)
* THIS SUROUTINE COMPUTES DERIVATIVE OF EACH ELEMENT OF THE MATRIX CREATED IN COEFF
      IMPLICIT REAL*8(A-H,O-Z)
      COMMON/T1/XXD(4)
      COMMON/T2/AL(2)
      COMMON/T3/E(2)
      COMMON/T4/U
      COMMON/T14/AR(3)
      DIMENSION FA(3,3),VR(2)
      DO 101 I=1,2
      AR(I)=EVV*DSQRT(E(I))
      VR(I)=DSQRT(E(I))
101  CONTINUE
      A1=-DSIN(AR(1)*XXD(2))*VR(1)*XXD(2)
      A2=-DSIN(AR(1)*XXD(2))/U-AR(1)*DCOS(AR(1)*XXD(2))*XXD(2)/U
      FA(1,1)=A1+AL(1)*VR(1)*A2
      FA(1,2)=-DCOS(AR(2)*XXD(2))*VR(2)*XXD(2)
      FA(1,3)=DSIN(AR(2)*XXD(2))*VR(2)*XXD(2)
      FA(2,1)=-AL(1)*DCOS(AR(1)*XXD(2))*E(1)*XXD(2)
      FA(2,2)=AL(2)*DCOS(AR(2)*XXD(2))*E(2)*XXD(2)
      FA(2,3)=AL(2)*DCOS(AR(2)*XXD(2))*E(2)*XXD(2)
      FA(3,1)=0.0
      FA(3,2)=-DSIN(AR(2)*XXD(3))*VR(2)*XXD(3)
      FA(3,3)=-DCOS(AR(2)*XXD(3))*VR(2)*XXD(3)
      RETURN
      END
      SUBROUTINE DATA(NX)
* THIS SURROUTINE READS OTHER DATA
      IMPLICIT REAL*8(A-H,O-Z)
      COMMON/T16/AA1,XD
      COMMON/T120/ML
      READ(3,*)AA1
      READ(3,*)XD
      READ(3,*)ML
      RETURN
      END
      SUBROUTINE EIGEN(VI1,VI2,EV)
* THIS SURROUTINE COMPUTES EIGENVALUES USING MODIFIED REGULA FALSI AND NEWTON'S METHOD
      IMPLICIT REAL*8(A-H,O-Z)
      DIMENSION AA(3,3),BB(3,3),CC(3,3)
      CALL COEFF(VI1,AA)
      CALL DETER(AA,3,3,AD1)
      CALL COEFF(VI2,BB)
      CALL DETER(BB,3,3,AD2)
      EV=(VI1*AD2-VI2*AD1)/(AD2-AD1)
2   CALL COEFF(EV,AA)
      CALL DCOEFF(EV,BB)
      SUM=0.0
      DO 1 I=1,3

```

```

CALL MAT(I,3,AA,BB,CC)
CALL DETER(CC,3,3,DV)
SUM=SUM+DV
1 CONTINUE
CALL DETER(AA,3,3,AD)
DEV=-AD/SUM
EV=EV+DEV
IF(DABS(DEV).GT.1.0D-12)GO TO 2
RETURN
END
SUBROUTINE MAT(JKF,NI,AB,BC,CA)
* THIS SURROUTINE ARRANGES JACOBIANS FOR NEWTON'S METHOD
IMPLICIT REAL*8(A-H,O-Z)
DIMENSION AB(NI,NI),BC(NI,NI),CA(NI,NI)
DO 2 I=1,NI
DO 2 J=1,NI
IF(I.EQ.JKF)THEN
CA(I,J)=BC(I,J)
ELSE
CA(I,J)=AB(I,J)
ENDIF
2 CONTINUE
RETURN
END
SUBROUTINE RADMIN
IMPLICIT REAL*8(A-H,O-Z)
COMMON/T11/EV(15000000),UD(15000000)
COMMON/T13/EI(2000),KK
COMMON/T14/AR(3)
COMMON/T16/AA1,XD
COMMON/T120/ML
DIMENSION AE1(2000),AE2(2000)
CALL AROOTS(ML)
MM=0
DER1=1.0
DER2=2.0
DO 1 L=1,ML-1
ULLAH=UD(L)/UD(L+1)
DER3=ULLAH
IF(ULLAH.LT.1.0D-10)THEN
MM=MM+1
AE1(MM)=EV(L)
AE2(MM)=EV(L+1)
ENDIF
1 CONTINUE
KK=MM
LX=1
K=1
DOWHILE (K.LE.KK)
PA=AE1(K)
FU=AE2(K)
CALL EIGEN(AE1(K),AE2(K),ABC)
IF(ABC.GT.FU.OR.ABC.LT.PA)GO TO 2
IF(DABS(ABC).LE.1.0D-5)GO TO 2
INDI=0
IF(LX.GT.1)THEN
DIFF=DABS(ABC-EI(LX-1))
IF(DIFF.LE.1.0D-03)INDI=1
ENDIF
IF(INDI.NE.0)GO TO 2
EI(LX)=ABC
LX=LX+1
2 K=K+1
ENDDO
KK=LX-1
RETURN
END
SUBROUTINE PRIME(TD,SUM,DERL,CDER)
* THIS SURROUTINE COMPUTES DIMENSIONLESS PRESSURE AND ITS DERIVATIVES
IMPLICIT REAL*8(A-H,O-Z)
COMMON/T13/EI(2000),KK
COMMON/T14/AR(3)

```

```

COMMON/T16/AA1,XD
DIMENSION FF(3,3),GG(3,3),P(2),Q(2)
CALL NOR(VA)
SUM=TD/VA
CDER=1.0/VA
SY=1.0
LX=1
K=1
  DOWHILE (K.LE.KK.AND.DABS(SY).GT.1.0D-17)
    CALL COEFF(EI(K),FF)
    DO 12 II=1,3
    DO 12 JJ=1,3
      GG(II,JJ)=FF(II,JJ)
12    CONTINUE
    CALL SOLVE(FF,P,Q)
    CALL SOURCE(P,Q,EI(K),TD,SY,SD)
    SUM=SUM+SY
    CDER=CDER+SD
2    K=K+1
    ENDDO
    DERL=CDER*(TD)**0.5
    RETURN
  END
  SUBROUTINE ARRAN(UU,D,G,H)
* THIS SUBROUTINE COMPUTES RESIDUE
  IMPLICIT REAL*8(A-H,O-Z)
  COMMON/T16/AA1,XD
  DIMENSION G(2),H(2),D(2),UU(3,3)
  G(1)=0.0
  H(1)=AA1
  G(2)=D(1)
  H(2)=D(2)
  DO 5 I=1,3
    V=H(1)*UU(I,2)+G(2)*UU(I,1)+H(2)*UU(I,3)
    IF(DABS(V).GE.1.0D-5) THEN
      PRINT*, 'WARNING! RESIDUE IS HIGH!!',V
    ENDIF
5    CONTINUE
  RETURN
  END
  SUBROUTINE AROOTS(LL)
* THIS SUBROUTINE COMPUTES DISCRETE POINTS TO CALCULATE ROOTS
  IMPLICIT REAL*8(A-H,O-Z)
  COMMON/T11/EV(15000000),UD(15000000)
  DIMENSION AA(3,3)
  EV(1)=0.000006
  DO 1000 L=1,LL
    CALL COEFF(EV(L),AA)
    CALL DETER(AA,3,3,UD(L))
    EV(L+1)=EV(L)+0.001
1000  CONTINUE
  RETURN
  END
  SUBROUTINE DETER(A,N,NP,D)
* THIS SUBROUTINE COMPUTES DETERMINANT OF A MATRIX
  IMPLICIT REAL*8(A-H,O-Z)
  DIMENSION A(NP,NP),INDX(6)
  CALL LUDCMP(A,N,NP,INDX,D)
  DO 11 J=1,N
    D=D*A(J,J)
11  CONTINUE
  RETURN
  END
  SUBROUTINE SOLVE(UU,P,Q)
  IMPLICIT REAL*8(A-H,O-Z)
  COMMON/T16/AA1,XD
  DIMENSION UU(3,3),W(2,2),Z(2),IND(2),P(2),Q(2)
  IP=2
  DO 1 II=1,2
  DO 1 JJ=1,2
    W(II,JJ)=UU(II,JJ+1)
1  CONTINUE

```



```

DO 5 II=1,2
Z(II)=-AA1*UU(II,1)
5 CONTINUE
CALL LUDCMP(W,2,IP,IND,F)
CALL LUBKSB(W,2,IP,IND,2)
CALL ARRAN(UU,2,P,Q)
RETURN
END
SUBROUTINE SOURCE(G,H,ALL,TD,SU,SUD)
* THIS SUBROUTINE COMPUTES SOURCE TERM
IMPLICIT REAL*8(A-H,O-Z)
COMMON/T1/XXD(4)
COMMON/T2/AL(2)
COMMON/T3/E(2)
COMMON/T5/N(3)
COMMON/T6/AD(3)
COMMON/T7/NTS(3)
COMMON/T8/QD(3,2),TPD(3,2),TSD(3,2)
COMMON/T10/CO(3)
COMMON/T14/AR(3)
COMMON/T16/AA1,XD
DIMENSION G(2),H(2)
TS=-ALL*ALL*TD
COED=DEXP(TS)
COE=1.0-COED
ARGU=AR(1)*XXD(1)
PSIA=G(1)*DSIN(ARGU)+H(1)*DCOS(ARGU)
SUU=PSIA*COE/(ALL*ALL)
ARU=AR(1)*XD
PC=G(1)*DSIN(ARU)+H(1)*DCOS(ARU)
CALL NORM(G,H,ABN)
SU=SUU*PC/AN
SUD=PSIA*PC*COED/AN
RETURN
END
SUBROUTINE NORM(AB)
* THIS SUBROUTINE COMPUTES NORM CORRESPONDING TO ZERO-EIGENVALUE
IMPLICIT REAL*8(A-H,O-Z)
COMMON/T1/XXD(4)
COMMON/T2/AL(2)
COMMON/T3/E(2)
COMMON/T14/AR(3)
AB=0.0
DO 1 I=1,2
XX=XXD(I+1)-XXD(I)
AB=AB-XX*AL(I)*E(I)
1 CONTINUE
RETURN
END
SUBROUTINE NORM(A,B,ABN)
* THIS SUBROUTINE COMPUTES NORM
IMPLICIT REAL*8(A-H,O-Z)
COMMON/T1/XXD(4)
COMMON/T2/AL(2)
COMMON/T3/E(2)
COMMON/T14/AR(3)
DIMENSION A(2),B(2)
ABN=0.0
DO 1 I=1,2
AA=A(I)*A(I)
BB=B(I)*B(I)
AB=A(I)*B(I)
XX1=XXD(I+1)-XXD(I)
XX2=XXD(I-1)-XXD(I)
XXR1=AR(I)*(XXD(I+1)+XXD(I))
XXR2=AR(I)*(XXD(I+1)-XXD(I))
SS=0.5*(AA+BB)*XX2
TT=-0.5*(AA-BB)*DCOS(XXR1)*DSIN(XXR2)/AR(I)
UU=AB*DSIN(XXR1)*DSIN(XXR2)/AR(I)
ABN=ABN+(E(I)*AL(I))*(SS+TT+UU)
1 CONTINUE
RETURN

```

```

      END
      SUBROUTINE LUDCMP(A,N,NP,INDX,D)
      • THIS SURROUTINE DEVELOPS DIAGONAL SYSTEM
      IMPLICIT REAL*8(A-H,O-Z)
      PARAMETER (NMAX=100,TINY=1.0D-20)
      DIMENSION A(NP,NP),INDX(N),VV(NMAX)
      D=1.0
      DO 12 I=1,N
        AAMAX=TINY
        DO 11 J=1,N
          IF (DABS(A(I,J)).GT.AAMAX) AAMAX=DABS(A(I,J))
11      CONTINUE
          IF (AAMAX.LE.TINY) PAUSE 'Singular Matrix !!!'
          VV(I)=1./AAMAX
12      CONTINUE
        DO 19 J=1,N
          DO 14 I=1,J-1
            SUM=A(I,J)
            DO 13 K=1,I-1
              SUM=SUM-A(I,K)*A(K,J)
13          CONTINUE
              A(I,J)=SUM
14          CONTINUE
              AAMAX=0.
              DO 16 I=J,N
                SUM=A(I,J)
                DO 15 K=1,J-1
                  SUM=SUM-A(I,K)*A(K,J)
15          CONTINUE
                  A(I,J)=SUM
                  DUM=VV(I)*DABS(SUM)
                  IF (DUM.GE.AAMAX) THEN
                    IMAX=I
                    AAMAX=DUM
                  ENDIF
16          CONTINUE
                  IF (J.NE.IMAX) THEN
                    DO 17 K=1,N
                      DUM=A(IMAX,K)
                      A(IMAX,K)=A(J,K)
                      A(J,K)=DUM
17          CONTINUE
                      D=-D
                      VV(IMAX)=VV(J)
                    ENDIF
                    INDX(J)=IMAX
                    IF (A(J,J).EQ.0.)A(J,J)=TINY
                    IF (J.NE.N) THEN
                      DUM=1./A(J,J)
                      DO 18 I=J-1,N
                        A(I,J)=A(I,J)*DUM
18          CONTINUE
                    ENDIF
19          CONTINUE
          RETURN
        END
      SUBROUTINE LUBKSB(A,N,NP,INDX,B)
      IMPLICIT REAL*8(A-H,O-Z)
      DIMENSION A(NP,NP),INDX(N),B(N)
      II=0
      DO 12 I=1,N
        LL=INDX(I)
        SUM=B(LL)
        B(LL)=B(I)
        IF (II.NE.0) THEN
          DO 11 J=II,I-1
            SUM=SUM-A(I,J)*B(J)
11          CONTINUE
          ELSE IF (SUM.NE.0.) THEN
            II=I
          ENDIF
        B(I)=SUM

```

```

12 CONTINUE
   DO 14 I=N,1,-1
     SUM=B(I)
     DO 13 J=I+1,N
       SUM=SUM-A(I,J)*B(J)
13   CONTINUE
     B(I)=SUM/A(I,I)
14 CONTINUE
   RETURN
   END

```

A.2 Input Files

* Input file: inld.d

```

0.0  0.5  1.0  <location of boundaries, XMD(I)>
0.0  0.0  <dimensionless initial pressure, PDO(I)>
1.0  100.0 <mobility ratios in compartments, EM(I)>
1.0  100.0 <storativity ratios in compartments, F(I)>
00100.0000 <skin factor at interface>
0.25 0.75 <location of wells, AD(I)>

```

* Input file: rdald.d

```

1.0 <constant in calculating roots of a linear, homogeneous syste>
0.2 <location where dimensionless pressure responses to be calculated>
9000 <number of segments to be considered for calculating eigenvalues, ML>

```

APPENDIX B

COMPUTER PROGRAM FOR TWO-DIMENSIONAL FLOW SYSTEM

This appendix presents the computer program for computing the numerical values from the analytical solution for a two-dimensional compartmentalized system as developed in Chapter 3.

B.1 Source Code

```

* Program: 2.f
.....
*   COMPARTMENTALIZED RESERVOIRS IN A 2-DIMENSIONAL SYSTEM
.....
*   Variable Identification List
.....
*   N = Number of compartments
*   XXD(I) = Locations of boundaries along x-axis
*   YYD(I) = Locations of boundaries along y-axis
*   ALX(I) = Defined in Eq. (3.16)
*   ALY(I) = Defined in Eq. (3.17)
*   EX(I) = Defined in Eq. (3.21)
*   EY(I) = Defined in Eq. (3.26)
*   UZ = 1/s (s = skin factor at an interface)
*   AD(I, J), BD(I, J) = Dimensionless coordinates of jth producing well at ith
*                       compartment
*   NW(I) = Number of wells in ith compartment
*   NTS(I, J) = Number of variable rates that the jth well at ith compartment
*              produces
*   QD(I, J, K) = Dimensionless production rate from ith compartment with jth
*               rate
*   TPD(I, J, K) = Dimensionless time at which jth production rate commences in
*                 well at ith compartment
*   TSD(I, J, K) = Dimensionless time at which jth production rate ceases in the
*                 well at ith compartment
*   TD = Dimensionless time
*   PD = Dimensionless pressure
*   SD = Semilog derivative
*   CD = Cartesian derivative
.....
IMPLICIT REAL*8(A-H,O-Z)
COMMON/T1/XXD(3),YYD(2)
COMMON/T2/ALX(2),ALY(2)
COMMON/T3/EX(2),EY(2)
COMMON/T4/UZ
COMMON/T5/NW(2)
COMMON/T6/AD(2,2),BD(2,2)
COMMON/T7/NTS(2,2)
COMMON/T8/QD(2,2,10),TDT(2,2,10)
COMMON/T11/AAL,XD,YD
COMMON/T21/AR(2)
COMMON/T101/T1(12000),T2(12000),S1(12000),S2(12000)
COMMON/T201/T1A(12000),T2A(12000),S1A(12000),S2A(12000)
COMMON/S50/ML
COMMON/S51/TD
OPEN(4,FILE='in9d.d')
OPEN(3,FILE='r9d.d')
OPEN(7,FILE='o.o')
CALL INPUT
CALL DATA
CALL PRE
CALL RADMIN(KK)
CALL PRES(KKK)
TD=0.01
WRITE(7,10)

```

```

10   FORMAT(8X,'TD',10X,'PD',10X,'SEMDER',10X,'CARDER')
      FAL=0.10
      DO 1 I=1,29
      IND=1
      CALL EQEV(KK,TD,PD,CD)
      CALL PCAL(KKK,PD,SD,CD)
      WRITE(7,11)TD,PD,SD,CD
11   FORMAT(F10.3,5X,F10.3,5X,F10.4,5X,F7.4)
      IF(TD.LT.FAL)THEN
      TD=TD+0.01
      IND=0
      ENDIF
      IF(IND.EQ.0)GO TO 1
      IF(TD.GT.FAL)THEN
      TD=2.0*TD
      ENDIF
1   CONTINUE
      STOP
      END
      SUBROUTINE INPUT
      IMPLICIT REAL*8(A-H,O-Z)
      COMMON/T1/XXD(3),YYD(2)
      COMMON/T2/ALX(2),ALY(2)
      COMMON/T3/EX(2),EY(2)
      COMMON/T4/UZ
      COMMON/T5/NW(2)
      COMMON/T6/AD(2,2),BD(2,2)
      COMMON/T7/NTS(2,2)
      COMMON/T8/QD(2,2,10),TDT(2,2,10)
      DIMENSION AMX(2),AMY(2),E(2)
      *   READING NO. OF COMPARTMENTS, NX
      READ(4,*)NX
      *   READING GEOMETRIC DIMENSIONS OF EACH COMPARTMENT IN X-DIR
      READ(4,*)XXD(1),XXD(2),XXD(3)
      READ(4,*)YYD(1),YYD(2)
      *   READING DIMENSIONLESS INITIAL PRESSURE IN EACH COMPARTMENT
      *   READING ROCK AND FLUID PROPERTIES IN EACH COMPARTMENT
      READ(4,*)(AMX(I),I=1,2)
      READ(4,*)(AMY(I),I=1,2)
      READ(4,*)(E(I),I=1,2)
      DO 1000 I=1,NX
      ALX(I)=E(I)*AMX(I)
      ALY(I)=E(I)*AMY(I)
      EX(I)=E(I)/ALX(I)
      EY(I)=E(I)/ALY(I)
1000 CONTINUE
      *   READING TRANSMISSIBILITY COEFFICIENT AT INTER-COMPARTMENT
      *   BOUNDARY
      READ(4,*)S
      UZ=1.0/S
      WRITE(7,*)'S=',S
      WRITE(7,*)'M1=',AMX(1),'M2=',AMY(2)
      WRITE(7,*)'F1=',E(1),'F2=',E(2)
      *   READING WHETHER A COMPARTMENT HAS A WELL, NW(L)=0 MEANS NO WELL
      *   READING LOCATION OF EACH WELL
      READ(4,*)NW(1),NW(2)
      DO 230 J=1,NX
      IF(NW(J).EQ.0)GO TO 231
      DO 23 I=1,NW(J)
      READ(4,*)AD(J,I),BD(J,I)
      *   READING NO. OF TIME-INTERVALS IN THE PRODUCTION
      *   SCHEDULE OF EACH WELL
      READ(4,*)NTS(J,I)
      *   READING DIMENSIONLESS PRODUCTION RATE, DIMENSIONLESS
      *   TIMES WHEN PRODUCTION STARTS
      DO 7 II=1,NTS(J,I)
      READ(4,*)QD(J,I,II)
      READ(4,*)TDT(J,I,II)
7   CONTINUE
23  CONTINUE
231 CONTINUE
230 CONTINUE

```

```

RETURN
END
SUBROUTINE DATA
  IMPLICIT REAL*8(A-H,O-Z)
  COMMON/T11/AA1,XD,YD
  COMMON/S50/ML
  READ(3,*)AA1
  READ(3,*)XD,YD
  READ(3,*)ML
  RETURN
END
SUBROUTINE COEFF(E1,E2,FA)
  IMPLICIT REAL*8(A-H,O-Z)
  COMMON/T1/XXD(3),YYD(2)
  COMMON/T2/ALX(2),ALY(2)
  COMMON/T3/EX(2),EY(2)
  COMMON/T4/UZ
  COMMON/T21/AR(2)
  DIMENSION FA(3,3)
  AR(1)=E1*DSQRT(EX(1))
  AR(2)=E2*DSQRT(EX(2))
  FA(1,1)=DCOS(AR(1)*XXD(2))-ALX(1)*AR(1)*DSIN(AR(1)*XXD(2))/UZ
  FA(1,2)=-DSIN(AR(1)*XXD(2))
  FA(1,3)=-DCOS(AR(1)*XXD(2))
  FA(2,1)=-ALX(1)*AR(1)*DSIN(AR(1)*XXD(2))
  FA(2,2)=-ALX(2)*AR(2)*DCOS(AR(2)*XXD(2))
  FA(2,3)=ALX(2)*AR(2)*DSIN(AR(2)*XXD(2))
  FA(3,1)=0.0
  FA(3,2)=DCOS(AR(2)*XXD(3))
  FA(3,3)=-DSIN(AR(2)*XXD(3))
  RETURN
END
SUBROUTINE DCOEFF(EV,FA)
  IMPLICIT REAL*8(A-H,O-Z)
  COMMON/T1/XXD(3),YYD(2)
  COMMON/T2/ALX(2),ALY(2)
  COMMON/T3/EX(2),EY(2)
  COMMON/T4/UZ
  COMMON/T21/AR(2)
  DIMENSION FA(3,3)
  V1=DSQRT(EX(1))
  V2=DSQRT(EX(2))
  A1=-DSIN(AR(1)*XXD(2))*V1*XXD(2)
  A2=-ALX(1)*V1*DSIN(AR(1)*XXD(2))/UZ
  A3=-ALX(1)*AR(1)*V1*XXD(2)*DCOS(AR(1)*XXD(2))/UZ
  FA(1,1)=A1+A2+A3
  FA(1,2)=-V2*XXD(2)*DCOS(AR(2)*XXD(2))
  FA(1,3)=V2*XXD(2)*DSIN(AR(2)*XXD(2))
  A4=-ALX(1)*AR(1)*V1*XXD(2)*DCOS(AR(1)*XXD(2))
  A5=-ALX(1)*V1*DSIN(AR(1)*XXD(2))
  FA(2,1)=A4+A5
  A6=-ALX(2)*V2*DCOS(AR(2)*XXD(2))
  A7=ALX(2)*AR(2)*V2*XXD(2)*DSIN(AR(2)*XXD(2))
  FA(2,2)=A6+A7
  A8=ALX(2)*V2*DSIN(AR(2)*XXD(2))
  A9=ALX(2)*AR(2)*V2*XXD(2)*DCOS(AR(2)*XXD(2))
  FA(2,3)=A8+A9
  FA(3,1)=0.0
  FA(3,2)=-DSIN(AR(2)*XXD(3))
  FA(3,3)=-DCOS(AR(2)*XXD(3))
  RETURN
END
SUBROUTINE EIGEN(VI1,VI2,EV)
  IMPLICIT REAL*8(A-H,O-Z)
  DIMENSION AA(3,3),BB(3,3),CC(3,3)
  CALL COEFF(VI1,VI1,AA)
  CALL DETER(AA,3,3,AD1)
  CALL COEFF(VI2,VI2,BB)
  CALL DETER(BB,3,3,AD2)
  EV=(VI1*AD2-VI2*AD1)/(AD2-AD1)
  M=0
  CALL COEFF(EV,EV,AA)

```

2

```

CALL DCOEFF(EV, BB)
M=M+1
SUM=0.0
DO 1 I=1, 3
CALL MAT(I, 3, AA, BB, CC)
CALL DETER(CC, 3, 3, DV)
SUM=SUM+DV
1 CONTINUE
CALL DETER(AA, 3, 3, AD)
DEV=-AD/SUM
EV=EV+DEV
IF(M.GT.1000)GO TO 3
IF(DABS(DEV).GT.1.0D-12)GO TO 2
3 IF(M.GT.1000)THEN
EV=1000000.0
ENDIF
RETURN
END
SUBROUTINE MAT(JKF, NI, AB, BC, CA)
IMPLICIT REAL*8(A-H, O-Z)
DIMENSION AB(NI, NI), BC(NI, NI), CA(NI, NI)
DO 2 I=1, NI
DO 2 J=1, NI
IF(I.EQ.JKF)THEN
CA(I, J)=BC(I, J)
ELSE
CA(I, J)=AB(I, J)
ENDIF
2 CONTINUE
RETURN
END
SUBROUTINE GUESS
IMPLICIT REAL*8(A-H, O-Z)
COMMON/T101/T1(12000), T2(12000), S1(12000), S2(12000)
PI=DACOS(-1.0D00)
DO 1 I=1, 300
T1(I)=PI
T2(I)=PI
1 CONTINUE
RETURN
END
SUBROUTINE PRE
IMPLICIT REAL*8(A-H, O-Z)
COMMON/T101/T1(12000), T2(12000), S1(12000), S2(12000)
DIMENSION SE(1000)
SUM=0.0
CALL GENEI(SE)
DO 1 I=1, 300
S1(I)=SE(I)
S2(I)=SE(I)
1 CONTINUE
RETURN
END
SUBROUTINE PRES(M)
IMPLICIT REAL*8(A-H, O-Z)
COMMON/T101/T1(12000), T2(12000), S1(12000), S2(12000)
COMMON/T201/T1A(12000), T2A(12000), S1A(12000), S2A(12000)
COMMON/S51/TD
DIMENSION SE(1000)
CALL GUESS
M=0
DO 3 J=1, 50
DO 2 I=1, 50
DS=S1(I)*S1(I)-S2(J)*S2(J)
IF(DABS(DS).LT.1.0D-09)GO TO 2
CALL FUNCT(I, DS)
IF(T1(I).LT.1.0D-10.OR.T2(I).LT.1.0D-10)GO TO 2
DIFF=T1(I)-T2(I)
IF(DABS(DIFF).LT.1.0D-05)GO TO 2
T1A(M)=T1(I)
T2A(M)=T2(I)
S1A(M)=S1(I)

```

```

        S2A(M)=S2(I)
        M=M+1
2      CONTINUE
3      CONTINUE
        M=M-1
        RETURN
        END
        SUBROUTINE FUNCT(I,DSQ)
        IMPLICIT REAL*8(A-H,O-Z)
        COMMON/T101/T1(12000),T2(12000),S1(12000),S2(12000)
        DIMENSION FF(3,3)
        MM=0
102     CALL F1(T1(I),T2(I),F10)
        F20=T1(I)*T1(I)-T2(I)*T2(I)+DSQ
        CALL D1D1(T1(I),T2(I),DF1)
        CALL D1D2(T1(I),T2(I),DF2)
        DF2DT1=2.0*T1(I)
        DF2DT2=-2.0*T2(I)
        V=DF1*DF2DT2-DF2*DF2DT1
        U1=(-F10*DF2DT2-F20*DF2)/V
        T1(I)=T1(I)+U1
        U2=(-F20*DF1-F10*DF2DT1)/V
        T2(I)=T2(I)-U2
        MM=MM+1
        IF(MM.GE.500)GO TO 103
        DEL=DABS(F10)+DABS(F20)
        IF(DEL.GT.1.0D-06)THEN
            IVUA=1
        ELSE
            IVUA=2
        ENDIF
        IF(IVUA.EQ.1)GO TO 102
        IF(IVUA.EQ.2)GO TO 104
103     T1(I)=100000.0
        T2(I)=100000.0
104     RETURN
        END
        SUBROUTINE F1(EV1,EV2,FA)
        IMPLICIT REAL*8(A-H,O-Z)
        COMMON/T1/XXD(3),YYD(2)
        COMMON/T2/ALX(2),ALY(2)
        COMMON/T3/EX(2),EY(2)
        COMMON/T4/UZ
        R1=DSQRT(EX(1))
        R2=DSQRT(EX(2))
        AR1=EV1*R1
        AR2=EV2*R2
        X=XXD(3)-XXD(2)
        W1=-AR2*DCOS(AR1*XXD(2))*DSIN(AR2*X)
        W2=ALX(1)*ALX(2)*AR1*AR2*DSIN(AR1*XXD(2))*DSIN(AR2*X)/UZ
        W3=-ALX(1)*AR1*DSIN(AR1*XXD(2))*DCOS(AR2*X)
        FA=W1+W2+W3
        RETURN
        END
        SUBROUTINE FCAL(NM,SU,SSD,SUD)
        IMPLICIT REAL*8(A-H,O-Z)
        COMMON/T21/AR(2)
        COMMON/T201/T1A(12000),T2A(12000),S1A(12000),S2A(12000)
        COMMON/S51/TD
        COMMON/S52/G(2),H(2)
        DIMENSION FF(3,3),GG(3,3)
        DO 1 I=1,NM
            A1=T1A(I)
            B1=T2A(I)
            C1=S1A(I)
            D1=S2A(I)
            ALU=A1*A1+C1*C1
            CALL COEFF(A1,B1,FF)
            DO 12 II=1,3
            DO 12 JJ=1,3
                GG(II,JJ)=FF(II,JJ)
12     CONTINUE

```



```

CALL SOLVE(FF,G,H)
CALL SOURCE(A1,B1,C1,D1,SY)
CALL PDSUM(A1,B1,C1,D1,S)
CALL SOUP(A1,B1,C1,D1,SD)
SU=SU+S*SY
SUD=SUD+SY*SD-ALU*S*SY
1 CONTINUE
SSD=TD*SUD
RETURN
END
SUBROUTINE INVAL(T,P,DP)
IMPLICIT REAL*8(A-H,O-Z)
COMMON/T1/XXD(3),YYD(2)
COMMON/T2/ALX(2),ALY(2)
COMMON/T3/EX(2),EY(2)
COMMON/T5/NW(2)
AN=0.0
QSU=0.0
DO 1 I=1,2
  AN=AN+EX(I)*ALX(I)*(XXD(I+1)-XXD(I))
DO 2 J=1,NW(I)
  IF(NW(I).EQ.0)GO TO 2
  CALL FTD(I,J,T,Q)
  QSU=QSU+EX(2)*ALX(2)*Q
2 CONTINUE
1 CONTINUE
AN=AN*(YYD(2)-YYD(1))
DP=QSU/AN
P=T*DP
RETURN
END
SUBROUTINE EQEV(KK,TD,SUM,SUD)
IMPLICIT REAL*8(A-H,O-Z)
COMMON/S2/EV(10000),UD(10000)
COMMON/S3/EI(2000)
COMMON/T11/AA1,XD,YD
COMMON/T21/AR(2)
COMMON/T101/T1(12000),T2(12000),S1(12000),S2(12000)
COMMON/S50/ML
COMMON/S52/G(2),H(2)
DIMENSION FF(3,3),GG(3,3)
CALL INVAL(TD,SUM,SUD)
SA1=0.0
SA2=0.0
DO 11 KY=1,300
DO 10 K=1,KK
  CALL COEFF(EI(K),EI(K),FF)
DO 12 II=1,3
DO 12 JJ=1,3
  GG(II,JJ)=FF(II,JJ)
12 CONTINUE
  ALU=EI(K)*EI(K)+S1(KY)*S1(KY)
  CALL SOLVE(FF,G,H)
  CALL SOURCE(EI(K),EI(K),S1(KY),S1(KY),SY)
  CALL PDSUM(EI(K),EI(K),S1(KY),S1(KY),S)
  CALL SOUP(EI(K),EI(K),S1(KY),S1(KY),SD)
  SUM=SUM+SY*S
  SUD=SUD+SY*SD-ALU*SY*S
10 CONTINUE
  ALY=S1(KY)*S1(KY)
  CALL PDSU(S1(KY),S1Y)
  SA1=SA1+S1Y
  CALL PDS(D(S1(KY),S2Y)
  SA2=SA2+S2Y-ALY*S1Y
11 CONTINUE
SUM=SUM+SA1
SUD=SUD+SA2
RETURN
END
SUBROUTINE RADMIN(LX)
IMPLICIT REAL*8(A-H,O-Z)
COMMON/S2/EV(1000000),UD(1000000)

```

```

COMMON/S3/EI(2000)
COMMON/S50/ML
DIMENSION AE1(2000),AE2(2000)
CALL AROOTS
LX=0
DO 1 L=1,ML-1
IF(DABS(UD(L)).LE.1.0D-12)THEN
  ABC=EV(L)
  GO TO 420
ENDIF
IF(DABS(UD(L+1)).LE.1.0D-12)THEN
  ABC=EV(L+1)
  GO TO 420
ENDIF
ULLAH=UD(L)/UD(L+1)
IF(ULLAH.GT.0.0)GO TO 1
PA=EV(L)
FU=EV(L+1)
CALL EIGEN(EV(L),EV(L+1),ABC)
IF(ABC.GT.FU.OR.ABC.LT.PA)GO TO 1
420 IF(ABC.LE.1.0D-5)GO TO 1
  INDI=0
  IF(LX.GT.1)THEN
    DIFF=DABS(ABC-EI(LX))
    IF(DIFF.LE.1.0D-03)INDI=1
  ENDIF
  IF(INDI.NE.0)GO TO 1
  LX=LX+1
  EI(LX)=ABC
1 CONTINUE
  LX=LX-1
  RETURN
END
SUBROUTINE GENEI(SE)
IMPLICIT REAL*8(A-H,O-Z)
COMMON/T1/XXD(3),YYD(2)
COMMON/T3/EX(2),EY(2)
DIMENSION SE(1000)
PI=DACOS(-1.0D+00)
DO 100 I=1,300
AI=FLOAT(I)
SE(I)=(AI-1.0)*PI/DSQRT(EY(1))
100 CONTINUE
RETURN
END
SUBROUTINE ARRAN(UU,D,G,H)
IMPLICIT REAL*8(A-H,O-Z)
COMMON/T11/AA1,XD,YD
DIMENSION G(2),H(2),D(2),UU(3,3)
G(1)=0.0
H(1)=AA1
G(2)=D(1)
H(2)=D(2)
DO 5 I=1,3
T=H(1)*UU(I,1)+G(2)*UU(I,2)-H(2)*UU(I,3)
IF(DABS(V).GE.1.0D-5) THEN
  PRINT*, 'WARNING! RESIDUE IS HIGH!!',V
ENDIF
5 CONTINUE
RETURN
END
SUBROUTINE AROOTS
IMPLICIT REAL*8(A-H,O-Z)
COMMON/S2/EV(10000000),UD(10000000)
COMMON/S50/ML
DIMENSION AA(3,3)
EV(1)=0.000006
DO 1000 L=1,ML
CALL COEFF(EV(L),EV(L),AA)
CALL DETER(AA,3,3,UD(L))
EV(L+1)=EV(L)+0.001
1000 CONTINUE

```

```

RETURN
END
SUBROUTINE DETER(A,N,NP,D)
IMPLICIT REAL*8(A-H,O-Z)
DIMENSION A(NP,NP),INDX(6)
CALL LUDCMP(A,N,NP,INDX,D)
DO 11 J=1,N
    D=D*A(J,J)
11 CONTINUE
RETURN
END
SUBROUTINE SOLVE(UU,P,Q)
IMPLICIT REAL*8(A-H,O-Z)
COMMON/T11/AAL,XD,YD
DIMENSION UU(3,3),W(2,2),Z(2),IND(2),P(2),Q(2)
N=2
IP=0
DO 1 II=1,2
DO 1 JJ=1,2
    W(II,JJ)=UU(II,JJ+1)
1 CONTINUE
DO 5 II=1,2
    Z(II)=-AAL*UU(II,1)
5 CONTINUE
CALL LUDCMP(W,2,IP,IND,F)
CALL LUBKSB(W,2,IP,IND,Z)
CALL ARRAN(UU,Z,P,Q)
RETURN
END
SUBROUTINE SOURCE(AL1,AL2,AY1,AY2,SU)
IMPLICIT REAL*8(A-H,O-Z)
COMMON/T3/EX(2),EY(2)
COMMON/T11/AAL,XD,YD
COMMON/T21/AR(2)
COMMON/S52/G(2),H(2)
DIMENSION FF(3,3),GG(3,3)
CALL NORM(G,H,AN)
ARY1=EY(1)*DSQRT(AY1)
DX=G(1)*DSIN(AR(1)*XD)-H(1)*DCOS(AR(1)*XD)
DY=DCOS(ARY1*YD)
PC=DX*DY
IF (CABS(AL1).LT.1.0D-08) THEN
    AN=1.5
ENDIF
IF (CABS(AY1).LT.1.0D-08) THEN
    AN=1.0*AN
ENDIF
SU=PC/(0.5*AN)
RETURN
END
SUBROUTINE PDSUM(AL1,AL2,AY1,AY2,PDS)
IMPLICIT REAL*8(A-H,O-Z)
COMMON/T1/XXD(3),YYD(2)
COMMON/T2/ALX(2),ALY(2)
COMMON/T3/EX(2),EY(2)
COMMON/T4/UZ
COMMON/T5/NW(2)
COMMON/T6/AD(2,2),BD(2,2)
COMMON/T7/NTS(2,2)
COMMON/T8/QD(2,2,10),TDT(2,2,10)
COMMON/T21/AR(2)
COMMON/S51/TD
COMMON/S52/G(2),H(2)
DIMENSION DUMT(20)
ARY1=AY1*DSQRT(EY(1))
ARY2=AY2*DSQRT(EY(2))
ALU=AL1*AL1+AY1*AY1
PDS=0.0
DO 220 IA=1,2
    IF (NW(IA).EQ.0) GO TO 201
    DO 200 JB=1,NW(IA)
        INDEX=1

```

```

DO 2 K=2,NTS(IA,JB)
IF(INDEX.EQ.0)GO TO 2
IF(TD.LE.TDT(IA,JB,K))THEN
    JFK=K-1
    INDEX=0
ENDIF
CONTINUE
IF(INDEX.EQ.0)THEN
    L=JKF
    ELSE
    L=NTS(IA,JB)
ENDIF
DO 50 KI=1,L
    DUMT(KI)=TDT(IA,JB,KI)
CONTINUE
DUMT(L+1)=TD
DO 1 I=1,L
    TT1=ALU*(DUMT(I)-TD)
    TT2=ALU*(DUMT(I+1)-TD)
    DFX=G(IA)*DSIN(AR(IA)*AD(IA,JB))+H(IA)*DCOS(AR(IA)*AD(IA,JB))
    IF(IA.EQ.1)THEN
        DFY=DCOS(ARY1*BD(IA,JB))
    ELSE
        DFY=DCOS(ARY2*BD(IA,JB))
    ENDIF
    VALU=ALY(2)*DFX*DFY/ALU
    PDS=PDS+QD(IA,JB,I)*(DEXP(TT2)-DEXP(TT1))*VALU
CONTINUE
CONTINUE
CONTINUE
CONTINUE
RETURN
END
SUBROUTINE PDSO(ALLY,PDS)
IMPLICIT REAL*8(A-H,O-Z)
COMMON/T1/XXD(3),YYD(2)
COMMON/T2/ALX(2),ALY(2)
COMMON/T3/EX(2),EY(2)
COMMON/T4/UZ
COMMON/T5/NW(2)
COMMON/T6/AD(2,2),BD(2,2)
COMMON/T7/NTS(2,2)
COMMON/T8/QD(2,2,10),TDT(2,2,10)
COMMON/T11/AAL,XD,YD
COMMON/SS1/TD
DIMENSION DUMT(20),ALV(2)
ALLY=ALLY*ALLY
PDS=0.0
INDI=0
IF(DABS(ALLY).LT.1.0D-3)THEN
    INDI=1
ENDIF
ENDIF
ALV(1)=ALLY*DSQRT(EY(1))
ALV(2)=ALLY*DSQRT(EY(2))
IF(INDI.EQ.1)GO TO 333
DO 1 I=1,2
    IF(NW(I).EQ.0)GO TO 1
    DO 2 J=1,NW(I)
        DFY=DCOS(ALV(I)*BD(I,J))
        DFYY=DCOS(ALV(I)*YD)
        CALL FTD(I,J,TD,Q)
        VALU=Q*DFY*DFYY*ALLY(2)
        PDS=PDS+VALU/0.5
CONTINUE
CONTINUE
RETURN
333
END
SUBROUTINE PDSU(ALLY,PDS)
IMPLICIT REAL*8(A-H,O-Z)
COMMON/T1/XXD(3),YYD(2)
COMMON/T2/ALX(2),ALY(2)
COMMON/T3/EX(2),EY(2)

```

```

COMMON/T4/UZ
COMMON/T5/NW(2)
COMMON/T6/AD(2,2),BD(2,2)
COMMON/T7/NTS(2,2)
COMMON/T8/QD(2,2,10),TDT(2,2,10)
COMMON/T11/AAL,XD,YD
COMMON/S51/TD
DIMENSION DUMT(20),ALV(2)
ALU=ALLY*ALLY
  INDI=0
PDS=0.0
ALV(1)=ALLY*DSQRT(EY(1))
ALV(2)=ALLY*DSQRT(EY(2))
IF(DABS(ALLY).LT.1.0D-3)THEN
  INDI=1
ENDIF
IF(INDI.EQ.1)GO TO 333
DO 220 IA=1,2
IF(NW(IA).EQ.0)GO TO 201
DO 200 JB=1,NW(IA)
INDEX=1
DO 2 K=2,NTS(IA,JB)
IF(INDEX.EQ.0)GO TO 2
IF(TD.LE.TDT(IA,JB,K))THEN
  JKF=K-1
  INDEX=0
ENDIF
CONTINUE
IF(INDEX.EQ.0)THEN
  L=JKF
ELSE
  L=NTS(IA,JB)
ENDIF
DO 50 KI=1,L
  DUMT(KI)=TDT(IA,JB,KI)
CONTINUE
DUMT(L+1)=TD
DO 1 I=1,L
  TT1=ALU*(DUMT(I)-TD)
  TT2=ALU*(DUMT(I-1)-TD)
  DFY=DCOS(ALV(IA)*BD(IA,JB))
  DFYY=DCOS(ALV(IA)*YD)
  VALU=ALV(2)*DFY*DFYY*(0.5*ALU)
  PDS=PDS-QD(IA,JB,I)*(DEXP(TT2)-DEXP(TT1))*VALU
CONTINUE
200 CONTINUE
201 CONTINUE
220 CONTINUE
333 RETURN
END

SUBROUTINE SOUP(AL1,AL2,AY1,AY2,SUB)
IMPLICIT REAL*8(A-H,O-Z)
COMMON/T1/XXD(3),YYD(2)
COMMON/T2/ALX(2),ALY(2)
COMMON/T3/EX(2),EY(2)
COMMON/T4/UZ
COMMON/T5/NW(2)
COMMON/T6/AD(2,2),BD(2,2)
COMMON/T7/NTS(2,2)
COMMON/T8/QD(2,2,10),TDT(2,2,10)
COMMON/T21/AR(2)
COMMON/S51/TD
COMMON/S52/G(2),H(2)
DIMENSION DUMT(20)
SUB=0.0
ALU=AL1*AL1+AY1*AY1
DO 200 I=1,2
IF(NW(I).EQ.0)GO TO 201
DO 202 J=1,NW(I)
CALL FTD(I,J,TD,QRATE)
DFX=G(I)*DSIN(AR(I)*AD(I,J))+H(I)*DCOS(AR(I)*AD(I,J))
IF(I.EQ.1)THEN

```

```

        AY=AY1*DSQRT(EY(1))
    ELSE
        AY=AY2*DSQRT(EY(2))
    ENDIF
    DFY=DCOS(AY*BD(I,J))
    SUB=SUB+QRATE*DFX*DFY*ALY(2)
202 CONTINUE
201 CONTINUE
200 CONTINUE
RETURN
END
SUBROUTINE FTD(I,J,T,Q)
IMPLICIT REAL*8(A-H,O-Z)
COMMON/T7/NTS(2,2)
COMMON/T8/QD(2,2,10),TDT(2,2,10)
INDEX=1
DO 1 K=2,NTS(I,J)
IF(INDEX.EQ.0)GO TO 1
IF(T.LT.TDT(I,J,K))THEN
Q=QD(I,J,K-1)
INDEX=0
ENDIF
CONTINUE
1 IF(INDEX.EQ.1)THEN
Q=QD(I,J,NTS(I,J))
ENDIF
RETURN
END
SUBROUTINE NORM(A,B,ABN)
IMPLICIT REAL*8(A-H,O-Z)
COMMON/T1/XXD(3),YYD(2)
COMMON/T2/ALX(2),ALY(2)
COMMON/T3/EX(2),EY(2)
COMMON/T21/AR(2)
DIMENSION A(2),B(2)
ABN=0.0
DO 1 I=1,2
AA=A(I)*A(I)
BB=B(I)*B(I)
AB=A(I)*B(I)
XX1=XXD(I+1)+XXD(I)
XX2=XXD(I-1)-XXD(I)
XXR1=AR(I)*(XXD(I+1)-XXD(I))
XXR2=AR(I)*(XXD(I-1)-XXD(I))
SS=0.5*(AA+BB)*XX2
TT=-0.5*(AA-BB)*DCOS(XXR1)*DSIN(XXR2)
UU=AB*DSIN(XXR1)*DSIN(XXR2)
ABN=ABN+EX(I)*(SS-TT-UU)*ALX(I)
1 CONTINUE
RETURN
END
SUBROUTINE LUDCMP(A,N,NP,INDX,D)
IMPLICIT REAL*8(A-H,O-Z)
PARAMETER (NMAX=100,TINY=1.0D-20)
DIMENSION A(NP,NP),INDX(N),VV(NMAX)
D=1.0
DO 12 I=1,N
AAMAX=0.
DO 11 J=1,N
IF (DABS(A(I,J)).GT.AAMAX) AAMAX=DABS(A(I,J))
11 CONTINUE
IF (AAMAX.EQ.0.) PAUSE 'Singular Matrix !!!'
VV(I)=1./AAMAX
12 CONTINUE
DO 19 J=1,N
DO 14 I=1,J-1
SUM=A(I,J)
DO 13 K=1,I-1
SUM=SUM-A(I,K)*A(K,J)
13 CONTINUE
A(I,J)=SUM
14 CONTINUE

```

```

      AAMAX=0.
      DO 16 I=J,N
        SUM=A(I,J)
        DO 15 K=1,J-1
          SUM=SUM-A(I,K)*A(K,J)
15     CONTINUE
        A(I,J)=SUM
        DUM=VV(I)*DABS(SUM)
        IF (DUM.GE.AAMAX) THEN
          IMAX=I
          AAMAX=DUM
        ENDIF
16     CONTINUE
        IF (J.NE.IMAX) THEN
          DO 17 K=1,N
            DUM=A(IMAX,K)
            A(IMAX,K)=A(J,K)
            A(J,K)=DUM
17     CONTINUE
          D=-D
          VV(IMAX)=VV(J)
        ENDIF
        INDX(J)=IMAX
        IF (A(J,J).EQ.0.)A(J,J)=TINY
        IF (J.NE.N) THEN
          DUM=1./A(J,J)
          DO 18 I=J-1,N
            A(I,J)=A(I,J)*DUM
18     CONTINUE
        ENDIF
19     CONTINUE
      RETURN
      END
      SUBROUTINE LUBKSB(A,N,NP,INDX,B)
      IMPLICIT REAL*8(A-H,O-Z)
      DIMENSION A(NP,NP),INDX(N),B(N)
      II=0
      DO 10 I=1,N
        LL=INDX(I)
        SUM=B(LL)
        B(LL)=B(I)
        IF(II.NE.0) THEN
          DO 11 J=II,I-1
            SUM=SUM-A(I,J)*B(J)
11     CONTINUE
          ELSE IF(SUM.NE.0.)THEN
            II=I
          ENDIF
        B(I)=SUM
12     CONTINUE
      DO 14 I=N,1,-1
        SUM=B(I)
        DO 13 J=I-1,N
          SUM=SUM-A(I,J)*B(J)
13     CONTINUE
        B(I)=SUM/A(I,I)
14     CONTINUE
      RETURN
      END
      SUBROUTINE D1D1(AL1,AL2,DF1DT1)
      IMPLICIT REAL*8(A-H,O-Z)
      COMMON/T1/XXD(3),YYD(2)
      COMMON/T2/ALX(2),ALY(2)
      COMMON/T3/EX(2),EY(2)
      COMMON/T4/UZ
      R1=DSQRT(EX(1))
      R2=DSQRT(EX(2))
      AR1=R1*AL1
      AR2=R2*AL2
      A1=ALX(2)*AR2*XXD(2)*R1*DSIN(AR1*XXD(2))
      A1=A1*DSIN(AR2*(XXD(3)-XXD(2)))
      A2=ALX(1)*ALX(2)*AR1*AR2*R1*XXD(2)*DCOS(AR1*XXD(2))/UZ

```

```

A3=A2*DSIN(AR2*(XXD(3)-XXD(2)))
A4=ALX(1)*ALX(2)*R1*AR2*DSIN(AR1*XXD(2))
A5=A4*DSIN(AR2*(XXD(3)-XXD(2)))/UZ
A6=-ALX(1)*R1*DSIN(AR1*XXD(2))*DCOS(AR2*(XXD(3)-XXD(2)))
A7=-ALX(1)*AR1*R1*XXD(2)*DCOS(AR1*XXD(2))
A7=A7*DCOS(AR2*(XXD(3)-XXD(2)))
DF1DT1=A1+A3+A5+A6+A7
RETURN
END
SUBROUTINE D1DC(AL1,AL2,DF1DT2)
IMPLICIT REAL*8(A-H,O-Z)
COMMON/T1/XXD(3),YYD(2)
COMMON/T2/ALX(2),ALY(2)
COMMON/T3/EX(2),EY(2)
COMMON/T4/UZ
R1=DSQRT(EX(1))
R2=DSQRT(EX(2))
AR1=R1*AL1
AR2=R2*AL2
A1=-ALX(2)*R2*DCOS(AR1*XXD(2))
A1=A1*DSIN(AR2*(XXD(3)-XXD(2)))
A2=-ALX(2)*R2*(XXD(3)-XXD(2))*AR2*DCOS(AR1*XXD(2))
A2=A2*DCOS(AR2*(XXD(3)-XXD(2)))
A3=ALX(1)*ALX(2)*AR1*R2*DSIN(AR1*XXD(2))/UZ
A3=A3*DSIN(AR2*(XXD(3)-XXD(2)))
A4=ALX(1)*ALX(2)*AR1*AR2*R2*(XXD(3)-XXD(2))/UZ
A4=A4*DSIN(AR1*XXD(2))*DCOS(AR2*(XXD(3)-XXD(2)))
A5=ALX(1)*AR1*DSIN(AR1*XXD(2))*R2*(XXD(3)-XXD(2))
A5=A5*DSIN(AR2*(XXD(3)-XXD(2)))
DF1DT2=A1+A2+A3+A4+A5
RETURN
END

```

B.2: Input Files

* Input file: input9d.d

```

2      <number of compartments>
0.0  0.5 1.0  <location boundaries in x-direction>
0.0  1.0      <location boundaries in y-direction>
1.0  1.0      <alx(1)>
1.0  1.0      <aly(1)>
0.1  0.1      <e(1)>
0.00000.0000 <skin factor>
1  1      <number of wells in each compartment, NW(I)>
0.25  0.5  <location of first well, AD(1,1),BD(1,1)>
2      <number of time steps in production schedule of first well, NTS(1,1)>
1.0  <QDT(1,1,1)>
0.0  <TDT(1,1,1)>
0.0  <QDT(1,1,2)>
100.0 <TDT(1,1,2)>
0.75  0.5  <location of second well, AD(2,1),BD(2,1)>
2      <number of time steps in production schedule of second well, NTS(2,1)>
0.0  <QDT(2,1,1)>
0.0  <TDT(2,1,1)>
1.0  <QDT(2,1,2)>
100.0 <TDT(2,1,2)>

```

* Input file: r9d.d

```

1.0  <AA1, a constant for solution of a linear system>
0.25  0.5000001  <location of measuring dimensionless pressure responses, XD, YD>
1000000  <ML, number of segments to be considered for calculating eigenvalues>

```


APPENDIX C

COMPUTER PROGRAM FOR THREE-DIMENSIONAL FLOW SYSTEM

This appendix presents the computer program for computing the numerical values from the analytical solution for a three-dimensional compartmentalized system as developed in Chapter 4.

C.1 Source Code

```

* Program: 3.f
.....
*   COMPARTMENTALIZED RESERVOIRS IN A 3-DIMENSIONAL SYSTEM
*   Stacked Channel Realization
.....
*   Variable Identification List
.....
*   N = Number of compartments
*   XXD(I) = Locations of boundaries along x-axis
*   YYD(I) = Locations of boundaries along y-axis
*   ZZD(I) = Locations of boundaries along z-axis
*   WD = Dimensionless width of each sand body
*   ALX(I) = Defined in Eq. (4.22)
*   ALY(I) = Defined in Eq. (4.23)
*   ALZ(I) = Defined in Eq. (4.24)
*   E(I) = Defined in Eq. (4.25)
*   EX(I) = Defined in Eq. (4.28)
*   EY(I) = Defined in Eq. (4.33)
*   EZ(I) = Defined in Eq. (4.38)
*   IS = 1/s (s = skin factor at an interface)
*   AD(I, J), BD(I, J) = Dimensionless areal coordinates of jth producing well at
*   ith compartment
*   HD1(I, J), HD2(I, J) = Extent of producing zone of jth producing well at
*   ith compartment (Fig. 4.2)
*   NW(I) = Number of wells in ith compartment
*   NTS(I, J) = Number of variable rates that the jth well at ith compartment
*   produces
*   QD(I, J, K) = Dimensionless production rate from ith compartment with jth
*   rate
*   TDT(I, J, K) = Dimensionless time at which jth production rate commences in
*   well at ith compartment
*   TD = Dimensionless time
*   PD = Dimensionless pressure
*   PARD = Particular derivative (eg. linear, radial or spherical)
*   CD = Cartesian derivative
.....
IMPLICIT REAL*8(A-H,O-Z)
COMMON/T1/XXD(4),YYD(4),ZZD(3)
COMMON/T2/ALX(2),ALY(2),ALZ(2)
COMMON/T3/EX(2),EY(2),EZ(2)
COMMON/T4/UZ
COMMON/T5/NW(6)
COMMON/T6/AD(6,2),BD(6,2),HD1(6,2),HD2(6,2)
COMMON/T7/NTS(6,2)
COMMON/T8/QD(6,2,20),TDT(6,2,20)
COMMON/T11/AA1,XD,YD,ZD
COMMON/T102/T1(1200),S1(1200),P1(1200)
COMMON/T103/T2(1200),S2(1200),P2(1200)
COMMON/T104/T3(1200),S3(1200),P3(1200)
COMMON/T105/T4(1200),S4(1200),P4(1200)
COMMON/T106/T5(1200),S5(1200),P5(1200)
COMMON/T107/T6(1200),S6(1200),P6(1200)
OPEN(4,FILE='in3d.d')
OPEN(3,FILE='r3d.d')

```

```

OPEN(7, FILE='5.0')
CALL INPUT
CALL DATA
CALL EQEV(M)
CALL EIGENV(M)
TD=0.001
WRITE(7,10)
10  FORMAT(8X, 'TD', 10X, 'PD', 10X, 'PARDER', 10X, 'CARDER')
    FAL=0.10
    DO 1 J=1,30
      IND=1
      CALL PCAL(M, TD, PD, CD)
      PARD=CD*(TD**0.5)
      WRITE(7, 11) TD, PD, PARD, CD
11  FORMAT(F10.3, 5X, F10.3, 5X, F10.4, 5X, F9.4)
      IF(TD.LT.FAL) THEN
        TD=TD+0.01
        IND=0
      ENDIF
      IF(IND.EQ.0) GO TO 1
      IF(TD.GT.FAL) THEN
        TD=2.0*TD
      ENDIF
1  CONTINUE
   STOP
   END
   SUBROUTINE INPUT
     IMPLICIT REAL*8(A-H,O-Z)
     COMMON/T1/XXD(4), YYD(4), ZZD(3)
     COMMON/T2/ALX(2), ALY(2), ALZ(2)
     COMMON/T3/EX(2), EY(2), EZ(2)
     COMMON/T4/UZ
     COMMON/T5/NW(6)
     COMMON/T6/AD(6,2), BD(6,2), HD1(6,2), HD2(6,2)
     COMMON/T7/NTS(6,2)
     COMMON/T8/QD(6,2,20), TDT(6,2,20)
     COMMON/T11/AA1, XD, YD, ZD
     * READING NO. OF COMPARTMENTS IN X, Y & Z-DIR, NX, NY & NZ
     READ(4,*) NX
     * READING GEOMETRIC DIMENSIONS OF EACH COMPARTMENT IN X-DIR
     READ(4,*) XXD(1), XXD(4)
     READ(4,*) WD
     XXD(2)=0.5*(XXD(4)-XXD(1))-0.5*WD
     XXD(3)=0.5*(XXD(4)-XXD(1))+0.5*WD
     READ(4,*) YYD(1), YYD(4)
     YYD(2)=0.5*(YYD(4)-YYD(1))-0.5*WD
     YYD(3)=0.5*(YYD(4)-YYD(1))+0.5*WD
     READ(4,*) (ZZD(I), I=1,3)
     * READING DIMENSIONLESS INITIAL PRESSURE IN EACH COMPARTMENT
     * READING ROCK AND FLUID PROPERTIES IN EACH COMPARTMENT
     READ(4,*) (ALX(I), I=1,2)
     READ(4,*) (ALY(I), I=1,2)
     READ(4,*) (ALZ(I), I=1,2)
     READ(4,*) (EX(I), I=1,2)
     READ(4,*) (EY(I), I=1,2)
     READ(4,*) (EZ(I), I=1,2)
     * READING TRANSMISSIBILITY COEFFICIENT AT INTER-COMPARTMENT
     * BOUNDARY
     READ(4,*) S
     UZ=1.0/S
     * READING WHETHER A COMPARTMENT HAS A WELL, N(L)=0 MEANS NO WELL
     READ(4,*) (NW(I), I=1, NX)
     * READING LOCATION OF EACH WELL
     DO 45 I=1, NX
       IF(NW(I).EQ.0) GO TO 45I
       DO 452 J=1, NW(I)
         READ(4,*) AD(I, J), BD(I, J)
         READ(4,*) HD1(I, J), HD2(I, J)
     * READING NO. OF TIME-INTERVALS IN THE PRODUCTION
     * SCHEDULE OF EACH WELL
     READ(4,*) NTS(I, J)
     * READING DIMENSIONLESS PRODUCTION RATE, DIMENSIONLESS TIMES WHEN PRODUCTION STARTS

```

```

DO 7 K=1,NTS(I,J)
READ(4,*)QD(I,J,K)
READ(4,*)TDT(I,J,K)
7 CONTINUE
452 CONTINUE
451 CONTINUE
45 CONTINUE
RETURN
END
SUBROUTINE DATA
IMPLICIT REAL*8(A-H,O-Z)
COMMON/T11/AA1,XD,YD,ZD
COMMON/T1100/WRS
READ(3,*)AA1
READ(3,*)XD,YD,ZD
READ(3,*)WRS
RETURN
END
SUBROUTINE GUESS
IMPLICIT REAL*8(A-H,O-Z)
COMMON/T101/T(6),S(6),P(6)
COMMON/T1100/WRS
PI=DACOS(-1.0D00)
DO 1 I=1,3
T(I)=WRS
1 CONTINUE
DO 2 I=4,6
S(I)=WRS
2 CONTINUE
P(2)=WRS
P(5)=WRS
RETURN
END
SUBROUTINE INVAL(T,P,DP)
IMPLICIT REAL*8(A-H,O-Z)
COMMON/T1/XXD(4),YYD(4),ZZD(3)
COMMON/T2/ALX(2),ALY(2),ALZ(2)
COMMON/T3/EX(2),EY(2),EZ(2)
COMMON/T5/NW(6)
COMMON/T6/AD(6,2),BD(6,2),HD1(6,2),HD2(6,2)
AN=0.0
AN1=0.0
QSU=0.0
DO 1 I=1,3
AN=AN+EX(I)*ALX(I)*(XXD(I+1)-XXD(I))
DO 2 J=1,NW(I)
IF(NW(I).EQ.0) GO TO 2
CALL FTD(I,J,T,Q)
QSU=QSU+Q
2 CONTINUE
1 CONTINUE
AN=AN*(YYD(3)-YYD(2))*(ZZD(2)-ZZD(1))
DO 3 I=1,3
AN1=AN1+EY(2)*ALY(2)*(YYD(I+1)-YYD(I))
DO 4 J=1,NW(I+3)
IF(NW(I+3).EQ.0) GO TO 4
CALL FTD(I-3,J,T,Q)
QSU=QSU+Q
4 CONTINUE
3 CONTINUE
AN=AN+AN1*(XXD(3)-XXD(2))*(ZZD(3)-ZZD(2))
DP=(ZZD(2)/XXD(4))*QSU/AN
P=T*DP
RETURN
END
SUBROUTINE PCAL(NM,TD,SU,SUD)
IMPLICIT REAL*8(A-H,O-Z)
COMMON/T11/AA1,XD,YD,ZD
COMMON/T102/T1(1200),S1(1200),P1(1200)
COMMON/T103/T2(1200),S2(1200),P2(1200)
COMMON/T104/T3(1200),S3(1200),P3(1200)
COMMON/T105/T4(1200),S4(1200),P4(1200)

```

```

COMMON/T106/T5(1200),S5(1200),P5(1200)
COMMON/T107/T6(1200),S6(1200),P6(1200)
COMMON/T108/A(3),B(3),C(3),D(3),F(2),G(2)
DIMENSION FX(5,5),FY(5,5),FZ(3,3)
CALL INVAL(TD,SU,SUD)
DO 1 I=1,NM
ALU=T1(I)*T1(I)+S1(I)*S1(I)+P1(I)*P1(I)
VUL=1.0-DEXP(-TD*ALU)
CALL FLX(T1(I),T2(I),T3(I),FX)
CALL SOLVE(5,FX,A,B)
CALL F2Y(S4(I),S5(I),S6(I),FY)
CALL SOLVE(5,FY,C,D)
CALL F3Z(P2(I),P5(I),FZ)
CALL SOLVE(3,FZ,F,G)
CALL SOURCE(I,S)
CALL PDSUM(I,TD,SUM)
CALL SOUP(I,TD,SUMD)
SU=SU+S*SUM
SUD=SUD+S*SUMD-ALU*S*SUM
CONTINUE
RETURN
END
SUBROUTINE EQEV(MM)
IMPLICIT REAL*8(A-H,O-Z)
COMMON/T1/XXD(4),YYD(4),ZZD(3)
COMMON/T3/EX(2),EY(2),EZ(2)
COMMON/T101/T(6),S(6),P(6)
COMMON/T102/T1(1200),S1(1200),P1(1200)
COMMON/T103/T2(1200),S2(1200),P2(1200)
COMMON/T104/T3(1200),S3(1200),P3(1200)
COMMON/T105/T4(1200),S4(1200),P4(1200)
COMMON/T106/T5(1200),S5(1200),P5(1200)
COMMON/T107/T6(1200),S6(1200),P6(1200)
COMMON/T100/WRS
DIMENSION SE1(1000),SE2(1000),SE3(1000),TE4(1000),
*TE5(1000),TE6(1000),PE1(1000),PE3(1000),PE4(1000),PE6(1000)
PI=DACOS(-1.0D-00)
WD=XXD(3)-XXD(2)
WD1=ZZD(2)-ZZD(1)
WD2=ZZD(3)-ZZD(2)
MM=0
CALL GUESS
DO 100 I=2,100
AI=FLOAT(I)
S(1)=(AI-1.0)*PI/(WD*EY(1))
S(2)=S(1)
S(3)=S(1)
T(4)=(AI-1.0)*PI/(WD*EX(2))
T(5)=T(4)
T(6)=T(4)
P(1)=(AI-1.0)*PI/(WD1*EZ(1))
P(3)=P(1)
P(4)=(AI-1.0)*PI/(WD2*EZ(2))
P(6)=P(4)
CALL FUNCT(NN,MM)
IF((NN-MM).EQ.1)THEN
MM=NN
ENDIF
100 CONTINUE
RETURN
END
SUBROUTINE EIGENV(MJ)
IMPLICIT REAL*8(A-H,O-Z)
COMMON/T1/XXD(4),YYD(4),ZZD(3)
COMMON/T3/EX(2),EY(2),EZ(2)
COMMON/T101/T(6),S(6),P(6)
COMMON/T102/T1(1200),S1(1200),P1(1200)
COMMON/T103/T2(1200),S2(1200),P2(1200)
COMMON/T104/T3(1200),S3(1200),P3(1200)
COMMON/T105/T4(1200),S4(1200),P4(1200)
COMMON/T106/T5(1200),S5(1200),P5(1200)
COMMON/T107/T6(1200),S6(1200),P6(1200)

```

```

      DIMENSION SE1(1000),SE2(1000),SE3(1000),TE4(1000),
#TE5(1000),TE6(1000),PE1(1000),PE3(1000),PE4(1000),PE6(1000)
      PI=DACOS(-1.0D+00)
      WD=XXD(3)-XXD(2)
      WD1=ZZD(2)-ZZD(1)
      WD2=ZZD(3)-ZZD(2)
      DO 100 I=1,10
      AI=FLOAT(I)
      SE1(I)=(AI-1.0)*PI/(WD*EY(1))
      SE2(I)=SE1(I)
      SE3(I)=SE1(I)
      TE4(I)=(AI-1.0)*PI/(WD*EX(2))
      TE5(I)=TE4(I)
      TE6(I)=TE4(I)
      PE1(I)=(AI-1.0)*PI/(WD1*EZ(1))
      PE3(I)=PE1(I)
      PE4(I)=(AI-1.0)*PI/(WD2*EZ(2))
      PE6(I)=PE4(I)
100  CONTINUE
      CALL GUESS
      NN=2
      DO 1 I1=1,NN
      S(1)=SE1(I1)
      DO 2 I2=1,NN
      S(2)=SE2(I2)
      DO 3 I3=1,NN
      S(3)=SE3(I3)
      DO 4 I4=1,NN
      T(4)=TE4(I4)
      DO 5 I5=1,NN
      T(5)=TE5(I5)
      DO 6 I6=1,NN
      T(6)=TE6(I6)
      DO 7 I7=1,NN
      P(1)=PE1(I7)
      DO 8 I8=1,NN
      P(3)=PE3(I8)
      DO 9 I9=1,NN
      P(4)=PE4(I9)
      DO 10 I10=1,NN
      P(6)=PE6(I10)
      IVAL=9-I10-I9-I8-I7-I6-I5-I4-I3-I2-I1
      IF(IVAL.EQ.0)GO TO 701
      CALL FUNCT(MI,MJ)
      IF((MI-MJ).EQ.1)THEN
      MJ=MI
      ENDIF
701  CONTINUE
10  CONTINUE
9    CONTINUE
8    CONTINUE
7    CONTINUE
6    CONTINUE
5    CONTINUE
4    CONTINUE
3    CONTINUE
2    CONTINUE
1    CONTINUE
      RETURN
      END
      SUBROUTINE FUNCT(MA,MB)
      IMPLICIT REAL*8(A-H,O-Z)
      COMMON/T101/T(6),S(6),P(6)
      COMMON/T102/T1(1200),S1(1200),P1(1200)
      COMMON/T103/T2(1200),S2(1200),P2(1200)
      COMMON/T104/T3(1200),S3(1200),P3(1200)
      COMMON/T105/T4(1200),S4(1200),P4(1200)
      COMMON/T106/T5(1200),S5(1200),P5(1200)
      COMMON/T107/T6(1200),S6(1200),P6(1200)
      DIMENSION F(8),F10(5,5),F20(5,5),F30(3,3),DF1(5,5),DF2A(5,5),
+DF2B(5,5),DF3A(5,5),DF3B(5,5),DF2(3,3),DF2A(3,3),DF2B(3,3),
-DF(8,8),DFE(8,8),DEA(8,8),U(8)

```

```

PI=DACOS(-1.0D+00)
MA=MB
MM=0
DO 1 J=1,8
DO 1 I=1,8
  DF(I,J)=0.0
1
CONTINUE
102 CALL FLX(T(1),T(2),T(3),F10)
CALL DETER(F10,5,5,F(1))
CALL F2Y(S(4),S(5),S(6),F20)
CALL DETER(F20,5,5,F(2))
CALL F3Z(P(2),P(5),F30)
CALL DETER(F30,3,3,F(3))
F(4)=T(1)*T(1)+S(1)*S(1)+P(1)*P(1)-T(2)*T(2)-S(2)*S(2)-P(2)*P(2)
F(5)=T(2)*T(2)+S(2)*S(2)+P(2)*P(2)-T(3)*T(3)-S(3)*S(3)-P(3)*P(3)
F(6)=T(4)*T(4)+S(4)*S(4)+P(4)*P(4)-T(5)*T(5)-S(5)*S(5)-P(5)*P(5)
F(7)=T(5)*T(5)+S(5)*S(5)+P(5)*P(5)-T(6)*T(6)-S(6)*S(6)-P(6)*P(6)
F(8)=T(2)*T(2)+S(2)*S(2)+P(2)*P(2)-T(5)*T(5)-S(5)*S(5)-P(5)*P(5)
CALL DF1D1(T(1),T(2),T(3),DF1)
CALL DETER(DF1,5,5,DF(1,1))
CALL DF1D2A(T(1),T(2),T(3),DF2A)
CALL DETER(DF2A,5,5,D1)
CALL DF1D2B(T(1),T(2),T(3),DF2B)
CALL DETER(DF2B,5,5,D2)
DF(1,2)=D1+D2
CALL DF1D3A(T(1),T(2),T(3),DF3A)
CALL DETER(DF3A,5,5,D1)
CALL DF1D3B(T(1),T(2),T(3),DF3B)
CALL DETER(DF3B,5,5,D2)
DF(1,3)=D1+D2
CALL DF2D4(S(4),S(5),S(6),DF1)
CALL DETER(DF1,5,5,DF(2,4))
CALL DF2D5A(S(4),S(5),S(6),DF2A)
CALL DETER(DF2A,5,5,D1)
CALL DF2D5B(S(4),S(5),S(6),DF2B)
CALL DETER(DF2B,5,5,D2)
DF(2,5)=D1+D2
CALL DF2D6A(S(4),S(5),S(6),DF3A)
CALL DETER(DF3A,5,5,D1)
CALL DF2D6B(S(4),S(5),S(6),DF3B)
CALL DETER(DF3B,5,5,D2)
DF(2,6)=D1+D2
CALL DF3D7(P(2),P(5),DF2)
CALL DETER(DF2,3,3,DF(3,7))
CALL DF3D8A(P(2),P(5),DF2A)
CALL DETER(DF2A,3,3,D1)
CALL DF3D8B(P(2),P(5),DF2B)
CALL DETER(DF2B,3,3,D2)
DF(3,8)=D1+D2
DF(4,1)=2.0*T(1)
DF(4,2)=-2.0*T(2)
DF(4,7)=-2.0*P(2)
DF(5,2)=2.0*T(2)
DF(5,3)=-2.0*T(3)
DF(5,7)=2.0*P(2)
DF(6,4)=2.0*S(4)
DF(6,5)=-2.0*S(5)
DF(6,8)=-2.0*P(5)
DF(7,5)=2.0*S(5)
DF(7,6)=-2.0*S(6)
DF(7,8)=2.0*P(5)
DF(8,2)=2.0*T(2)
DF(8,5)=-2.0*S(5)
DF(8,7)=2.0*P(2)
DF(8,8)=-2.0*P(5)
DO 101 J=1,8
DO 101 I=1,8
  DFA(I,J)=DF(I,J)
101 CONTINUE
CALL DETER(DFA,8,8,V)
DEL=0.0
DELU=0.0

```

```

DO 100 I=1,8
CALL MATAR(I,F,DF,DF)
CALL DETER(DF,8,8,U(I))
U(I)=U(I)/V
DEL=DEL+DABS(F(I))
DELU=DELU+DABS(U(I))
100 CONTINUE
T(1)=T(1)+U(1)
T(2)=T(2)+U(2)
T(3)=T(3)+U(3)
S(4)=S(4)+U(4)
S(5)=S(5)+U(5)
S(6)=S(6)+U(6)
P(2)=P(2)+U(7)
P(5)=P(5)+U(8)
MM=MM+1
IF(MM.GE.200)GO TO 103
IVU=0
IF(DEL.GE.1.0D-06)IVU=1
IF(DELU.GE.1.0D-08)IVU=1
IF(IVU.EQ.1)GO TO 102
IND=0
DO 43 KK=1,6
IF(T(KK).LT.0.0)IND=1
IF(T(KK).GT.1.0D+10)IND=1
IF(S(KK).LT.0.0)IND=1
IF(S(KK).GT.1.0D+10)IND=1
IF(P(KK).LT.0.0)IND=1
IF(P(KK).GT.1.0D+10)IND=1
43 CONTINUE
IF(IND.EQ.1)GO TO 103
MA=MB+1
T1(MA)=T(1)
T2(MA)=T(2)
T3(MA)=T(3)
T4(MA)=T(4)
T5(MA)=T(5)
T6(MA)=T(6)
S1(MA)=S(1)
S2(MA)=S(2)
S3(MA)=S(3)
S4(MA)=S(4)
S5(MA)=S(5)
S6(MA)=S(6)
P1(MA)=P(1)
P2(MA)=P(2)
P3(MA)=P(3)
P4(MA)=P(4)
P5(MA)=P(5)
P6(MA)=P(6)
IF(IVU.EQ.0)GO TO 104
103 CALL GUESS
104 CONTINUE
RETURN
END
SUBROUTINE MATAR(K,FU,DFU,RFU)
IMPLICIT REAL*8(A-H,O-Z)
DIMENSION FU(8),DFU(8,8),RFU(8,8)
DO 1 J=1,8
DO 1 I=1,8
IF(J.EQ.K) THEN
RFU(I,J)=-FU(I)
ELSE
RFU(I,J)=DFU(I,J)
ENDIF
CONTINUE
RETURN
END
SUBROUTINE FLX(EV1,EV2,EV3,FA)
IMPLICIT REAL*8(A-H,O-Z)
COMMON/T1/XXD(4),YYD(4),ZZD(3)
COMMON/T2/ALX(2),ALY(2),ALZ(2)

```

```

COMMON/T3/EX(2),EY(2),EZ(2)
DIMENSION FA(5,5)
DO 102 I=1,5
DO 102 J=1,5
  FA(I,J)=0.0
102 CONTINUE
AR1=EV1*DSQRT(EX(1))
AR2=EV2*DSQRT(EX(1))
AR3=EV3*DSQRT(EX(1))
CO1=ALX(1)*AR1
CO2=ALX(1)*AR2
CO3=ALX(1)*AR3
FA(1,1)=-CO1*DSIN(AR1*XXD(2))
FA(1,2)=CO2*DSIN(AR2*XXD(2))
FA(1,3)=-CO2*DCOS(AR2*XXD(2))
FA(2,1)=DCOS(AR1*XXD(2))
FA(2,2)=-DCOS(AR2*XXD(2))
FA(2,3)=-DSIN(AR2*XXD(2))
FA(3,2)=-CO2*DSIN(AR2*XXD(3))
FA(3,3)=CO2*DCOS(AR2*XXD(3))
FA(3,4)=CO3*DSIN(AR3*XXD(3))
FA(3,5)=-CO3*DCOS(AR3*XXD(3))
FA(4,2)=DCOS(AR2*XXD(3))
FA(4,3)=DSIN(AR2*XXD(3))
FA(4,4)=-DCOS(AR3*XXD(3))
FA(4,5)=-DSIN(AR3*XXD(3))
FA(5,4)=-DSIN(AR3*XXD(4))
FA(5,5)=DCOS(AR3*XXD(4))
RETURN
END
SUBROUTINE F2Y(EV1,EV2,EV3,FA)
IMPLICIT REAL*8(A-H,O-Z)
COMMON/T1/XXD(4),YYD(4),ZZD(3)
COMMON/T2/ALX(2),ALY(2),ALZ(2)
COMMON/T3/EX(2),EY(2),EZ(2)
DIMENSION FA(5,5)
DO 102 I=1,5
DO 102 J=1,5
  FA(I,J)=0.0
102 CONTINUE
AR1=EV1*DSQRT(EY(2))
AR2=EV2*DSQRT(EY(2))
AR3=EV3*DSQRT(EY(2))
CO1=ALY(2)*AR1
CO2=ALY(2)*AR2
CO3=ALY(2)*AR3
FA(1,1)=-CO1*DSIN(AR1*YYD(2))
FA(1,2)=CO2*DSIN(AR2*YYD(2))
FA(1,3)=-CO2*DCOS(AR2*YYD(2))
FA(2,1)=DCOS(AR1*YYD(2))
FA(2,2)=-DCOS(AR2*YYD(2))
FA(2,3)=-DSIN(AR2*YYD(2))
FA(3,2)=-CO2*DSIN(AR2*YYD(3))
FA(3,3)=CO2*DCOS(AR2*YYD(3))
FA(3,4)=CO3*DSIN(AR3*YYD(3))
FA(3,5)=-CO3*DCOS(AR3*YYD(3))
FA(4,2)=DCOS(AR2*YYD(3))
FA(4,3)=DSIN(AR2*YYD(3))
FA(4,4)=-DCOS(AR3*YYD(3))
FA(4,5)=-DSIN(AR3*YYD(3))
FA(5,4)=-DSIN(AR3*YYD(4))
FA(5,5)=DCOS(AR3*YYD(4))
RETURN
END
SUBROUTINE F3Z(EV1,EV2,FA)
IMPLICIT REAL*8(A-H,O-Z)
COMMON/T1/XXD(4),YYD(4),ZZD(3)
COMMON/T2/ALX(2),ALY(2),ALZ(2)
COMMON/T3/EX(2),EY(2),EZ(2)
COMMON/T4/UZ
DIMENSION FA(3,3)
AR1=EV1*DSQRT(EZ(1))

```



```

AR2=EV2*DSQRT(EZ(2))
CO1=ALZ(1)*AR1
CO2=ALZ(2)*AR2
FA(1,1)=-UZ*DCOS(AR1*ZZD(2))+CO1*DSIN(AR1*ZZD(2))
FA(1,2)=UZ*DCOS(AR2*ZZD(2))
FA(1,3)=UZ*DSIN(AR2*ZZD(2))
FA(2,1)=-CO1*DSIN(AR1*ZZD(2))
FA(2,2)=CO2*DSIN(AR2*ZZD(2))
FA(2,3)=-CO2*DCOS(AR2*ZZD(2))
FA(3,1)=0.0
FA(3,2)=-DSIN(AR2*ZZD(3))
FA(3,3)=DCOS(AR2*ZZD(3))
RETURN
END
SUBROUTINE DF1D1(EV1, EV2, EV3, FA)
IMPLICIT REAL*8(A-H, O-Z)
COMMON/T1/XXD(4), YYD(4), ZZD(3)
COMMON/T2/ALX(2), ALY(2), ALZ(2)
COMMON/T3/EX(2), EY(2), EZ(2)
DIMENSION FA(5,5)
DO 102 I=1,5
DO 102 J=1,5
  FA(I,J)=0.0
102 CONTINUE
AR1=EV1*DSQRT(EX(1))
AR2=EV2*DSQRT(EX(1))
AR3=EV3*DSQRT(EX(1))
CO1=ALX(1)*AR1
CO2=ALX(1)*AR2
CO3=ALX(1)*AR3
COX=DSQRT(EX(1))
COO=ALX(1)*COX
COO1=ALX(1)*EX(1)*EV1
FA(1,1)=-COO*DSIN(AR1*XXD(2))-COO1*XXD(2)*DCOS(AR1*XXD(2))
FA(1,2)=CO2*DSIN(AR2*XXD(2))
FA(1,3)=-CO2*DCOS(AR2*XXD(2))
FA(2,1)=-COX*XXD(2)*DSIN(AR1*XXD(2))
FA(2,2)=-DCOS(AR2*XXD(2))
FA(2,3)=-DSIN(AR2*XXD(2))
FA(3,2)=-CO2*DSIN(AR2*XXD(3))
FA(3,3)=CO2*DCOS(AR2*XXD(3))
FA(3,4)=CO3*DSIN(AR3*XXD(3))
FA(3,5)=-CO3*DCOS(AR3*XXD(3))
FA(4,2)=DCOS(AR3*XXD(3))
FA(4,3)=DSIN(AR2*XXD(3))
FA(4,4)=-DCOS(AR3*XXD(3))
FA(4,5)=-DSIN(AR3*XXD(3))
FA(5,4)=-DSIN(AR3*XXD(4))
FA(5,5)=DCOS(AR3*XXD(4))
RETURN
END
SUBROUTINE DF1D2A(EV1, EV2, EV3, FA)
IMPLICIT REAL*8(A-H, O-Z)
COMMON/T1/XXD(4), YYD(4), ZZD(3)
COMMON/T2/ALX(2), ALY(2), ALZ(2)
COMMON/T3/EX(2), EY(2), EZ(2)
DIMENSION FA(5,5)
DO 102 I=1,5
DO 102 J=1,5
  FA(I,J)=0.0
102 CONTINUE
AR1=EV1*DSQRT(EX(1))
AR2=EV2*DSQRT(EX(1))
AR3=EV3*DSQRT(EX(1))
CO1=ALX(1)*AR1
CO2=ALX(1)*AR2
CO3=ALX(1)*AR3
COX=DSQRT(EX(1))
COO=ALX(1)*COX
COO2=ALX(1)*EV2*EX(1)
FA(1,1)=-CO1*DSIN(AR1*XXD(2))
FA(1,2)=COO*DSIN(AR2*XXD(2))+CO2*XXD(2)*DCOS(AR2*XXD(2))

```

```

FA(1,3)=-CO2*DCOS(AR2*XXD(2))
FA(2,1)=DCOS(AR1*XXD(2))
FA(2,2)=COX*XXD(2)*DSIN(AR2*XXD(2))
FA(2,3)=-DSIN(AR2*XXD(2))
FA(3,2)=-COO*DSIN(AR2*XXD(3))-COO2*XXD(3)*DCOS(AR2*XXD(3))
FA(3,3)=CO2*DCOS(AR2*XXD(3))
FA(3,4)=CO3*DSIN(AR3*XXD(3))
FA(3,5)=-CO3*DCOS(AR3*XXD(3))
FA(4,2)=-COX*XXD(3)*DSIN(AR2*XXD(3))
FA(4,3)=DSIN(AR2*XXD(3))
FA(4,4)=-DCOS(AR3*XXD(3))
FA(4,5)=-DSIN(AR3*XXD(3))
FA(5,4)=-DSIN(AR3*XXD(4))
FA(5,5)=DCOS(AR3*XXD(4))
RETURN
END
SUBROUTINE DF1D2B(EV1,EV2,EV3,FA)
IMPLICIT REAL*8(A-H,O-Z)
COMMON/T1/XXD(4),YYD(4),ZZD(3)
COMMON/T2/ALX(2),ALY(2),ALZ(2)
COMMON/T3/EX(2),EY(2),EZ(2)
DIMENSION FA(5,5)
DO 102 I=1,5
DO 102 J=1,5
FA(I,J)=0.0
102 CONTINUE
AR1=EV1*DSQRT(EX(1))
AR2=EV2*DSQRT(EX(1))
AR3=EV3*DSQRT(EX(1))
CO1=ALX(1)*AR1
CO2=ALX(1)*AR2
CO3=ALX(1)*AR3
COX=DSQRT(EX(1))
COO=ALX(1)*COX
COO2=ALX(1)*EX(1)*EV2
FA(1,1)=-CO1*DSIN(AR1*XXD(2))
FA(1,2)=CO2*DSIN(AR2*XXD(2))
FA(1,3)=-COO*DCOS(AR2*XXD(2))+COO2*XXD(2)*DSIN(AR2*XXD(2))
FA(2,1)=DCOS(AR1*XXD(2))
FA(2,2)=-DCOS(AR2*XXD(2))
FA(2,3)=-COX*XXD(2)*DCOS(AR2*XXD(2))
FA(3,2)=-CO2*DSIN(AR2*XXD(3))
FA(3,3)=COO*DCOS(AR2*XXD(3))-COO2*XXD(3)*DSIN(AR2*XXD(3))
FA(3,4)=CO3*DSIN(AR3*XXD(3))
FA(3,5)=-CO3*DCOS(AR3*XXD(3))
FA(4,2)=DCOS(AR2*XXD(3))
FA(4,3)=COX*XXD(3)*DCOS(AR2*XXD(3))
FA(4,4)=-DCOS(AR3*XXD(3))
FA(4,5)=-DSIN(AR3*XXD(3))
FA(5,4)=-DSIN(AR3*XXD(4))
FA(5,5)=DCOS(AR3*XXD(4))
RETURN
END
SUBROUTINE DF1D3A(EV1,EV2,EV3,FA)
IMPLICIT REAL*8(A-H,O-Z)
COMMON/T1/XXD(4),YYD(4),ZZD(3)
COMMON/T2/ALX(2),ALY(2),ALZ(2)
COMMON/T3/EX(2),EY(2),EZ(2)
DIMENSION FA(5,5)
DO 102 I=1,5
DO 102 J=1,5
FA(I,J)=0.0
102 CONTINUE
AR1=EV1*DSQRT(EX(1))
AR2=EV2*DSQRT(EX(1))
AR3=EV3*DSQRT(EX(1))
CO1=ALX(1)*AR1
CO2=ALX(1)*AR2
CO3=ALX(1)*AR3
COX=DSQRT(EX(1))
COO=ALX(1)*COX
COO3=ALX(1)*EX(1)*EV3

```

```

FA(1,1)=-CO1*DSIN(AR1*XXD(2))
FA(1,2)=CO2*DSIN(AR2*XXD(2))
FA(1,3)=-CO2*DCOS(AR2*XXD(2))
FA(2,1)=DCOS(AR1*XXD(2))
FA(2,2)=-DCOS(AR2*XXD(2))
FA(2,3)=-DSIN(AR2*XXD(2))
FA(3,2)=-CO2*DSIN(AR2*XXD(3))
FA(3,3)=CO2*DCOS(AR2*XXD(3))
FA(3,4)=COO*DSIN(AR3*XXD(3))+COO3*XXD(3)*DCOS(AR3*XXD(3))
FA(3,5)=-CO3*DCOS(AR3*XXD(3))
FA(4,2)=DCOS(AR2*XXD(3))
FA(4,3)=DSIN(AR2*XXD(3))
FA(4,4)=COX*XXD(3)*DSIN(AR3*XXD(3))
FA(4,5)=-DSIN(AR3*XXD(3))
FA(5,4)=-COX*XXD(4)*DCOS(AR3*XXD(4))
FA(5,5)=DCOS(AR3*XXD(4))
RETURN
END
SUBROUTINE DF1D3B(EV1,EV2,EV3,FA)
IMPLICIT REAL*8(A-H,O-Z)
COMMON/T1/XXD(4),YYD(4),ZZD(3)
COMMON/T2/ALX(2),ALY(2),ALZ(2)
COMMON/T3/EX(2),EY(2),EZ(2)
DIMENSION FA(5,5)
DO 102 I=1,5
DO 102 J=1,5
FA(I,J)=0.0
102 CONTINUE
AR1=EV1*DSQRT(EX(1))
AR2=EV2*DSQRT(EX(1))
AR3=EV3*DSQRT(EX(1))
CO1=ALX(1)*AR1
CO2=ALX(1)*AR2
CO3=ALX(1)*AR3
COX=DSQRT(EX(1))
COO=ALX(1)*COX
COO3=ALX(1)*EX(1)*EV3
FA(1,1)=-CO1*DSIN(AR1*XXD(2))
FA(1,2)=CO2*DSIN(AR2*XXD(2))
FA(1,3)=-CO2*DCOS(AR2*XXD(2))
FA(2,1)=DCOS(AR1*XXD(2))
FA(2,2)=-DCOS(AR2*XXD(2))
FA(2,3)=-DSIN(AR2*XXD(2))
FA(3,2)=-CO2*DSIN(AR2*XXD(3))
FA(3,3)=CO2*DCOS(AR2*XXD(3))
FA(3,4)=CO3*DSIN(AR3*XXD(3))
FA(3,5)=-COO*DCOS(AR3*XXD(3))+COO3*XXD(3)*DSIN(AR3*XXD(3))
FA(4,2)=DCOS(AR2*XXD(3))
FA(4,3)=DSIN(AR2*XXD(3))
FA(4,4)=-DCOS(AR3*XXD(3))
FA(4,5)=-COX*XXD(3)*DCOS(AR3*XXD(3))
FA(5,4)=-DSIN(AR3*XXD(4))
FA(5,5)=-COX*XXD(4)*DSIN(AR3*XXD(4))
RETURN
END
SUBROUTINE DF2D4(EV1,EV2,EV3,FA)
IMPLICIT REAL*8(A-H,O-Z)
COMMON/T1/XXD(4),YYD(4),ZZD(3)
COMMON/T2/ALX(2),ALY(2),ALZ(2)
COMMON/T3/EX(2),EY(2),EZ(2)
DIMENSION FA(5,5)
DO 102 I=1,5
DO 102 J=1,5
FA(I,J)=0.0
102 CONTINUE
AR1=EV1*DSQRT(EY(2))
AR2=EV2*DSQRT(EY(2))
AR3=EV3*DSQRT(EY(2))
CO1=ALY(2)*AR1
CO2=ALY(2)*AR2
CO3=ALY(2)*AR3
COX=DSQRT(EY(2))

```

```

COO=ALY(2)*COX
COO1=ALY(2)*EY(2)*EV1
  FA(1,1)=-COO*DSIN(AR1*YYD(2))-COO1*YYD(2)*DCOS(AR1*YYD(2))
  FA(1,2)=CO2*DSIN(AR2*YYD(2))
  FA(1,3)=-CO2*DCOS(AR2*YYD(2))
  FA(2,1)=-COX*YYD(2)*DSIN(AR1*YYD(2))
  FA(2,2)=-DCOS(AR2*YYD(2))
  FA(2,3)=-DSIN(AR2*YYD(2))
  FA(3,2)=-CO2*DSIN(AR2*YYD(3))
  FA(3,3)=CO2*DCOS(AR2*YYD(3))
  FA(3,4)=CO3*DSIN(AR3*YYD(3))
  FA(3,5)=-CO3*DCOS(AR3*YYD(3))
  FA(4,2)=DCOS(AR2*YYD(3))
  FA(4,3)=DSIN(AR2*YYD(3))
  FA(4,4)=-DCOS(AR3*YYD(3))
  FA(4,5)=-DSIN(AR3*YYD(3))
  FA(5,4)=-DSIN(AR3*YYD(4))
  FA(5,5)=DCOS(AR3*YYD(4))
RETURN
END
SUBROUTINE DF2D5A(EV1,EV2,EV3,FA)
IMPLICIT REAL*8(A-H,O-Z)
COMMON/T1/XXD(4),YYD(4),ZZD(3)
COMMON/T2/ALX(2),ALY(2),ALZ(2)
COMMON/T3/EX(2),EY(2),EZ(2)
DIMENSION FA(5,5)
DO 102 I=1,5
DO 102 J=1,5
  FA(I,J)=0.0
102 CONTINUE
AR1=EV1*DSQRT(EY(2))
AR2=EV2*DSQRT(EY(2))
AR3=EV3*DSQRT(EY(2))
CO1=ALY(2)*AR1
CO2=ALY(2)*AR2
CO3=ALY(2)*AR3
COX=DSQRT(EY(2))
COO=ALY(2)*COX
COO2=ALY(2)*EY(2)*EV2
  FA(1,1)=-CO1*DSIN(AR1*YYD(2))
  FA(1,2)=COO*DSIN(AR2*YYD(2))+COO2*YYD(2)*DCOS(AR2*YYD(2))
  FA(1,3)=-CO2*DCOS(AR2*YYD(2))
  FA(2,1)=DCOS(AR1*YYD(2))
  FA(2,2)=COX*YYD(2)*DSIN(AR2*YYD(2))
  FA(2,3)=-DSIN(AR2*YYD(2))
  FA(3,2)=-COO*DSIN(AR2*YYD(3))-COO2*YYD(3)*DCOS(AR2*YYD(3))
  FA(3,3)=CO2*DCOS(AR2*YYD(3))
  FA(3,4)=CO3*DSIN(AR3*YYD(3))
  FA(3,5)=-CO3*DCOS(AR3*YYD(3))
  FA(4,2)=-COX*YYD(3)*DSIN(AR2*YYD(3))
  FA(4,3)=DSIN(AR2*YYD(3))
  FA(4,4)=-DCOS(AR3*YYD(3))
  FA(4,5)=-DSIN(AR3*YYD(3))
  FA(5,4)=-DSIN(AR3*YYD(4))
  FA(5,5)=DCOS(AR3*YYD(4))
RETURN
END
SUBROUTINE DF2D5B(EV1,EV2,EV3,FA)
IMPLICIT REAL*8(A-H,O-Z)
COMMON/T1/XXD(4),YYD(4),ZZD(3)
COMMON/T2/ALX(2),ALY(2),ALZ(2)
COMMON/T3/EX(2),EY(2),EZ(2)
DIMENSION FA(5,5)
DO 102 I=1,5
DO 102 J=1,5
  FA(I,J)=0.0
102 CONTINUE
AR1=EV1*DSQRT(EY(2))
AR2=EV2*DSQRT(EY(2))
AR3=EV3*DSQRT(EY(2))
CO1=ALY(2)*AR1
CO2=ALY(2)*AR2

```

```

CO3=ALY(2)*AR3
COX=DSQRT(EY(2))
COO=ALY(2)*COX
COO2=ALY(2)*EY(2)*EV2
FA(1,1)=-CO1*DSIN(AR1*YYD(2))
FA(1,2)=CO2*DSIN(AR2*YYD(2))
FA(1,3)=-COO*DCOS(AR2*YYD(2))+COO2*YYD(2)*DSIN(AR2*YYD(2))
FA(2,1)=DCOS(AR1*YYD(2))
FA(2,2)=-DCOS(AR2*YYD(2))
FA(2,3)=-COX*YYD(2)*DCOS(AR2*YYD(2))
FA(3,2)=-CO2*DSIN(AR2*YYD(3))
FA(3,3)=COO*DCOS(AR2*YYD(3))-COO2*YYD(3)*DSIN(AR2*YYD(3))
FA(3,4)=CO3*DSIN(AR3*YYD(3))
FA(3,5)=-CO3*DCOS(AR3*YYD(3))
FA(4,2)=DCOS(AR2*YYD(3))
FA(4,3)=COX*YYD(3)*DCOS(AR2*YYD(3))
FA(4,4)=-DCOS(AR3*YYD(3))
FA(4,5)=-DSIN(AR3*YYD(3))
FA(5,4)=-DSIN(AR3*YYD(4))
FA(5,5)=DCOS(AR3*YYD(4))
RETURN
END
SUBROUTINE DF2D6A(EV1,EV2,EV3,FA)
IMPLICIT REAL*8(A-H,O-Z)
COMMON/T1/XXD(4),YYD(4),ZZD(3)
COMMON/T2/ALX(2),ALY(2),ALZ(2)
COMMON/T3/EX(2),EY(2),EZ(2)
DIMENSION FA(5,5)
DO 102 I=1,5
DO 102 J=1,5
FA(I,J)=0.0
102 CONTINUE
AR1=EV1*DSQRT(EY(2))
AR2=EV2*DSQRT(EY(2))
AR3=EV3*DSQRT(EY(2))
CO1=ALY(2)*AR1
CO2=ALY(2)*AR2
CO3=ALY(2)*AR3
COX=DSQRT(EY(2))
COO=ALY(2)*COX
COO3=ALY(2)*EY(2)*EV3
FA(1,1)=-CO1*DSIN(AR1*YYD(2))
FA(1,2)=CO2*DSIN(AR2*YYD(2))
FA(1,3)=-CO2*DCOS(AR2*YYD(2))
FA(2,1)=DCOS(AR1*YYD(2))
FA(2,2)=-DCOS(AR2*YYD(2))
FA(2,3)=-DSIN(AR2*YYD(2))
FA(3,2)=-CO2*DSIN(AR2*YYD(3))
FA(3,3)=CO2*DCOS(AR2*YYD(3))
FA(3,4)=COO*DSIN(AR3*YYD(3))+COO3*YYD(3)*DCOS(AR3*YYD(3))
FA(3,5)=-CO3*DCOS(AR3*YYD(3))
FA(4,2)=DCOS(AR2*YYD(3))
FA(4,3)=DSIN(AR2*YYD(3))
FA(4,4)=COX*YYD(3)*DSIN(AR3*YYD(3))
FA(4,5)=-DSIN(AR3*YYD(3))
FA(5,4)=-COX*YYD(4)*DCOS(AR3*YYD(4))
FA(5,5)=DCOS(AR3*YYD(4))
RETURN
END
SUBROUTINE DF2D6B(EV1,EV2,EV3,FA)
IMPLICIT REAL*8(A-H,O-Z)
COMMON/T1/XXD(4),YYD(4),ZZD(3)
COMMON/T2/ALX(2),ALY(2),ALZ(2)
COMMON/T3/EX(2),EY(2),EZ(2)
DIMENSION FA(5,5)
DO 102 I=1,5
DO 102 J=1,5
FA(I,J)=0.0
102 CONTINUE
AR1=EV1*DSQRT(EY(2))
AR2=EV2*DSQRT(EY(2))
AR3=EV3*DSQRT(EY(2))

```

```

CO1=ALY(2)*AR1
CO2=ALY(2)*AR2
CO3=ALY(2)*AR3
COX=DSQRT(EY(2))
COO=ALY(2)*COX
COO3=ALY(2)*EY(2)*EV3
FA(1,1)=-CO1*DSIN(AR1*YYD(2))
FA(1,2)=CO2*DSIN(AR2*YYD(2))
FA(1,3)=-CO3*DCOS(AR2*YYD(2))
FA(2,1)=DCOS(AR1*YYD(2))
FA(2,2)=-DCOS(AR2*YYD(2))
FA(2,3)=-DSIN(AR2*YYD(2))
FA(3,2)=-CO2*DSIN(AR2*YYD(3))
FA(3,3)=CO2*DCOS(AR2*YYD(3))
FA(3,4)=CO3*DSIN(AR3*YYD(3))
FA(3,5)=-COO*DCOS(AR3*YYD(3))+COO3*YYD(3)*DSIN(AR3*YYD(3))
FA(4,2)=DCOS(AR2*YYD(3))
FA(4,3)=DSIN(AR2*YYD(3))
FA(4,4)=-DCOS(AR3*YYD(3))
FA(4,5)=-COX*YYD(3)*DCOS(AR3*YYD(3))
FA(5,4)=-DSIN(AR3*YYD(4))
FA(5,5)=-COX*YYD(4)*DSIN(AR3*YYD(4))
RETURN
END
SUBROUTINE DF3D7(EV1, EV2, FA)
IMPLICIT REAL*8(A-H, O-Z)
COMMON/T1/XXD(4), YYD(4), ZZD(3)
COMMON/T2/ALX(2), ALY(2), ALZ(2)
COMMON/T3/EX(2), EY(2), EZ(2)
COMMON/T4/UZ
DIMENSION FA(3,3)
DO 102 I=1,3
DO 102 J=1,3
  FA(I,J)=0.0
102 CONTINUE
AR1=EV1*DSQRT(EZ(1))
AR2=EV2*DSQRT(EZ(2))
CO1=ALZ(1)*AR1
CO2=ALZ(2)*AR2
COX1=DSQRT(EZ(1))
COX2=DSQRT(EZ(2))
COO1=ALZ(1)*COX1
COO2=ALZ(2)*COX2
COO3=ALZ(1)*EZ(1)*EV1
FA(1,1)=UZ*COX1*ZZD(2)*DSIN(AR1*ZZD(2))-COO1*DSIN(AR1*ZZD(2))
FA(1,2)=FA(1,1)-COO3*ZZD(2)*DCOS(AR1*ZZD(2))
FA(1,3)=UZ*DCOS(AR2*ZZD(2))
FA(2,1)=UZ*DSIN(AR2*ZZD(2))
FA(2,2)=-COO1*DSIN(AR1*ZZD(2))-COO3*ZZD(2)*DCOS(AR1*ZZD(2))
FA(2,3)=CO2*DSIN(AR2*ZZD(2))
FA(2,4)=-CO2*DCOS(AR2*ZZD(2))
FA(3,2)=-DSIN(AR2*ZZD(3))
FA(3,3)=DCOS(AR2*ZZD(3))
RETURN
END
SUBROUTINE DF3D8A(EV1, EV2, FA)
IMPLICIT REAL*8(A-H, O-Z)
COMMON/T1/XXD(4), YYD(4), ZZD(3)
COMMON/T2/ALX(2), ALY(2), ALZ(2)
COMMON/T3/EX(2), EY(2), EZ(2)
COMMON/T4/UZ
DIMENSION FA(3,3)
DO 102 I=1,3
DO 102 J=1,3
  FA(I,J)=0.0
102 CONTINUE
AR1=EV1*DSQRT(EZ(1))
AR2=EV2*DSQRT(EZ(2))
CO1=ALZ(1)*AR1
CO2=ALZ(2)*AR2
COX1=DSQRT(EZ(1))
COX2=DSQRT(EZ(2))

```

```

COO1=ALZ(1)*COX1
COO2=ALZ(2)*COX2
COO3=ALZ(2)*EZ(2)*EV2
  FA(1,1)=-UZ*DCOS(AR1*ZZD(2))+CO1*DSIN(AR1*ZZD(2))
  FA(1,2)=-UZ*COX2*ZZD(2)*DSIN(AR2*ZZD(2))
  FA(1,3)=UZ*DSIN(AR2*ZZD(2))
  FA(2,1)=-CO1*DSIN(AR1*ZZD(2))
  FA(2,2)=COO2*DSIN(AR2*ZZD(2))+COO3*ZZD(2)*DCOS(AR2*ZZD(2))
  FA(2,3)=-CO2*DCOS(AR2*ZZD(2))
  FA(3,2)=-COX2*ZZD(3)*DCOS(AR2*ZZD(3))
  FA(3,3)=DCOS(AR2*ZZD(3))
RETURN
END
SUBROUTINE DF3D8B(EV1,EV2,FA)
IMPLICIT REAL*8(A-H,O-Z)
COMMON/T1/XXD(4),YYD(4),ZZD(3)
COMMON/T2/ALX(2),ALY(2),ALZ(2)
COMMON/T3/EX(2),EY(2),EZ(2)
COMMON/T4/UZ
DIMENSION FA(3,3)
DO 102 I=1,3
DO 102 J=1,3
  FA(I,J)=0.0
102 CONTINUE
  AR1=EV1*DSQRT(EZ(1))
  AR2=EV2*DSQRT(EZ(2))
  CO1=ALZ(1)*AR1
  CO2=ALZ(2)*AR2
  COX1=DSQRT(EZ(1))
  COX2=DSQRT(EZ(2))
  COO1=ALZ(1)*COX1
  COO2=ALZ(2)*COX2
  FA(1,1)=-UZ*DCOS(AR1*ZZD(2))+CO1*DSIN(AR1*ZZD(2))
  FA(1,2)=UZ*DCOS(AR2*ZZD(2))
  FA(1,3)=UZ*COX2*ZZD(2)*DCOS(AR2*ZZD(2))
  FA(2,1)=-CO1*DSIN(AR1*ZZD(2))
  FA(2,2)=CO2*DSIN(AR2*ZZD(2))
  FA(2,3)=-COO2*DCOS(AR2*ZZD(2))+CO2*ZZD(2)*DSIN(AR2*ZZD(2))
  FA(3,2)=-DSIN(AR2*ZZD(3))
  FA(3,3)=-COX2*ZZD(3)*DSIN(AR2*ZZD(3))
RETURN
END
SUBROUTINE ARRAN(N,UU,D,G,H)
IMPLICIT REAL*8(A-H,O-Z)
COMMON/T11/AA1,XD,YD,ZD
DIMENSION G(3),H(3),D(N-1),UU(N,N)
G(1)=AA1
H(1)=0.0
  LM=1
  L=(N+1)/2
DO 89 LL=2,L
  G(LL)=D(LM)
  H(LL)=D(LM-1)
  LM=LM+2
89 CONTINUE
DO 5 I=1,N
  V=G(1)*UU(I,1)+G(2)*UU(I,2)+H(2)*UU(I,3)
  IF(L.GT.2)THEN
    V=V+G(3)*UU(I,4)+H(3)*UU(I,5)
  ENDIF
  IF(DABS(V).GE.1.D-5) THEN
    PRINT*, 'WARNING! RESIDUE IS HIGH!!',V
  ENDIF
5 CONTINUE
RETURN
END
SUBROUTINE DETER(A,N,NP,D)
IMPLICIT REAL*8(A-H,O-Z)
DIMENSION A(NP,NP),INDX(NP)
CALL LUDCMP(A,N,NP,INDX,D)
DO 11 J=1,N
  D=D*A(J,J)

```

```

11 CONTINUE
RETURN
END
SUBROUTINE SOLVE(N,UU,G,H)
IMPLICIT REAL*8(A-H,O-Z)
COMMON/T11/AA1,XD,YD,ZD
DIMENSION UU(N,N),W(N-1,N-1),D(N-1),G(3),H(3),IND(N-1)
DO 1 II=1,N-1
DO 1 JJ=1,N-1
W(II,JJ)=UU(II,JJ+1)
1 CONTINUE
DO 5 II=1,N-1
D(II)=-AA1*UU(II,1)
5 CONTINUE
CALL LUDCMP(W,N-1,N-1,IND,F)
CALL LUBKSB(W,N-1,N-1,IND,D)
CALL ARRAN(N,UU,D,G,H)
RETURN
END
SUBROUTINE SOURCE(L,SU)
IMPLICIT REAL*8(A-H,O-Z)
COMMON/T11/AA1,XD,YD,ZD
COMMON/T108/A(3),B(3),C(3),D(3),F(2),G(2)
COMMON/T109/ARX(6),ARY(6),ARZ(6)
COMMON/T110/AX1(6),AX2(6),AY1(6),AY2(6),AZ1(6),AZ2(6)
CALL NORM(L,AN)
DX=AX1(5)*DCOS(ARX(5)*XD)+AX2(5)*DSIN(ARX(5)*XD)
DY=C(2)*DCOS(ARY(5)*YD)+D(2)*DSIN(ARY(5)*YD)
DZ=F(2)*DCOS(ARZ(5)*ZD)+G(2)*DSIN(ARZ(5)*ZD)
PC=DX*DY*DZ
SU=PC/AN
RETURN
END
SUBROUTINE PDSUM(LL,TD,PDS)
IMPLICIT REAL*8(A-H,O-Z)
COMMON/T1/XXD(4),YYD(4),ZED(3)
COMMON/T2/ALX(2),ALY(2),ALZ(2)
COMMON/T3/EX(2),EY(2),EZ(2)
COMMON/T5/NW(6)
COMMON/T6/AD(6,2),BD(6,2),HD1(6,2),HD2(6,2)
COMMON/T7/NTS(6,2)
COMMON/T9/QD(6,2,20),TDT(6,2,20)
COMMON/T11/AA1,XD,YD,ZD
COMMON/T102/T1(1200),S1(1200),P1(1200)
COMMON/T103/T2(1200),S2(1200),P2(1200)
COMMON/T104/T3(1200),S3(1200),P3(1200)
COMMON/T105/T4(1200),S4(1200),P4(1200)
COMMON/T106/T5(1200),S5(1200),P5(1200)
COMMON/T107/T6(1200),S6(1200),P6(1200)
COMMON/T108/A(3),B(3),C(3),D(3),F(2),G(2)
COMMON/T109/ARX(6),ARY(6),ARZ(6)
COMMON/T110/AX1(6),AX2(6),AY1(6),AY2(6),AZ1(6),AZ2(6)
DIMENSION DUMT(20)
ALU=T1(LL)*T1(LL)+S1(LL)*S1(LL)+P1(LL)*P1(LL)
PDS=0.0
DO 220 IA=1,6
IF(NW(IA).EQ.0)GO TO 201
DO 200 JB=1,NW(IA)
INDEX=1
DO 2 K=2,NTS(IA,JB)
IF(INDEX.EQ.0)GO TO 2
IF(TD.LE.TDT(IA,JB,K))THEN
JKF=K-1
INDEX=0
ENDIF
CONTINUE
IF(INDEX.EQ.0)THEN
L=JKF
ELSE
L=NTS(IA,JB)
ENDIF
DO 50 KI=1,L

```



```

      DUMT(KI)=TDT(IA,JB,KI)
50  CONTINUE
      DUMT(L+1)=TD
      DO 1 I=1,L
      TT1=ALU*(DUMT(I)-TD)
      TT2=ALU*(DUMT(I+1)-TD)
      DFX=AX1(IA)*DCOS(ARX(IA)*AD(IA,JB))
      #+AX2(IA)*DSIN(ARX(IA)*AD(IA,JB))
      DFY=C(IA-3)*DCOS(ARY(IA)*BD(IA,JB))
      #+D(IA-3)*DSIN(ARY(IA)*BD(IA,JB))
      DFZ=AZ1(IA)
      DHD=(HD2(IA,JB)-HD1(IA,JB))/ZZD(2)
      IF(ARZ(IA).GT.1.0D-10)THEN
      V1=0.5*ARZ(IA)*(HD1(IA,JB)+HD2(IA,JB))
      V2=0.5*ARZ(IA)*(HD2(IA,JB)-HD1(IA,JB))
      DFZ=F(IA-3)*DCOS(V1)*DSIN(V2)+G(IA-3)*DSIN(V1)*DSIN(V2)
      DFZ=2.0*DFZ/ARZ(IA)
      ENDIF
      VALU=DFX*DFY*DFZ/(DHD*ALU)
      PDS=PDS+QD(IA,JB,I)*(DEXP(TT2)-DEXP(TT1))*VALU
1  CONTINUE
200 CONTINUE
201 CONTINUE
220 CONTINUE
      RETURN
      END
      SUBROUTINE SOUP(L,TD,SUB)
      IMPLICIT REAL*8(A-H,O-Z)
      COMMON/T1/XXD(4),YYD(4),ZZD(3)
      COMMON/T2/ALX(2),ALY(2),ALZ(2)
      COMMON/T3/EX(2),EY(2),EZ(2)
      COMMON/T5/NW(6)
      COMMON/T6/AD(6,2),BD(6,2),HD1(6,2),HD2(6,2)
      COMMON/T7/NTS(6,2)
      COMMON/T8/QD(6,2,20),TDT(6,2,20)
      COMMON/T102/T1(1200),S1(1200),P1(1200)
      COMMON/T103/T2(1200),S2(1200),P2(1200)
      COMMON/T104/T3(1200),S3(1200),P3(1200)
      COMMON/T105/T4(1200),S4(1200),P4(1200)
      COMMON/T106/T5(1200),S5(1200),P5(1200)
      COMMON/T107/T6(1200),S6(1200),P6(1200)
      COMMON/T108/A(3),B(3),C(3),D(3),F(2),G(2)
      COMMON/T109/ARX(6),ARY(6),ARZ(6)
      COMMON/T110/AX1(6),AX2(6),AY1(6),AY2(6),AZ1(6),AZ2(6)
      DIMENSION DUMT(20)
      ALU=T1(L)*T1(L)+S1(L)*S1(L)+P1(L)*P1(L)
      SUB=0.0
      DO 200 I=1,6
      IF(NW(I).EQ.0)GO TO 201
      DO 202 J=1,NW(I)
      CALL FTD(I,J,TD,QRATE)
      DFX=AX1(I)*DCOS(ARX(I)*AD(I,J))+AX2(I)*DSIN(ARX(I)*AD(I,J))
      DFY=C(I-3)*DCOS(ARY(I)*BD(I,J))+D(I-3)*DSIN(ARY(I)*BD(I,J))
      DFZ=AZ1(I)
      DHD=(HD2(I,J)-HD1(I,J))/ZZD(2)
      IF(ARZ(I).GT.1.0D-10)THEN
      V1=0.5*ARZ(I)*(HD1(I,J)+HD2(I,J))
      V2=0.5*ARZ(I)*(HD2(I,J)-HD1(I,J))
      DFZ=F(I-3)*DCOS(V1)*DSIN(V2)+G(I-3)*DSIN(V1)*DSIN(V2)
      DFZ=2.0*DFZ/ARZ(I)
      ENDIF
      SUB=SUB+QRATE*DFX*DFY*DFZ/DHD
202 CONTINUE
201 CONTINUE
200 CONTINUE
      RETURN
      END
      SUBROUTINE FTD(I,J,T,Q)
      IMPLICIT REAL*8(A-H,O-Z)
      COMMON/T7/NTS(6,2)
      COMMON/T8/QD(6,2,20),TDT(6,2,20)
      INDEX=1

```

```

DO 1 K=2,NTS(I,J)
IF(INDEX.EQ.3)GO TO 1
IF(T.LT.TDT(I,J,K))THEN
Q=QD(I,J,K-1)
INDEX=0
ENDIF
CONTINUE
IF(INDEX.EQ.1)THEN
  Q=QD(I,J,NTS(I,J))
ENDIF
RETURN
END
SUBROUTINE NORM(L,ABN)
IMPLICIT REAL*8(A-H,O-Z)
COMMON/T1/XXD(4),YYD(4),ZZD(3)
COMMON/T2/ALX(2),ALY(2),ALZ(2)
COMMON/T3/EX(2),EY(2),EZ(2)
COMMON/T11/AA1,XD,YD
COMMON/T102/T1(1200),S1(1200),P1(1200)
COMMON/T103/T2(1200),S2(1200),P2(1200)
COMMON/T104/T3(1200),S3(1200),P3(1200)
COMMON/T105/T4(1200),S4(1200),P4(1200)
COMMON/T106/T5(1200),S5(1200),P5(1200)
COMMON/T107/T6(1200),S6(1200),P6(1200)
COMMON/T108/A(3),B(3),C(3),D(3),E(2),G(2)
COMMON/T109/ARX(6),ARY(6),ARZ(6)
COMMON/T110/AX1(6),AX2(6),AY1(6),AY2(6),AZ1(6),AZ2(6)
DIMENSION E(2)
E(1)=ALX(1)*EX(1)
E(2)=ALX(2)*EX(2)
ABN=0.0
ARX(1)=T1(L)*DSQRT(EX(1))
ARX(2)=T2(L)*DSQRT(EX(1))
ARX(3)=T3(L)*DSQRT(EX(1))
ARX(4)=T4(L)*DSQRT(EY(2))
ARX(5)=T5(L)*DSQRT(EY(2))
ARX(6)=T6(L)*DSQRT(EY(2))
ARY(1)=S1(L)*DSQRT(EY(1))
ARY(2)=S2(L)*DSQRT(EY(1))
ARY(3)=S3(L)*DSQRT(EY(1))
ARY(4)=S4(L)*DSQRT(EY(2))
ARY(5)=S5(L)*DSQRT(EY(2))
ARY(6)=S6(L)*DSQRT(EY(2))
ARZ(1)=P1(L)*DSQRT(EZ(1))
ARZ(2)=P2(L)*DSQRT(EZ(1))
ARZ(3)=P3(L)*DSQRT(EZ(1))
ARZ(4)=P4(L)*DSQRT(EZ(2))
ARZ(5)=P5(L)*DSQRT(EZ(2))
ARZ(6)=P6(L)*DSQRT(EZ(2))
AY1(1)=AA1
ASD=S1(L)*YYD(3)*DSQRT(EY(1))
AY2(1)=AA1*DSIN(ASD)/DCOS(ASD)
AZ1(1)=AA1
AZ2(1)=0.0
AY1(2)=AA1
ASD=S2(L)*YYD(3)*DSQRT(EY(1))
AY2(2)=AA1*DSIN(ASD)/DCOS(ASD)
AZ1(2)=F(1)
AZ2(2)=G(1)
AY1(3)=AA1
ASD=S3(L)*YYD(3)*DSQRT(EY(1))
AY2(3)=AA1*DSIN(ASD)/DCOS(ASD)
AZ1(3)=AA1
AZ2(3)=0.0
YY1=YYD(3)+YYD(2)
YY2=YYD(3)-YYD(2)
ZZ1=ZZD(2)+ZZD(1)
ZZ2=ZZD(2)-ZZD(1)
ZZ3=ZZD(3)-ZZD(2)
DO 1 I=1,3
AA=A(I)*A(I)
BB=B(I)*B(I)

```

```

AB=A(I)*B(I)
XX1=XXD(I+1)+XXD(I)
XX2=XXD(I+1)-XXD(I)
XXR1=ARX(I)*XX1
XXR2=ARX(I)*XX2
SS=0.5*(AA+BB)*XX2
TT=0.0
UU=0.0
IF(ARX(I).GT.1.0D-10)THEN
  TT=0.5*(AA-BB)*DCOS(XXR1)*DSIN(XXR2)/ARX(I)
  UU=AB*DSIN(XXR1)*DSIN(XXR2)/ARX(I)
ENDIF
F1=E(1)*(SS+TT+UU)
AA=AY1(I)*AY1(I)
BB=AY2(I)*AY2(I)
F2=0.5*(AA+BB)*YY2
AA=AZ1(I)*AZ1(I)
BB=AZ2(I)*AZ2(I)
AB=AZ1(I)*AZ2(I)
ZZR1=ARZ(I)*ZZ1
ZZR2=ARZ(I)*ZZ2
SS=0.5*(AA+BB)*ZZ2
TT=0.0
UU=0.0
IF(1.EQ.2.AND.ARZ(I).GT.1.0D-10)THEN
  TT=0.5*(AA-BB)*DCOS(ZZR1)*DSIN(ZZR2)/ARZ(I)
  UU=AB*DSIN(ZZR1)*DSIN(ZZR2)/ARZ(I)
ENDIF
F3=SS+TT+UU
ABN=ABN+F1+F2+F3
CONTINUE
AX1(4)=AA1
ASD=T4(L)*XXD(3)*DSQRT(EX(2))
AX2(4)=AA1*DSIN(ASD)/DCOS(ASD)
AZ1(4)=AA1
ASD=P4(L)*ZZD(3)*DSQRT(EZ(2))
AZ2(4)=AA1*DSIN(ASD)/DCOS(ASD)
AX1(5)=AA1
ASD=T5(L)*XXD(3)*DSQRT(EX(2))
AX2(5)=AA1*DSIN(ASD)/DCOS(ASD)
AZ1(5)=F(2)
AZ2(5)=G(2)
AX1(6)=AA1
ASD=T6(L)*XXD(3)*DSQRT(EX(2))
AX2(6)=AA1*DSIN(ASD)/DCOS(ASD)
AZ1(6)=AA1
ASD=P6(L)*ZZD(3)*DSQRT(EZ(2))
AZ2(6)=AA1*DSIN(ASD)/DCOS(ASD)
XX1=XXD(3)+XXD(2)
XX2=XXD(3)-XXD(2)
ZZ3=ZZD(3)+ZZD(2)
ZZ4=ZZD(3)-ZZD(2)
DO 2 I=4,6
  AA=C(I-3)*C(I-3)
  BB=D(I-3)*D(I-3)
  AB=C(I-3)*D(I-3)
  YY1=YYD(I-2)+YYD(I-3)
  YY2=YYD(I-2)-YYD(I-3)
  YYR1=ARY(I)*YY1
  YYR2=ARY(I)*YY2
  SS=0.5*(AA+BB)*YY2
  TT=0.0
  UU=0.0
  IF(ARY(I).GT.1.0D-10)THEN
    TT=0.5*(AA-BB)*DCOS(YYR1)*DSIN(YYR2)/ARY(I)
    UU=AB*DSIN(YYR1)*DSIN(YYR2)/ARY(I)
  ENDIF
  F4=E(2)*(SS+TT+UU)
  AA=AX1(I)*AX1(I)
  BB=AX2(I)*AX2(I)
  AB=AX1(I)*AX2(I)
  F5=0.5*(AA+BB)*XX2

```

```

AA=AZ1(I)*AZ1(I)
BB=AZ2(I)*AZ2(I)
AB=AZ1(I)*AZ2(I)
ZZR1=ARZ(I)*ZZ3
ZZR2=ARZ(I)*ZZ4
SS=0.5*(AA+BB)*ZZ4
TT=0.0
UU=0.0
IF(I.EQ.5.AND.ARZ(I).GT.1.0D-10)THEN
  TT=0.5*(AA-BB)*DCOS(ZZR1)*DSIN(ZZR2)/ARZ(I)
  UU=AB*DSIN(ZZR1)*DSIN(ZZR2)/ARZ(I)
ENDIF
F6=SS+TT+UU
ABN=ABN-F4*F5*F6
2 CONTINUE
RETURN
END
SUBROUTINE LUDCMP(A,N,NP,INDX,D)
IMPLICIT REAL*8(A-H,O-Z)
PARAMETER (NMAX=100,TINY=1.0D-20)
DIMENSION A(NP,NP),INDX(N),VV(NMAX)
D=1.0
DO 12 I=1,N
  AAMAX=0.
  DO 11 J=1,N
    IF (DABS(A(I,J)).GT.AAMAX) AAMAX=DABS(A(I,J))
11 CONTINUE
  IF (AAMAX.EQ.0.) PAUSE 'Singular Matrix !!!'
  VV(I)=1./AAMAX
12 CONTINUE
DO 19 J=1,N
  DO 14 I=1,J-1
    SUM=A(I,J)
    DO 13 K=1,I-1
      SUM=SUM-A(I,K)*A(K,J)
13 CONTINUE
    A(I,J)=SUM
14 CONTINUE
  AAMAX=0.
  DO 16 I=J,N
    SUM=A(I,J)
    DO 15 K=1,J-1
      SUM=SUM-A(I,K)*A(K,J)
15 CONTINUE
    A(I,J)=SUM
    DUM=VV(I)*DABS(SUM)
    IF (DUM.GE.AAMAX) THEN
      IMAX=I
      AAMAX=DUM
    ENDIF
16 CONTINUE
    IF (J.NE.IMAX) THEN
      DO 17 K=1,N
        DUM=A(IMAX,K)
        A(IMAX,K)=A(J,K)
        A(J,K)=DUM
17 CONTINUE
      D=-D
      VV(IMAX)=VV(J)
    ENDIF
    INDX(J)=IMAX
    IF (A(J,J).EQ.0.)A(J,J)=TINY
    IF (J.NE.N) THEN
      DUM=1./A(J,J)
      DO 18 I=J+1,N
        A(I,J)=A(I,J)*DUM
18 CONTINUE
    ENDIF
19 CONTINUE
RETURN
END
SUBROUTINE LUBKSB(A,N,NP,INDX,B)

```

```

      IMPLICIT REAL*8(A-H,O-Z)
      DIMENSION A(NP,NP),INDX(N),B(N)
      II=0
      DO 12 I=1,N
        LL=INDX(I)
        SUM=B(LL)
        B(LL)=B(I)
        IF(II.NE.0) THEN
          DO 11 J=II,I-1
            SUM=SUM-A(I,J)*B(J)
11        CONTINUE
          ELSE IF(SUM.NE.0.)THEN
            II=I
          ENDIF
          B(I)=SUM
12        CONTINUE
        DO 14 I=N,1,-1
          SUM=B(I)
          DO 13 J=I+1,N
            SUM=SUM-A(I,J)*B(J)
13          CONTINUE
          B(I)=SUM/A(I,I)
14        CONTINUE
      RETURN
      END

```

C.2 Input Files

* Input file: in3d.d

```

6      <number of compartments>
0.0  1.0      <location of extreme boundaries in x-direction>
0.3      <dimensionless width of each body>
0.0  1.0      <location of extreme boundaries in y-direction>
0.0  0.05 0.1 <location of boundaries in z-direction>
1.0  1.0      <ALX(I)>
1.0  1.0      <ALY(I)>
1.0  1.0      <ALZ(I)>
1.0  1.0      <EX(I)>
1.0  1.0      <EY(I)>
1.0  1.0      <EZ(I)>
010000.0    <skin factor>
0 0 0 1 0    <number of well(s) in each compartment, N(I)>
0.5 0.5      <areal location of well in 5th compartment>
0.521 0.526 <completed interval of well in 5th compartment, h1D(5),h2D(2)>
2      <number of time steps in production schedule of well in 5th compartment,
      NTS(I,J)>
1.0      <QD(5,1,1)>
0.0      <TDT(5,1,1)>
1.0      <QD(5,1,2)>
1.0      <TDT(5,1,2)>

```

* Input File: r3d.d

```

1.0      <AA1, a constant for solving a linear system of equation>
0.51 0.5 0.022 <location of observing pressure responses, xo, yo, zo>
3.01     <WRS, Initial guess for eigenvalues>

```

APPENDIX D

THREE-DIMENSIONAL FLOW IN A HOMOGENEOUS AND ISOTROPIC RECTANGULAR PARALLELEPIPED

D.1 Introduction

Sometimes a producing well penetrates the formation partially, rather than fully. The presence of bottom water and/or a gas cap may lead to such a situation. The primary objective of this Appendix is to develop analytical solutions for the transient potential in a homogeneous and isotropic rectangular parallelepiped which is producing through a partially-penetrating well. Here, an extension of the procedure for developing the solutions for a two-dimensional rectangular system, as outlined by *Hovanessian* (1961), will be followed.

Muskat (1949) presented an analytical solution for the potential distribution in a bounded reservoir under steady-state conditions producing through a partially-penetrating well. This author used a continuous distribution of flux elements, each of which is provided with a series of images in the bounding planes such that the net flow across the bounding planes cancels to zero. *Seth* (1968) developed an analytical solution for transient pressure in finite reservoirs in radial systems producing through a partially-penetrating well. *Kazemi* and *Seth* (1969) generated numerical solutions for transient-pressure responses using a finite-difference technique for finite and infinite reservoirs producing through partially-penetrating wells. These authors examined the effect of anisotropy and stratification on transient-pressure analysis of wells with restricted flow entry. *Streltsova-Adams* (1979) developed analytical solutions for transient pressure in an oil reservoir producing through a partially-penetrating well in the presence of a gas cap. These solutions have been shown to become the solution for a situation with impervious top and bottom boundaries as a limiting case. *Marett et al.* (1991) have derived analytical

solutions for steady-state pressure distribution due to production through a partially-perforated wellbore in a three-dimensional cylindrical system.

Raghavan and Ozkan (1994) have presented the solutions in Laplace space for transient pressure for a line-source well placed inside a homogeneous and isotropic parallelepiped with various boundary conditions using the method of images. These authors considered the cases of all the boundaries being closed and of where up to four boundaries (out of six boundaries) are being maintained at a constant pressure.

Therefore, in the following Sections, analytical solutions will be developed for transient-potential responses in a homogeneous and isotropic parallelepiped producing through a partially-penetrating well at a constant rate. Considering the importance of incorporating the effects of gravity in the solutions, this problem (with diffusivity equation and conditions) is formulated based on the force form of potential as illustrated in Section 4.1, Chapter 4.

D.2 Development of Solutions

A homogeneous and isotropic rectangular parallelepiped, whose domain is defined by R , is producing through a partially-penetrating (or partially completed) well as shown in Fig. D.1. In this Appendix, the analytical solutions in closed form for the dimensionless potential of this system following a procedure similar to that of *Hovanessian (1961)* are developed. Here the solutions are developed for two sets of boundary conditions. The boundary conditions considered are:

- All boundaries are closed (no flow)
- All boundaries are kept at a constant potential.

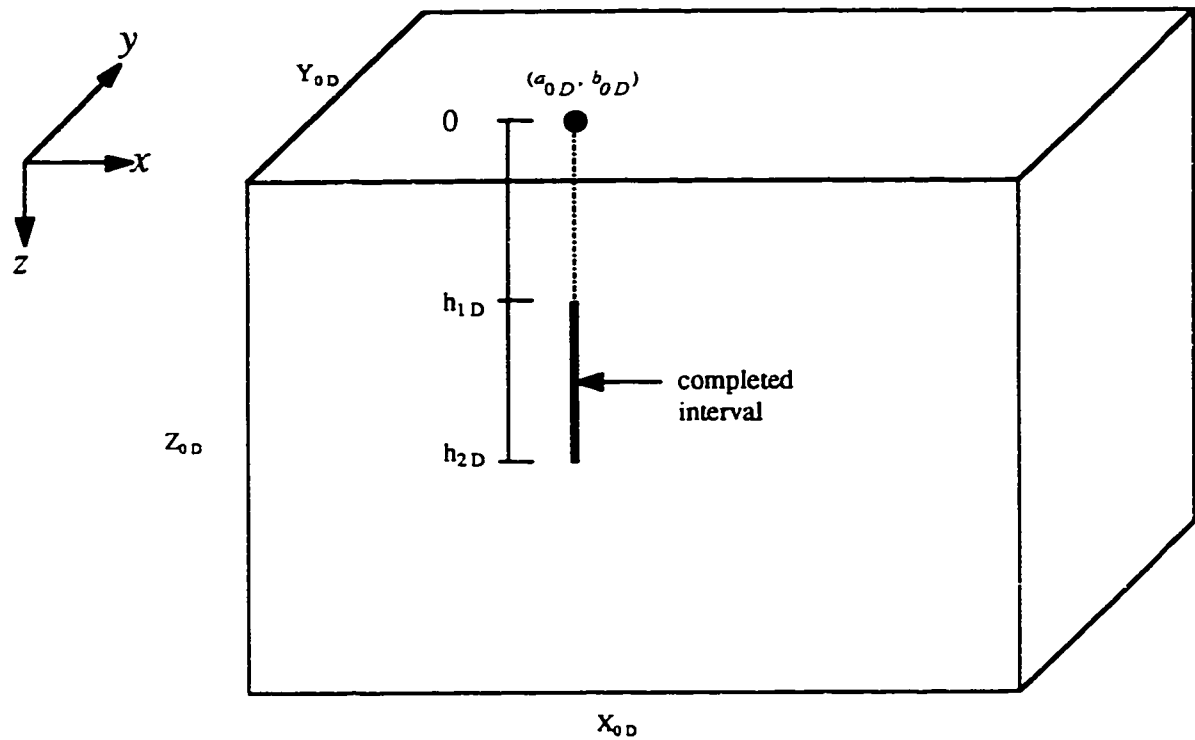


Figure D.1: Schematic of three-dimensional flow in a homogeneous parallelepiped.

The dimensionless form of the diffusivity equation for a slightly-compressible fluid with a constant compressibility in the three-dimensional, Cartesian co-ordinate system due to production through a completed interval between $z_D = h_{1D}$ and $z_D = h_{2D}$ of the partially-penetrating well located at (a_{0D}, b_{0D}) areally (on x - y plane) at a dimensionless rate of q_D is given by:

$$\frac{\partial^2 \Phi_D}{\partial x_D^2} + \frac{\partial^2 \Phi_D}{\partial y_D^2} + \frac{\partial^2 \Phi_D}{\partial z_D^2} + \frac{q_D}{h_{2D} - h_{1D}} [H(z_D - h_{1D}) - H(z_D - h_{2D})] \delta(x_D - a_{0D}) \delta(y_D - b_{0D}) = \frac{\partial \Phi_D}{\partial t_D} \quad \text{.....(D.1)}$$

The above equation is valid for $0 \leq x_D \leq X_{0D}$, $0 \leq y_D \leq Y_{0D}$, $0 \leq z_D \leq Z_{0D}$, $t_D > 0$. The dimensionless variables are defined in Section 4.2, Chapter 4.

For a uniform, initial potential, the initial condition to Eq. (D.1) is prescribed as:

$$\Phi_D(x_D, y_D, z_D, 0) = 0 \quad \text{.....(D.2)}$$

In the following Sections, the solutions for $\Phi_D(x_D, y_D, z_D, t_D)$ to Eq. (D.1) with the initial condition, expressed by Eq. (D.2), are derived for two sets of boundary conditions.

D.3 Case: All Boundaries Closed

All the boundaries are kept closed while the partially-penetrating well is producing. In this case, the boundary conditions in dimensionless form are prescribed as:

$$\left[\frac{\partial \Phi_D}{\partial x_D} \right]_{x_D=0} = \left[\frac{\partial \Phi_D}{\partial x_D} \right]_{x_D=X_{0D}} = 0 \quad \text{.....(D.3)}$$

$$\left[\frac{\partial \Phi_D}{\partial y_D} \right]_{y_D=0} = \left[\frac{\partial \Phi_D}{\partial y_D} \right]_{y_D=Y_{0D}} = 0 \quad \text{.....(D.4)}$$

$$\left[\frac{\partial \Phi_D}{\partial z_D} \right]_{z_D=0} = \left[\frac{\partial \Phi_D}{\partial z_D} \right]_{z_D=Z_{0D}} = 0 \dots \dots \dots (D.5)$$

The homogeneous, Neumann-type of boundary conditions, expressed by Eqs. (D.3) through (D.5), suggest that one needs to use the finite, Fourier cosine transform (*Sneddon*, 1951). There will be eight auxiliary solutions to Eq. (D.1), the algebraic summation of which will result in the complete solution for Φ_D . Thus,

$$\Phi_D(x_D, y_D, z_D, t_D) = \sum_{i=1}^8 \Phi_{iD} \dots \dots \dots (D.6)$$

Table D.1 shows the kernel functions (operators) for the finite, Fourier cosine transform used for these auxiliary solutions. In the following, the derivation for Φ_{1D} is shown. The other auxiliary solutions can be derived in a similar way.

To get the Fourier cosine transformation of the diffusivity equation, multiplying both sides of Eq. (D.1) by the operator, $\cos\left(\frac{l' \pi x_D}{X_{0D}}\right) \cos\left(\frac{m' \pi y_D}{Y_{0D}}\right) \cos\left(\frac{n' \pi z_D}{Z_{0D}}\right) dx_D dy_D dz_D$, and integrating over the domain of the rectangular parallelepiped, R , one has:

$$\begin{aligned} & \iiint_R \left(\frac{\partial^2 \Phi_D}{\partial x_D^2} + \frac{\partial^2 \Phi_D}{\partial y_D^2} + \frac{\partial^2 \Phi_D}{\partial z_D^2} \right) \cos\left(\frac{l' \pi x_D}{X_{0D}}\right) \cos\left(\frac{m' \pi y_D}{Y_{0D}}\right) \cos\left(\frac{n' \pi z_D}{Z_{0D}}\right) dx_D dy_D dz_D \\ & + \frac{q_D}{h_{2D} - h_{1D}} \iiint_R [H(z_D - h_{1D}) - H(z_D - h_{2D})] \delta(x_D - a_{0D}) \delta(y_D - b_{0D}) \\ & \quad \cdot \cos\left(\frac{l' \pi x_D}{X_{0D}}\right) \cos\left(\frac{m' \pi y_D}{Y_{0D}}\right) \cos\left(\frac{n' \pi z_D}{Z_{0D}}\right) dx_D dy_D dz_D \\ & = \iiint_R \frac{\partial \Phi_D}{\partial t_D} \cos\left(\frac{l' \pi x_D}{X_{0D}}\right) \cos\left(\frac{m' \pi y_D}{Y_{0D}}\right) \cos\left(\frac{n' \pi z_D}{Z_{0D}}\right) dx_D dy_D dz_D \dots \dots \dots (D.7) \end{aligned}$$

TABLE D.1: KERNEL FUNCTIONS FOR AUXILIARY SOLUTIONS FOR CLOSED BOUNDARIES

Auxiliary Solution, Φ_{iD}	Kernel Function
Φ_{1D}	$\cos\left(\frac{l' \pi x_D}{X_{0D}}\right) \cos\left(\frac{m' \pi y_D}{Y_{0D}}\right) \cos\left(\frac{n' \pi z_D}{Z_{0D}}\right)$
Φ_{2D}	$\cos\left(\frac{l' \pi x_D}{X_{0D}}\right) \cos\left(\frac{m' \pi y_D}{Y_{0D}}\right)$
Φ_{3D}	$\cos\left(\frac{l' \pi x_D}{X_{0D}}\right)$
Φ_{4D}	$\cos\left(\frac{l' \pi x_D}{X_{0D}}\right) \cos\left(\frac{n' \pi z_D}{Z_{0D}}\right)$
Φ_{5D}	$\cos\left(\frac{n' \pi z_D}{Z_{0D}}\right)$
Φ_{6D}	$\cos\left(\frac{m' \pi y_D}{Y_{0D}}\right) \cos\left(\frac{n' \pi z_D}{Z_{0D}}\right)$
Φ_{7D}	$\cos\left(\frac{m' \pi y_D}{Y_{0D}}\right)$
Φ_{8D}	C (an arbitrary constant)

Simplification of Eq. (D.7) involves evaluation of integrals and substitution of the boundary condition, Eqs. (D.3) through (D.5). Then, solving the resulting equation with the initial condition, one gets,

$$\bar{\Phi}_{D1l'm'n'}(t_D) = \frac{Q_{01l'm'n'}}{\vartheta_{1l'm'n'}^2} (1 - e^{-\vartheta_{1l'm'n'}^2 t_D}) \dots \dots \dots (D.8)$$

where,

$$\bar{\Phi}_{D1l'm'n'}(t_D) = \iiint_R \Phi_D \cos\left(\frac{l' \pi x_D}{X_{0D}}\right) \cos\left(\frac{m' \pi y_D}{Y_{0D}}\right) \cos\left(\frac{n' \pi z_D}{Z_{0D}}\right) dx_D dy_D dz_D \dots \dots \dots (D.9)$$

$$Q_{01l'm'n'} = \frac{q_D Z_{0D}}{n' \pi (h_{2D} - h_{1D})} \cos\left(\frac{l' \pi a_{0D}}{X_{0D}}\right) \cos\left(\frac{m' \pi b_{0D}}{Y_{0D}}\right) \left\{ \sin\left(\frac{n' \pi h_{2D}}{Z_{0D}}\right) - \sin\left(\frac{n' \pi h_{1D}}{Z_{0D}}\right) \right\} \dots \dots \dots (D.10)$$

$$\vartheta_{1l'm'n'}^2 = \pi^2 \left(\frac{l'^2}{X_{0D}^2} + \frac{m'^2}{Y_{0D}^2} + \frac{n'^2}{Z_{0D}^2} \right) \dots \dots \dots (D.11)$$

Inversion of Eq. (D.8) results in the following equation (Sneddon, 1951):

$$\Phi_{1D} = \frac{\delta}{X_{0D} Y_{0D} Z_{0D}} \sum_{l'=1}^{\infty} \sum_{m'=1}^{\infty} \sum_{n'=1}^{\infty} \bar{\Phi}_{D1l'm'n'}(t_D) \cos\left(\frac{l' \pi x_D}{X_{0D}}\right) \cos\left(\frac{m' \pi y_D}{Y_{0D}}\right) \cos\left(\frac{n' \pi z_D}{Z_{0D}}\right) \dots \dots \dots (D.12)$$

Having derived the other auxiliary solutions (for Φ_{2D} , Φ_{3D} ,....., Φ_{8D}) and then substituting all the auxiliary solutions into Eq. (D.6), one has, for the complete solution:

$$\begin{aligned}
\Phi_D(x_D, y_D, z_D, t_D) = & \frac{q_D t_D}{X_{0D} Y_{0D} Z_{0D}} + \frac{8}{X_{0D} Y_{0D} Z_{0D}} \sum_{l'=1}^{\infty} \sum_{m'=1}^{\infty} \sum_{n'=1}^{\infty} \left[\frac{Q_{01l'm'n'}}{\vartheta_{1l'm'n'}^2} (1 - e^{-\vartheta_{1l'm'n'} t_D}) \right. \\
& \left. \cdot \cos\left(\frac{l' \pi x_D}{X_{0D}}\right) \cos\left(\frac{m' \pi y_D}{Y_{0D}}\right) \cos\left(\frac{n' \pi z_D}{Z_{0D}}\right) \right] \\
& + \frac{4}{X_{0D} Y_{0D} Z_{0D}} \sum_{l'=1}^{\infty} \sum_{m'=1}^{\infty} \left[\frac{Q_{02l'm'}}{\vartheta_{2l'm'}^2} (1 - e^{-\vartheta_{2l'm'} t_D}) \cos\left(\frac{l' \pi x_D}{X_{0D}}\right) \cos\left(\frac{m' \pi y_D}{Y_{0D}}\right) \right] \\
& + \frac{2}{X_{0D} Y_{0D} Z_{0D}} \sum_{l'=1}^{\infty} \left[\frac{Q_{03l'}}{\vartheta_{3l'}^2} (1 - e^{-\vartheta_{3l'} t_D}) \cos\left(\frac{l' \pi x_D}{X_{0D}}\right) \right] \\
& + \frac{4}{X_{0D} Y_{0D} Z_{0D}} \sum_{m'=1}^{\infty} \sum_{n'=1}^{\infty} \left[\frac{Q_{04m'n'}}{\vartheta_{4m'n'}^2} (1 - e^{-\vartheta_{4m'n'} t_D}) \cos\left(\frac{m' \pi y_D}{Y_{0D}}\right) \cos\left(\frac{n' \pi z_D}{Z_{0D}}\right) \right] \\
& + \frac{2}{X_{0D} Y_{0D} Z_{0D}} \sum_{m'=1}^{\infty} \left[\frac{Q_{05m'}}{\vartheta_{5m'}^2} (1 - e^{-\vartheta_{5m'} t_D}) \cos\left(\frac{m' \pi y_D}{Y_{0D}}\right) \right] \\
& + \frac{4}{X_{0D} Y_{0D} Z_{0D}} \sum_{l'=1}^{\infty} \sum_{n'=1}^{\infty} \left[\frac{Q_{06l'n'}}{\vartheta_{6l'n'}^2} (1 - e^{-\vartheta_{6l'n'} t_D}) \cos\left(\frac{l' \pi x_D}{X_{0D}}\right) \cos\left(\frac{n' \pi z_D}{Z_{0D}}\right) \right] \\
& + \frac{2}{X_{0D} Y_{0D} Z_{0D}} \sum_{n'=1}^{\infty} \left[\frac{Q_{07n'}}{\vartheta_{7n'}^2} (1 - e^{-\vartheta_{7n'} t_D}) \cos\left(\frac{n' \pi z_D}{Z_{0D}}\right) \right] \dots \dots \dots (D.13)
\end{aligned}$$

where,

$$Q_{02l'm'} = q_D \cos\left(\frac{l' \pi a_{0D}}{X_{0D}}\right) \cos\left(\frac{m' \pi b_{0D}}{Y_{0D}}\right) \dots \dots \dots (D.14)$$

$$\vartheta_{2l'm'}^2 = \pi^2 \left(\frac{l'^2}{X_{0D}^2} - \frac{m'^2}{Y_{0D}^2} \right) \dots \dots \dots (D.15)$$

$$Q_{03l'} = q_D \cos\left(\frac{l' \pi a_{0D}}{X_{0D}}\right) \dots \dots \dots (D.16)$$

$$\vartheta_{3l'}^2 = \frac{\pi^2 l'^2}{X_{0D}^2} \dots \dots \dots (D.17)$$

$$Q_{04m'n'} = \frac{q_D Z_{0D}}{n' \pi (h_{2D} - h_{1D})} \cos\left(\frac{m' \pi b_{0D}}{Y_{0D}}\right) \left\{ \sin\left(\frac{n' \pi h_{2D}}{Z_{0D}}\right) - \sin\left(\frac{n' \pi h_{1D}}{Z_{0D}}\right) \right\} \dots \dots \dots (D.18)$$

$$\vartheta_{4m'n'}^2 = \pi^2 \left(\frac{m'^2}{Y_{0D}^2} + \frac{n'^2}{Z_{0D}^2} \right) \dots \dots \dots (D.19)$$

$$Q_{05m'} = q_D \cos\left(\frac{m' \pi b_{0D}}{Y_{0D}}\right) \dots\dots\dots (D.20)$$

$$\vartheta_{5m'}^2 = \frac{\pi^2 m'^2}{Y_{0D}^2} \dots\dots\dots (D.21)$$

$$Q_{06l'n'} = \frac{q_D Z_{0D}}{n' \pi (h_{2D} - h_{1D})} \cos\left(\frac{l' \pi a_{0D}}{X_{0D}}\right) \left\{ \sin\left(\frac{n' \pi h_{2D}}{Z_{0D}}\right) - \sin\left(\frac{n' \pi h_{1D}}{Z_{0D}}\right) \right\} \dots\dots\dots (D.22)$$

$$\vartheta_{6l'n'}^2 = \pi^2 \left(\frac{l'^2}{X_{0D}^2} + \frac{n'^2}{Z_{0D}^2} \right) \dots\dots\dots (D.23)$$

$$Q_{07n'} = \frac{q_D Z_{0D}}{n' \pi (h_{2D} - h_{1D})} \left\{ \sin\left(\frac{n' \pi h_{2D}}{Z_{0D}}\right) - \sin\left(\frac{n' \pi h_{1D}}{Z_{0D}}\right) \right\} \dots\dots\dots (D.24)$$

$$\vartheta_{7n'}^2 = \frac{\pi^2 n'^2}{Z_{0D}^2} \dots\dots\dots (D.25)$$

Therefore, Eq. (D.13) is the ultimate solution to the problem.

D.4 Case: All Boundaries Maintained at a Constant Potential

All the boundaries are maintained at a constant potential (initial potential) while the partially-penetrating well is producing. Thus, the boundary conditions in dimensionless form are as follows:

$$[\Phi_D]_{x_D=0} = [\Phi_D]_{x_D=X_{0D}} = 0 \dots\dots\dots (D.26)$$

$$[\Phi_D]_{y_D=0} = [\Phi_D]_{y_D=Y_{0D}} = 0 \dots\dots\dots (D.27)$$

$$[\Phi_D]_{z_D=0} = [\Phi_D]_{z_D=Z_{0D}} = 0 \dots\dots\dots (D.28)$$

Following *Sneddon* (1951), the homogenous, Dirichlet-type of boundary conditions, expressed by Eqs. (D.26) through (D.28), suggest that one should use the finite, Fourier sine transform. Unlike the case of closed boundary system considered in Section D.3, the ultimate solution is reached by carrying out the derivation with one kernel function

(operator) only. Thus, multiplying both sides of the diffusivity equation, expressed by Eq. (D.1), by the operator, $\sin\left(\frac{l' \pi x_D}{X_{0D}}\right) \sin\left(\frac{m' \pi y_D}{Y_{0D}}\right) \sin\left(\frac{n' \pi z_D}{Z_{0D}}\right) dx_D dy_D dz_D$, and integrating over the domain of the rectangular parallelepiped, R , and following a similar procedure to that described in Section D.3, one obtains,

$$\Phi_D(x_D, y_D, z_D, t_D) = \frac{8}{X_{0D} Y_{0D} Z_{0D}} \sum_{l'=1}^{\infty} \sum_{m'=1}^{\infty} \sum_{n'=1}^{\infty} \left[\frac{Q_{0l'm'n'}}{\vartheta_{l'm'n'}^2} (1 - e^{-\vartheta_{l'm'n'}^2 t_D}) \cdot \sin\left(\frac{l' \pi x_D}{X_{0D}}\right) \sin\left(\frac{m' \pi y_D}{Y_{0D}}\right) \sin\left(\frac{n' \pi z_D}{Z_{0D}}\right) \right] \dots \text{(D.29)}$$

where,

$$Q_{0l'm'n'} = - \frac{q_D Z_{0D}}{n' \pi (h_{2D} - h_{1D})} \sin\left(\frac{l' \pi a_{0D}}{X_{0D}}\right) \sin\left(\frac{m' \pi b_{0D}}{Y_{0D}}\right) \left\{ \cos\left(\frac{n' \pi h_{2D}}{Z_{0D}}\right) - \cos\left(\frac{n' \pi h_{1D}}{Z_{0D}}\right) \right\} \dots \text{(D.30)}$$

$$\vartheta_{l'm'n'}^2 = \pi^2 \left(\frac{l'^2}{X_{0D}^2} + \frac{m'^2}{Y_{0D}^2} + \frac{n'^2}{Z_{0D}^2} \right) \dots \text{(D.31)}$$

Therefore, Eq. (D.29) is the ultimate solution to the problem.

APPENDIX E

PROOF OF APPLICABILITY OF PRINCIPLE OF RECIPROCITY

Consider a compartmentalized system with two hydraulically-communicating compartments A and B. This system is subject to two-dimensional flow when the condition at each extreme boundary is of the homogeneous, Dirichlet-type. It will be shown that the principle of reciprocity holds for this kind of situation. Initially, both compartments are at an identical, uniform pressure. The points $(x_{D A}, y_{D A})$ and $(x_{D B}, y_{D B})$ are the two arbitrary points in these compartments, respectively, where an active well and an observation well are to be located. Let $p_{D A}(x_{D A}, y_{D A}, t_D)$ be the dimensionless pressure response at an observation well, located at $(x_{D A}, y_{D A})$ in compartment A, due to the production through an active well, located at $(x_{D B}, y_{D B}, t_D)$ in compartment B, and also let $p_{D B}(x_{D B}, y_{D B}, t_D)$ be the dimensionless pressure response at an observation well, located at $(x_{D B}, y_{D B})$ in compartment B, due to production through an active well, located at $(x_{D A}, y_{D A})$ in compartment A, at dimensionless time t_D . In both cases, a dimensionless production rate of $q_D(t_D)$ as a function of t_D is considered.

Applying the solution for dimensionless pressure responses from Eq. (3.40), taking care that an appropriate Dirichlet-type conditions is used at all the extreme boundaries (Section 3.2.7 in Chapter 3), one gets,

$$p_{D A}(x_{D A}, y_{D A}, t_D) = h_{p D} \sum_{I=1}^{\infty} U_{I B}(x_{D B}, y_{D A}) V_{I B}(x_{D B}, y_{D B}) U_{I A}(x_{D A}, y_{D A}) V_{I A}(x_{D A}, y_{D A}) \int_0^{t_D} q_D(\tau) e^{-\lambda_I^2 \tau} d\tau \dots\dots\dots (E.1)$$

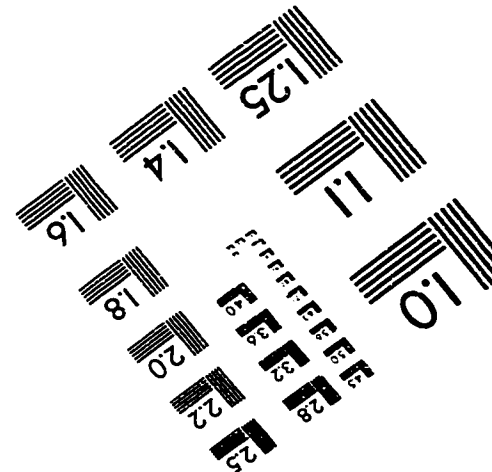
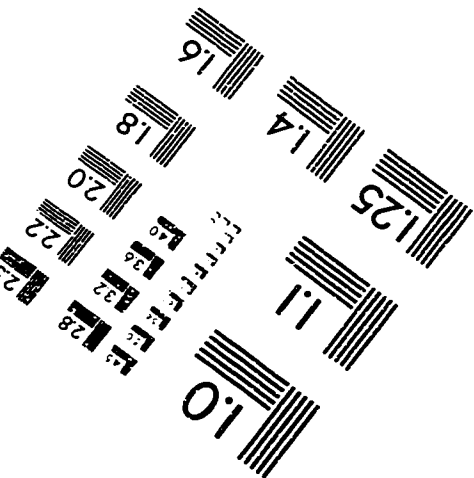
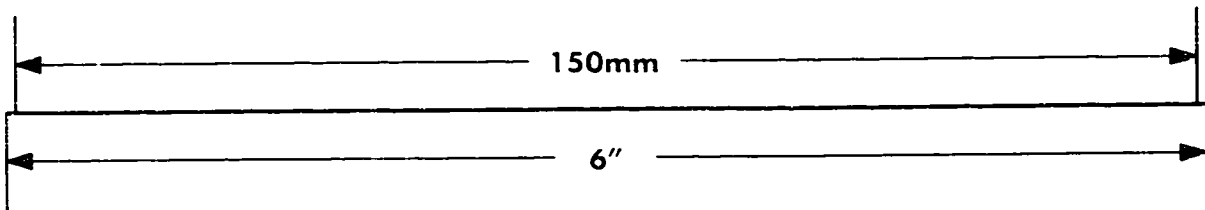
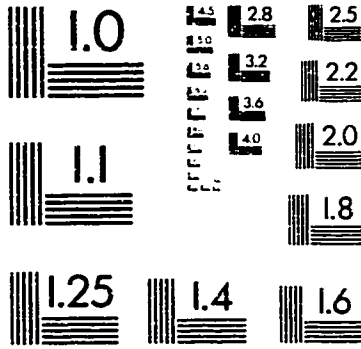
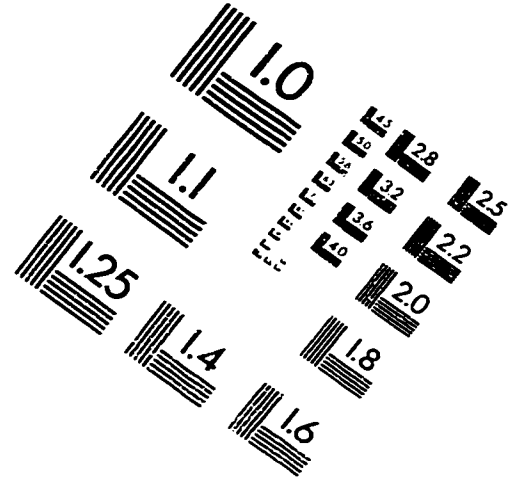
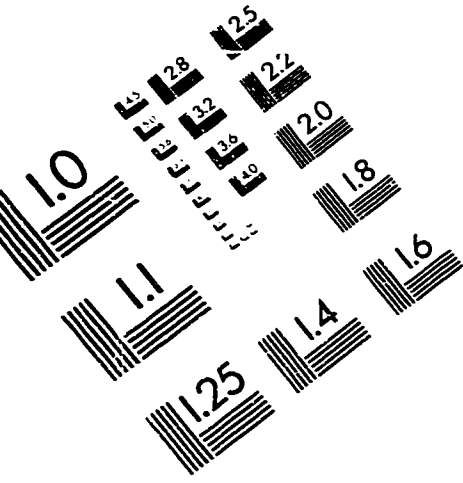
$$p_{D B}(x_{D B}, y_{D B}, t_D) = h_{p D} \sum_{I=1}^{\infty} U_{I A}(x_{D A}, y_{D A}) V_{I A}(x_{D A}, y_{D A}) U_{I B}(x_{D B}, y_{D B}) V_{I B}(x_{D B}, y_{D B}) \int_0^{t_D} q_D(\tau) e^{-\lambda_I^2 \tau} d\tau \dots\dots\dots (E.2)$$

From Eqs. (E.1) and (E.2), one has,

$$p_{DA}(x_A, y_A, t_D) = p_{DB}(x_{DB}, y_{DB}, t_D) \dots \dots \dots (E.3)$$

Hence the principle of reciprocity holds when all the conditions at the extreme boundaries are of the homogeneous, Dirichlet-type. Similarly, one can show that this principle is applicable even when the conditions are of the homogeneous, Nuemann-type or a combination of homogeneous, Dirichlet- and Nuemann-types.

IMAGE EVALUATION TEST TARGET (QA-3)



APPLIED IMAGE, Inc
 1653 East Main Street
 Rochester, NY 14609 USA
 Phone: 716/482-0300
 Fax: 716/288-5989

© 1993, Applied Image, Inc., All Rights Reserved